Electrophysiological correlates of event segmentation: how does the human mind process ongoing activity?

Richard M. Sharp

Doctor of Philosophy

Neuroinformatics Doctoral Training Centre

School of Informatics

University of Edinburgh

2010

Declaration

I declare that this thesis is of my own composition, that it contains no material previously submitted for the award of any other degree except as specified, and that the work reported in this thesis has been completed on my own except where explicitly indicated in the text.

Richard M. Sharp

Abstract

The human mind decodes, processes, and makes sense of a continual flow of dynamic information, taken from an array of sensory inputs. Compelling behavioural and neuroimaging evidence reveals that humans segment activities into meaningful chunks for processing, and this phenomenon has profound implications for learning, memory and understanding the world around us (Newtson, 1973; Zacks and Tversky, 2001; Zacks et al., 2001). Whilst the existence of event segmentation is widely accepted, it remains unclear what cognitive mechanisms drive this ability.

This thesis constitutes a series of behavioural and neuroimaging experiments that investigate top-down and bottom-up influences on event segmentation. The neuroimaging studies presented here are novel; they extend the field by investigating event segmentation using scalp-recorded electroencephalography (EEG). Event Related Potentials (ERPs, derived from EEG using signal-averaging procedures) showed that the perceptual processing of event boundaries is differentially sensitive to the segmentation of activities into small or large chunks, consistent with findings from previous neuroimaging research (Zacks et al., 2001). In contrast with previous findings, the electrophysiological investigations elicited responses that were clearly affected by manipulating top-down information (e.g., participant's knowledge about the activity being segmented). The results from the studies reported in the thesis support an account of the perceptual processing of event boundaries, which incorporates both top-down and bottom-up influences.

Acknowledgments

Chiefly, I would like to acknowledge the Doctoral Training Centre (DTC), funded by the Engineering and Physical Sciences Research Council (EPSRC) and the Medical Research Council (MRC), for providing me with the opportunity to develop my scientific skills and pursue my personal research interests.

I would also like to thank all of the members of the Psychological Imaging Laboratory (PIL), Stirling University, where all Event Related Potential (ERP) studies reported in this thesis were conducted. Sincere thanks, in particular, go to Professor David Donaldson for supervising my research and nurturing my scientific interests.

Gratitude goes to Associate Professor Jeff Zacks, Washington University in St. Louis, for inspiration, guidance and stimulus materials. I would like to thank Dr John Lee for supervising my research and providing endless support and encouragement. Additionally. I would like to thank Catriona Bruce for technical assistance, and Pat Ferguson for administrative support and moral.

Finally, I would like to acknowledge all of my family, colleagues and friends, particularly William McCrea, for their invaluable support while I pursued my research interests.

Table of Contents

1 Human processing of ongoing activity

1.1 Event perception

Human consciousness is an exceptional ability that is often taken for granted. The surrounding environment presents the human multi-sensory processing system with an influx of continuous, dynamic information that is seemingly processed with relative ease. Simply to function in the world around us requires a vast amount of mental processing and even from birth, the human mind is learning how to process and structure environmental information. The more we learn the better we become at recognising our environment and anticipating what might happen next; quickly we learn how to cope. So how does the human mind process all this environmental information, and what are the cognitive mechanisms that facilitate our ability to draw meaning from events that surround us? How humans are able pick out parts from the constant information stream that bombards our sensory system, and how we construct relationships between these parts to bring order and meaning, are key questions for psychology.

Compelling evidence suggests that humans are able to process ongoing activity by breaking the world around us down into manageable chunks (Newtson, 1973, 1976; Zacks, Braver, et al., 2001; Zacks & Tversky, 2001). When considered from this perspective, we can see that even a mundane day is filled with activities that humans are able to segment into meaningful parts. For example, as part of our morning routine we brush our teeth. This activity appears to have clearly defined boundaries: we start brushing our teeth, and then we finish. However, not only does this simple task have event boundaries, so do its constituent parts, e.g. pick up the

toothbrush, pick up the toothpaste, apply the toothpaste to the brush, and so on. From this example alone it is clear that the world can be thought of as a series of goal-driven *events* that appear to form a rough hierarchy.

The term *event* can be used to cover a variety of activities, spanning a variety of timescales ranging from seconds to years. Zacks & Tversky (2001, p. 17) define the term event as "a segment of time at a given location that is conceived by an observer to have a beginning and an end". For example, something as momentous as World War II could be described as an event that lasted several years, and similarly, getting a coffee from the vending machine could be described as an event lasting only a couple of minutes. Although natural events such as flooding may not necessarily be goal-directed, events that involve humans generally do, for example you wash your clothes to make them clean.

The comprehension and completion of everyday tasks clearly rely upon experience, as the more familiar we become with a task the less cognitive effort we require to complete the task; just think how second nature brushing your teeth is compared to driving a car for the first time. Performing an everyday task is likely to invoke a cognitive schema based upon experience; from this, we can reliably extract the temporal sequence of *sub-tasks* that must be completed to achieve the goal of the *task*. For example, to make a cup of tea we know we must put a tea bag in the cup, fill the kettle, and boil the kettle and so on. This example illustrates how the human mind is able to retrieve a cognitive schema that includes the goals, structure and constituent parts of the task.

Conversely, processing a task that we are unfamiliar with is an example of failing to retrieve a reliable schema. Faced with an unfamiliar set of events, cognitive schemas that are judged similar to the task may be

retrieved to provide tentative predictions. In this scenario, we could expect the formation of a new or amended schema, guided by bottom-up features of the task (such as movement) while correcting for errors in prediction. Generally, the more we learn about a task the less attention we need to pay to the details and less attention we require for prediction error correction. Considering the use of a cognitive schema in the perception of familiar and unfamiliar tasks in the aforementioned ways, indicates the differential engagement of cognitive functions during event segmentation that are sensitive to the amount of experience we have with the task, and influenced by different features of the task.

Zacks, Tversky, & Iyer (2001) suggest that segmenting activities into events reflects a psychological reality, in which people perceive their surroundings in terms of discrete parts, and that ongoing cognitive resources are devoted to this perceptual process. Furthermore, it is argued that breaking the world around us down into manageable portions is an automatic process that has consequences for memory and learning (Zacks, Speer, Swallow, Braver, & Reynolds, 2007).

1.2 Investigating event segmentation

Early research investigating perception and event segmentation began with the formulation of a now well-used paradigm; asking people to mark the boundaries of events in activities by pressing a button (Newtson, 1973). Both early and current studies of event segmentation apply the paradigm by asking participants to segment videos of everyday activities based upon their own perceptual judgements. Specifically, participants are asked to segment the activities into large (coarse-grain) and small (fine-grain) parts in separate viewings, to measure the internal representation of information on multiple

levels. To illustrate this point, consider the everyday activity of making your bed. The goal of making the bed may be segmented into sub-events such as changing the pillow cover, changing the duvet cover etc., and likewise, these sub-event have many of their own sub-event such as; removing the pillow cover, preparing the fresh pillow cover, putting the fresh pillow cover on, and so on. From this example, we can see how one might conceptualise an activity on multiple psychological levels.

Newtson's initial work, in combination with further follow-up studies (Newtson, 1976), revealed that repeated segmentation trials produced similar behavioural patterns, and that timings of event boundaries were broadly similar across all participants. Recent research has additionally shown that the perception of event boundaries is reliable, e.g. Speer, Swallow, & Zacks, 2003 showed that participants identified the same event boundaries in stimuli that they had done so one year previously. These behavioural results provide support for the suggestion that event segmentation is an automatic process that is common in human perception.

1.2.1 Cognitive schemata

The role that cognitive schemas might play in perception has been investigated by studying narrative comprehension. Investigating internal representations in this way reveals important implications for event segmentation, as narratives are discourses that describe a set of actions. A number of studies have supported an account of internally representing activities as a hierarchically organised structure (Bower, 1982; Mandler & Johnson, 1977; Schank & Abelson, 1977; Thorndyke, 1977). In particular, Rumelhart (1977) proposes a model that accounts for narrative

comprehension by initially selecting a pre-existing cognitive schema that best fits the narrative. The model also suggests that schemata exhibit a hierarchical structure organised around goals and sub-goals, and that mental tasks such as summarising are undertaken by accessing higher organisational levels of the schemata. These studies appear to suggest that cognitive schemas are employed as a part of ongoing perception, and that schemas comprise of hierarchically organised parts and sub-part structures. But what may be the motivators for forming a schema? Further work investigating this question has given rise to models of narrative comprehension, which suggest that schemas are formed around people and objects, and are driven by changes in time, space and activity goals (Gernsbacher, 1990; Zwaan, Langston, & Graesser, 1995).

1.2.2 Event boundaries

If the human mind is processing activities by accessing and forming cognitive schemas that are organised hierarchically around parts and sub-parts, it reasonable to expect there to be some evidence for the mental processing of event boundaries. Further narrative comprehension studies investigating the mental processing of event boundaries revealed a number of key findings. One study demonstrated that reading time increases at narrative changes in time and goal-direction (Zwaan, Magliano, & Graesser, 1995). Similarly, further studies have found reading time increases at shifts in characters and their goals (Rinck & Weber, 2003; Zwaan, Radvansky, Hilliard, & Curiel, 1998). Finally, Speer & Zacks (2005) were able to demonstrate that temporal discontinuities in a narrative, such as "an hour later", influenced the perception of event boundaries, with participants being more likely to align event boundaries with clauses that contained the

temporal discontinuity. The study also showed that, in contrast with the previous studies showing increases in reading time around event boundaries, clauses containing temporal discontinuities slowed reading time.

The investigation of event boundary perceptions has also provided useful data from domains out with narrative comprehension studies and experiments measuring behavioural responses. For example, the diameter of the pupil has been shown to provide an online measure of cognitive processing load (Beatty & Lucero-Wagoner, 2000), and in one study participants viewed movies while their pupil diameters and eye movements were recorded (Swallow & Zacks, 2004). The study revealed that pupil diameter transiently increased at boundaries, indicating a fluctuation in cognitive load when an event boundary is perceived.

Taken together, these studies support an account of the perceptual processing of event boundaries that is sensitive to the continuity of the information. The differential sensitivity shown in reading times may reflect a shift in the cognitive processing of ongoing activity, as the mind adjusts to changes it had not anticipated. If cognitive schemata play an important role in event segmentation, the results may be interpreted as reflecting a prediction error, as the unexpected change did not match a schema drawn from memory.

This section has highlighted some of the evidence that support a role for cognitive schemas in event perception, and the continuity-sensitive cognitive processing of event boundaries. The following section discusses the structure of activities, and the consequences for the internal representations that we form for activities as part of ongoing perception.

1.3 The structure of events

The previous section discussed evidence which suggested that the human mind imposes (creates) structures upon the information it receives (e.g., Bower, Black, & Turner, 1979; Graesser & Clark, 1985; Schank & Abelson, 1977), and this may reflect the involvement of cognitive schemas in perception. Furthermore, the knowledge structure of a goal-directed everyday activity has been argued as being both hierarchically ordered and temporally organised (Abbott, Black, & Smith, 1985; Zacks & Tversky, 2001).

Of course, in reality, the world around us is not always hierarchical in nature; events such as wars may be described as being heterarchical as they comprise of overlapping and similar sub-events, such as multiple conflicts. It is important to note that research of event segmentation typically focuses on the perception of short (1-10 minutes) hierarchically structured goal-orientated activities, and therefore cannot reflect all aspects of human perception. Nonetheless, such short measurements of perception can provide meaningful insight, particularly when hierarchically structured events can exhibit differing structural characteristics. To explain this point, Zacks & Tversky (2001) draw an analogy from perceptual psychology; events are likened to objects as they too both belong to categories and also have parts. Further, the relationship between objects and events can be exploited to reveal two distinct hierarchical structures: partonomies and taxonomies.

A partonomic structure reflects the hierarchical grouping of parts, and sub-parts, based upon relationships and casual structure, e.g. a tyre is a "part of" the wheel, and the wheel is a part of the car. Conversely, taxonomic structures reflect grouping based on categories e.g., a Ford Escort is a "type of" car, which is a type of motor vehicle. It is likely, however, that as our environment is comprised of a mixture of partonomic and taxonomic

structures this composition is reflected in the structure of a cognitive schema. Consequently, cognitive schemata may comprise of a mixture of partonomic and taxonomic organisations, and this concurrence is believed to facilitate bridges between perception and function or behaviour (Tversky & Hemenway, 1984).

Despite the apparent complexities of events and their structures, research investigating event segmentation is, therefore, ultimately concerned with the perception of partonomic, goal-orientated activities. Nevertheless, structuring internal representations of events in this way has been shown to drive narrative comprehension, memory and planning (Zacks & Tversky, 2001), and is therefore considered to play a key role in perception.

1.3.1 The hierarchical structure of event segmentation

Having discussed the implications of structure in event segmentation in the previous section, we now try to understand how goal-driven, partonomically-structured events are represented as part of ongoing perception.

Zacks, Tversky et al. (2001) asked participants to segment videotaped activities into large meaningful (coarse-grain), and small meaningful (fine-grain) units by pressing a button. From these behavioural data, the investigators were able to extract the timings of event boundaries marked by participants, and subsequently compare the distributions of coarse and fine-grain boundaries over time. The investigators found that by breaking the length of the activities into one-second time bins, they could identify time bins that contained both a coarse and fine-grained boundary, so called "overlapping" time bins. The number of recorded overlapping time bins was

found to be consistently higher than the number generated by chance, suggesting that participants used the coarse-grain boundaries to mark groups of fine-grain units. These results allowed the investigators to deduce that temporally overlapping event boundaries exist, perceived on different psychological levels, reflecting participants encoding activity in terms of goals and sub-goals (i.e. partonomically).

Event boundary alignment has also been observed by Hard, Lozano, & Tversky (2006), who additionally revealed that the timings of coarse-grain boundaries were slightly behind those of fine-grain boundaries to which they were closest. Hard, Lozano, & Tversky hypothesised that the delay in coarse-grain boundary timing reflects the fact that conceptually, large units subsume small units, thus forming a partonomic structure. Interestingly, studies investigating memory and understanding (e.g., Lichtenstein & Brewer, 1980; Rumelhart, 1977), have argued that hierarchically structured representations are important for relating ongoing activity, therefore, implying that the structural perception of events is a core feature of psychological processing. Taken together, these studies appear to show that the perception of coarse and fine-grain events follow a partonomic strucutre, and argue for an account of the human mind structuring internal representations of ongoing activity hierarchically.

1.4 The development of event segmentation

So far, this introductory chapter has discussed how the human mind might process ongoing activity, in terms of the structure imposed upon mental representations. Overall, there appears to be compelling evidence to support a theory of event segmentation in ongoing perception, and so this section aims to discuss the broader implications of event segmentation.

If, as suggested, event segmentation is an automatic process that plays a key role in the perception of ongoing activity, then one could expect to find evidence across all demographics. So far, we have seen evidence from studies typically performed on young, healthy adults, however complementary data do exist. For example, Wynn (1996) revealed that children are able to segment a continuous activity such as going to a birthday party into discrete events. This finding is supported by Nelson & Gruendel (1986), who demonstrated that infants knew the parts of common events (e.g. going to school). Additional studies also investigating narrative comprehension in 4-6-year olds, collectively indicate that infant's memory for activity reflects a hierarchical pattern of recall, and furthermore, is affected by activity goals (e.g., Hudson, 1988; van den Broek, Lorch, & Thurlow, 1996). The influence of internal representation structure and activity goals on memory for activity has also been observed in toddlers as young as 15 months (e.g., Bauer & Mandler, 1989; Travis, 1997).

How event segmentation plays a role in later life, was investigated as part of a memory and understanding study (Zacks, Speer, Vettel, & Jacoby, 2006). Here, participants that segmented movies of everyday activities were studied in three groups; young healthy adults, older healthy adults, and older adults diagnosed with mild dementia of the Alzheimer type. Agreement over event boundaries was found to be less reliable in older adults compared to younger adults, and less reliable still, for older adults diagnosed with mild dementia. Subsequent memory tests revealed that recall was poorer among older adults with poor event boundary agreement. Zacks et al. also indicate that impaired semantic knowledge for events was associated with memory deficits, and argue that semantic event knowledge guides encoding, which facilitates later memory.

In summary, the studies discussed in this section reinforce the view that event segmentation is an instinctive ability, which plays a role in ongoing perception. Moreover, they show that internally representing events in goal-orientated, partonomic structures is common through the age demographic. The affect of event segmentation for memory has also been seen across the studies in this section; better understanding of event knowledge structures is associated with better memory for events.

1.5 Influences on event segmentation

Much of the discussion thus far has concentrated on identifying a reliable strategy that accounts for the cognitive processing of ongoing activity. We have seen that partonomically structured cognitive schemas organised around goals and sub-goals, appear to reflect how the human mind represents events. Furthermore, the ability to use cognitive schemas appears to have implications for memory. However, we still do not know what the mechanisms are that drive event segmentation, i.e. what influences the identification of event segments. This section aims to discuss the possible cognitive drivers of event segmentation.

As previously discussed, events can be interpreted as exhibiting a partonomic, hierarchical structure, and the cognitive schemas that we employ to represent information appear to follow a similar partonomic structure. Much of the research discussed, investigates event segmentation using the paradigm set out by Newtson (1973), whereby movies of activities are segmented into large (coarse-grain) and small (fine-grain) chunks. These studies have shown that coarse-grain event boundaries are typically used to indicate the grouping of smaller, fine-grain events, which reflects the

hierarchical nature of event segmentation (e.g., Newtson & Engquist, 1976; Zacks & Tversky, 2001). Critically, this hierarchical structure of events and sub-events clearly shows the involvement of top-down knowledge, such as the goal of the task. For example, to brush our teeth, we can identify many sub-goals such as applying paste to the brush, and the temporal order of the sub-goals that must be completed to accomplish the overall goal. From this example, we can see that identifying the common parts of an activity clearly rely on the application of familiar event knowledge structures. Therefore, we can assume that top-down knowledge influences at least coarse-grain event segmentation.

To understand top-down influences, Newtson, Engquist, & Bois (1977) analysed the relationship between the movement of actors in movie stimuli, revealing that event boundary perceptions were influenced most by the pose of the actor. Supporting evidence suggests that the perception of event boundaries is influenced by the object features of a stimulus (Avrahami & Kareev, 1994). Furthering these qualitive studies, J.M. Zacks (2004) investigated the influence of movement and intentions to understand simple events quantatively. Based on the hypothesis that observers segment on-going activity into meaningful temporal parts, Zacks investigated the influence of top-down knowledge and bottom-up cues (e.g., the physical characteristics of the activity, or the cognitive representation of events, respectively). Using movies of simple animations, Zacks revealed that the movement features of the movie stimuli (e.g., acceleration and object relative position), could be used to predict where participants perceived event boundaries.

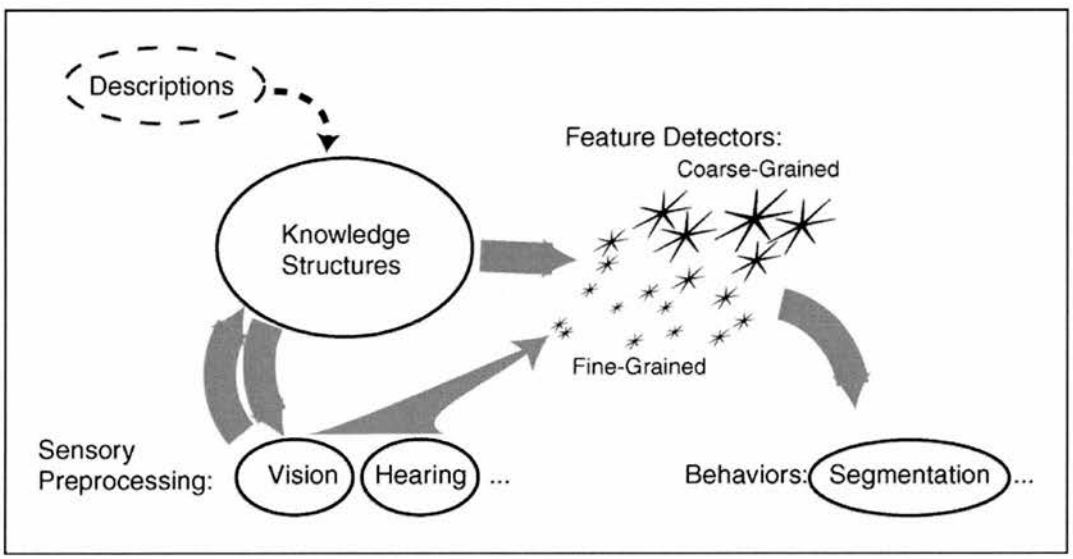

Figure 1-1: A model of the role of movement features in event segmentation. A bottom-up processing stream computes event segments from sensory characteristics, using feature detectors that vary in their temporal grain. This processing stream interacts bi-directionally with knowledge structures, which allow attributes such as actors' intentions to influence processing. Knowledge structures have their strongest effects on coarse-grained feature detectors. Dashed lines indicate that the mechanism by which explicit descriptions of the activities (i.e., the interpretation manipulations) are interpreted and active knowledge structures is outside the scope of the model. Adapted from Zacks (2004).

Given the evidence for top-down and bottom-up influences on event segmentation, Zacks proposed a conceptual model of event segmentation (Figure 1-1). The model illustrates how bottom-up features of an activity influence the perception of fine-grain, and to lesser extent coarse-grain event boundaries. Bottom-up features are also shown to interact with top-down knowledge, as familiar event knowledge structures are updated with features of the current activity. Top-down influences are described in the model as the existence of familiar knowledge structures, which affect the perception of coarse-grain events, and to lesser extent fine-grain events.

The evidence and conceptual model discussed in this section clearly indicate multiple sources that may influence the perception of an event.

However, from the studies described so far we can begin to understand how top-down knowledge and bottom-up features influence the segmentation of everyday activities into coarse and fine grain chunks. In particular, Zacks indicated that coarse-grain event perception would be influenced mostly (although not exclusively) by event knowledge structures. Furthermore, Zacks argued that bottom-up features of the activity such as movement and object position should have a greater influence on fine-grain when compared to coarse-grain event perception.

1.6 Implications of event segmentation for memory

Previously discussed studies have identified event segmentation as having implications for memory (e.g., Bauer & Mandler, 1989; Zacks, et al., 2006; Zacks & Tversky, 2001; Zacks et al., 2001). The perception of events is likely to rely upon the memories of similar event structures. However, during perception it is also likely that existing cognitive schema for an event is updated by unexpected events that occur and the goals and sub-goals of the event change. Therefore, it appears likely, and has been suggested that (Zacks, 2004), the flow of information between memory and the perceptual system is in a constant feedback loop. This section aims to discuss some of the evidence for an interaction between event perception and memory. First, we will consider the role of cognitive schemas in learning.

1.6.1 Event segmentation and learning

The influence that hierarchically organised events play in learning was investigated in a primate study (Byrne, 2002). Byrne demonstrated that the hierarchical features of a structure activity were key to learning a new task.

Similarly, Zacks & Tversky (2003) were able to demonstrate in humans that hierarchically structuring information aided learning, and the lack of a hierarchical structure hindered learning; top-down principles alone were insufficient when constructing an effective interface design to facilitate learning. Therefore, Zacks & Tversky argued that a combination of top-down and bottom-up influences best-aided learning. Humans have also been found to form segments, or "chunks", of semantic knowledge during learning (Gobet et al., 2001). Taken together, these studies appear to show that encoding structured activity in terms of their partonomic relationships, certainly aids, if not underpins, the human mind's ability to learn.

1.6.2 Event segmentation and working memory

The consequences of temporal event structure for memory have been demonstrated by varying the passage of events in text (e.g., Bower & Rinck, 2001; Glenberg & Kaschak, 1987; Morrow, Bower, & Greenspan, 1989; Rinck & Bower, 2000). These studies revealed that altering the temporal structure of events impedes retrieval, suggesting that in addition to the importance of hierarchical structuring to learning, temporal event structure also influences memory encoding.

Trabasso & van den Broek (1985), revealed the importance to memory of predictability in an activity; this study showed that events are recalled best when they feature the goals of individuals and the consequences of these goals. Finding goal-driven activities easier to recall is a view supported further by Abbott et al. (1985) and Graesser & Clark (1985).

The interaction between memory and event segmentation has also been researched in media studies. For example, Gernsbacher (1985) was able

to show that retrieval for images was greater if the images appeared in the same structural episode, suggesting that memories for sub-events are grouped partonomically. Similarly, a study conducted in Virtual Reality (VR), showed that memory for recently seen objects was reduced after passing through a doorway; an action which may be interpreted as a boundary between room orientated events (Radvansky & Copeland, 2006). The findings in these two studies have been further supported by Swallow, Zacks, & Abrams (2007), who argued that memory for objects was affected by the presence of a perceived event boundary. From the evidence discussed so far, it is clear that goal-directed partonomically structured event segmentation plays a role in the encoding and retrieval of both short-term and long-term memory.

1.6.3 Event segmentation and long-term memory

As with many fields of psychological research, neuro-imaging technology is used to isolate and identify neurological activation arising in response to a specific experimental tasks (e.g., Squire & Zola-Morgan, (1991) demonstrated that the hippocampus plays a key role in long-term memory). To investigate the role of event segmentation in long-term memory, Swallow, Zacks, & Abrams (2007) used a functional Magnetic Resonance Imaging (fMRI) scanner to measure brain activity during experimental trials. The authors revealed activation in the hippocampus, but only when participants attempted to recall objects prior to a recent boundary perception. Importantly, this finding suggests that memory for within-event objects is encoded to long-term memory at around event boundary perception, for cross-event retrieval.

Other studies have also investigated the influence of event boundary perception in memory. Pictures have been found to be better recalled at event boundaries rather than between event boundaries (Newtson & Engquist, 1976). Boltz (1992) found that memory for movies was better when interruptions (commercials) were placed at event boundaries. The effect of placing interruptions at event boundaries on memory suggests that memories are better encoded when an episode is judged complete, and consequently long-term memory is updated with working-memory. In a similar study, memory for movies was found to be better when deletions occurred within event boundaries (Schwan & Garsoffky, 2004), suggesting in agreement with Boltz, that event boundaries are critical for encoding memories. Taken together, the long-term memory experiments suggest that the most likely explanation for the influence of event boundary perception on memory is the transferral of working memory to long-term memory, occurring at the time a new event is perceived.

In summary, it is clear from the evidence presented thus far that event segmentation and the structuring of cognitive schema influence many aspects of memory. In particular, the hierarchical structure of representations are key in the encoding of memories when learning a new task. Furthermore, the perceiving of the beginning of a new event part, appears to act as an indicator as to what memories are grouped together and saved for long-term storage. Grouping memories may reflect the role of a partonomically structured cognitive schema, which mediates between retrieval and encoding functions during event perception.

1.7 Modelling event segmentation

Given the wealth and variety of evidence supporting a role for event segmentation in perception, some authors have proposed conceptual models which aim to capture the characteristics of event segmentation (e.g., Zacks, 2004). This section aims to discuss the most recent model refinement, called Event Segmentation Theory (EST), presented by Zacks et al. (2007).

1.7.1 Event Segmentation Theory (EST)

Zacks et al. argue that, in line with the evidence discussed throughout this chapter, perception can be described as a roughly hierarchical process in which ongoing activity is mapped to cognitive schema. Recollecting pre-existing event structures based upon a set of sensory cues facilitates prediction, which in evolutionary terms is a key skill (e.g., avoiding interception by predators and intercepting prey). It is further argued by Zacks et al., that event segmentation occurs as a side effect of trying to anticipate upcoming information. As part of their case for EST, Zacks et al. identified three key properties of perception; that it is hierarchical, recurrent and cyclical. We can consider these properties thus; firstly, perception may be regarded as a hierarchical process; sensory inputs present information that must be interpreted, a familiar event structure is then likely recalled, and finally, predictions are generated based upon the recalled schema. Secondly, it is likely that the later engagement of cognitive schema affect how early sensory information is interpreted, so forming a recurrent flow of information. Lastly, predictions are likely to be constantly compared with the 'here and now', which permits the perceptual system to accommodate correction of erroneous predictions. Error corrected cognitive schema may

then be used to compare against sensory information, thus forming a cyclic perceptual pattern.

As pointed out by Zacks et al., these three notions - hierarchy, recurrence, and cyclicality - are working assumptions in many different theories of perception (Neisser, 1967), neurophysiology (Carpenter & Grossberg, 2003; Fuster, 1991), and language processing (van Dijk & Kintsch, 1983). Furthermore, a number of authors have developed recurrent neural network models based upon these three properties. For example, in applications of word learning (Elman, 1990), action learning (Jordan & Rumelhart, 1992), and event perception (Hanson & Hanson, 1996). EST shares these three properties, and is illustrated in Figure 1-2.

EST proposes that our instinct to predict upcoming events is core to perception, and this gives rise to the theory that event segmentation is a side effect of perceptual prediction. Specifically, the model states that when features of the ongoing activity change, prediction becomes more difficult and errors in prediction increase transiently. In addition to the previously discussed evidence for memory updating at event boundaries (e.g., Speer, Zacks, & Reynolds, 2007), EST suggests that people update memory representations when errors in prediction are detected. Perceiving a transient increase in error and consequently updating memory, may reflect subjective experience that a new event has begun (Kurby & Zacks, 2008). In summary, the authors argue that perception is guided by cognitive-schema-based prediction and that unexpected changes in ongoing activity, serve as a cue for the perception of an event boundary. During the perception of a new event, the cognitive schema is updated thus improving future predictions.

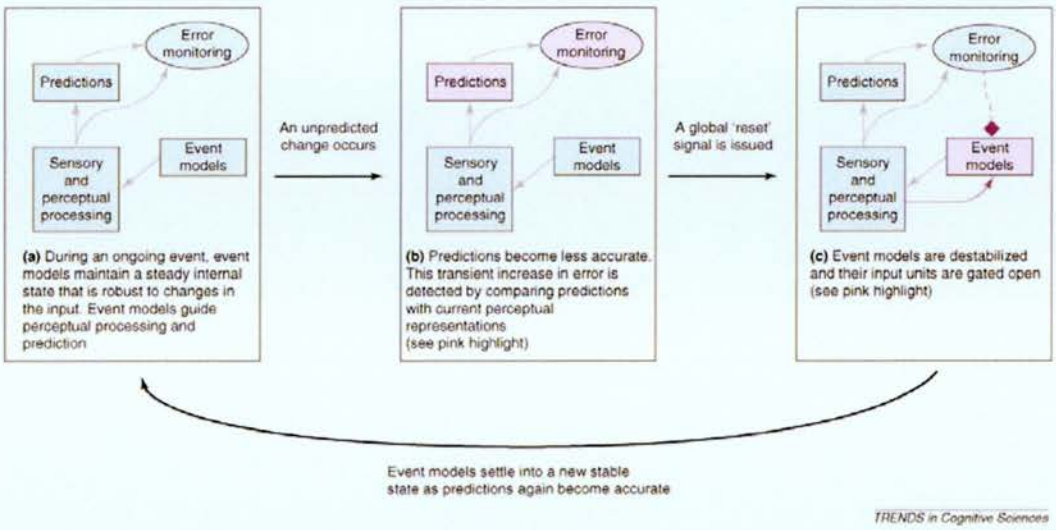

Figure 1-2: A schematic depiction of how event segmentation emerges from perceptual prediction and the updating of event models. (a) Most of the time, sensory and perceptual processing leads to accurate predictions, guided by event models that maintain a stable representation of the current event. Event models are robust to moment-to-moment fluctuations in the perceptual input. (b) When an unexpected change occurs, prediction error increases and this is detected by error monitoring processes. (c) The error signal is broadcast throughout the brain. The states of event models are reset based on the current sensory and perceptual information available; this transient processing is an event boundary. Prediction error then decreases and the event models settle into a new stable state. Adapted from Kurby & Zacks (2008).

EST encapsulates a body of evidence that implicates event segmentation as a key component of perception. The model also adequately accounts for theories discussed in this chapter (e.g., hierarchically structured perception that is influenced by top-down knowledge and bottom-up features), and is implicated in memory function. Furthermore, the model adheres to commonly regarded key principles of perception, and provides insight into the perception of events (e.g. the importance of prediction to event segmentation). In conclusion, EST may be regarded as a robust theory of perception.

1.8 Summary

This chapter has discussed how the human mind processes ongoing activity. A number of factors have become clear due to the compelling evidence supporting a theory of event segmentation. Perception in itself can be regarded as hierarchical due to the various layers of cognitive function between sensing our environment and deciding how to react. Moreover, the structure of events and the cognitive schema that we use to represent activity appear to exhibit a partonomic structure. There is a large amount of evidence to support the notion that we process event boundaries, and we have seen evidence to implicate the perceptual cues that drive event segmentation, e.g. top-down knowledge, bottom-up characteristics, and errors in prediction. Investigating the perception of events has also revealed the interdependency between perception and memory, served by hierarchically structured cognitive schema that are organised around goals and sub-goals. The role of hierarchically structured event segmentation in perception has been shown to be key in the encoding, retrieval, and continual updating of cognitive schema. We have also seen evidence to suggest that event segmentation is a core skill that is with us throughout our development.

The evidence discussed in this chapter has allowed an understanding of how the perceptual system might operate. However, a number of fundamental issues remain unanswered. Hierarchical structures have been identified as a common feature across perception, however, whether or not this is a *requirement* of perception and learning remains unclear. Similarly, interdependences between event segmentation and memory have been identified, but the implications of processing unfamiliar events have not been fully explored. Some behavioural data do exist that suggest unfamiliar activities are segmented into smaller parts (Hard, Tversky, & Lang, 2006), but

this effect is not robust (Zacks, Tversky, et al., 2001). Based upon the evidence discussed in this chapter we could conclude that processing unfamiliar activity would increase cognitive load, due to prediction correction, however this requires clarification. Nonetheless, both top-down knowledge, such as activity goals, and bottom-up features, such as the physical correlates of ongoing activity, have been shown to influence the perception of an event. Zacks (2004) revealed how bottom-up features influence the perception of abstract activities, but how this differs from the perception of everyday activities is not clear. Lastly, much of the research investigating event segmentation follows the paradigm used by Newtson (1973), however as this paradigm assumes that by marking event breakpoints, one event or sub-event ends just as another begins. Whether or not this reflects a psychological reality, gives rise to questions such as "how does the perceptual system process events that do not occur in quick succession", and "do gaps between events provide the perceptual system a chance to update (reset the cognitive schema)"?

Collectively, the studies support an account of event segmentation as an automatic process that has implications for perception, learning and memory, and raise a number of interesting challenges for future studies. The following chapter aims to discuss how the psychological questions raised in this chapter can be address with neuroimaging.

2 Event-related potentials

2.1 Introduction

Electroencephalography (EEG) is the measurement of the human brain's response to an event, expressed as variations in voltage plotted against time. Voltage variations are recorded by attaching a pair of electrodes to the surface of the human scalp, connected to a differential amplifier. The amplitudes of normal EEG traces vary between -100 and +100 μV and the frequency ranges to 40Hz. EEG, defined such that it is time locked to the presentation of a stimulus or behavioural response, is called an epoch. Time-locking EEG responses to different stimuli facilitate the comparison of voltage amplitudes for different experimental conditions. Significant changes in EEG activity specifically related to the brain's response to a stimulus, collated over many trials, constitute an Event-Related Potential (ERP).

Hans Berger (1929) first demonstrated that electrical fields generated by the brain could be measured at the scalp. Evidence collected by Berger revealed that the electrical activity reflects the current mental states of a participant, and suggested that further analysis may reveal ongoing cognitive processes. And since Berger first published his findings, the use of EEG in cognitive psychology has indeed revealed insights into cognitive functions such as memory, perception and language.

EEG recordings actually reveal little about participant's ongoing mental processes in their raw form, as they represent the sum of all measurable activity generated by the brain plotted against time. As raw EEG recordings are continuous waveforms reflecting only small voltage fluctuations (-100 to 100 microvolts or μV), the data must be processed in order to extract the signal from the background EEG. Typically, epochs are

formed time-locked to a set of events, then averaged together to reveal the signal of interest.

This chapter will introduce ERPs and their neural sources. Additionally, ERPs will be discussed in terms of the processing required to form them, the analysis techniques used to asses them and the inferences that may be drawn from them. The aim is to examine the methodological issues related to ERP-based research.

2.2 The Neural Origin of ERPs

ERPs reflect electrical activity from the brain; however, the precise relationship between the underlying brain activity and ERPs is not well understood. Nonetheless, it is widely believed that net electrical fields produced by sizeable populations of neurons constitute the source of the electrical potentials measurable at the scalp. This section aims to describe the generation of these post-synaptic potentials and their relation to the activity measured at the scalp.

2.2.1 Electrogenesis

Neurons pass information to one another via chemical processes and electrical signals called action potentials. An action potential is provoked if the neuron's membrane (as shown in Figure 2-1) is depolarised sufficiently. At rest, the voltage across the axonal membrane is typically -70 millivolts (mV), and this is regulated by the different concentrations of ions inside and outside of the cell, which is referred to as the concentration gradient. A neuron's stable-state, or resting membrane potential, reflects equilibrium in the concentration gradient. Specifically, ionic equilibrium potential occurs

when the electrical force of the neuron is equal to that of the diffusion force produced by the ion gradients.

Depolarisation occurs as a result of an action potential in an adjacent cell initiating the release of neurotransmitter. Receptors on connecting neurons bind with the released neurotransmitter, and this in turn causes voltage-sensitive ion channels on the neuronal membrane to either open (have an excitatory effect), or close (have an inhibitory effect). If the ion channels are opened electrically charged sodium ions [Na+] flow into the neuron, and potassium ions [K+] flow out. The flow of ions facilitates further depolarisation by allowing current to flow into the axon and this process causes the membrane to 'fire'. The neuron now enters a positive feedback loop which causes the neuron's voltage to rise rapidly before returning to its resting state. If depolarisation is sufficient to initiate the positive feedback loop, a neuron will fire; such neurons may be described as 'all-or-none'. Neurons actually overshoot both the threshold value required to create an action potential (hyper-polarisation), and the resting membrane potential (hyper-depolarisation).

After firing, voltage sensitive channels open which allow the flow of current out of the cell. Furthermore, the ion channels now allow the sodium ions to flow out of the cell and potassium ions to flow back in. These processes facilitate the restoration of the membrane potential to the initial resting state. The time taken for the neuron to return to the resting membrane potential is known as the refractory period.

As the action potential propagates through the cell dendrites, it travels rapidly down the axon and this movement is regulated by the opening and closing of voltage sensitive ion channels. After travelling down the axon, the action potential will reach the end of the axon (the axon terminal), at which

point its presence initiates the secretion of neurotransmitters. The junction at which connecting neurons meet is called the synapse, and the gap between the pre-synaptic axon terminal and the post-synaptic dendritic spine is known as the synaptic cleft. Neurotransmitters released into the synaptic cleft bind with receptors on the post-synaptic neuron at which point if the neuron is excitatory, the process of action potential generation is repeated.

Changes in the membrane potential of the post-synaptic terminal of the synapse are referred to as postsynaptic potentials. In contrast to action potentials, which maintain their voltage as they travel along the neuronal axon, postsynaptic potentials are graded as their magnitude decays over distance travelled. Due to signal degradation of graded potentials, their presence may not necessarily initiate sufficient depolarisation in the neuron that would cause it to 'fire'.

Biophysical and neurophysical studies suggest that the net electrical fields produced by neurons which are measurable at the scalp, principally reflect post-synaptic activity. In particular, Lorente de Nó (1947a) used single cell recordings of action potentials in peripheral nerves to demonstrate that, as activation moves along an axon, an electrode recording extracellular potential will produce a triphasic waveform. Lorente de Nó's research illustrated that the potentials from different neurons summate at all locations in extracellular space, which is known as the principle of superposition. The principle of superposition states that temporally synchronous potentials, with similar firing latencies and that share the same polarity, will summate to produce large amplitude potentials that can be recorded at a considerable distance from the nerve cell (i.e. the scalp). A second type of extracellular potential, also identified by Lorente de Nó, is associated with graded post-synaptic potentials in the soma (the cell body) and the dendrites of the nerve

cell (Figure 2-1). Graded post-synaptic potentials can be either excitatory (Excitatory Post-Synaptic Potentials, or EPSPs) which produce a similar pattern of extracellular potentials, or inhibitory (Inhibitory Post-Synaptic Potentials, or IPSPs) which cause the polarity to be reversed. Knight (2003) concluded that the majority of scalp recorded EEG is due to the summation of post-synaptic potentials, and action potentials play a minor role.

Synchronously firing neuron populations with specific geometric configurations have been shown to produce measurable fields. A dipolar field reflects the summation of neuron configurations that yield individual fields of electrical activity. 'Open field' configurations are neuron populations aligned in a parallel orientation, in relation to the scalp. Neuron populations arranged in an open field configuration produce synchronous depolarisation at the somas and this produces individual potential fields orientated in the same direction. The summation of activity produced by neurons aligned in an open field configuration (Figure 2-2) may be detected at some distance (Lorenete de Nó, 1947b).

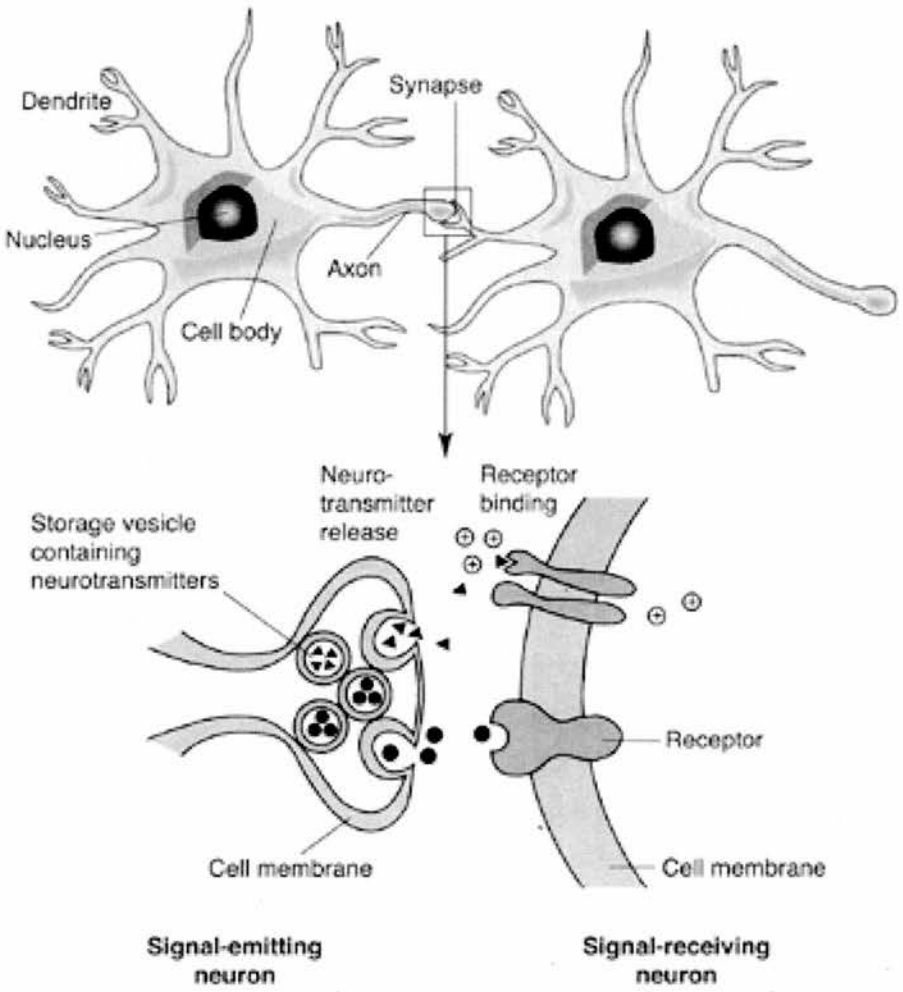

Figure 2-1: The structure of a typical neuron which comprises dendrites, a cell body (soma) and an axon. Action potentials propagate along the axon via a wave of depolarisation resulting from ion flow across the membrane. Information passes between connecting neurons at synapses. The arrival of an action potential at the synapse causes release of neurotransmitters from the pre-synaptic cells which bind to receptors in the postsynaptic cells. This causes opening or closing of ion channels, leading to voltage change in the post-synaptic membrane which results in (excitatory or inhibitory) postsynaptic potentials. Adapted from www.niaaa.nih.gov/Resources/GraphicsGallery/Neuroscience/synapse.htm

The limited ability to detect neuronal processes brings consequences for the interpretation of recorded data, as much of the activity of the brain may never be detected at the scalp. Neuron populations must have an open

field configuration, and fire synchronously, to produce a measurable field. Of course, one advantage of the partial volume of the scalp is that too much information may become too complex and undecipherable. By contrast, however, too little information limits detection possibilities, so rendering numerous functional neuronal processes undetectable.

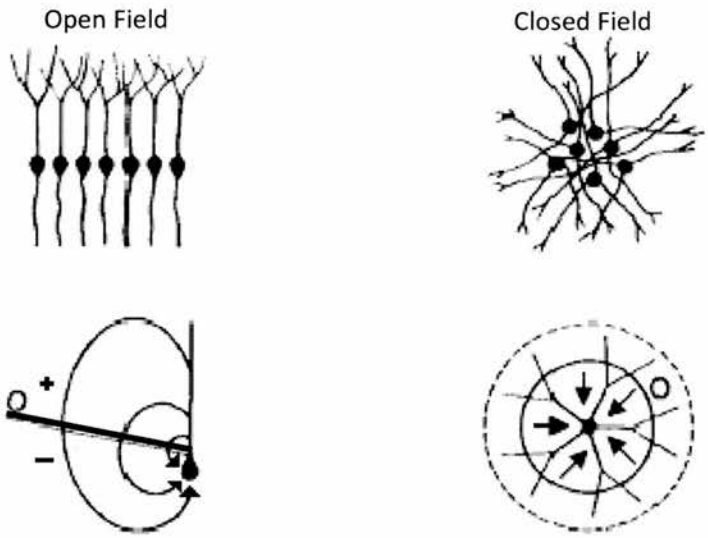

Figure 2-2: Predicted current flow and potential field produced by synchronous depolarisation of the cell bodies of a row of neurons with parallel orientation (open field), and a group with cell bodies clustered in the centre and dendrites spreading radially (closed field). Adapted from Allison et al. (1986).

2.2.2 Volume Conduction

The previous section discussed the generation of neural activity which is detectable at the scalp. More specifically, scalp-recorded EEG reflects the post-synaptic activity of sizeable populations of neurons that fire synchronously and are aligned in a specific configuration as to allow their activity to be recorded at the scalp. In fact, the electrical activity generated by

neuronal sources propagates to the scalp because the skull and scalp act as volume conductors.

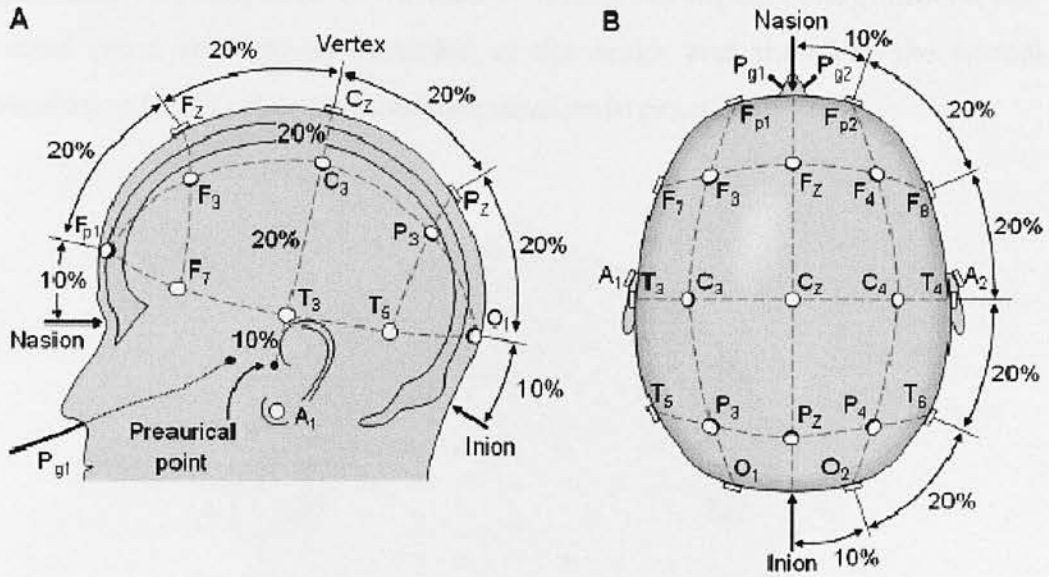

Figure 2-3: The International 10-20 system for electrode placement seen from (A) left and (B) above the head. The reference points refer to the following: A = ear lobe, C = central, Pg = nasopharyngeal, T = temporal, P = parietal, F = frontal, Fp = frontal polar, O = occipital. Adapted from Jasper (1958).

However, the low conductivity of the skull attenuates the signal, and this causes lateral spreading which masks the signal of interest. Differences between the size and shape of subject's skulls mean that identification of the source activity reflected by an ERP are difficult. The problem of source localisation is known as the inverse problem and this is the main factor that contributes to the low spatial resolution EEG has to offer. Existing techniques which attempt to circumvent the inverse problem, such as Principal and Independent Component Analysis (PCA and ICA respectively) produce mathematical based estimates as to the likely source of activity reflected in

ERP data. The use of PCA and ICA can only provide an estimate as to the source of the activity, and therefore the putative relationship between neural generators and scalp recorded activity is still weak. This weak relationship is primarily a consequence of the infinite number of dipole configurations that could cause the activity recorded at the scalp, and therefore the spatial resolution of EEG data remains intermediate in practice.

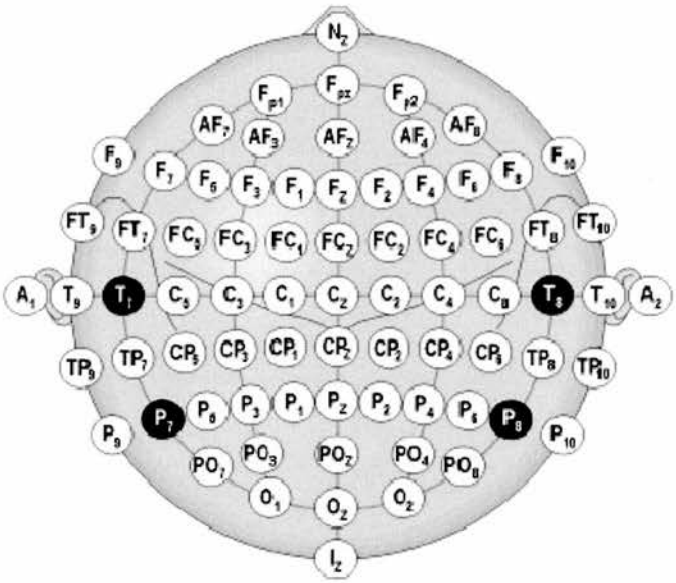

Figure 2-4: The Extended International 10-20 system for electrode placement, standardised by the American Electroencephalographic Society. Adapted from American Electroencephalographic Society (1994).

Despite the poor spatial resolution EEG has to offer, the main advantage of using this technique as a means of neuro-imaging remains its fine temporal resolution. The electrical activity generated by the brain which propagates to the scalp can be sampled at intervals n the range of milliseconds using EEG. The high sampling rate capabilities can capture

voltage changes which reflect almost instantaneous brain function, and this granularity allows researchers to examine cognitive operations precisely.

2.3 Recording ERPs

2.3.1 Active Electrodes

EEG records neuro-electric activity by measuring the resulting voltage present at the scalp. Voltage is the difference in electrical potential at two points and as such at least two electrodes are required: an active electrode (EA) and a reference electrode (ER). Electrodes placed on the scalp record not just the 'signal' of interest but also background activity, known as 'noise'. To eliminate noise from the recordings a ground electrode (EG) is also used so that the difference between the background activity and the activity recorded at the scalp can be measured and subtracted. Differential amplifiers are used to amplify the electrical signals before the difference in voltage at pairs of electrodes is calculated, as follows: (EA-EG) minus (ER-EG). Thus, contributions from the ground electrode which are assumed to be background environmental electrical activity are eliminated from the data by subtraction, leaving only contributions from the active electrode (relative to the reference electrode).

As voltage waveforms may vary in their morphology (amplitude, latency and polarity) many active electrodes are employed in order to characterise the scalp distribution of the activity recorded. Employing a montage of electrodes allows voltage waveforms to be differentiated on the basis of their distribution, and eye movement artefacts more readily observed (Picton et al., 2000). Scalp electrodes are usually arranged based

upon the International 10-20 system (Jasper, 1958). The International 10-20 system dictates that 21 electrodes are placed on the scalp according to the features of the skull, i.e. the nasion, inion and the left and right pre-auricular points (Figure 2-3). Using the features of the skull to constrain electrode placement allows the montage to define lines of latitude and longitude upon which electrodes can be placed at regular intervals. It is important to note however that the system assumes that head is symmetrical and as previously discussed this is typically not the case in practice. The International 10-20 system was extended by the American Electroencephalographic Society (American Electroencephalographic Society 1994) facilitating the placement of a greater number of electrodes. Note that this thesis employs the extended montage system for electrode placement.

2.3.2 Reference Electrodes

The adoption of an internationally recognised system by researchers using EEG underlines the importance of electrode placement. Nevertheless, it cannot be assumed that the activity recorded at electrode sites reflects a neural generator located directly below the electrode site. The principles of volume conduction and supersistion mean that the post-synaptic activity generated by active neurons may feasibly summate at every point on the scalp (Allison et al., 1986). Consequently, the activity recorded at the scalp may have been generated from a distant source, not necessarily in close proximity to the electrode site where the activity has been recorded. Consideration should also be given to the fact that the measured activity reflects a relative difference in voltage between the active and reference electrodes, thus the activity at the reference site will contribute equally to all active electrodes.

Researchers using EEG normally use a reference electrode that is common to all active electrodes. Employing a common reference electrode allows an equal contribution to be made to all active electrode sites, and therefore voltage differences between the active electrodes will remain informative (Dien, 1998). In practice, two reference electrodes are typically used in order to avoid inducing a hemispheric bias, which could occur if only a single reference electrode was placed on one side of the skull. In practice, most ERP researchers place one reference electrode behind the left ear and one behind the right. Activity is then recorded from both reference electrodes and averaged together to yield a 'virtual' reference electrode. (Miller et al., 1991). One alternative method of referencing EEG data averages all active electrodes, and assuming that all activity it recorded evenly approximates reference activity to zero (Picton et al., 1994). Note that the data presented in this thesis are recorded using Miller's technique of linked mastoid references, whose activity is averaged, thus producing a virtual reference electrode.

2.3.3 Analogue-digital (A/D) conversion

In order to facilitate the processing and analysis of EEG data, the small voltages recorded by the scalp electrodes are amplified and digitised, with data sampling occurring every 5ms (200Hz) for example. Furthermore, after the signal is amplified it is passed through two filters; firstly high-pass filters to attenuate high frequencies and secondly low-pass filters to attenuate low frequencies. It is important to note however, that digitising an analogue signal that contains high frequencies at a low sampling rate, can produce spurious low frequencies in the data. However, the Nyquist Theorem states that aliasing is eliminated when the sampling rate is at least twice the highest frequency present in the analogue signal (Luck, 2005).

2.4 Extracting the signal from the noise

Filtering of EEG data attenuates low and high frequencies present in the signal, however the data are still contaminated with artefacts such as muscle activity and eye blinks. Therefore the ERP must be extracted from the background noise in order to isolate the signal of interest. This section will discuss the steps that may be taken in order to reduce background noise.

2.4.1 Ocular artefact reduction

The majority of background noise may be attributed to artefacts generated by ocular activity. To facilitate the removal ocular based artefacts, eye blinking and movement is recorded by the electrooculogram or EOG. Specifically, the EOG measures the relatively large differences in electrical potential (millivolts as compared to brain activity in microvolts) by placing electrodes above and below one eye (vertical EOG, or VEOG) and on the outer canthi to the left and right of the eyes (horizontal EOG, or HEOG). The VEOG is used primarily to measure eye blinks, and the HEOG to measure eye movement; both actions dominate activity recorded over frontal and inferior electrode sites.

Eye movement and eye blinks propagate throughout the scalp as electrical frequencies. Frequency propagation occurs because the eyeball functions like an electrical dipole, with positive and negative charge on either side. Minimising eye related artefacts require practical steps to be taken, such as asking the participant to focus on a particular point during trials, and blinking only at designated points during an experiment.

Imposing constraints on the participant, may however add a level of complexity to captured data, as the participant will concentrate on following the constraints. Alternatively, all epochs including artefacts of this nature may be disregarded, thus eliminating the problem of contamination during processing. Elimination of eye blink and other artefact-infected epochs however, may also lead to the elimination of a significant amount of data from the entire experiment. Epoch elimination may not be desirable if it leaves an insufficient number of epochs available for analysis. Furthermore, substantially reducing the data set may ultimately result in data which is unrepresentative of the complete data set (Gratton, 1998).

Modern approaches to the problem of artefact removal rely on estimating the contribution of eye related artefacts, and subtracting this contribution from the data set. Subtracting eye blink contributions is an advantageous approach as it allows a far greater number of trials to be included in the data set for analysis. Due to the superior trial retention rate, it is assumed that this method is more representative of data set than when simply rejecting trials in which ocular movement occurs. Nevertheless, it is important to consider that if ERP effects are observed over fronto-polar electrodes close to the eyes, this reduction method may contaminate the perceived signal.

2.4.2 Averaging

As discussed, ocular artefact reduction seeks to remove the effect of unwanted eye movements from EEG data. However, the EEG still includes background noise such as concurrent mental processes, muscle activity, etc., and this renders the ERP signal weak by comparison. Data averaging is a popular technique used to extracting ERP signals from EEG samples.

Typically, epochs of EEG data are formed relative to a stimulus onset or event. Once formed, epochs containing responses to corresponding events are averaged together to produce an ERP which reflects a particular event (Coles & Rugg, 1995).

It is important to note that four assumptions underlie averaging (Glaser & Ruchkin, 1976; Spencer, 2005): it is firstly assumed that the signal and noise sum linearly to produce the recorded waveform; secondly, that the signal waveform is the same for each corresponding event; thirdly, that the noise is sufficiently irregular from event to event to be considered as statistically independent samples of a random process; and lastly, that the noise is stationary (i.e. the means and variance of each sample are similar). If all four assumptions are met, then the square root rule of averaging, which states that reduction of noise is directly proportional to the root mean square of the noise and inversely proportional to the square root of the number of samples, will apply (Perry, 1966).

In particular, the fourth assumption of averaging states that noise is stationary, which is not usually the case. For example, during testing participant's muscle activity is likely to contribute to the EEG signal differentially over time. Additionally, the second assumption requires that the signal is the equivalent over all trials. However participant fatigue, boredom and attention lapses all tend to produce ERP voltage fluctuations as the recording session progresses (Ruchkin, 1988). In fact, the signal may even be absent from some trials (e.g., as a result of guessing in a memory experiment).

Additionally, it is important to consider that ERP waveform may be distorted by variations in the onset of a signal (jitter). As the trials of subjects are averaged together to form an ERP, jitter can cause the amplitude to be

spread over time, thus reducing the signal-to-noise ratio. Steps may be taken to minimise the effect of jitter, such as excluding participants if they fail to contribute a sufficient number of trials to individual participant ERPs. To maximise the signal-to-noise ratio, this thesis only includes data from participants who produced a minimum of 16 artefact free trials for each condition.

2.5 Drawing Inferences from ERPs

The foregoing section described the processing steps that must be taken in order to extract the ERP signal from background EEG noise. Averaging across participants for each condition yields grand average waveforms which are used as a basis for interpretation. The following section discusses the inferences that may be drawn from grand average ERP data about the underlying cognitive processes the ERP reflects.

2.5.1 Components

The morphology of an ERP waveform may include both positive and negative peaks in amplitude, which are plotted over time, and measured relative to a baseline (Figure 2-5, A). Baselines are usually defined as the mean voltage level for a time period preceding the ERP (usually 200ms). However, in some instances pre-stimulus activity may also be of interest, and therefore, alternative baseline methods may be employed e.g., the entire epoch interval may be averaged to yield a mean voltage, to which the positive and negative peaks are plotted relative to. Note that the data presented in this thesis are baseline corrected using the entire interval method.

Importantly, it is not possible to infer cognitive processes purely from waveform morphology, as ERPs represent the summation of all electrical activity recorded at the scalp. As stated by the principles of volume conduction and superposition, separate and unidentifiable regions of the brain may form the ERP, known as the problem of component overlap (Coles & Rugg, 1995, p8). To resolve the problem of component overlap, components of interest are defined as the difference between two separate experimental conditions. Defining a component according to this functional approach, means that understanding of the ERP is solely based upon its relationship with experimental variables. Subtracting ERPs elicited by two different conditions isolates the component of interest, which is assumed to reflect the cognitive process underlying the experimental manipulation.

The method of subtraction is predicated on two assumptions which are important to consider. The first assumption states that the latency of the equivalent component in separate conditions must be identical. A difference in component latencies across conditions would produce separate peaks in the subtraction waveforms, suggesting that the underlying functions differed qualitatively (Coles & Rugg, 1995). The second assumption, which underpins all subtraction methodology, is known as the pure insertion principle (Donders, 1968). The pure insertion principle states that cognitive functions are additive and act independently of each other (Sternberg, 1969; 2001), however, cognitive functions are often not additive (Friston et al., 1996; Price & Friston, 1997). By definition, the two conditions being subtracted will also most likely have several shared components, but it is important to note that these components will be affected by the presence of additional components. Therefore, a subtraction component represents the interaction between shared components and additional components which are not shared across

conditions. The likelihood of detecting components that are not shared across conditions implies that the principle of pure insertion is not strictly adhered to in electrophysiology. However, this problem is not unique to ERP data, for instance, comparisons of behavioural measures between two conditions also depend on the principle of pure insertion. Notwithstanding concerns about it, this thesis uses the subtraction method, and as such, experiments are designed with this in mind.

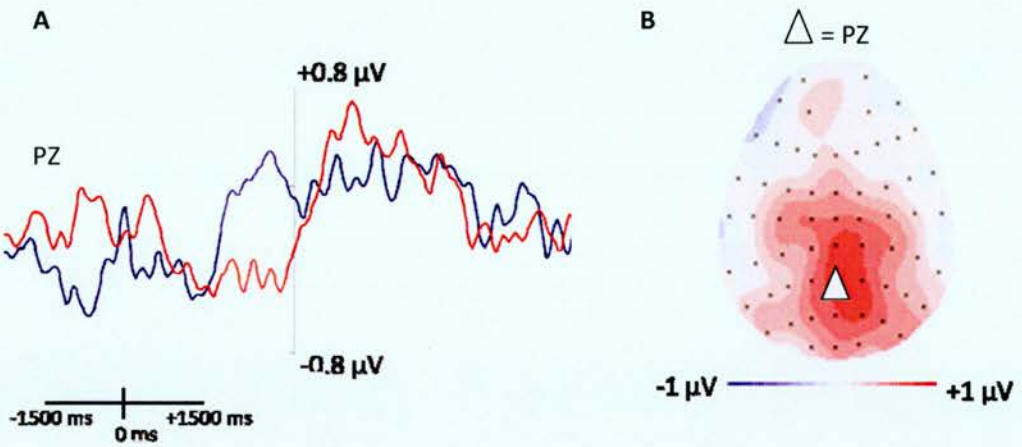

Figure 2-5: Two examples of ERPs. Panel A represents the Grand average ERP waveforms from two different conditions: one shown in blue, the other shown in red. 0ms marks the event breakpoint, the duration of the epoch is approximately 3000 ms, and positivity is plotted upwards. The time window selected for analysis captures a diverge in the waveforms from around -300 ms pre-event breakpoint. B depict topographic map of the difference voltage between two conditions (as shown on the scale bar below the figure). The map represents a birds-eye view of the head, with anterior sites towards the top of the page. The dots represent the electrode positions, the difference voltages in the intervening areas are estimated using a spline interpolation technique (Perrin et al., 1987; 1989). Data from Sharp et al. (2007).

2.5.2 Inferences from amplitude and temporal differences

In order to draw inferences from ERPs, data are quantified to reveal effects between conditions (Figure 2-5, A). The ERPs from two separate conditions may vary in magnitude, and if this is found to be the case, it can be inferred that the underlying cognitive processes responsible for the activity are differentially engaged. It is important to consider however, that differences found between the conditions only provide an upper-bound estimate of the time it takes the brain to differentiate between the two conditions. As such, earlier differences may have been present in brain regions, but the signal may not have propagated to the scalp (Rugg & Coles, 1995; Otten & Rugg, 2005).

In practice, ERP researchers are able to infer differences between cognitive operations if the resultant activity from one condition elicits a greater response than the other. Variances in the magnitude of ERPs may be quantified by employing inferential statistical models i.e. ANOVA (ANalysis Of VAriance), which allow the assessment of the reliability of magnitude variances. Once reliable differences between conditions have been identified, the distribution of the effects is assessed by submitting the ERP data for qualification. Reliable differences in the magnitude and qualitive differences in the distribution of ERPs, lead to the conclusion that different cognitive processes are in operation.

2.5.3 Inferences from topographic differences

As discussed in the previous section, ERP researchers infer differences in cognitive operations based upon quantitative magnitude differences and qualitive distribution differences. However, due to the inability to reliably

detect the sources of activity in EEG data (the inverse problem), qualitive differences fail to account for the neural generators responsible for topographic distributions (Figure 2-5, B). Nevertheless, qualitive differences do clearly imply the presence of components that are not shared across conditions and therefore that differential cognitive operations are engaged.

As with magnitude analysis, inferential statistics may be used to analyse differences in the distribution of ERPs. However, the use of inferential statistical models to analyse ERP data poses a problem; the ANOVA model is additive while ERP data are multiplicative (McCarthy & Wood, 1985). For ERP data to be additive, a neural generator would have to have an equal effect on all electrodes. This is not the case, as a generator may lie in closer proximity to one electrode than another, and its dipole projection may, therefore, affect one area of electrodes and not another. ANOVA interprets data as qualitative rather than quantitative and this could result in spurious interactions. To solve the problem, ERP data are normalised, which eliminates amplitude differences between conditions. The normalisation procedure preserves the relative pattern of difference across electrodes whilst reducing the likelihood of Type 1 error in terms of qualitive differences.

The applicability of data normalisation however, is a topic of debate in the ERP community. Opponents to the normalisation process, (e.g., Haig et al., 1997; Urbach & Kutas, 2002) argue that it fails to consider differences in variance between conditions, and therefore obscures genuine differences (maximum/minimum method), or produces spurious differences (vector method). However, proponents (such as Ruchkin et al., 1999; Wilding, 2006), argue that normalising ERP data should occur prior to topographic analysis, and that significant results should only be interpreted as confirming the presence of a distributional differences between conditions. The nature of the

distributional differences should then be inferred from the observed pattern in the quantitative analysis of ERP data. Applying the proponent's arguments may produce conservative results, but despite this, normalising ERP data so that distributional differences may be statistically analysed is a useful method. As such, the data presented in this thesis are normalised prior to topographic analysis using the maximum/minimum method of McCarthy & Wood (1985).

2.6 Summary

The precise nature of the relationship between cognitive operations and ERP components remains unclear. However, assuming a one-to-one mapping allows meaningful inferences to be drawn about cognitive operations. Currently, the methods outlined in this dissertation section, combined with sound psychologically meaningful and well defined experiments, can provide useful real information about the way brain systems support complex cognitive processes such as those involved in event segmentation. Having described how ERPs are used to study cognitive operations generally, the following chapter will describe how ERPs can be used to investigate the phenomenon of event segmentation.

3 The neural correlates of event segmentation

The previous chapters have discussed the role of event segmentation in perception, and how neural activity may be measured with EEG to answer psychological questions. This chapter aims to summarise existing neuroimaging evidence related to event segmentation, and discuss the use of ERPs in investigating event segmentation.

3.1 Investigating the neural correlates of event segmentation

In addition to behavioural evidence supporting an account of event segmentation, and neurophysiological evidence indicating the role of the hippocampus in event segmentation, a number of studies have investigated the neural correlates of event segmentation.

Perhaps the most influential neuroimaging study of event segmentation was conducted by Zacks et al. (2001). In their study, participants were asked to segment movies of everyday activities in accordance with the paradigm used by Newtson (1973). However, Zacks et al. extended this paradigm by recording neural activity in an fMRI scanner while participants viewed and segmented the movies. Crucially, participants first viewed the movies passively (e.g. without any knowledge of the experimental task), before actively segmenting the movies by pressing a button during subsequent viewings. From this data, Zacks et al. extracted the timings of perceived event boundaries, and overlaid these points onto the neural data recorded during passive viewing. Overlaying the event boundaries onto the passive data, allowed neural activity to be time-locked to perceived event boundaries when no explicit task was inferred. Measuring

neural responses to the perception of event boundaries during passive viewing is a critical manipulation of the Newtson paradigm, not least because it should better reflect ongoing perception as part of everyday life. In accordance with the Newtson paradigm, participants were required to segment movies of everyday activities into large (coarse-grain) and small (fine-grain) chunks, during subsequent viewings.

The fMRI study revealed a network of regions within the brain that were perpetually tuned to salient event boundaries. Neural responses were recorded from similar brain regions during both active and passive viewings, which implies that event segmentation is an automatic cognitive process active during everyday perception. Furthermore, neural responses that were aligned to the perception of coarse-grained event boundaries were found to be greater than those aligned to fine-grained event boundaries. Neural responses to the perception of coarse and fine-grain event boundaries are illustrated in Figure 3-1.

The authors argue that greater responses to coarse-grained events reflect the hierarchical nature of perception; a theory that aligns with interpretations of behavioural data (e.g., Newtson 1973; Zacks and Tversky 2001). As discussed previously, perception may be interpreted as a cascade of cognitive processes; from low-level sensory interpretation and the retrieval of an appropriate cognitive schema, to high-level prediction generation that forms the basis of anticipation. If, as suggested, perceptions of coarse-grain event boundaries reflect a psychological grouping of fine-grain events, the greater responses reported by Zacks et al. may reflect up-stream cognitive functions, such as event structuring and prediction re-alignment. Activation of similar neural networks during coarse and fine-grain event boundary perception may reflect the continual assessment of our environment, while

the differences in response strength suggest the involvement of differential cognitive functions, as previously suggested.

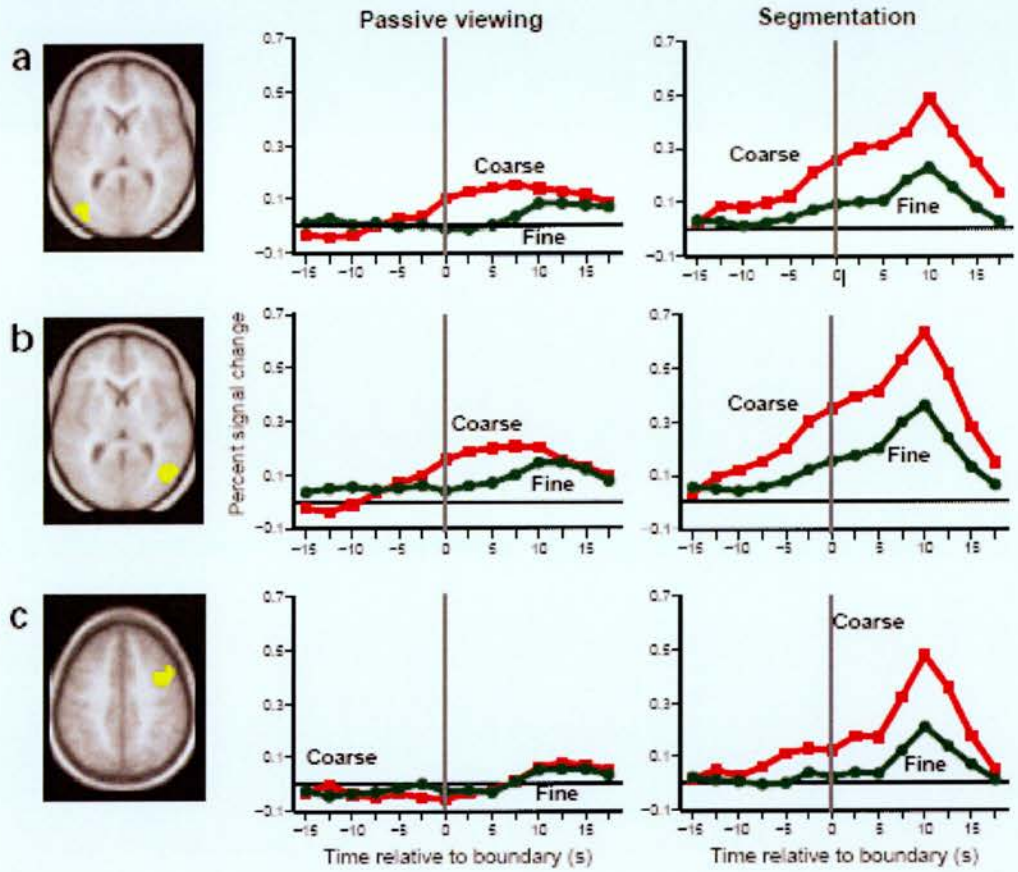

Figure 3-1: Time courses of focal brain activity in a subset of actived locations. Data from the strongest left posterior focus (cluster 2, Talairach coordinates –37, –81, 3) (**a**), strongest right posterior focus (cluster 1, Talairach coordinates 46, –69, 3) (**b**) and the right frontal focus (cluster 6, Talairach coordinates 40, 9, 39) (**c**). (The homologous left-hemisphere precentral location showed no evidence of time-locked activity, even with a more lenient criterion of $Z > 3.0$.) In each panel, the left image shows the extent of the cluster, superimposed on an averaged anatomical image for the 16 participants. The graphs to the right show the time course of activity of that location in the passive viewing and active segmentation conditions, respectively. Green lines plot activity correlated with fine unit boundaries; red lines plot activity correlated with coarse unit boundaries. Vertical lines indicate the frame at which a segment boundary was placed during the intentional segmentation scans, on which the time courses were aligned for estimation using the general linear model. Adapted from Zacks, et al. (2001).

The regions of the brain that displayed the most robust activity in response to passive and active event segmentations are shown in Figure 3-1. Region (a) shows activation at the occipital / temporal junction (or Brodman's areas 19/37 bilaterally). The region labelled (b) is located posteriorally over the right hemisphere, and is in close proximity to the Human MT (or V5) complex, which has been implicated in motion processing and in processing biological motion and human action (Sekuler, Watamaniuk et al. 2002). The precentral suclus highlighted as (c) is also referred to as Brodman's area 6, and is located in close proximity to the human analog of the Frontal Eye Field (FEF) of the monkey. The FEF has been previously shown to be active during shifts in spatial attention and related to eye movements (Corbetta et al., 1998). These data clearly indicate a network of brain regions that respond to the perception of an event boundary. Furthermore, the spatial locations of the regions imply the use of sensory processing functions, specifically attending to movement in the movie. However, as the neural network is not solely limited to areas supporting sensory processing, we may assume that network activation also reflects additional cognitive processes, most likely attributed to the processing of event boundaries.

Interestingly, visual inspection of the data clearly shows activation in regions (a) and (b) that commences *before* the explicit perception of an event boundary. To quantify the build up of activity, Zacks et al. submitted pre-boundary fMRI scan frames for analysis. Pre-boundary activation was detected during active segmentation for both coarse and fine-grain segmentations. Importantly, pre-boundary neural activity was detected during passive viewing when perceiving coarse-grain event boundaries in the right frontal region (a). Zacks et al. suggest that the pre-stimulus activity

reflects a build-up of information that anticipates the explicit report of an event boundary, i.e. based on active monitoring rather than simple reactive processing. However, during active segmentation viewings, participants are explicitly told to segment the movies by pressing a button. Consequently, pre-boundary activity during active viewing may reflect cognitive functions actively seeking to identify an event boundary; moreover, participants may be preparing psychologically to press the button. Despite active segmentation pre-boundary neural responses potentially containing cognitive artefacts, it cannot be ruled out that the perceptual system actively seeks out event boundaries as a part of ongoing perception. Bearing this in mind, the presence of pre-boundary activity during passive viewing goes someway to supporting the authors claim, albeit exhibiting only partial network activation during the perception of coarse-grain events.

Discussing their results, Zacks et al. speculate on the role of the neocortex in the perception of event boundaries. Firstly, the authors argue that the network of cortical areas active during passive viewing is a core component of event perception. Secondly, it is suggested that the stronger responses noted for coarse-grain response when compared to fine-grain boundaries, reflects the hierarchical nature of event perception. Thirdly, areas in close proximity to the human MT complex and FEF are argued to be heavily involved in perceptual event segmentation. Lastly, responses recorded in the neocortex network that began substantially before an event boundary, are suggested as being reflective of continual monitoring; necessary to facilitate the anticipation of upcoming event boundaries. In sum, Zacks et al. concluded that the neuroimaging study provides convincing data to support a theory of event segmentation as a part of ongoing perception.

3.2 Extending the primary evidence

As previously discussed, a right-frontal region of the network lay in close proximity to the FEF, which is associated with eye movement. Also discussed was a right-parietal region of the network lay in close proximity to the MT complex, which is associated with motion processing. The authors argue that the FEF and MT complex may be heavily involved in event perception, however, to what extent was not revealed in the neuroimaging study.

Consequently, a follow-up fMRI-based study investigated the role of the FEF and MT complex in the perception of events, using a set of neural localiser tasks (Speer et al., 2003). Specifically, participants viewed stimuli designed to elicit responses from either MT+ or FEF; the resultant data were compared against MT+ and FEF activation present during the perception of an event boundary. The investigation demonstrated the role of the MT complex in event segmentation (due to similar responses elicited during localiser trials and event segmentation trials), however, involvement of the FEF was effectively ruled out (due to dissimilar responses between localiser and event segmentation trials). The authors concluded that because of their findings, motion cues, and possibly eye movements, might play key roles in the perception of events. With this insight, a further study specifically investigated the role of the MT complex in event perception, and the influence of motion on event perception (Zacks et al,. 2006). This study used simple animations of geometric objects as stimuli, so that a quantitative analysis of the influence of movement on event segmentation could be conducted. Results revealed that activity in the MT complex was correlated with the speed of the object's motion, and additionally with the presence of event boundaries.

Taken together, these studies clarify the role of the FEF an MT complex in event perception. Firstly, the FEF is effectively ruled out as a component of event segmentation due to its spatial disparities with the neighbouring area identified in the event segmentation neural network. Secondly, the MT complex is implicated in the perception of event boundaries and the processing of motion, giving rise to the notion that the perception of an event boundary may be driven (at least in part), by perceived ongoing motion.

3.3 Converging fMRI evidence

Converging with the previously discussed studies, neuroimaging investigations of event perception have been conducted in other fields of interest, including music perception and narrative comprehension. This section aims to summarise the findings of these studies, and discuss their implications for the theory of event segmentation.

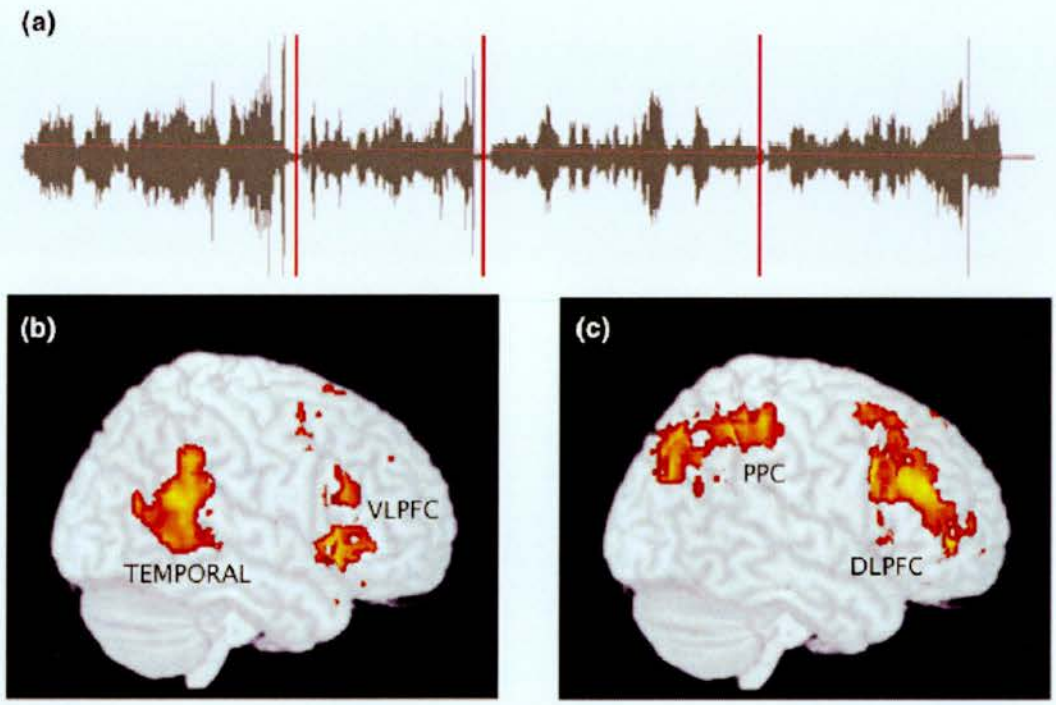

Figure 3-2: The boundaries between musical movements elicited increased activity at a network of brain regions. (a) In Western concert music, symphonies are made up of movements. The sound wave is plotted, and the breaks between movements are illustrated with red lines. Sridharan et al. (2007) had musically untrained participants listen to two 8-10-min segments of symphonies by William Boyce, consisting of movements lasting an average of 1 min and 10 s, while their brain activity was recorded using fMRI. (b) A ventral network including the ventrolateral prefrontal cortex (VLPFC) and posterior temporal cortex (TEMPORAL) increased in activity first at movement boundaries. (c) A dorsal network including the dorsolateral prefrontal cortex (DLPFC) and posterior parietal (PPC) increased in activity slightly later. Both networks were lateralized to the right hemisphere. The authors interpreted these data by suggesting that the response of the ventral network reflected the processing of violations of musical expectancy, whereas the response of the dorsal network reflected consequent top-down modulation of the processing of new musical information. Adapted from Kurby & Zacks (2008).

Unlike the previous studies which used visual stimuli as a basis for event segmentation, Sridharan, Levitin, Chafe, Berger, & Menon (2007) investigated the perception of event structure in music. Musically untrained listeners segmented audio clips of Western concert music into coarse-grained events, while having their brain activity recorded in an fMRI scanner.

Sridharan and colleagues examined the extent to which listeners used transitions between movements as a basis for the perception of an event boundary. Figure 3-2 illustrates two dissociable networks in the right brain hemisphere that were differentially active at transitions between movements. These results indicate that event segmentation may play a role in the perception of music, and provide further evidence to support a wider role for event segmentation in ongoing perception.

Similarly, in a study of narrative comprehension, Speer, Zacks, & Reynolds (2007) recorded participants neural responses in an fMRI scanner. During the investigation, participants read narrative text one word at a time, before actively segmenting the texts in subsequent readings. Mimicking the paradigm used in the Zacks et al. (2001) study, perceived event boundaries were overlaid onto initial passive readings, allowing the examination of neural data time-locked to event breakpoints. Speer and colleagues revealed a network of regions that responded to the perception of an event; importantly, these regions corresponded substantially with the regions that increased at event boundaries in movies.

3.4 Neurophysiological investigations of event segmentation

Neuroimaging studies that use fMRI measure changes of blood flow in the brain, and such activity may be located on a fine spatial scale, whereas studies that employ EEG reveal changes in electrical activity on a fine temporal scale. Data from fMRI and EEG studies are not directly comparable, principally due to different types of signal being measured; EEG measures changes in electrical activity at the scalp, whereas fMRI measures changes in blood flow. However, results from EEG experiments can complement fMRI data, providing additional psychological insight.

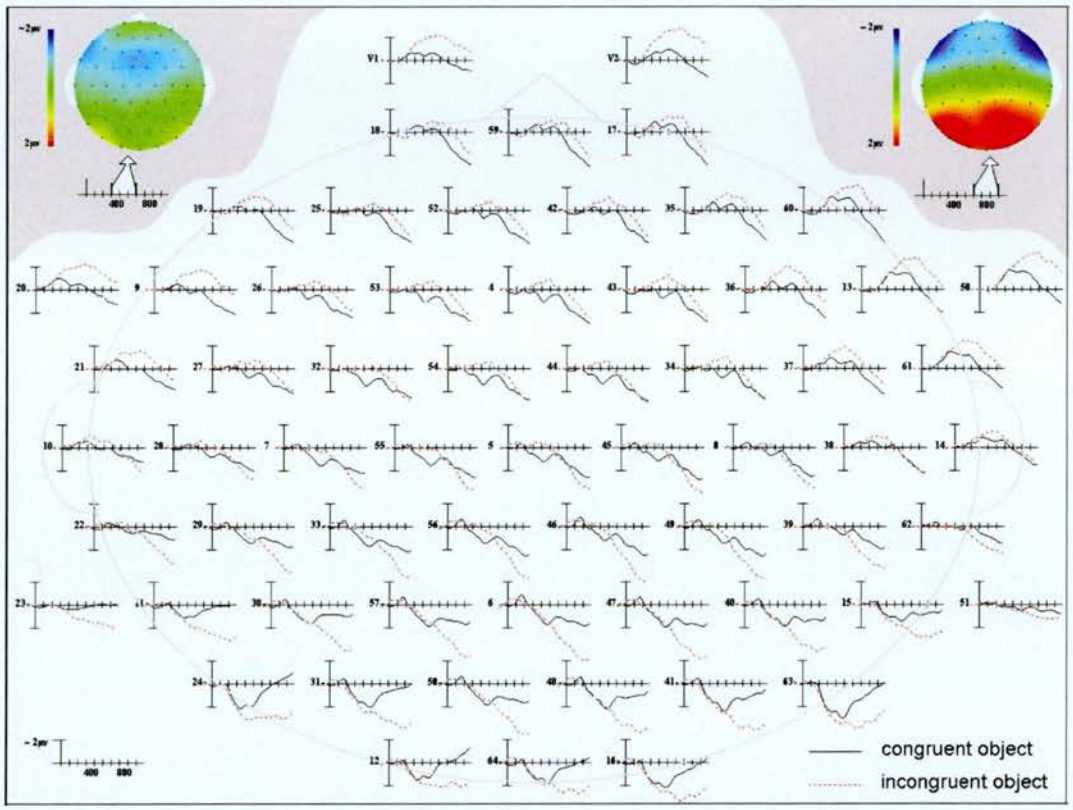

Figure 3-3: Average ERPs elicited by target objects in videos, and the corresponding voltage maps of the ERP differences in the N400 (top left) and LPC (top right) time-windows. Adapted from Sitnikova, et al. (2003).

In a study of semantic integration in movies of real-world events, Sitnikova, Kuperberg, & Holcomb (2003) used EEG to measure evoked responses to the appearance of incongruent objects. Contextually appropriate and inappropriate objects appeared in movie clips of everyday activities; brain activity was time-locked to these events, from which ERPs were formed. The ERP study revealed a greater negative-going deflection over left-parietal regions for incongruent objects when compared to congruent object appearance, as illustrated in Figure 3-3. Differences were also found over right-frontal electrode sites, with the ERPs for incongruent objects found to be more positive going than those for congruent objects. The onset

of the effect found over left-parietal electrode sites was detected shortly after object presentation, which Sitnikova et al. claim, reflects a rapid online component of semantic integration in real-world perception. Furthermore, the authors argue that later evoked responses to incongruent objects reflect a psychological triggering of cognitive functions that attempt to integrate incongruent information. Despite the lack of EEG comparability with similar fMRI studies (e.g., Michelon, Snyder et al. 2003), the data do reveal interesting findings.

Considering the evidence for a cascade of cognitive processes, these results may be interpreted as supporting the previously discussed common hypotheses, which describe perception as a hierarchical thought process. Additionally, the study provides further insight into the nature of perception; evidence suggests that objects are integrated as a part of ongoing perception, and that integrating unanticipated objects engages differential cognitive processes. A more recent study that further investigated the ERP components identified by Sitnikova, Kuperberg, & Holcomb, concluded that the components might reflect two neurophysiologically distinct semantic integration mechanisms, that mediate visual comprehension of the real world (Sitnikova et al., 2008).

3.5 Summary

Currently no electrophysiological studies have specifically investigated event segmentation during perception. In their fMRI study, Zacks et al. (2001) report a cortical network of activity that responded to the perception of an event boundary. Techniques exploiting fMRI technology are particularly accurate in identifying specific regions of the brain; however, the spatial accuracy is compromised by the lack of temporal resolution. An

electrophysiological investigation of event segmentation should provide temporal data of a high-resolution that capture the neural correlates of event perception. Additionally, ERP experiments may also be used to answer psychological questions regarding event segmentation, such as, "what effect does familiarity have upon the perception of event"? The aim of this thesis is to ask psychological questions of event segmentation theories, and provide evidence in a fine temporal domain using EEG and ERPs. The following chapter discusses the results of a pilot EEG study investigating the perception of events.

4 General methods

4.1 Experimental procedure

The core experimental design used across all experiments in this thesis follows the adapted Newtson (1973) paradigm, as used by Zacks et al. in 2001. With the exception of Experiment 1, participants were asked firstly to watch four video clips, typically of real world activates each lasting around five minutes, with no knowledge of the experimental paradigm. Specially, participants were asked to maintain attention during the passive viewings. Upon subsequent viewings, participants were asked to actively segment the videos into as many large meaningful chunks as possible (coarse grain), and into as small meaningful chunks as possible (fine grain). Participants were asked to mark the boundaries between events by tapping a button. The order of fine grain vs. coarse grain segmentations were counterbalanced across participants.

4.1.1 Stimuli materials

All the experiments reported in this thesis used a set of four short video clips (typically 5 minutes playing time) as stimuli. Four sets of stimuli were used; three sets were fixed shot, single scene recordings of an actor performing one goal-directed task, a further set of video stimuli depicted abstract shapes moving around the screen. Active segmentations were overlaid onto the passive viewing for each video, from which ERPs were formed time-locked to the participant's response.

4.1.1.1 Stimuli for Experiment 1

The purpose of the first experiment was to evaluate the use of ERPs as a valid means of measuring the perception of event boundaries. As such, the study sought to replicate the Zacks et al. (2001) fMRI study as closely as possible. Kindly, Jeffrey M. Zacks (University of Washington, St. Louis), provided the video stimuli used in his 2001 fMRI study of event segmentation. The four activities were fertilising a houseplant (148 seconds), making the bed (255 seconds), doing the dishes (245 seconds), and ironing a shirt (300 seconds). Figure 4-1 shows four frames taken from the video 'ironing a shirt'.

Figure 4-1: Four frames from the video 'ironing a shirt'.

4.1.1.2 Stimuli for Experiments 2 and 5

Video stimuli material for experiments 2 and 5, again supplied by Jeffrey M. Zacks, also showed actors performing an everyday activities; doing the laundry (300 seconds), making the bed (320 seconds), planting plants (360 seconds) and washing the car (450 seconds). The four videos used in Experiment 2 and 5, were found to be of a higher quality i.e. clearer picture resolution, while similarly to the Zacks et al. (2001) video stimuli, depicting everyday tasks shot in a single scene from a fixed camera position.

4.1.1.3 Stimuli for Experiment 3

The videos used in Experiment 3 were recorded using volunteer actors (a sample of frames from the video 'making a table' are shown in Figure 4-2). Each video was a fixed shot, single scene recording of one actor performing an obscure task that would not be, at least initially, recognisable to participants. The four activities were erecting a clothes rail (424 seconds), constructing a table (444 seconds), setting up a confocal microscope (327 seconds), and setting up electronic musical equipment (324 seconds). Each activity was deemed to be equally and sufficiently ambiguous, in addition to including an ample amount of distinguishable sub-events.

Figure 4-2: Three frames from the video 'making a table'.

4.1.1.4 Stimuli for Experiment 4

Unlike the previous experimental stimuli featuring real-world activities, the video clips used in Experiment 4 displayed coloured geometric shapes (a green circle and a red square, as illustrated in Figure 4-3), moving around a white background. This set of videos were produced by Jeffrey M. Zacks and used in his study of 2004 (see Zacks, 2004, Experiment 3). The movements of the shapes are generated randomly, however, the mean speeds and acceleration magnitudes of the objects are matched to parameters taken from participants playing a video game e.g. circle chases square. Video clips were

selected if they were considered to typically reflect the game being played; the four video clips used in Experiment 4 in this thesis were shapes fighting, shapes chasing, shapes courting and shapes playing (all 300 seconds).

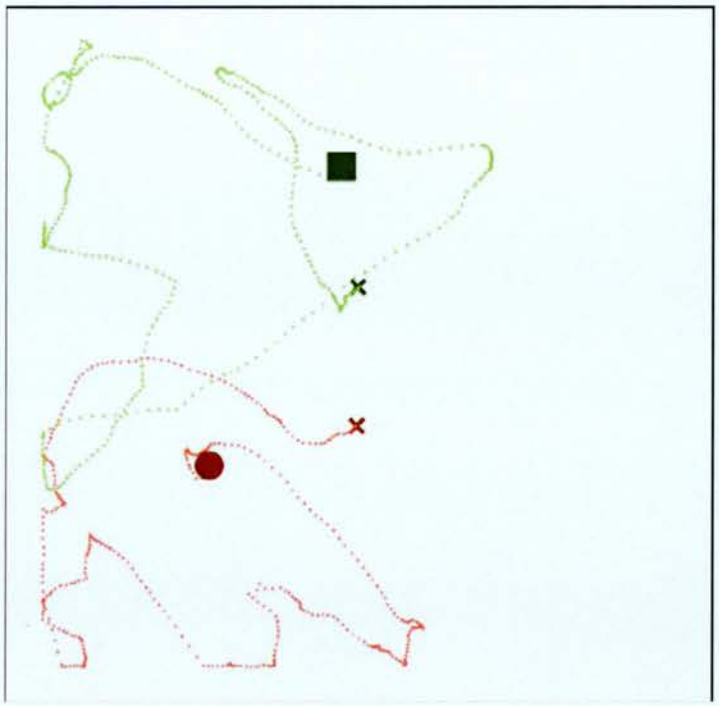

Figure 4-3: An example of the trajectories taken by the objects (green square and red circle) over a 40 second time period; the trajectories paths are marked by the small dots. The centred crosses represent the starting position of the objects. Adapted from Zacks (2004).

The use of this set of video stimuli is best believed to serve the purpose of Experiment 4, as firstly; the stimuli provide an abstract activity (one preventing the engagement of pre-existing cognitive schema), and secondly; the stimuli provide activities that are both randomly generated and can be inferred as representing a goal-directed activity, thus neither group of participants can be wholly influenced by the stimuli alone. Therefore, the

stimuli lend themselves to the subtle manipulations of top-down inference investigated in the experiment.

4.1.2 Participants

Participants with no known psychological impairment were recruited from the University of Stirling, age range 17-35, all having normal or corrected-to-normal vision. Each participant was remunerated either at a rate of £5 per hour, or with a combination of partial payment and course credits. All participants gave informed consent prior to, and were fully debriefed after the experimental session.

4.2 ERP data acquisition and processing

4.2.1 Acquisition

An electrode cap was fitted to each participant, with instructions to minimise eye movement during the experimental phase to reduce eye muscle artefact in the EEG data. Participants were seated in a darkened room approximately 1 metre from a 17" monitor screen. Each video was centrally positioned on the monitor screen with a black background, leaving only the video clearly visible during the experiment.

Video playback was controlled by Psyscope software package (see http://psyscope.psy.cmu.edu) run on an Apple Mac computer. The participants controlled activation of the video via a button box connected to the Mac, and marked segmentation breakpoints by pressing a separate buttons box, controlled via E-Prime software package (see http://www.pstnet.com). Button presses were relayed via E-Prime to the

EEG acquisition software: Neuroscan (see http://www.neuro.com). Both E-Prime and Neuroscan were controlled from a booth adjacent to participant testing.

EEG data were recorded by 61 silver/silver-chloride electrodes based upon the standard 10-20 montage system devised by Jasper (1958). Electrodes were placed onto the scalp using a 'QuickCap', supplied by Neuro-medical Supplies (see http://www.neuro.com), in which the electrodes are embedded in an elastic cap. The channels are listed as follows: FP1, FP2, AF3, AF4, AF7, AF8, Fz, F1, F2, F3, F4, F5, F6, F7, F8, FCz, FC1, FC2, FC3, FC4, FC5, FC6, FT7, FT8, Cz, C1, C2, C3, C4, C5, C6, T7, T8, CPz, CP1, CP2, CP3, CP4, CP5, CP6, TP7, TP8, Pz, P1, P2, P3, P4, P5, P6, P7, POz, PO1, PO2, PO3, PO4, PO5, PO6, PO7, PO8, Oz, O1, O2.

Additional electrodes were placed to the side of each eye (left and right horizontal EOG) to monitor eye movement, and above and below the participants left eye (upper and lower vertical EOG), to monitor eye blinks. Two further electrodes (M1 and M2) were placed behind the participant's left and right ear respectively, to act as reference electrodes. Electrode impedance was below 5kΩ to ensure good quality recording of the EEG. All channels were connected to and amplified by Contact Precision amplifiers, filtered between 0.01 and 40 Hz. All data were acquired using a sampling frequency of 200Hz.

4.2.2 Processing procedure

Data were processed using Neuroscan 4.3 Edit software (Neuromedical Supplies); processing was automated by the development of configurable scripts written in the tcl programming language, which implemented Neuroscan Batch commands. Additionally, the scripts were used to form the

passive viewing ERPs; timings of event breakpoints marked during active segmentation viewings were extracted and superimposed onto passive viewing data, as illustrated in Figure 4-4. Passive viewing ERPs were then formed time-locked to the overlaid breakpoints for processing.

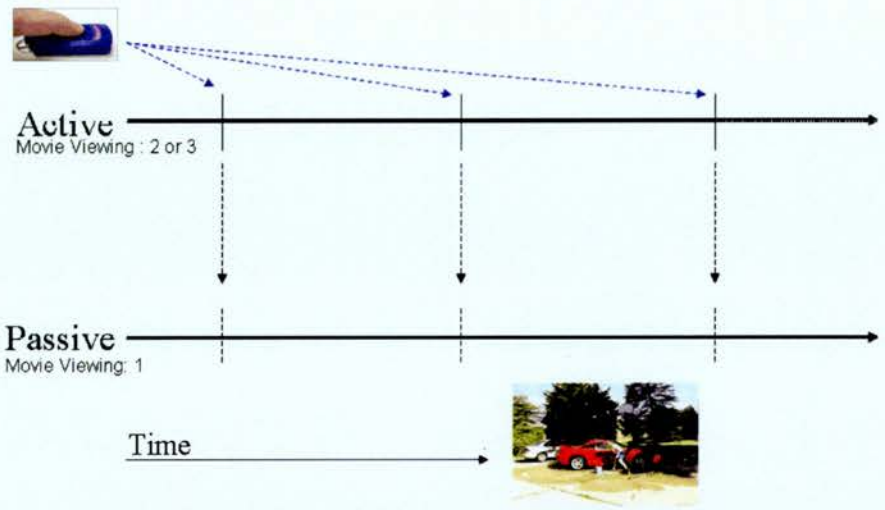

Figure 4-4: Overlaying the passive viewing with participant event points recorded during active segmentation.

Prior to forming Grand Average ERPs for each experimental condition, a number of steps must be taken to eliminate potential artefact from the data. In particular, eye movements are the most prominent and frequent sources of EEG artefact; electrodes placed in the frontal and temporal regions of the scalp are particularly susceptible to ocular artefact. These artefacts were removed by performing a regression analysis; an average ocular artefact response is constructed from which transmission coefficients are computed (by estimating the covariance of the averaged potentials in the ocular channel with the EEG channels). Combining

regression analysis with ocular artefact averaging yields a reliable method for artefact removal (Semlitsch et al., 1986).

Subsequently, EEG data were separated into epochs time-locked to segmentation perceptions; passive viewing epochs lasted from -1500ms to +1500ms, while active viewing epochs lasted from -200ms to 1500ms. Epochs were excluded from analysis when: (a) amplifier saturation occurred; (b) where voltage drift between the start to the end of the epoch exceeded ±75μV; (c) where voltage activity exceeded ±100μV; or (d), when visual inspection of the data identified muscular activity. The data were then smoothed; each datum point was averaged with the two preceding and two proceeding adjacent data points to create a smoother waveform. The passive-viewing EEG data were baseline corrected relative to the mean amplitude of the entire 3000ms interval, whereas the active viewing EEG data were plotted relative to the average activity over a pre-stimulus baseline period of 200ms. Finally, the data must be adjusted for the linked mastoid reference; during recording EEG electrodes are referenced against the left mastoid (M1), which is placed behind the participants left ear, introducing lateral asymmetry to the EEG data. Therefore, to correct the EEG data, the right mastoid (M2, recorded separately to assess the quality of the EEG data) is used to calculate and adjust the linked mastoid reference.

Following these processing steps, the remaining accepted epochs are grouped together by experimental condition, before averaging to form the ERP conditions for each participant. Individual participant average ERP data are then averaged together to produce a Grand Average ERP (a waveform that represents the averaged data for each participant for each ERP condition). Grand averaging is performed separately for each experimental condition.

4.3 Data analysis

The following sections describe the steps taken to analyse the behavioural and ERP data.

4.3.1 Behavioural data

4.3.1.1 Investigating the concurrence of event perception

To validate the hypotheses of event segmentation, in addition to validating the experimental paradigm and video stimuli, an analysis of participant agreement over segmentation points was performed. For ease of data visualisation, plotting participant segmentation points in a raster plot provided the most appropriate solution, as illustrated in Figure 4-5.

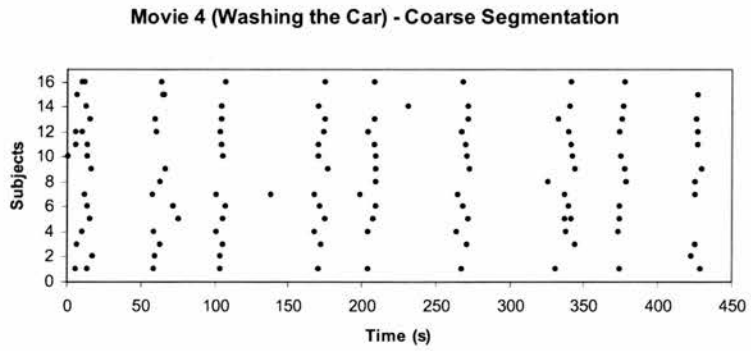

Figure 4-5: Example raster plot of data showing participant agreement of segmentation points.

4.3.1.2 Investigating the hierarchical nature of event segmentation

4.3.1.2.1 Time-bin overlap analysis

Given the exploratory nature of the ERP studies of event segmentation, replications were sought of transferrable analyses to build confidence. In line with the Zacks fMRI study, each movie was segmented into one second time-bins, which were classified as *overlap* time-bins if both a coarse and fine-grained segmentation was present (Zacks, Tversky & Iyer, 2001). The mean number of overlap time-bins was calculated and scaled as per-minute values, thus allowing comparison across movies with varying durations. To qualify the assumption that participants parsed the activity into groups of sub-parts (i.e., formed a hierarchical relationship between parts and sub-parts), the number of recorded overlap time-bins were compared against the number of overlap time-bins that would occur by chance (see Equation 4-1).

$$Overlaps = \frac{Fine}{Bins} \times \frac{Coarse}{Bins} \times Bins = \frac{Fine \times Coarse}{Bins}$$

Equation 4-1: Calculation used to estimate the number of overlap time-bins that would occur by chance. Adapted from Zacks, Tversky and Iyer (2001).

Notwithstanding the three second epoch used in the succeeding ERP analyses, the overlap analyses maintain the use of one second time-bins throughout this thesis to facilitate direct comparison with results from the literature.

4.3.1.2.2 Event enclosure analysis

Coarse-grain event boundaries were paired with the fine-grain event boundaries that lay in closest temporal proximity. The resulting coarse- and

fine-grain pairs were analysed to determine which participants marked first in time. The mean number of coarse-grain boundaries found first and fine-grain boundaries found first were calculated, thus allowing comparison across the experiment

4.3.2 ERP data

4.3.2.1 Implications of hierarchical structuring for ERPs

The hierarchical analysis procedure outlined in section 4.3.1.2.1, aims to demonstrate that participants tend to align sub-part boundaries with those of larger part boundaries. As independent conditions are formed for coarse and fine-grained event segmentation, the presence of overlapping time-bins identified in the hierarchical analysis will suggest that there must be ERPs with overlapping epochs. ERP epochs have a length of 3000ms, whereas time-bins have a length of 1000ms, thus when two time-bins overlap this is indicative of overlapping ERPs. No matter whether the segmentation occurs at the start or the end of a time-bin, due to the larger ERP epoch length an overlap time-bin denotes coarse and fine grain ERP overlap. Thus, by necessity, any condition that has overlapping epochs with another condition will be contaminated by the presence of the other condition. For ERPs, the contamination will result in weakening of the signal-to-noise ratio; as a result, the strength of the comparison between the overlapping conditions will also be weakened.

To investigate the effect of overlapping epochs upon the signal-to-noise ratio, the contribution of the conditions to one another was calculated. Both coarse and fine segmentations from Experiment 1 were summed and

compared with the number of overlapping time-bins found in Experiment 1; the percentage of ERPs with overlapping epochs is shown in Table 4-1. Calculating the percentage of overlapping epochs allows evaluation of the contribution of coarse and fine ERPs to one another.

Video	Coarse-grain	Fine-grain
Fertilising a plant	100%	43%
Making the bed	100%	31%
Doing the dishes	100%	29%
Ironing a shirt	100%	36%
Mean Percentage	**100%**	**35%**

Table 4-1: Percentage of overlapping epochs found for coarse and fine event segmentations across the four activities taken from Experiment 1. Mean values across activities are shown on the bottom row.

As is clear from Table 4-1, every coarse-grain event segmentation epoch overlapped that of a fine-grain event segmentation point. The overlapping epochs of fine grain ERPs will, therefore, weaken the signal-to-noise ratio of coarse grain ERPs. As part of the ERP extraction process, ERPs are averaged across all subjects, and across all activities, in order to reduce noise and isolate the ERP components. Furthermore, epochs are rejected if they contain undesirable noise levels (following the process set out in section 4.3.2.3), thus increasing the signal-to-noise ratio. Averaging and noise rejection reduces the effect of overlapping fine grain ERPs, however coarse gain ERPs must still be considered to contain an element of fine grain event segmentation.

Overlapping epochs occurred on average in 35% of all fine grain ERP epochs. Correspondingly, fine grain ERPs are averaged across all subjects

and all participants, in addition to being rejected based upon their noise levels, in order to maximise the signal-to-noise ratio. Nonetheless, fine grain ERPs must still be considered to be comprised in part, of coarse grain event segmentation. However, with overlaps comprised 35% of fine grain epochs compared to 100% of coarse grain epochs, it is reasonable to assume that fine grain ERP signal-to-noise ratios are affected to a lesser extent than coarse grain ERPs.

The presence of unwanted signals owing to overlapping epochs is likely to have an impact on ERP analysis, for example, as the signal-to-noise ration decreases variability in the signal increases; thus, statistical reliability is expected to be weakened. Furthermore, the comparison of coarse- and fine-grain ERPs is liable to yield the comparably weakest set of statistical results, as both sets of ERPs include signals generated by the other. Nevertheless, the strong brain imaging results reported by Zacks et al. (2001), give rise to the prospect that distinguishable neural correlates may still be revealed using electrophysiological data.

4.3.2.2 Generating the baseline ERP condition

In this thesis, effects of task are identified by comparing coarse and fine grain ERPs, whereas inter-experimental effects are identified by contrasting two conditions such as familiar and unfamiliar activity segmentation. However, in correspondence with et al. (2001) fMRI study, main effects in Experiments 1 and 2 are identified by their reliable divergence from an estimation of background neurological activity over time. Specifically, a baseline (rest state) condition was estimated by placing breakpoints at random intervals throughout participant passive-viewing blocks from which ERPs were formed.

In practice, particularly in the case of frequently perceived fine-grain breakpoints, epochs formed around randomly placed breakpoints overlap epochs containing breakpoint perceptions. To counter this problem, a high number of breakpoints were generated and randomly placed before averaging to minimise the signal strength of segmentation point perceptions. Typically, 512 breakpoints were generated and placed at random points in time for each participant, with around half rejected during ERP formation and processing. For example, in Experiment 2, which attempts to replicate the Zacks et al. (2001) paradigm, the mean number of trials (± SD) contributing to the baseline ERPs was 300 (136); resulting randomly-placed breakpoint ERPs appear close to flat, as would be expected of background activity.

Nevertheless, it is important to consider that the baseline condition is an estimation of background activity, and as such, is primarily used to guide the analysis approach taken in subsequent experiments. Moreover, the majority of the ERP analyses presented in this thesis show the comparison of two inter-experiment conditions such as activity familiar and unfamiliar participant groups, or start- versus end-breakpoint perceptions.

4.3.2.3 Data mining approach

The following section outlines the approach taken to indentify and analyse ERP components of interest, and the rationale employed to limit the scope of the analyses to a reasonable level.

4.3.2.4 Time window classification

The application of ERPs to the event segmentation paradigm is novel; no published ERP data exist for this field of research. Furthermore, in the following studies the participants are defining the 'trial' structure of the experiment, based upon their behaviour after EEG data are recorded. This contrasts with the traditional ERP paradigm, where the experimenter defines trial structures through the presentation of discrete stimuli. Because self-paced designs are not prevalent in the field of ERPs, a standard approach to statistical analysis may not be taken (e.g., a more traditional approach would use published effects as a basis for defining time window selection and selecting electrodes for statistical analysis).

Consequently, a data-driven approach is taken in the current study, based on the data mining tradition within informatics (Hand et al., 2001; Han and Kamber, 2001). Analysis is driven by mining initial overview statistical data in an effort to aid the selection of time windows and electrodes, which will be subsequently submitted to ANOVA.

Firstly, to provide an overview of the event segmentation data, each condition comparison analysis had its 3000ms epoch split into thirty 100ms time windows. For each 100 ms time window, the mean voltage value for all 61 electrodes was calculated. Two conditions were selected for analysis, with the resulting mean values for the electrodes in each condition being compared for significant differences using a two-tailed paired t-test. Differences in electrode mean voltage values across conditions were calculated for each of the 100 ms time windows.

Secondly, to counter the problem of high false positive data produced by performing huge numbers of t-tests, additional criteria were applied to filter these data. Data providing significant t-test results was only considered

for further analysis if the p-value was less than 0.05 (i.e., no marginally significant t-test results were included). More importantly, significant t-test results were then grouped according to their location on the scalp. The scalp map of electrodes was segmented into quadrants; left-frontal, right -frontal, right-parietal and left-parietal. Electrode clusters were only formed if at least three significant electrode comparisons were found within a scalp quadrant. By only including significant t-tests, and then by only considering electrodes which were found to form part of a localised group, these layers of filtering minimise randomly significant or isolated electrodes which may not represent a real effect.

To provide a consistent summary of the statistical effects across experiments, within the ERP literature the same electrodes are typically selected for analysis in each experiment. However, due to the current study providing the first set of event segmentation ERPs, no *a priori* basis existed for selecting electrodes for analysis. Moreover, the use of video stimuli in this experiment is likely to invoke far greater amounts of eye-movement than traditional ERP studies; even with stringent instructions participants watching the movies will likely scan the entire viewing screen as they examine the scenario and track the movements of agents. Owing to the increased likelihood of eye-movement generated artefact, anterior and fronto-temporal electrode sites are excluded from the selection. Consequently, two sets of electrodes were proposed for data mining, each representing the different electrode hemispheres, locations and sites on the scalp. The two sets of electrodes are as follows; (i) left-frontal { F5, F3, F1 }, right-frontal { F2, F4, F6 }, right-parietal { P2, P4, P6 } and left-parietal { P5, P3, P1 }, and (ii); left-frontal { FC5, FC3, FC1 }, right-frontal { FC2, FC4, FC6 }, right-parietal { PC2, PC4, PC6 } and left-parietal { PC5, PC3, PC1 }. These two

electrode sets are shown in Figure 4-6, which highlights the different distributions.

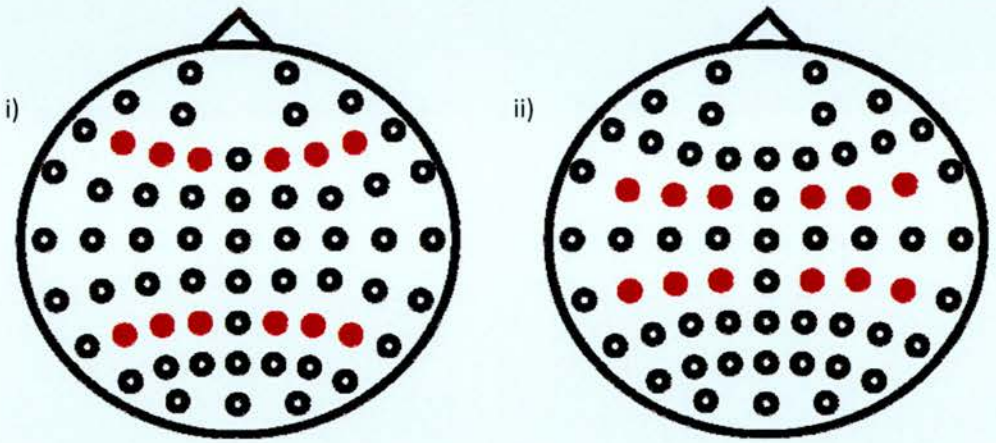

Figure 4-6: Scalp maps (looking down on the scalp, nose to the front) showing the two electrode distributions considered for ANOVA. Distribution (i) shows the 'outer' electrode set, which reflects a more widespread area of coverage than distribution (ii), the 'inner' electrode set that reflects a more central area of scalp coverage.

Lastly, the data mined clusters of significant electrodes that were identified in step two, were compared against the two sets of proposed electrode clusters (i & ii) listed above. If a data mined cluster of significant electrodes included an electrode that was listed in the proposed electrode cluster, then that data mined cluster was selected for further analysis. These steps produced two sets of data, each arranged over time; the first contained data mined clusters with at least one electrode location that matched an electrode location listed in the first proposed electrode set (i); the second data was produced in similar fashion for the second proposed electrode cluster (ii). The purpose of this step was to produce an overview of scalp quadrant effects for both of the proposed electrode clusters. Based on the generation of overview tables for each condition comparison, across all experiments

reported in this thesis, the first proposed electrode set (i) was selected because it best reflected the most prevalent effects present in the ERP waveforms.

Using the overview tables and visually inspecting the waveforms for each comparison allowed time windows to be refined such that the main ERP effects are elicited. Overview tables for each condition comparison, spanning all experiments, for the first set of proposed electrodes are available in Appendix A.

4.3.2.5 Time window selection

The production of summary tables for all experiments in this thesis revealed, in most cases, a number of candidate time windows of interest from each condition comparison. Based purely upon the experimental conditions defined in this thesis, the number of comparisons to be submitted for analysis totalled 56. The amount of comparison analyses can be reduced by assuming that the less interesting differences between active and passive conditions are so prevalent, that only one set of analyses should be conducted (in this first empirical chapter). Discounting the comparison of active versus passive conditions from all further experiments reduces the number of condition comparison analyses to 42. Nevertheless, selecting several time windows from each comparison would lead to an insurmountable number of analyses being reported within the confines of this thesis. As a result, pragmatism forces a minimalist approach to time window selection and analysis, although this must clearly be balanced against the need to provide a thorough investigation.

Considering that one of the main findings of Zacks et al. (2001) was the presence of pre-segmentation neural activity in addition to post-segmentation neural activity, a targeted analysis strategy is thus proposed: each condition comparison includes, where possible, one pre-segmentation time window and one post-segmentation time window to be submitted for analysis. In the case where more than one candidate time window is identified in either pre- or post-segmentation time, the time window that is temporally closest to the segmentation point is selected for further analysis. The choice is based on the following rationale; the aim of this thesis is to investigate the neural correlates of event segmentation, time windows that lie in close temporal proximity to the segmentation point are of greater interest than those that do not. As previously discussed, overlapping ERPs are likely to impact the analysis, and so by discounting time windows which lie further from the segmentation point it is hoped that the effect of overlapping ERPs will also be minimised.

Adopting this strategy imposes conservative reporting of between-condition effects, but importantly, facilitates the presentation of a manageable yet broad spectrum of analyses of interest across the thesis. Moreover, the analyses are reported in a format that allows comparisons to be drawn with the results reported by Zacks et al. (2001). Albeit that the approach focuses on time windows that lie in close proximity to the perception of an event boundary, each experiment presents the full three second epoch window to maintain consistency across the studies. Further, as each investigation is novel, a long-lasting epoch window is used to provide a comprehensive overview in each experimental chapter.

4.3.2.6 Analysis procedure

Following the selection of appropriate time windows as outlined in the previous sections, these data are submitted to ANOVA for statistical analysis. Notwithstanding the pre-generation of t-tests for each time window as a result of the data mining approach, t-test data will only be presented if the results from ANOVA indicate follow-up tests are required e.g. interactions revealed with factors of hemisphere or location would justify subsidiary ANOVAs, or t-tests, to further analyse the scalp quadrants. All analyses presented in this thesis follow the procedures outlined in this chapter.

4.4 Controlling for eye movement artefacts

Given the use of video clips in the experiments, it is likely that excessive lateral eye movement will be evoked when compared to a typical ERP study. Therefore, notwithstanding the steps taken to eliminate horizontal eye from the data as described in Section 4.2.2, additional consideration must be attributed to further control ocular artefact.

A number of steps were taken to ensure the affect of lateral eye movement was minimised upon the data; firstly, participants were instructed to limit their gaze to within the monitor display area; secondly, the data were analysed to eliminate voltage drift that may occur due to shifts in gaze; thirdly, the voltage in each channel was compared against a threshold value, thereby eliminating any sudden shifts in gaze that would likely produce a voltage fluctuation; fourthly, as illustrated in Figure 4-6, both sets of electrode clusters selected for analysis excluded fronto-polar, temporal and fronto-temporal channels, all of which are likely to be affected the most by

ocular artefact; and lastly, visual inspection of Grand Average ERPs cross referenced HEOG waveform morphology against the distribution of activity found over frontal and temporal electrode sites, collectively ensuring lateral ocular artefact is minimised.

4.5 Further considerations

In practice, participants that did not provide a minimum of 16 artefact free trials from which to form an ERP were excluded from analysis (due to a lack statistical strength). Further, participants were monitored during testing any who were deemed to have misinterpreted the guidance e.g. marking substantially more segmentation points, were re-briefed. However, whilst these practices excluded subjects based upon a lower-limit threshold and judgement based upper-limit, no formal method is taken in this thesis to exclude outlying subjects that provided an abnormally high amount of trials.

In principle, outlying or unusual participants could be identified using statistical methods such as examining the distribution of participant responses to gauge confidence intervals. Participants response frequencies who lay either three (outlying 99% of the population), or two (outlying 95% of the population) standard deviations from the mean may be excluded depending on the level of confidence required. Nevertheless, as the experiments relied upon perceptions rather than a set of pre-determined responses, this thesis presents data form participants that provided a minimum of 16 segmentation points per condition and were monitored during testing for abnormal response patterns.

5 Directed event segmentation

5.1 Introduction

In 2001, Zacks et al. investigated the phenomenon of event segmentation by showing participants videos of everyday tasks while recording their brain activity. By using the Newtson (1973) paradigm in an fMRI experiment, Zacks et al. were able to reveal the location of neural responses to event segmentations. Zacks et al. reported three regions of interest that responded to salient event boundaries. All three areas showed activation in response to segmentations, with two of the three regions exhibiting pre-stimulus activity (i.e., a response leading up to the event segmentation). Zacks et al. also found evidence of hierarchical structuring in event segmentation, which reflected participant's propensity to segment activities in terms of their parts and their constituent sub-parts. Although the fMRI data allowed neural activity to be examined on a fine spatial scale, the temporal resolution is poor (in the order of seconds) and by no means reflects the fine temporal scale on which the brain operates.

In order to reveal the neural correlates of event segmentation on a temporal scale more akin to the timing of neural functions, an alternative imaging method must be employed. Electroencephalography (EEG) allows small fluctuations of electrical activity to be measured from electrodes on the scalp, and with data sampled in terms of milliseconds, is an ideal alternative to fMRI. Of course, using EEG to investigate event segmentation will produce neural data with a fine temporal resolution but a poor spatial resolution. In particular, difficulty in localising the source of the electrical activity measured at the scalp is a serious limitation of EEG. Due to their distinct underlying causes and the contrasts of spatial and temporal

resolution available in the different imaging techniques, EEG findings can be expected to be not directly comparable with the results reported by Zacks et al. However, using an alternative imaging method will provide a useful alternative analysis of the neural correlates of event segmentation, particularly given that the high temporal resolution of EEG should better capture the temporal nature of event segmentation.

This chapter more closely explores the effectiveness of employing the Newtson (1973) event segmentation paradigm in an EEG study. In correspondence with the Zacks et al. study, participants watched videos of everyday activities passively, before marking segmentation points by pressing a button on subsequent viewings. Segmentations are then overlaid onto the neural data recorded during passive viewing, thus allowing ERPs to be formed time locked to the segmentations. The Zacks et al. study revealed activity in eight neural populations in response to event segmentations. It is therefore assumed that the same populations of neurons will be actived; given their location within the cerebral cortex these regions are reasonably likely to produce ERP signals. However, as neuron populations must be aligned in a configuration that allows their activity to be measured, and with the problem of scalp source mixing, it cannot be safely assumed that the activation of all three sources will be independently measurable with ERPs. Despite the limitations of EEG, it is hypothesised that at least some populations of neurons responding to event segmentations will be measurable at the scalp and detectable in the averaged ERPs.

The critical question to be addressed in the current study is whether, assuming ERP correlates of event segmentation exist, clear pre- or post segmentation activity will be evident, and whether differences between coarse and fine grain segmentation will be present. Moreover, given the fine

temporal resolution of EEG, it is of particular interest as to whether ERP data will reveal temporally finer grained neural correlates of event segmentation, when compared with the Zacks (2001) study.

5.2 Experiment 1: Investigating the effect of coaching on event segmentation using ERPs

5.2.1 Methods

In addition to the General Methods (see Chapter 4), the following sections detail experimental methods specific to this experiment.

5.2.1.1 Stimuli

The videos used in this experiment were provided by Jeffrey M. Zacks (University of Washington, St. Louis), taken from his 2001 fMRI study of event segmentation. Each video was a fixed shot, single scene recording of one actor performing an everyday task. The four activities were fertilising a houseplant, making the bed, doing the dishes and ironing a shirt. Active segmentations were overlaid onto the passive viewing for each video, from which ERPs were formed time-locked to the participant's responses.

5.2.1.2 Participants

Twenty-two participants took part, as per the criteria set out in the General Methods chapter. Data from two participants was discarded due to behavioural non-compliance; twenty participants remained in the group (9 male, age range 19-32).

5.2.1.3 Procedure

The current procedure differed from that employed in the original paradigm (Newtson, 1973) in several respects. Firstly, participants neural activity was recorded via scalp mounted electrodes to allow ERPs to be formed time-locked to their responses, as described in the General Methods chapter. Secondly, participants watched one video while under instruction to maintain attention, and then actively segmented the video into large or small segments on subsequent viewings (with the order of coarse and fine segmentation counterbalanced across participants). Each video followed the same procedure; the overall paradigm therefore differed from the original paradigm in which participants actively segmented videos. Thus, the current procedure also differed from Zacks et al. (2001), in which participants watched all videos passively before actively segmenting the videos.

5.2.2 Behavioural results

The following section contains analysis of behavioural data collected from 20 participants as they performed the event segmentation experiment.

5.2.2.1 Investigating the concurrence of event perception

Experiments investigating event segmentation rely upon participants marking coarse and fine event boundaries, as they perceive them. Although participants can consciously mark event boundaries when instructed to do so, whether or not event segmentation is an automatic process is debatable. One way to investigate the process of event segmentation is to study participant agreement across event boundary perception.

For easy visualisation of participant event-boundary perceptions over time, the data for each video, for both coarse and fine conditions, are displayed as raster plots in Figure 5-1. From visual inspection of the raster plots, it is clear, particularly for the coarse conditions, that there is across-participant agreement over event segmentation points. The coarse raster plots display clearly defined columns of data points, indicating that many participants marked the same point in the movie as an event boundary. Participant agreement is also evident in the fine-grain segmentation raster plots; again columns of data may be identified. For example, in the activity 'doing the dishes', the fine grain event segmentation raster plot shows columns of data points amongst the many segmentation points that each individual participant would select during a fine grain segmentation viewing.

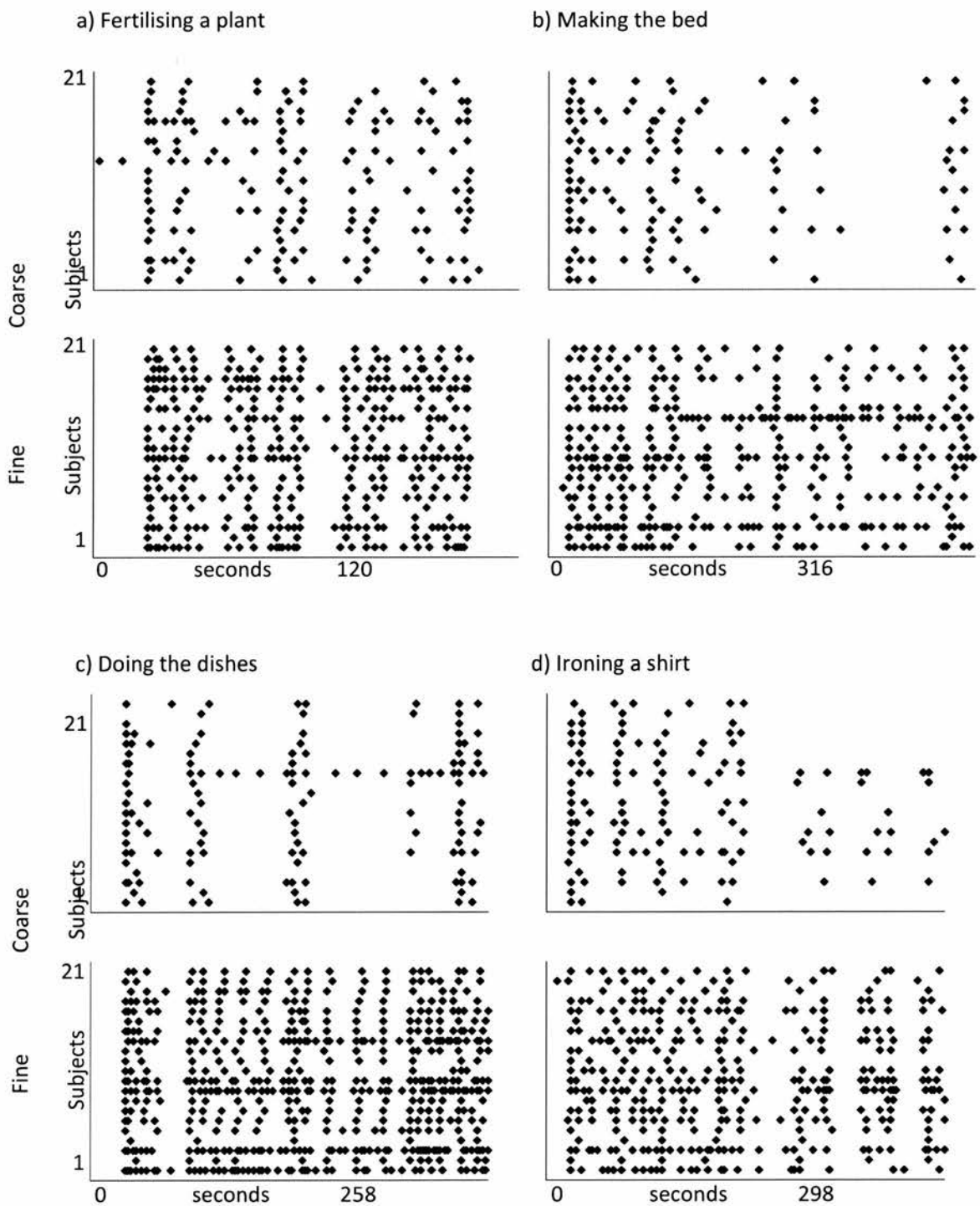

Figure 5-1: Raster plots of segmentation timings (x-plane) for each participant (y-plane), shown separately for each movie (a-d), for fine and coarse conditions. Each individual data point reflects a single segmentation response.

In summary, the raster plot data suggest that participants shared a common perception of where segmentation points occur, perceiving many events in the same way, despite the presence of segmentation points that were unique to individual participants. As the results reveal at least a degree of common strategy in the perception of events, one interpretation could be that existing hypotheses, which state that event segmentation is an automatic process, are supported. Alternatively, the results could simply suggest that participants consciously employ a common strategic approach to identifying event boundaries. Notwithstanding this concern, the results do align with previous experiments, and therefore, are at least encouraging for the scope of this experiment.

5.2.2.2 Investigating the hierarchical nature of event segmentation

Based upon the criteria set out in the General Methods chapter, two measures of hierarchical event structuring were extracted from the behavioural data collected during active segmentation.

Firstly, mean values for recorded and randomly placed overlap time-bins were calculated for each activity, as illustrated in Figure 5-2. ANOVA with factors of condition (recorded/randomly placed) and activity (fertilising a houseplant, making the bed, doing the dishes and ironing a shirt), revealed a main effect of condition [$F(1,19) = 98.96$; $p < 0.001$], reflecting the greater chance of participants overlapping fine and coarse-grain segmentation points than when the segmentations are generated randomly. A further interaction between condition and activity was revealed [$F(1.98,37.63) = 7.97$; $p < 0.005$], reflecting the different structures of the activities, for example, participants may feel that making a bed does not contain as many parts as fertilising a

house plant. In addition, t-tests (reported in Table 5-1) were run comparing recorded and randomly placed overlap time bin mean values; significant differences were revealed for each activity. Secondly, coarse- and fine-grain pairs were analysed to determine which breakpoint participants marked first in time (see Figure 5-3); however, analysis of the data failed to reveal a tendency to mark coarse-grain event boundaries slightly after fine-grain event boundaries [$p > 0.1$].

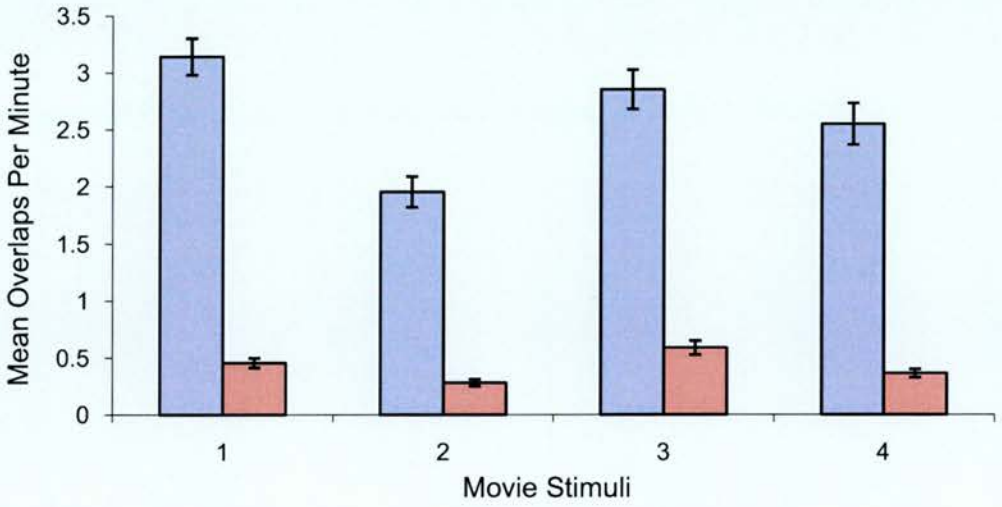

Figure 5-2: Mean number of overlap time-bins for recorded (blue) and randomly placed (red) segmentations per minute are shown for each video; (1) fertilising a house plant, (2) making the bed, (3) doing the dishes and (4) ironing a shirt. Error bars represent one standard error of the mean. For all four movies, significantly larger numbers of overlapping time-bins were recorded than would occur randomly.

T-test results for overlapping coarse- and fine-grain event perception

Activity	T-test result
Fertilising a house plant	[t(19) = -10.96; p < 0.001]
Making a bed	[t(19) = -7.52; p < 0.001]
Doing the dishes	[t(19) = -9.26; p < 0.001]
Ironing a shirt	[t(19) = -7.21; p < 0.001]

Table 5-1: Resulting p-values from the two-tailed t-tests performed on each activity. The results reflect the clear differences present between actual overlapping time bins recorded and those arising purely by chance.

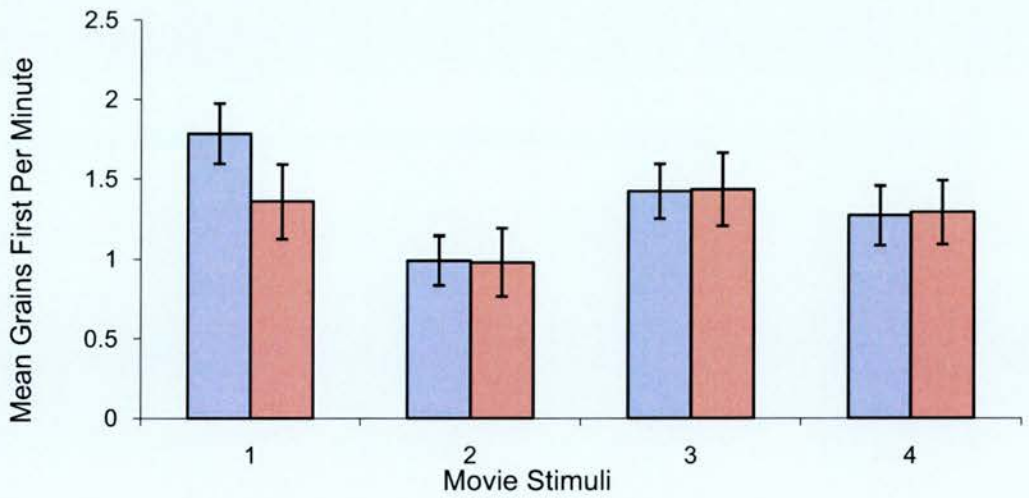

Figure 5-3: Mean number of fine- before coarse-grain segmentations (light blue), and coarse-before fine-grain segmentations (light red) per minute are shown for each video; (1) fertilising a house plant , (2) making a bed, (3) doing the dishes and (4) ironing a shirt. Error bars represent one standard error of the mean. None of the movies demonstrated significantly larger numbers of fine- before coarse-grain segmentations than coarse- before fine-grain segmentations.

In summary, the hierarchical analyses reported conflicting results; the striking probability of participants overlapping coarse- and fine-grained event breakpoints, supports the conclusion that participants encoded the

activity in terms of hierarchical relationships between parts and sub-parts. However, the second analysis failed to support previous findings (see Hard et al., 2001), suggesting that participants did not use coarse-grain event boundaries to group fine-grain event parts.

5.2.3 ERP results

5.2.3.1 Investigating directed-passive-coarse grain segmentation

Figure 5-4 shows the grand average directed-passive-coarse and randomly generated segmentation point waveforms for passive segmentation from 61 EEG electrode sites; the mean number of trials (± SD) contributing to the ERPs was 38 (19) for directed-passive-coarse. Several features of the ERP data are reliable. First, the random condition is evidently close to flat – as would be expected for random background EEG. Second, the segmentation ERP is clearly not flat; the waveform exhibits a distinct morphology, with a changing pattern of activity over time.

Third, in comparing the two sets of ERPs the waveforms clearly show an early divergence from -1500ms pre-segmentation over the right-frontal electrode locations, with the ERPs for directed-passive-coarse becoming less negative towards the segmentation at 0ms. Parietal electrode sites exhibit a positive-going divergence that starts at approximately -1300ms pre-segmentation, with the ERPs for directed-passive-coarse becoming less positive towards -1000ms. A further positive-going divergence is present over all electrodes at around -400ms, with the ERPs for directed-passive-coarse continuing to remain positive until approximately 0ms. Post-segmentation divergences appear to show long lasting effects from

approximately 300ms to 1000ms. During this time window waveforms for directed-passive-coarse are more positive than random, particularly over right-frontal electrode sites, but more negative than random over parietal electrode sites.

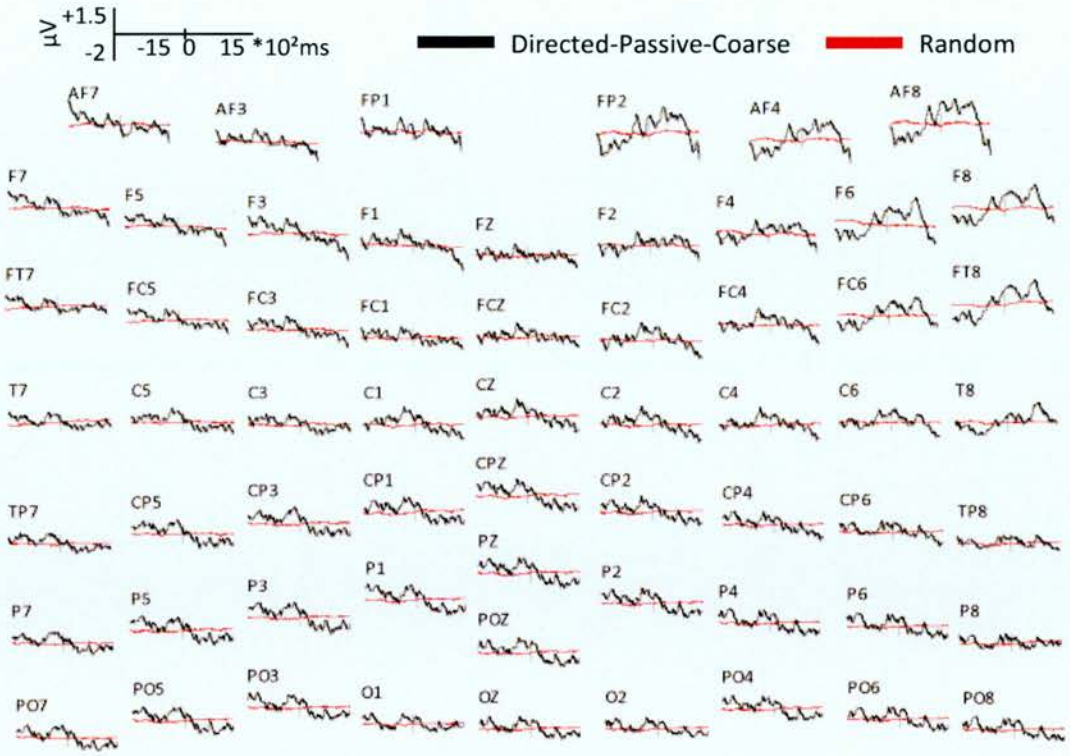

Figure 5-4: Grand average ERPs elicited for directed-passive-coarse (black) and random (red). Positive-going activity is present globally for directed-passive-coarse compared to random ERPs, particularly between -400 and -100ms. Parietal electrodes show more negative-going activity, particularly between 400 and 1000ms, and right-frontal electrodes appear to show more positive-going activity between 400 and 1200ms.

Directed-Passive-Coarse Segmentation

Time window (*10²ms)	-15	-14	-13	-12	-11	-10	-9	-8	-7	-6	-5	-4	-3	-2	-1
Left Frontal												*			
Right Frontal							*								
Right Parietal				*									*	*	
Left Parietal			*	*								*	*	*	

Time window (*10²ms)	0	1	2	3	4	5	6	7	8	9	10	11	12	13	14
Left Frontal															
Right Frontal	*		*					*	*						
Right Parietal						*				*					
Left Parietal					*	*	*		*	*					

Event Boundary Perception

Table 5-2: Overview table showing the comparison of directed-passive-coarse and random conditions. The 3000ms epoch window for each condition was split into 100ms time-bins for analysis, with the data mined effects identified in the scalp quadrants listed. The purpose of the overview table is to aid the identification of appropriate time windows to be used in focussed ERP analyses. Time windows are selected by visually inspecting both the ERP waveforms and the grouping patterns of scalp quadrant effects over time. In order to demonstrate the correlation between the ERP grand average waveforms and the overview data, the first time window used in the first condition comparison may be used as an example: the first row in the table shows a number of scalp quadrant effects present during the -400 to -100ms time window. The effects listed in the overview table during the -400 to -100ms time window indicate the presence of an effect - in this case reflective of the positive-going waveforms present globally for the directed-passive-coarse condition visible in the grand average waveforms during -400 to 0ms as shown in Figure 5-4. Utilising the overview data allows visually identified time window definitions to be refined, thus revealing the most robust effects.

5.2.3.1.1 Pre-segmentation time window (-400 to -100ms)

To characterise the ERP results and subject the data to a more focused analysis, one time window was selected from pre-segmentation time, and one from post-segmentation time. The current pre-segmentation, time window was selected based upon visual inspection of the grand average waveforms (Figure 5-4), and refined using the overview table generated for the current condition comparison (see Table 5-2). Two pre-segmentation time windows were initially identified as possible time window candidates; the first captured an early parietal effect from -1300 to -1000ms, and the second captured a later widespread effect from -400 to 0ms. The second time window was selected for analysis as the ERPs indicated it to contain the stronger effect, in addition to the overview data confirming longer-lasting divergences.

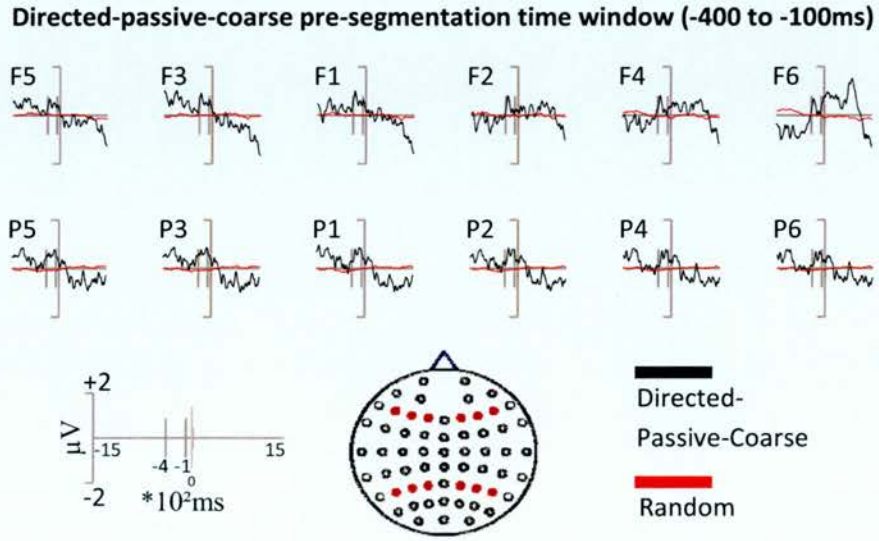

Figure 5-5: Grand average ERPs elicited for directed-passive-coarse (black) and random (red). Frontal and parietal electrodes demonstrate more positive-going activity for directed-passive-coarse compared to random ERPs between -400 and -100ms.

Figure 5-5 shows the grand average ERPs time-locked to directed-passive-coarse and randomly generated segmentation points, at electrodes chosen for statistical testing. ANOVA with factors of condition (directed-passive-coarse/random), location (frontal/parietal), hemisphere (left/right) and site (superior/medial/inferior), revealed a main effect of condition [$F(1, 19) = 7.96$; $p < 0.05$]. This finding, in combination with the fact that no further interactions were revealed, reflects the global differences present between the directed-passive-coarse and random conditions over the scalp electrodes.

5.2.3.1.2 Post-segmentation time window (400 to 1000ms)

The post-segmentation time window was identified for analysis using the same process that was employed to identify the first time window. During the period of 400ms to 1000ms, the waveforms indicate, and the overview data in Table 5-2 confirm, the presence of a long lasting parietal effect. In addition to capturing the parietal effect, the long time window also captures the right-frontal effect visible in the waveforms, and was therefore deemed a suitable candidate for analysis. Figure 5-6 shows the grand average ERPs time-locked to directed-passive-coarse and randomly generated segmentation points, at electrodes chosen for statistical testing.

ANOVA with factors of condition (directed-passive-coarse/random), location (frontal/parietal), hemisphere (left/right) and site (superior/medial/inferior), revealed a significant interaction between condition and location [$F(1, 19) = 6.69$; $p < 0.05$], reflecting the negative-going waveforms for directed-passive-coarse over parietal electrode sites, and the positive-going waveforms for directed-passive-coarse over right-frontal electrode sites.

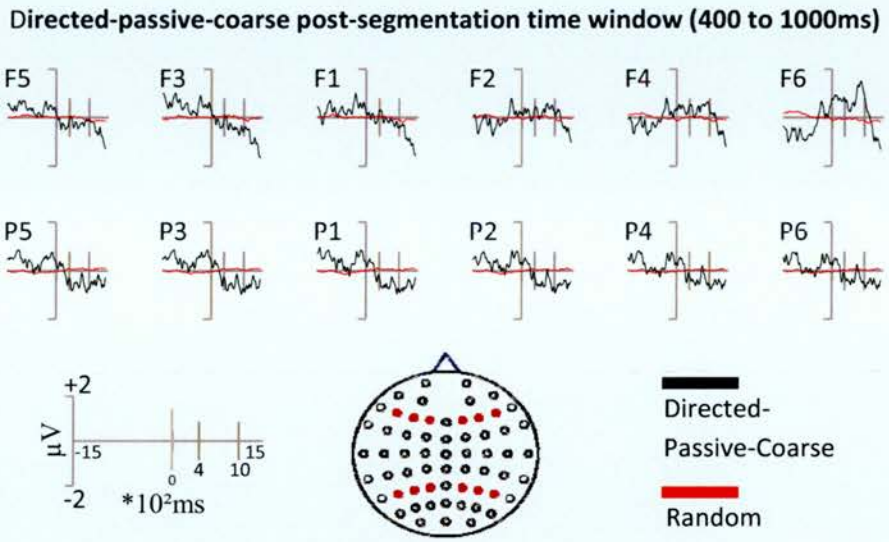

Figure 5-6: Grand average ERPs elicited for directed-passive-coarse (black) and random (red). Parietal electrodes demonstrate more negative-going activity for passive-coarse compared to random, and right-frontal electrodes demonstrate more positive-going activity between 400 and 1000ms.

A further interaction between condition and hemisphere [$F(1, 19) = 12.09$; $p < 0.01$] reflects the strong differences between the left and right hemispheres, which is most evident at frontal electrodes (see Figure 5-6). A 3-way interaction was also revealed between condition, location and hemisphere [$F(1, 19) = 5.01$; $p < 0.05$], which reflects the positive-going waveforms for directed-passive-coarse over right-frontal electrode sites as compared to the lateralized negative-going waveforms for directed-passive-coarse over parietal electrode sites. Finally, an additional 3-way interaction between condition, hemisphere and site [$F(1.42, 26.99) = 3.94$; $p < 0.05$] reflects the fact that the effects present over left-lateralised sites are largest over superior electrodes, whereas in right-lateralised sites the effects are

largest at inferior electrodes, as illustrated in Figure 5-7 and detailed in Table 5-3.

T-test results for directed-passive-coarse and random conditions

Left-Frontal Electrodes		Right-Frontal Electrodes	
F5	-	F6	[t(19) = -3.16; p < 0.01]
F3	-	F4	-
F1	-	F2	-
Left-Parietal Electrodes		**Right-Parietal Electrodes**	
P5	[t(19) = -3.19; p < 0.01]	P6	[t(19) = -2.05; p < 0.1 (0.055)]
P3	[t(19) = -3.22; p < 0.01]	P4	[t(19) = -2.21; p < 0.05]
P1	[t(19) = -2.79; p < 0.05]	P2	[t(19) = -2.55; p < 0.05]

Table 5-3: Resulting p-values from the two-tailed t-tests performed on each electrode included in the ERP analysis of directed-passive-coarse and random conditions in the post-segmentation time window 400 to 1000ms. The results reflect the wide spread parietal nature of the effect, and the divergences in waveforms found over the right-frontal electrodes.

Voltage magnitudes for directed-passive-coarse and random conditions

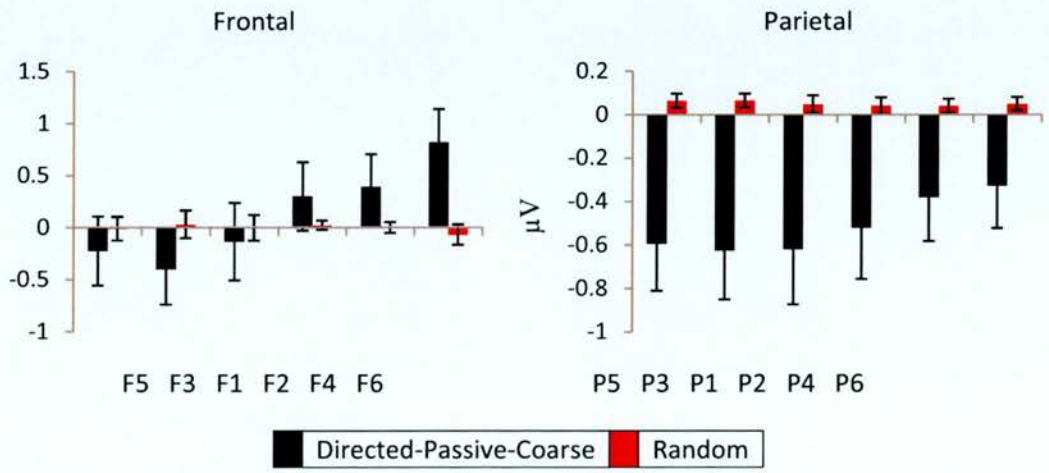

Figure 5-7: Differences in effect size at frontal and parietal electrode sites are shown for directed-passive-coarse (black) and random (red) segmentation points; right-lateralised frontal, and bi-lateral parietal sites display significantly different magnitudes.

5.2.3.1.3 Topographic analysis

Figure 5-8 shows the scalp distributions of the differences between directed-passive-coarse and random conditions for both pre- and post-segmentation time windows, illustrating a clear change in the pattern of effects over time.

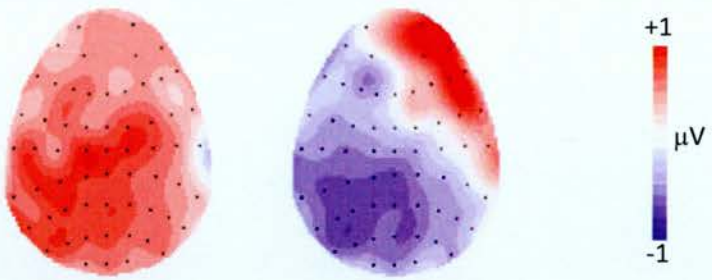

Figure 5-8: Topographic distributions of the directed-passive-coarse/random difference for the pre- and post-segmentations. Each cartoon shows the distribution of the difference between directed-passive-coarse and randomly generated segmentations, averaged across a 300ms period for the first time window (-400 to -100ms), and across 600ms for the second (400 to 1000ms). The front of the head is at the top of each map, and the left hemisphere is on the left-hand side. Each dot represents a recording electrode. The scale bar indicates the range of activity (in microvolts). The effect in the first time window has a centro-left-lateralised and centro-posterior distribution; whereas the effect in the second time window exhibits left-lateralised negativity over parietal electrodes and a right-lateralised positivity over frontal electrodes.

ANOVA with factors of epoch (-400 to -100ms/400 to 1000ms), location (frontal/parietal), hemisphere (left/right) and site (superior/medial/inferior), revealed a main effect of epoch [$F(1, 19) = 5.89$; $p < 0.05$], which reflects the broad differences present in the scalp distributions over the two time windows - notably the changing polarity of the effect over time. The presence of a significant interaction between epoch and hemisphere [$F(1, 19) = 4.98$; $p < 0.05$], indicates that the effects do exhibit distinct topographies, with a slight left greater than right asymmetry during

the first time window and the opposite right greater than the left asymmetry in the later time window.

Although the topographic maps shown in Figure 5-8 suggest that the later effect exhibits a strong frontal/posterior difference, no significant interactions involving location were present. Nonetheless, the topographic analyses confirm that the pattern of effects is distributionally different pre- and post-segmentation, inferring the engagement of at least partially, if not wholly, different sets of neural generators.

5.2.3.2 Investigating directed-passive-fine grain segmentation

Figure 5-9 shows the grand average directed-passive-fine and randomly generated event segmentation waveforms for passive segmentation from all 61 EEG electrode sites. The mean number of trials (± SD) contributing to the ERPs was 122 (59) for directed-passive-fine. As previously noted, the randomly generated ERPs are evidently close to flat, reflecting random background EEG. In contrast, the segmentation ERP is clearly not flat, exhibiting a distinct morphology, with a changing pattern of activity over time.

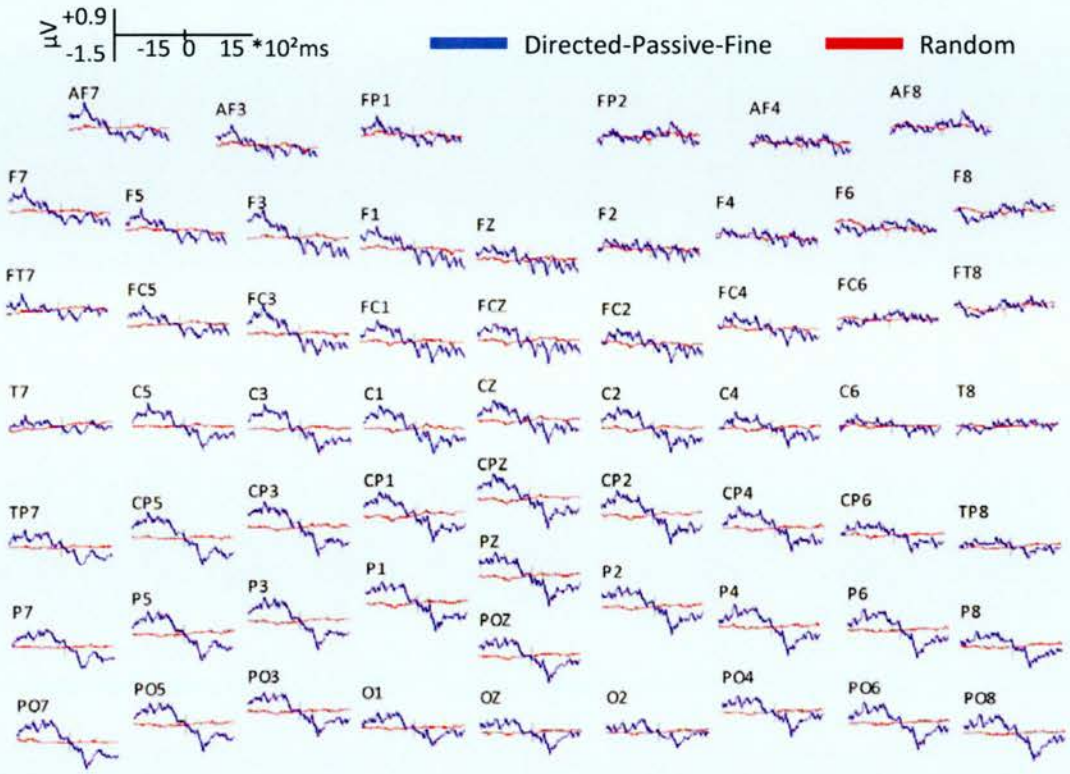

Figure 5-9: Grand average ERPs elicited for directed-passive-fine (blue) and random (red). More positive-going activity is present over left-frontal for directed-passive-fine compared to random ERPs between -400 and -100ms. Parietal electrodes show more negative-going activity between 400 and 1000ms, and right-frontal electrodes appear to show more positive-going activity between 400 and 1200ms.

5.2.3.2.1 Pre-segmentation time window (-1100 to -400ms)

As previously, a pre-segmentation time window was selected; the ERPs in Figure 5-9 clearly show a pre-segmentation divergence in the waveforms bi-laterally over parietal electrodes, and this is reflected in the overview data shown in Table 5-4. To capture the bi-lateral nature of the parietal divergence, a time-window from -1100ms to -400ms was selected.

Directed-Passive-Fine Segmentation

Time window (*10²ms)	-15	-14	-13	-12	-11	-10	-9	-8	-7	-6	-5	-4	-3	-2	-1
Left Frontal		*	*	*	*	*	*		*						
Right Frontal															
Right Parietal					*	*	*	*	*	*	*	*			
Left Parietal		*	*	*	*	*	*	*	*	*	*				

Time window (*10²ms)	0	1	2	3	4	5	6	7	8	9	10	11	12	13	14
Left Frontal		*			*	*	*				*		*		
Right Frontal															
Right Parietal				*	*	*	*	*	*	*		*			
Left Parietal	*	*	*	*	*	*	*	*	*	*	*	*	*	*	

Event Boundary Perception

Table 5-4: Overview table showing the data mined comparison of directed-passive-fine and random conditions. To demonstrate the correlation between the ERP grand average waveforms and the overview data an example is provided: the first row in the table shows a left frontal scalp quadrant effect present during from -1400 to -800ms, indicating the presence of an effect - in this case reflective of the positive-going waveforms present over left frontal electrode sites for the directed-passive-fine condition, as shown in Figure 5-9. Overview data allow visually identified time window definitions to be refined, thus revealing the most robust effects.

Figure 5-10 shows the grand average ERPs time-locked to directed-passive-fine and randomly generated segmentation points; ANOVA with factors of condition (directed-passive-fine/random), location (frontal/parietal), hemisphere (left/right) and site (superior/medial/inferior), revealed a main effect of condition [$F(1, 19) = 12.96$; $p < 0.01$]. A further interaction was revealed between condition and hemisphere [$F(1, 19) = 9.06$; $p < 0.01$] reflecting the larger divergences present over electrodes over the left hemisphere.

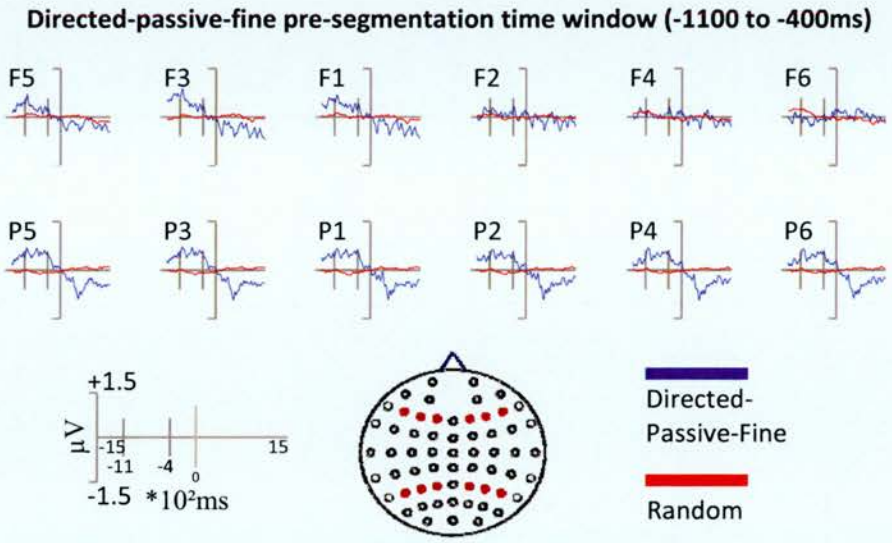

Figure 5-10: Grand average ERPs elicited for directed-passive-fine (blue) and random (red). Left-frontal and bi-lateral parietal electrodes demonstrate more positive-going activity for directed-passive-fine compared to random between -1100 and -400ms.

Additionally, a 3-way interaction was revealed between condition, hemisphere and site: [$F(1, 19) = 11.56$; $p < 0.01$], reflecting the stronger nature of the effect present on medial sites over the left hemisphere. A further 3-way interaction was revealed between condition, location and site [$F(1.43, 27.23) = 4.36$; $p < 0.05$], reflecting the stronger medial nature of the effect present over frontal electrode sites, which is not seen over parietal sites. Subsidiary t-tests (listed in Table 5-5) and voltage magnitudes (illustrated in Figure 5-11) for the electrodes submitted to ANOVA over frontal and parietal locations, reveal stronger effects for directed-passive-fine are found bi-laterally over parietal and left-frontal sites.

T-test results for directed-passive-fine and random conditions

Left-Frontal Electrodes		Right-Frontal Electrodes	
F5		F6	
F3	[t(19) = 2.92; p < 0.01]	F4	
F1	[t(19) = 2.36; p < 0.05]	F2	
Left-Parietal Electrodes		**Right-Parietal Electrodes**	
P5	[t(19) = 3.88; p < 0.005]	P6	[t(19) = 4.16; p < 0.005]
P3	[t(19) = 3.89; p < 0.005]	P4	[t(19) = 3.75; p < 0.005]
P1	[t(19) = 3.41; p < 0.01]	P2	[t(19) = 3.05; p < 0.01]

Table 5-5: Resulting p-values from the two-tailed t-tests performed on each electrode included in the ERP analysis of directed-passive-fine and random conditions in the pre-segmentation time window -1100 to -400ms. The results reflect the wide spread parietal nature of the effect, and the effect found over the left-frontal electrodes.

Voltage magnitudes for directed-passive-fine and random conditions

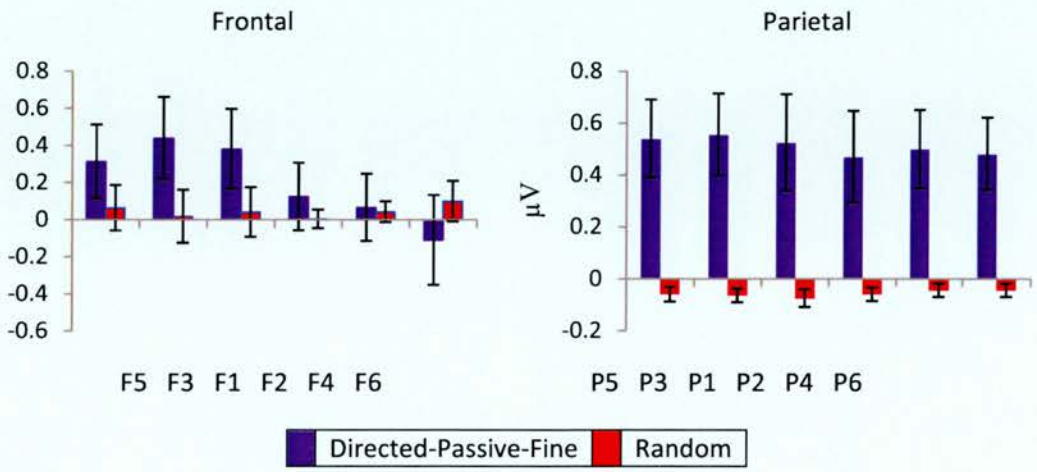

Figure 5-11: The magnitude of ERP effects from -1100 to -400ms, at frontal and parietal electrode sites are shown for directed-passive-fine (blue) and random (red) segmentation points. Error bars represent one standard error of the mean. Significantly larger effect sizes were present for directed-passive-fine compared to random segmentation ERPs bi-laterally over parietal electrode sites, and medially over left-frontal sites.

5.2.3.2.2 Post-segmentation time window (300 to 1000ms)

The post-segmentation time window from 300 to 1000ms was identified for analysis owing to the ERP waveforms (shown in Figure 5-9) indicating, and the overview data confirming (listed in Table 5-4), the presence of a long lasting parietal effect. Grand average ERPs time-locked to directed-passive-fine and randomly generated segmentation points are illustrated in Figure 5-12.

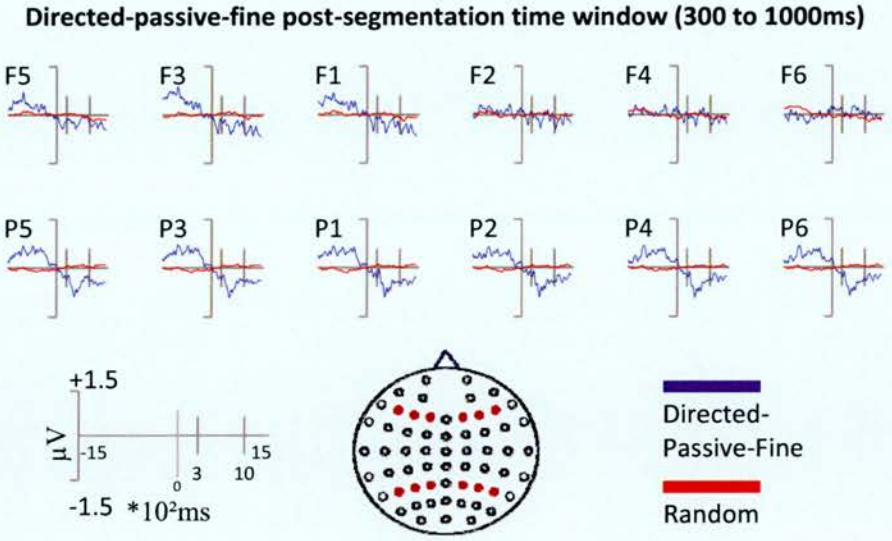

Figure 5-12: Grand average ERPs elicited for directed-passive-fine (blue) and random (red). Parietal electrodes demonstrate more negative-going activity for directed-passive-fine compared to random between 300 and 1000ms.

ANOVA with factors of condition (directed-passive-fine/random), location (frontal/parietal), hemisphere (left/right) and site (superior/medial/inferior), revealed a main effect of condition [$F(1, 19) = 15.38$; $p < 0.001$]. Further interactions were found between condition and location [$F(1, 19) = 7.37$; $p < 0.05$] and between condition and hemisphere [$F(1, 19) = 5.14$; $p < 0.05$], reflecting the parietal and left-sided nature of the

effect respectively. A further interaction was revealed between condition and site [$F(1.31, 24.88) = 4.17$; $p < 0.05$], which reflects the superior-medial nature of the effect. A 3-way interaction was revealed between condition, location and hemisphere [$F(1, 19) = 7.27$; $p < 0.05$] which reflects the strong bi-lateral nature of the effect present over parietal sites, and the left-sided nature of the effect present over frontal sites.

As justified by the proceeding analyses, individual two tailed t-tests were performed on the electrodes selected for analysis (see Table 5-6), revealing significant segmentation effects present predominantly over parietal electrodes. Figure 5-13 shows the voltage magnitudes for the electrodes submitted to ANOVA over frontal and parietal locations.

T-test results for directed-passive-coarse and random conditions

Left-Frontal Electrodes		Right-Frontal Electrodes	
F5	-	F6	-
F3	[t(19) = -2.96; p < 0.01]	F4	-
F1	[t(19) = -2.24; p < 0.05]	F2	-
Left-Parietal Electrodes		**Right-Parietal Electrodes**	
P5	[t(19) = -4.24; p < 0.001]	P6	[t(19) = -4.37; p < 0.001]
P3	[t(19) = -4.36; p < 0.001]	P4	[t(19) = -4.06; p < 0.005]
P1	[t(19) = -3.81; p < 0.005]	P2	[t(19) = -3.51; p < 0.01]

Table 5-6: Resulting p-values from the two-tailed t-tests performed on each electrode included in the ERP analysis of directed-passive-fine and random conditions in the post-segmentation time window 300 to 1000ms. The results reflect the wide spread parietal nature of the effect, and the effect found superiorly and medially over left-frontal electrode sites.

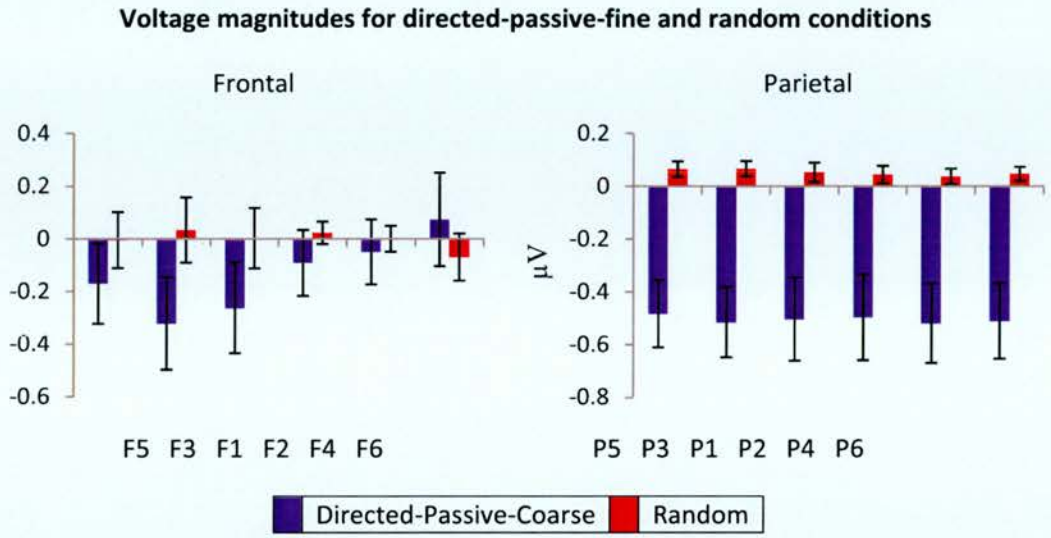

Figure 5-13: Differences in effect size at frontal and parietal electrode sites are shown for directed-passive-fine (blue) and random (red) segmentation points. Significantly larger effect sizes were present for directed-passive-fine compared to random segmentation points over left-frontal electrode sites and bi-laterally over parietal sites.

5.2.3.2.3 Topographic analysis

Figure 5-14 shows the scalp distributions of the differences between directed-passive-fine and random conditions for both pre- and post-segmentation time windows, illustrating a clear change in the pattern of effect over time. ANOVA with factors of epoch (-1100 to -400ms/300 to 1000ms), location (frontal/parietal), hemisphere (left/right) and site (superior/medial/inferior), revealed a main effect of epoch [$F(1, 19) = 15.53$; $p < 0.01$], which reflects the broad differences present in the scalp distributions over the two time windows - notably the changing polarity of the effect over time. The presence of a significant interaction between epoch and location [$F(1, 19) = 5.23$; $p < 0.05$], reflects the positive-going effect over parietal sites when compared to frontal sites during the pre-segmentation

time window, then shifting to become more negative-going when compared to frontal electrode sites during the post-segmentation time window.

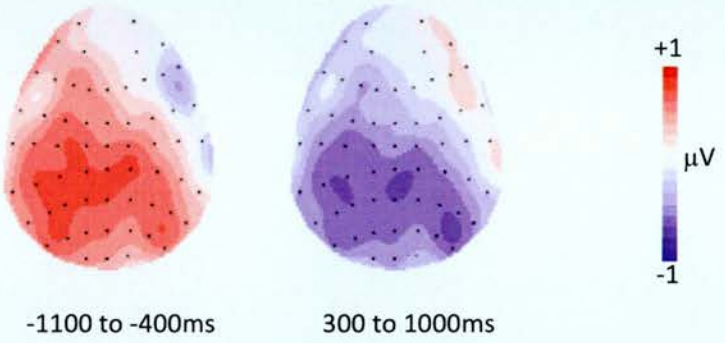

Figure 5-14: Topographic distributions of the directed-passive-fine/random difference for the pre- and post-segmentations. Each cartoon shows the distribution of the difference between directed-passive-fine and randomly generated segmentations, averaged across a 700ms period for the first time window (-1100 to -400ms), and across 700ms for the second (300 to 1000ms). The front of the head is at the top of each map, and the left hemisphere is on the left-hand side. Each dot represents a recording electrode. The scale bar indicates the range of activity (in microvolts). The effect in the first time window has a centro-left-lateralised and centro-posterior distribution; whereas the effect in the second time window exhibits left-lateralised negativity over parietal electrodes and a right-lateralised positivity over frontal electrodes.

A further interaction was revealed between epoch and hemisphere [$F(1, 19) = 8.25$; $p < 0.05$], which reflects the left-lateralised positive-going nature of the effect present during the pre-segmentation time window that changes polarity over time, becoming more negative-going when compared to the right hemisphere during the post-segmentation time window. An additional 2-way interaction between epoch and site [$F(1.26, 23.96) = 4.35$; $p < 0.05$] was revealed, and this reflects the superior-medial nature of the effect during the pre-segmentation time window, which changes to inferior-medial during the post-segmentation time window. A 3-way interaction was revealed between epoch, location and hemisphere [$F(1, 19) = 11.24$; $p < 0.01$],

reflecting the strongest differences found over left-parietal electrode sites, which change in polarity over time. Additionally, a 3-way interaction between epoch, location and site [$F(1.38, 26.21) = 3.81$; $p = 0.05$] reflects the medial nature of the effect over frontal sites when compared to parietal sites during the pre-segmentation time window, which changes to inferior in nature over frontal sites when compared to parietal sites during the post-segmentation time widow. In summary, the topographic analyses confirm that the pattern of effects is distributionally different pre- and post-segmentation, inferring the differential engagement of neural generators.

5.2.3.3 Comparing directed-passive-coarse and fine grain segmentation

Figure 5-15 shows the grand average directed-passive-coarse and directed-passive-fine waveforms for passive segmentation from all 61 EEG electrode sites. Despite the problem of overlapping epochs, the waveforms do appear to display clear differences in waveform morphology; divergences are present from approximately -1450ms pre-segmentation, with the ERPs for directed-passive-coarse becoming more negative than those for directed-passive-fine over right-frontal electrode sites until approximately -700ms. At approximately -400ms pre-segmentation the ERPs for directed-passive-coarse become more positive-going than for directed-passive-fine over left-parietal sites, central sites and bi-laterally over frontal sites.

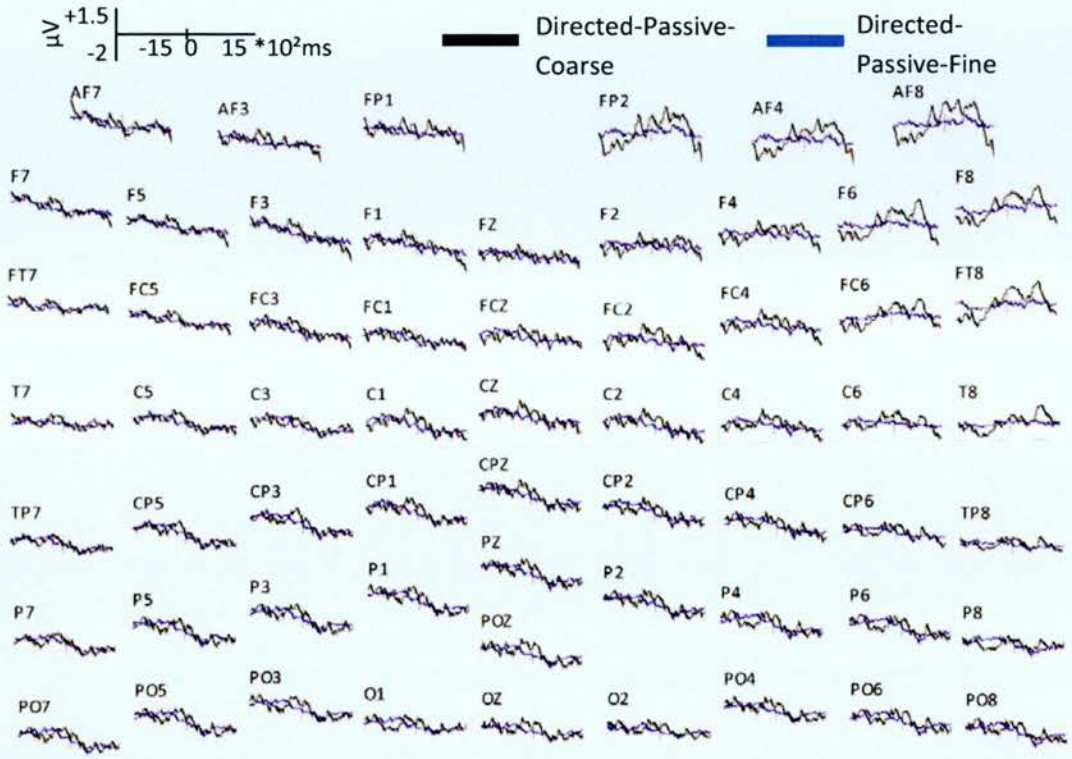

Figure 5-15: Grand average ERPs elicited for directed-passive-coarse (black) and directed-passive-fine (blue). More positive-going activity is present globally for directed-passive-coarse compared to directed-passive-fine ERPs between -400 and -100ms. Right-frontal electrodes show more positive-going activity between 400 and 1200ms.

The positive-going deflection for directed-passive-coarse ERPs continues until approximately 300ms over left-parietal, central and left-frontal electrodes sites, with the effect continuing until approximately 1200ms over right-frontal sites. Also notable, is a pre-segmentation divergence present over right-parietal electrode sites, with the ERPs for directed-passive-coarse becoming more negative-going than for directed-passive-fine from approximately -800ms and continuing until -400ms.

Directed-Passive-Coarse versus Directed-Passive-Fine Segmentation

Time window (*10²ms)	-15	-14	-13	-12	-11	-10	-9	-8	-7	-6	-5	-4	-3	-2	-1
Left Frontal															
Right Frontal															
Right Parietal				*											
Left Parietal														*	

Time window (*10²ms)	0	1	2	3	4	5	6	7	8	9	10	11	12	13	14
Left Frontal															
Right Frontal									*	*					
Right Parietal		*													
Left Parietal															

Event Boundary Perception

Table 5-7: Overview table showing the data mined comparison of directed-passive-coarse and directed-passive-fine conditions; the pattern of data is reflective of the divergences present in Figure 5-15.

5.2.3.3.1 Pre-segmentation time window (-200 to -100ms)

In line with the analyses in previous sections, a pre-segmentation time window between-100 and -200ms was selected by identifying divergences in the ERP waveforms (Figure 5-15) and confirming their presence using the overview data (Table 5-7). Figure 5-16 shows the grand average ERPs time-locked to directed-passive-coarse and directed-passive-fine segmentation points over the electrode sites selected for analysis.

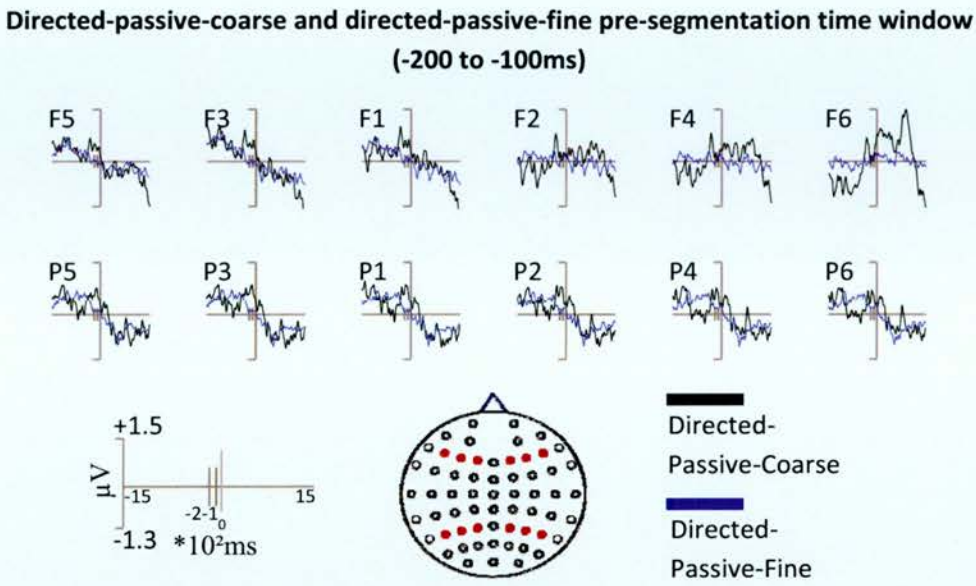

Figure 5-16: Grand average ERPs elicited for directed-passive-coarse (black) and directed-passive-fine (blue). Parietal electrodes demonstrate more positive-going activity for directed-passive-coarse compared to directed-passive-fine between -200 and -100ms.

ANOVA with factors of condition (directed-passive-coarse/directed-passive-fine), location (frontal/parietal), hemisphere (left/right) and site (superior/medial/inferior), revealed only a marginal effect of condition [$F(1, 19) = 3.08$; $p < 0.1$ (0.095)], perhaps owing to the problems with overlapping epochs (see General Methods, Section 4.2.3.1).

5.2.3.3.2 Post-segmentation time window (800 to 1000ms)

As previous, a post-segmentation time window from 800ms to 1000ms was selected for analysis (overview data available in Table 5-7); Figure 5-17 shows the grand average ERPs time-locked to directed-passive-coarse and directed-passive-fine segmentation points over the electrode sites selected for analysis.

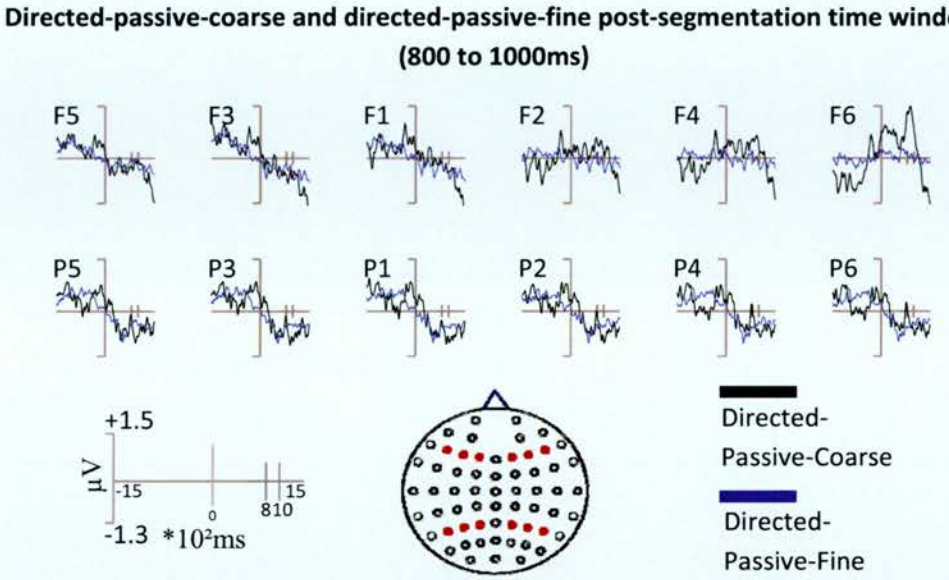

Figure 5-17: Grand average ERPs elicited for directed-passive-coarse (black) and directed-passive-fine (blue). Right-frontal electrodes appear to demonstrate more positive-going activity for directed-passive-coarse compared to directed-passive-fine between 800 and 1000ms.

To examine the pattern of directed-passive-coarse/directed-passive-fine effects during the selected time window, the data were submitted to ANOVA with factors of condition (directed-passive-coarse/directed-passive-fine), location (frontal/parietal), hemisphere (left/right) and site (superior/medial/inferior), which failed to reveal a main effect of directed-passive-coarse/ directed-passive-fine. However, significant interactions were revealed between condition and hemisphere [$F(1, 19) = 13.21$; $p < 0.01$], reflecting the right-lateralised nature of the effect. Finally, in addition, a 3-way interaction was revealed between condition, hemisphere and site [$F(1.41, 26.8) = 4.64$; $p < 0.05$], which reflects the increasing size of the effect over inferior right-sided sites relative to the lack of interactions over any sites over the left hemisphere, as illustrated in Figure 5-18. These data were subsequently subjected to a series of t-tests (reported in Table 5-8); significant

segmentation effects are only present over inferior right-frontal parietal electrode sites.

T-test results for direct-passive-coarse and directed-passive-fine conditions

Left-Frontal Electrodes		Right-Frontal Electrodes	
F5	-	F6	[t(19) = -3.44; p < 0.01]
F3	-	F4	-
F1	-	F2	-

Left-Parietal Electrodes		Right-Parietal Electrodes	
P5	-	P6	-
P3	-	P4	-
P1	-	P2	-

Table 5-8: Resulting p-values from the two-tailed t-tests performed on each electrode included in the ERP analysis of directed-passive-coarse and directed-passive-fine conditions in the post-segmentation time window 800 to 1000ms. The results reflect the specific right-frontal nature of the effect.

Voltage magnitudes for directed-passive-coarse and directed-passive-fine conditions

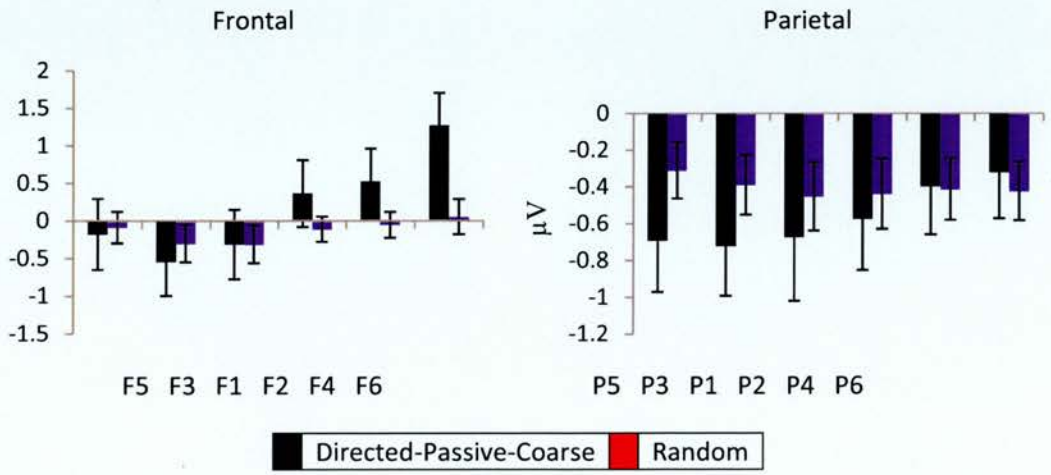

Figure 5-18: Differences in effect size at frontal and parietal electrode sites are shown for directed-passive-coarse (black) and directed-passive-fine (blue) segmentation points. A significantly larger effect sizes was present for directed-passive-coarse compared to directed-passive-fine segmentation points inferiorly over right-frontal parietal electrode sites.

5.2.3.3.3 Topographic analysis

Figure 5-19 illustrates a clear change in the pattern of effect over time. ANOVA with factors of directed-passive-coarse minus random/directed-passive-fine minus random, epoch (-200 to -100ms/800 to 1000ms), location (frontal/parietal), hemisphere (left/right) and site (superior/medial/inferior), revealed only a marginally significant 3-way interaction between directed-passive-coarse minus random/directed-passive-fine minus random, epoch and location [$F(1, 19) = 3.29$; $p < 0.1$ (0.86)], reflecting the marginally parietal greater than frontal distribution pre-segmentation, when compared to the frontal greater than parietal distribution post-segmentation. Focussed contrasts directly comparing locations, hemispheres and sites across directed-passive-coarse and directed-passive-fine pre-event segmentation failed to reveal any interactions. Conversely, analysis of post-segmentation topographic data revealed a significant 3-way interaction between directed-passive-coarse minus random/directed-passive-fine minus random, hemisphere and site [$F(1.31, 24.84) = 4.04$; $p < 0.05$], which reflects the inferiorly distributed positive-going effect over right-lateralised electrodes, when compared to the broad distribution of the effect present over left-lateralised electrode sites. Therefore, the topographic analyses failed to confirm that the pattern of effects is distributionally different for the directed-passive-coarse minus random/directed-passive-fine minus random ERPs between pre- and post-segmentation. Furthermore, focussed analysis failed to reveal any differential engagement during pre-segmentation time. Nevertheless, the analyses do confirm the differential engagement of neural generators between the conditions post-segmentation.

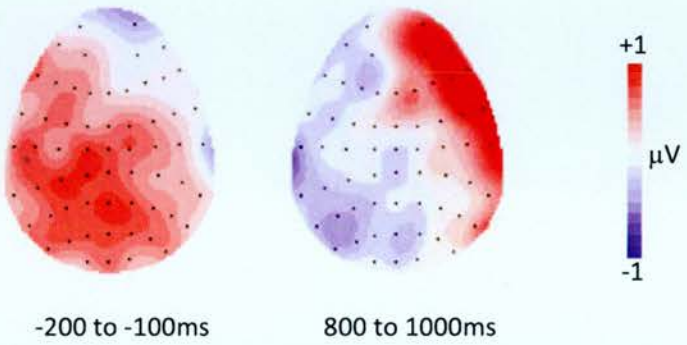

Figure 5-19: Topographic distributions of the directed-passive-coarse/directed-passive-fine difference for the pre- and post-segmentations. Each cartoon shows the distribution of the difference between directed-passive-coarse and directed-passive-finely generated segmentations, averaged across a 100ms period for the first time window (-200 to -100ms), and across 200ms for the second (800 to 1000ms). The front of the head is at the top of each map, and the left hemisphere is on the left-hand side. Each dot represents a recording electrode. The scale bar indicates the range of activity (in microvolts. The effect in the first time window has a centro-left-lateralised and centro-posterior distribution; whereas the effect in the second time window exhibits left-lateralised negativity over parietal electrodes and a right-lateralised positivity over frontal electrodes.

5.2.3.4 Active segmentation

5.2.3.4.1 Introduction

The examination of neurophysiological data thus far has focussed on passive-event segmentation, in line with the Zacks et al (2001) study. However, participant's neural activity was also measured during active segmentation. Contrasting with passive-event segmentation, active-event segmentation requires participants to actively mark event boundaries by pressing a button. The physical action of pressing a button is a primary consequence of the primary motor cortex instructing a limb to move, thus, neural activity is generated in the motor cortex. Consequently, it is likely that

active-event segmentation ERPs will reflect the culmination of primary motor cortex activation, and cognitive functions correlated with event segmentation.

To investigate active segmentation data and the activation of motor activity, average ERPs were formed. ERPs were time-locked to the segmentation point, with a -200 to 1500ms epoch. These data are shown in Figure 5-20 which reveals that neural activity generated in the primary motor cortex is predominant in active ERPs as illustrates, and therefore, it may be assumed that this magnitude of predominance will be present throughout all studies reported in this thesis. Consequently, this section aims to investigate the magnitude of primary motor cortex activation as an index of cognitive load during active segmentation present during this experiment.

Magnitude differences in primary motor cortex responses may be indicative of the underlying cognitive function specific to the experimental task. In particular, the difference in task between coarse and fine-grain event segmentation may give rise to differing magnitudes of activation if, for example, participants reflectively place more emphasis on larger event segments owing to the hierarchical nature of event segmentation. Therefore, it is hypothesised that significance of larger event segments will elicit greater responses for coarse-grain as compared to fine-grain segmentation, which would be in line with the Zacks et al. study. Furthermore, it is reasonable to assume that cumulative neurophysiological responses measured at the scalp may be affected by the experimental manipulations presented in this thesis. The following sections outline the analysis strategy employed to analyse motor cortex activation during active-event segmentation.

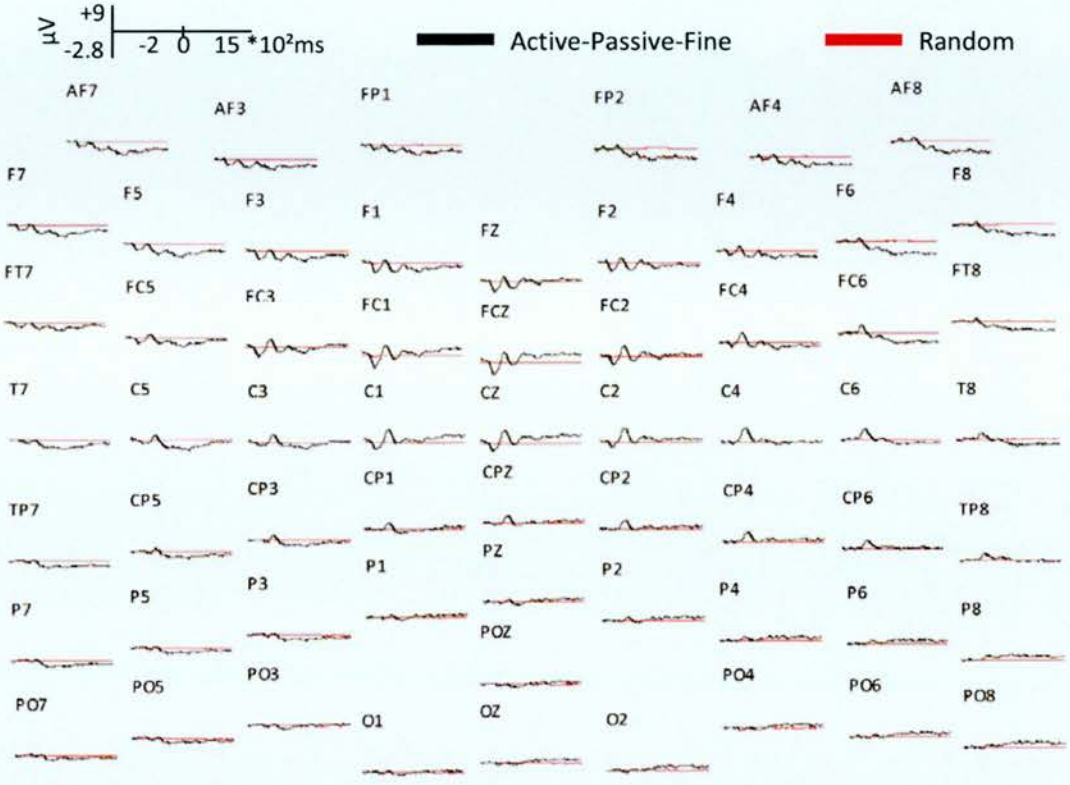

Figure 5-20: Grand average ERPs elicited for active-fine (black) and random (red). More negative-going activity is present across frontal electrodes sites for active-fine compared to random ERPs between 0ms and 1500ms. Significantly however, distinctive negative and positive-going waveform morphology is present across central electrodes sites subsequent to active-segmentation; most likely a result of primary motor cortex activation, generated when participants press a button to mark an event boundary.

5.2.3.4.2 Selecting an electrode site

Owing to the uncertainty of topographical distribution exhibited by experimental effect, a rigorous approach was taken when investigating passive-event segmentation; multiple broadly-distributed electrodes were selected for analysis. Conversely, the investigation of active-event segmentation focuses on a single electrode: CZ, as shown in Figure 5-21 (b).

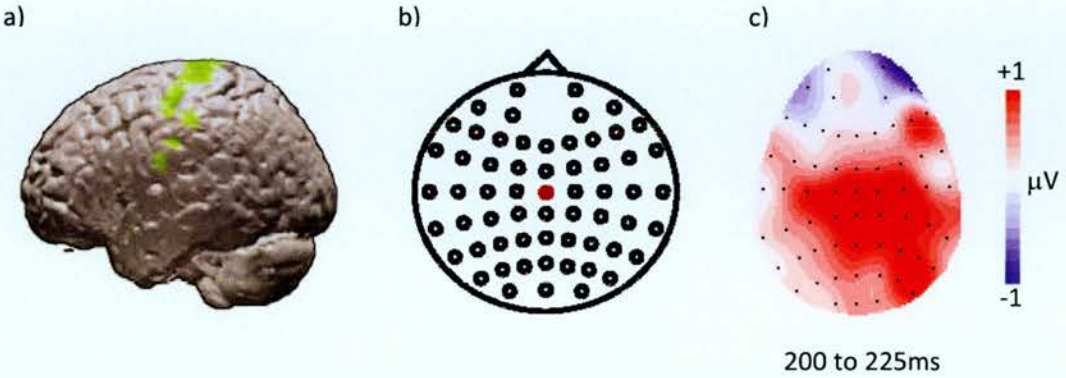

Figure 5-21: The centralised locality of electrode site CZ is hypothesised to be the electrode most likely to reflect primary motor cortex activation. (a) Side-elevation of a representation of the human brain, the left hemisphere is in view, with the front of the brain pointing left. The areas marked green show activation of the motor cortex measured in the fine-spatial domain of fMRI (image courtesy of http://upload.wikimedia.org/wikipedia). (b) Scalp map of electrode site positioning used in the fine temporal domain of EEG based on the International 10-20 montage system. The central-midline electrode site CZ selected for analysis is highlighted in red. (c) Topographic distribution of the difference between active-fine and random conditions sampled in this chapter, averaged across a 25ms time period between 200 and 225ms (surrounding the greatest centralised positive-going waveforms). The front of the head is at the top of the map, and the left hemisphere is on the left-hand side. Each dot represents a recording electrode. The scale bar indicates the range of activity (in microvolts). The effect is clearly distributed across centralised electrode sites, mostly likely reflecting motor cortex activation.

The location of the primary motor cortex in the human brain is illustrated in Figure 5-21 (a), showing neural activity present in the dorsal part of the precentral gyrus and the anterior bank of the central sulcus (also known as Brodmann area 4). Figure 5-21 (c) shows a scalp map of the topographic differences between active-fine and random ERPs, which clearly demonstrate a centralised distribution of effect. In comparing the known location of the primary motor cortex (upper middle of the brain, in relatively close proximity to the scalp) and the active segmentation scalp map (showing centrally distributed activity, over the top of the scalp), it is reasonable to assume that the activity displayed in the scalp map reflects mostly primary

motor cortex activation. Therefore, the central midline electrode CZ was selected for analysis owing to its central proximity in relation to the scalp and the effect shown in Figure 5-21 (c).

5.2.3.4.3 ERP method

Pre-segmentation activity has been reported in the previous analysis reported in this chapter, and in the Zacks et al. (2001) study. However, as this section is investigating the magnitudes of primary motor cortex activation across experiments, the neural correlates of anticipating active segmentation are not as interesting. This is in no small part because active segmentation ERPs reflect conscious decisions being taken to mark event boundaries, in an activity that has been viewed shortly before. In addition, pre-segmentation activity is most likely to reflect anticipatory motor responses, due to the large amount of activity measured in the time surrounding the button press. Consequently, the analysis in this chapter focuses solely on post-segmentation time, in which primary motor cortex activity is recorded e.g. slightly after the button press. Therefore, a pre-segmentation baseline of 200ms is used to reference the 1500ms post-segmentation activity time window. Visual inspection of the waveforms in Figure 5-20 clearly show primary motor cortex activation to be maximal at around 200ms, thus a time window of 200ms to 225ms is used to isolate positive-going activity. The following section contains the results of the magnitude analyses of primary motor cortex activity across all experiments.

5.2.3.4.4 Results

To investigate the magnitudes of motor cortex activation during active-coarse- and active-fine-grain segmentation, the central midline electrode CZ was selected for analysis. Figure 5-22 shows the grand average ERPs for active-coarse and active-fine segmentation on electrode CZ. Activity surrounding the maximal positive-going deflections in the waveforms e.g. the most notable waveform morphology over centralised electrodes, was selected for magnitude analysis. These data were subjected to a t-test examination on electrode CZ.

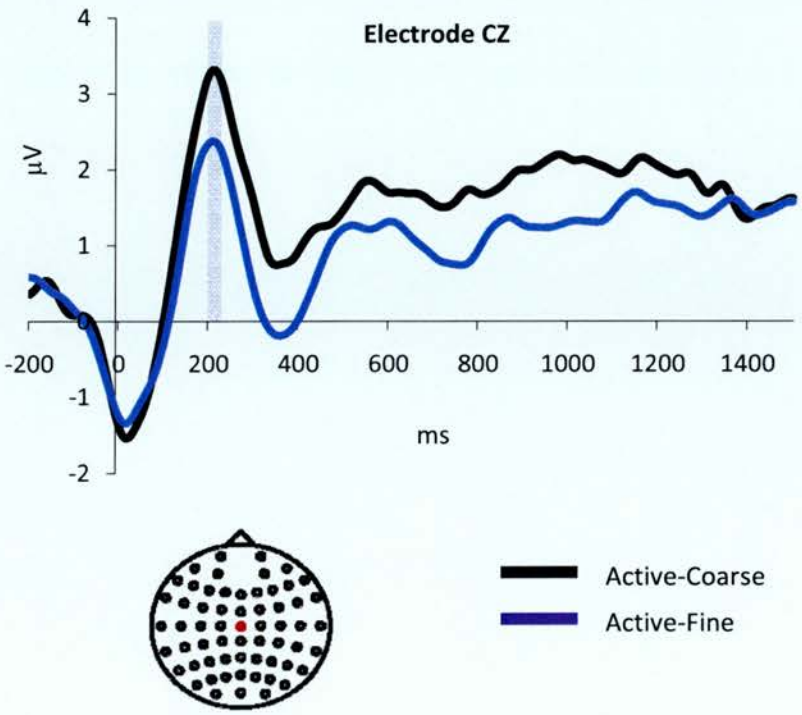

Figure 5-22: Grand average ERPs elicited for active-coarse (black) and active-fine (blue) on the electrode site CZ (shown as the red dot on the scalp map). More positive-going activity is present for active-coarse ERPs compared to active-fine ERPs during the 200 to 225ms time window (shaded grey).

Analysis of the data revealed a clear difference in magnitude between active-coarse and active-fine segmentation [$t(19) = 2.48$; $p < 0.05$], with the ERPs for active-coarse more positive-going than those for active-fine. For illustrative purposes, the magnitude analysis and topographic distribution are illustrated Figure 5-23 (a) and (b) respectively.

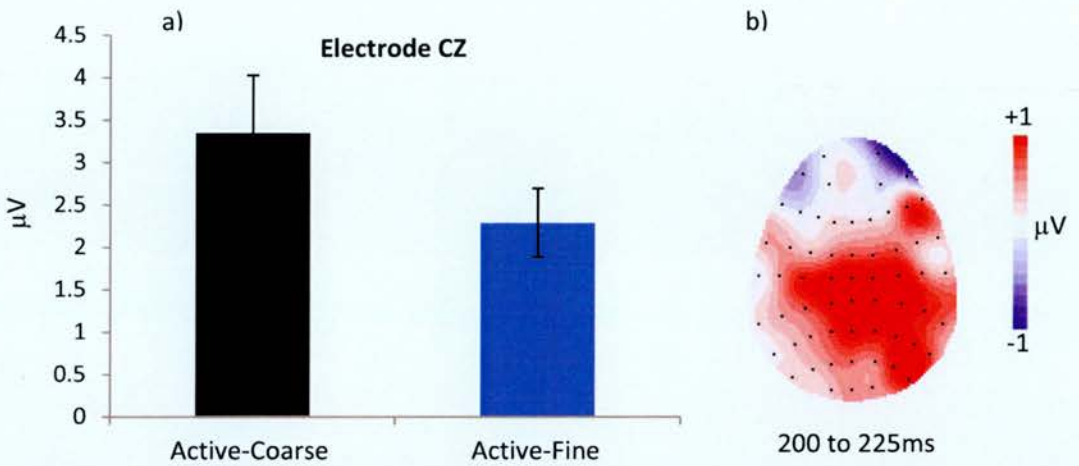

Figure 5-23: (a) Differences in effect sizes at electrode site CZ are shown for active-coarse (black) and active-fine (blue) segmentation points. Significantly larger effect sizes were present for active-coarse compared to active-fine segmentation points. (b) Topographic distribution of the active-coarse/active-fine difference averaged across a 25ms time period (200 to 225ms). The front of the head is at the top of the map, and the left hemisphere is on the left-hand side. Each dot represents a recording electrode. The scale bar indicates the range of activity (in microvolts). The effect is clearly distributed across the central electrodes, mostly likely reflecting the magnitude differences originating in the motor cortex. Additionally, the effect shows a centro-right-lateralised and centro-posterior distribution.

In summary, the results clearly demonstrate greater voltage magnitude for active-coarse segmentation when compared to active-fine segmentation, indicating higher significance participants may place upon coarse grain segmentation boundaries. Moreover, the results are analogous

and supportive of the coarse-greater-than-fine results reported in the Zacks et al. (2001) study.

5.2.4 Discussion

The aim of the experiment was to investigate whether the effects reported by Zacks et al. (2001) in their fMRI study of event segmentation could be replicated using ERPs. The experiment was based upon the paradigm set out by Newtson (1973) and employed by Zacks et al. (2001), but crucially, participants in the current experiment were aware of the requirement to actively segment the activities depicted in the videos during 'passive' viewing. As the passive viewings also reflect participant's knowledge of the experimental task, the passive viewings are referred to as 'directed-passive' viewings. In line with the original paradigm, participants viewed the movies under three conditions; passive (or directed-passive), coarse-grain segmentation and fine-grain segmentation. To compare the conditions, a baseline set of ERPs was produced which reflects background EEG activity.

5.2.4.1 Summary and interpretation

ERPs for directed-passive-coarse showed the presence of a positive-going pre-segmentation effect over parietal electrodes, when compared to the baseline ERPs. Additionally, when comparing the ERPs for directed-passive-coarse and randomly generated segmentation points, a positive-going post-segmentation effect was revealed over right-frontal electrode sites, and a negative-going effect was found bi-laterally over posterior sites. Most notably, the effects found over parietal sites shift in polarity over time, more specifically they swap polarity at approximately the point of event

segmentation (0ms). Topographic analyses revealed the engagement of differential neural generators over time, suggesting that at least partially, if not wholly, different psychological processes are engaged pre- and post directed-passive-coarse segmentation.

In contrast with the ERPs for directed-passive-coarse, ERPs for directed-passive-fine showed the emergence of an earlier, and longer-lasting, effect present over parietal electrode sites pre-segmentation. Similarly, however, the pre-segmentation effects for both directed-passive-coarse and directed-passive-fine were found over parietal electrode sites, and exhibited the same polarity when compared to the baseline randomly generated ERPs. In correspondence with the ERPs for directed-passive-coarse, the ERPs for directed-passive-fine shift in polarity from positive-going to negative-going when compared with the baseline ERPs, at around the time of segmentation. Post-segmentation effects were also revealed when comparing directed-passive-fine ERPs with baseline ERPs, which at least partially mirror the comparison of directed-passive-coarse and baseline ERPs; both effects present over parietal electrode sites are negative-going and occur over more or less the same post-segmentation period. In contrast with the ERPs for directed-passive-coarse, the ERPs for directed-passive-fine do not contain a post-segmentation effect present over right-sided frontal electrode sites. Nonetheless, topographic analyses revealed corresponding results with those performed on directed-passive-coarse ERPs, with strong evidence indicating the engagement of different psychological processes, pre- and post-segmentation.

In comparing the ERPs from directed-passive-coarse with those from directed-passive-fine, less convincing evidence was found for the engagement of different sets of neural generators. Only a marginally

significant difference was found pre-segmentation over left-parietal electrode sites. However, analysis of post-segmentation data did reveal an inferiorly distributed positive-going effect over right-lateralised electrodes, when compared with the broad distribution of the ERP differences present over left-lateralised electrodes. Despite the problem of overlapping ERPs discussed earlier, the analysis of post-segmentation scalp distributions infers the differential engagement of neural generators between directed-passive-coarse and directed-passive-fine conditions.

In summary, the ERPs for directed-passive-coarse and directed-passive-fine are broadly similar, particularly over parietal electrode sites. Both exhibit positive-going pre-segmentation and negative-going post-segmentation effects when compared to the baseline ERPs over parietal sites. However, the ERPs for directed-passive-coarse and directed-passive-fine do also differ, notably with right-sided frontal effects found post-segmentation in directed-passive-coarse ERPs. Both sets of ERPs show reliable differences in the pattern of effects over time, and analysis confirmed the presence of differentially engaged neural generators, pre- and post-segmentation. Given the problem of overlapping ERPs as discussed in section 5.2.3.1, it is perhaps unsurprising that similarities exist between directed-passive-coarse and directed-passive-fine ERP. Nevertheless, it is clear from the analyses that at least partially, if not wholly, different sets of neural generators are engaged during directed-passive-coarse and directed-passive-fine post-segmentation. The ERP evidence therefore supports the suggestion that participants are capable of passively segmenting events on differing levels of granularity, and that different psychological processes are engaged when segmenting at different grains. Moreover, it may be inferred that different sets of psychological processes are engaged pre- and post-segmentation, when

segmenting events at both a coarse and fine grain. Fundamentally, and perhaps most importantly, the data support the hypothesis that the regions of the brain that respond to event segmentation are measurable with EEG.

5.2.4.2 Comparison with Zacks et al. (2001) study

It is clear that a number of similarities exist between the results of the current ERP experiment and the Zacks study. Firstly, both pre- and post-segmentation neural responses were recorded during passive video viewings. Secondly, responses were measured during both passive and active segmentation runs. Thirdly, distinguishable neural correlates were revealed for coarse- and fine-grained segmentation during passive and active viewings in both studies. Lastly, although the link between the fine spatial locations revealed by fMRI and the broad scalp distributions are weak due to the inverse problem and skull attenuation, it is interesting to note that the regions of the scalp over which ERPs effects are present, roughly correlate with the network of regions identified in the Zacks study. More specifically, bi-lateral effects were revealed posteriorly, and right-sided effects were present over frontal electrodes in both studies.

Although the ERP study and the Zacks study do have many comparable results, several differences exist between the studies that must also be considered. Firstly, perhaps the most striking difference in the results is the apparent difference in the pattern of responses elicited for coarse compared to fine grain segmentation during passive viewing. The Zacks study reported stronger activity for coarse- than fine-grain segmentation only in posterior locations, and only after the segmentation. By contrast, there is, however, some evidence in the ERP study for stronger responses

occurring in passive-coarse grain segmentation as compared to passive-fine grain that occurs pre-segmentation. Specifically, data from the pre-segmentation time window (when comparing passive-coarse and passive-fine grain segmentation ERPs) exhibit a difference, but one that is difficult to isolate to posterior electrodes; significant differences in magnitude were present over parietal locations at individual electrode sites, but no interaction with location was found when the data were analysed further. Nevertheless, given the nature of the effects present in passive-fine and passive-coarse segmentation ERPs (i.e., positive-going deflections relative to the baseline), the evidence indicates the effect for passive-coarse segmentation is stronger (more positive-going) than that for passive-fine segmentation during the pre-segmentation time window. In contrast, there is very little evidence to support greater responses in passive-coarse segmentation than in passive-fine segmentation in the post-segmentation window. An effect was noted over the right-frontal electrode locations when comparing the ERPs; however, it cannot be suggested that ERPs share a common polarity as the ERPs for passive-fine segmentation are relatively close to flat, compared with positive-going ERPs for passive-coarse segmentation over right-frontal electrode sites.

Conversely, and although focussed as described in section 5.2.3.6.2, the magnitude analysis performed on active segmentation ERPs clearly demonstrated a greater response elicited for coarse-grain segmentation than for fine post-segmentation, which is in line with the data presented by Zacks et al. (2001).

Another striking difference with the Zacks study is the identification of differential neural activity between pre- and post-segmentation. The current experiment indicates that pre- and post-segmentation activity is

temporally distinct, and moreover, separated by a time period surrounding segmentation at 0ms in which no significant activity was reported. Confirmation of the differential engagement of sets of neural generators pre- and post-segmentation in both passive-coarse- and passive-fine-grain segmentation further extends, and additionally confirms the discrepancy. This result is somewhat surprising given that the data produced in the Zacks study suggests that a single set of neural generators were active, onsetting before segmentation and continuing until after segmentation. To some extent, from a hierarchical perspective, this might be considered surprising; given that the segmentation point is considered to be significant in terms of how ongoing information is processed, there might be expected to be changes in the pattern of processing before and after segmentation occurs.

In the Zacks study, the fMRI data revealed varying levels of response pre- and post-segmentation time (i.e., the response increased in size, being much larger after the segmentation). The evidence reported in this study strongly suggests that different sets of neural generators are active during pre- and post-segmentation. Why then should the fMRI and ERP data reveal such different results? One possibility is that they reflect different underlying signals, revealing two equally valued views of the neural basis of event segmentation. However, another possibility exists; the differences between the studies may reflect the difference in task knowledge levels between the studies (i.e., during the Zacks study participants had no knowledge of the segmentation task during passive viewing, while conversely, participants in the current study were aware of the paradigm prior to passive viewing). Certainly, if as hypothesised in the literature, coarse-grain event segmentation were influenced mostly by top-down knowledge, differences between the Zacks study and the current study would be expected to be

found, particularly in relation to the coarse-grain condition. Differences in the fine-grain condition would be expected to be minimal if this process is influenced mostly by bottom-up knowledge, such as the physical correlates of the activity. Although these hypothesised differences are difficult to assess with the current study and Zacks study results, it is proposed that the following chapter follow the exact paradigm used in the original Zacks study, thus allowing a comparison of directed-passive and true (or task naive) passive event segmentation solely with ERPs.

The use of ERPs to measure the neural correlates of event segmentation does require some consideration when interpreting the results. For example, as discussed in the ERPs chapter, the problems of skull attenuation and dipole alignment may render some neural activity immeasurable with EEG and difficult to interpret topographically. Therefore, it may be possible that the lack of reported neural activity surrounding the perception of an event breakpoint in this experiment, is due to the inherent problems of EEG recording. Moreover, the source of activity is unrecoverable due to the inverse problem, and therefore EEG data lacks ability to isolate activity on a fine spatial resolution like the Zacks study. Nonetheless, the ERPs do provide sufficient neurophysiological data to facilitate the disclosure of clearly defined effects of event segmentation. Additionally, and perhaps owing to the fine temporal resolution of EEG, the ERP data demonstrate the engagement of different sets of neural generators; information that is unique to the field of event segmentation.

What then does this data add to the theory of event segmentation? One implication may be that the perception of an event boundary reflects multiple cognitive functions engaged when processing information. If existing cognitive representations are retrieved to increase prediction

accuracy, while also updated based upon errors in prediction as proposed by Event Segmentation Theory (EST), it may be assumed that multiple cognitive functions facilitate these actions. Furthermore, if as the data suggest events are internally represented as hierarchical structures, one might expect the engagement of additional cognitive function as sub-events are defined and grouped. Finally, the Zacks data suggest that neural activity surrounding the perception of an event boundary may be in part generated by the processing of motion and interpretation of movement. Thus, it may be reasonable to expect the activation of additional neural generators during event segmentation; activity which at least partially reflects lower-level cognitive functions such as motion processing.

In sum, the ERP data facilitate a more complex model of event segmentation, one in which different neural generators are active pre- and post-segmentation, and additionally for coarse- and fine-grain segmentation. This model may reflect more accurately the likely numerous psychological tasks active when processing information. Moreover, despite the conservative analysis strategy (e.g. selecting only one time window from pre-segmentation and one time window from post-segmentation time), and the resulting likelihood that additional neural activity was not revealed, the data and analysis strategy do provide sufficient evidence for the engagement of multiple neurological processes.

5.2.4.3 Comparison with event segmentation literature

In addition to the similarities in neurological terms with the Zacks study, the behavioural results also share similar attributes with previous investigations, i.e., participants segmented the activities in terms of parts and sub-parts forming a hierarchical relationship between coarse and fine grain

segmentation (see Zacks, Tversky, et al., 2001; Zacks et al. (2001). Furthermore, the raster plots shown in Figure 5-1 suggest that there is common agreement between participants as to where the natural boundaries between event parts occur, and this finding is in line with broadly agreed views of event segmentation (e.g. Newtson, 1973a; Zacks & Tversky, 2001; Bower et al., 1979). However, also in similarity with the neurological data, differences exist between the behavioural results of the current experiment and event segmentation literature. Specifically, the study failed to replicate the findings of Hard et al. (2001), which reported that coarse-grain event boundaries lay significantly after fine-grain boundaries in temporal space. Hard et al. conclude that the results reflect a psychological consequence of event segmentation; coarse-grain boundaries are used to subsume fine-grain events parts. Furthermore, the authors interpret these findings as a reflection of the hierarchical nature of internally represented event structures. Given the abovementioned replication of hierarchical analyses, it is perhaps surprising that the current study fails to replicate the results of the Hard et al. hierarchical analysis. One area of culpability for the idiosyncratic results may lie with presence of task knowledge in the current study. Therefore, the call for following study to exactly replicate the paradigm followed by Zacks et al. in 2001 is further supported, so that clarity may be brought to the behavioural results.

5.3 Conclusions

The chapter reported an experiment that investigated the effects of event segmentation in both the behavioural and neural domains. There was evidence to suggest that the study is broadly in line with previous research in event segmentation. Namely, that the participant agreement over event boundaries, and partial behavioural evidence for hierarchical structuring, is consistent with the literature. Furthermore, the neural data contained several comparable features with the Zacks study, including neural responses to passive and active event segmentation, present for both coarse- and fine-grain segmentation. There was little evidence to support the claims made by Zacks et al. (2001) that coarse-grain segmentation elicits greater responses than fine-grain event segmentation during passive segmentation, although a similar effect was noted pre-segmentation in the ERP study. Nonetheless, analysis of active segmentation data did reveal a greater magnitude present for coarse-gain event segmentation when compared with fine-grain event segmentation.

In real life, breaking ongoing activity down into manageable chunks for processing is likely to invoke many psychological processes such as ongoing retrieval and refinement of existing cognitive schemata, prediction engineering and sensory perceptual processing. Therefore, the data presented in the current study appear to fit such a complex model of information processing; multiple neural generators are differentially active during event boundary perception. The data support the view that event segmentation takes place on multiple levels of granularity; a feature which reflects the importance of event structure in information processing, and perhaps the differential influence of top-down knowledge and bottom-up processing upon coarse- and fine-grain event segmentation.

Fundamentally, given the success of this study in proving that neural responses during directed event segmentation can be measured using EEG, the following study should follow the original paradigm used in the Zacks study to investigate whether the pattern of ERP effect revealed during task naive passive segmentation will be more directly comparable with the Zacks study.

6 The perception of everyday events

6.1 Introduction

The previous experiment demonstrated that the neural correlates of event segmentation could be measured using scalp recorded EEG. Moreover, the experiment revealed that the neural processing of event boundaries was differentially sensitive to coarse and fine grain segmentation, and differentially engaged neural generators pre- and post-segmentation. Participants were also found to encode the activities shown in the movies into parts and their constituent sub-parts, thus forming a segmentation hierarchy, which supported previous findings. Importantly however, the previous experiment differed from the Zacks et al. (2002) study, in that participants had explicit knowledge of the experimental task prior to watching the activities passively.

The experiment reported in this chapter extends the previous pilot experiment firstly; by employing a larger number of participants to increase statistical power and secondly; by replicating the event segmentation paradigm exactly (i.e. by excluding participants knowledge of the paradigm). This chapter aims to replicate the Zacks et al. study to investigate whether the neural correlates of *passive* event segmentation may be measured with scalp recorded EEG. Given the relative success of the pilot study, it is hypothesised that the current study will reveal the neural correlates of passive event segmentation using EEG. Furthermore, it is hypothesised that the differential processing of event boundaries will be reflected in the results of this study in line with the pilot and Zacks et al. studies, and moreover, given the results of the pilot study, that different neural generators will be present pre- and post-segmentation. Additionally, a replication of the

hierarchical nature of event segmentation reported in the pilot and Zacks et al. studies is expected. It is further hypothesised that withholding task knowledge from participants in the current experiment, will produce a replication of the hierarchical findings reported by Hard et al. (2001).

In summary, the critical question to be addressed in this experiment is whether a close replication of the paradigm employed in the Zacks study will elicit clear pre- or post segmentation activity, and whether differences between coarse and fine grain segmentation will be present.

6.2 Experiment 2: Investigating passive segmentation of everyday events using ERPs

6.2.1 Methods

The following sections detail the experimental methods followed in this experiment.

6.2.1.1 Stimuli

Jeffrey M. Zacks (University of Washington, St. Louis) provided the videos used in this experiment. Each video was a fixed shot, single scene recording of one actor performing an everyday task. The four activities were doing the laundry, making the bed, planting plants and washing the car.

6.2.1.2 Participants

Twenty-seven participants with took part in the experiment; the data from three participants was discarded due to behavioural non-compliance, leaving 24 participants (8 male, age range 18-37).

6.2.1.3 Procedure

The current procedure differed from that employed in the original paradigm (Newtson, 1973) as participants neural activity was recorded via scalp mounted electrodes to allow ERPs to be formed time-locked to their responses, as described in the General Methods chapter. Importantly, the current procedure replicated Zacks et al. (2001) by excluding task knowledge; participants were asked to simply watch the videos while maintaining attention. Participants watched all videos passively, and then actively segmented the videos into large or small segments on subsequent viewings.

6.2.2 Behavioural results

The following section contains analysis of behavioural data collected from 24 participants as they performed the event segmentation experiment.

6.2.2.1 Investigating the concurrence of event perception

As in the previous experiment the automaticity of event segmentation was investigated by examining participant agreement, illustrated in Figure 6-1. In line with the findings from the pilot study, visual inspection of the raster plots clearly indicates a common perception of event boundaries in time, particularly for the coarse conditions.

Correlation results for coarse- and fine-grain event perception

Activity	Coarse-grain and fine-grain
Doing the laundry	$r(299) = 0.501$; $p < 0.001$
Making the bed	$r(311) = 0.448$; $p < 0.001$
Planting plants	$r(353) = 0.418$; $p < 0.001$
Washing the car	$r(430) = 0.606$; $p < 0.001$

Table 6-1: Resulting p-values from the correlation tests performed on the temporal response distributions for coarse- with fine-grain segmentation. As expected, the results reflect the strong relationship between coarse- and fine-grain event perceptions, clearly indicating that participants perceive separate levels of event segmentation to be interdependent.

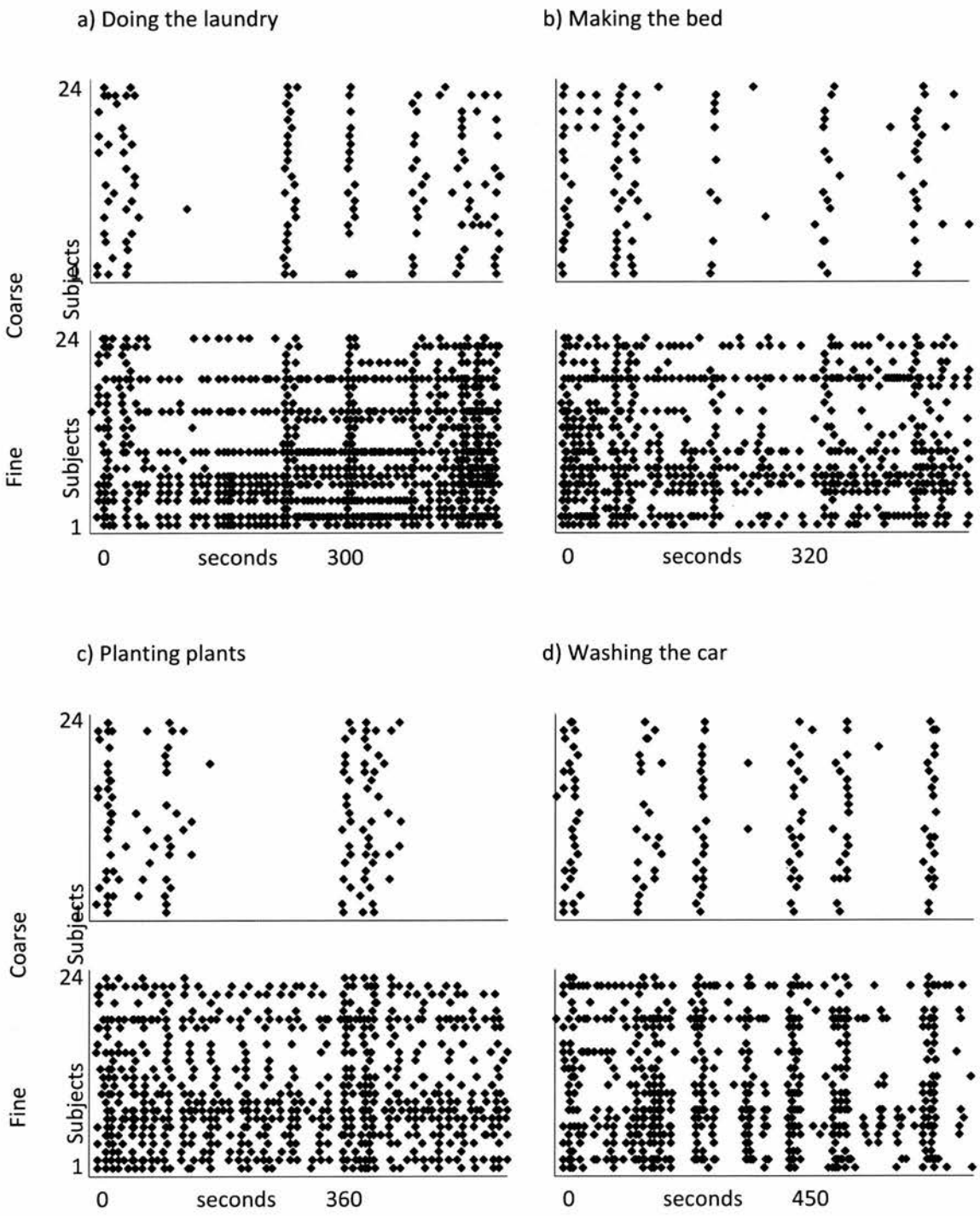

Figure 6-1: Raster plots of segmentation timings (x-plane) for each participant (y-plane), shown separately for each movie (a-d), for fine and coarse conditions. Each individual data point reflects a single segmentation response.

As described in the General Methods chapter, Temporal Response Distributions (TDRs) were formed for participant responses to examine the relationship between fine- and coarse-grain event boundary perceptions. The results (listed in Table 6-1) demonstrate a high-level of association between coarse- and fine-grain boundary perceptions across all activities, suggesting that participants perceive separate levels of event segmentation to be interdependent.

6.2.2.2 Investigating the hierarchical nature of event perception

Figure 6-2 shows the mean value of recorded and randomly placed overlap time-bins calculated for each activity. ANOVA with factors of condition (recorded/randomly placed) and activity (doing the laundry, making the bed, planting plants and washing the car), revealed a main effect of condition overlap time-bins [$F(1,23) = 359.31$; $p < 0.001$], reflecting the greater chance of participants overlapping fine and coarse-grain segmentation points than when the segmentations are generated randomly. No interaction was revealed between condition overlap time bins and activity, reflecting the broadly similar strategy present across all movie stimuli. T-test results (reported in Table 6-2), demonstrate that hierarchical performance was present for each movie. In summary, the behavioural results clearly indicate that participants encoded the activity in terms of hierarchical relationships between parts and sub-parts.

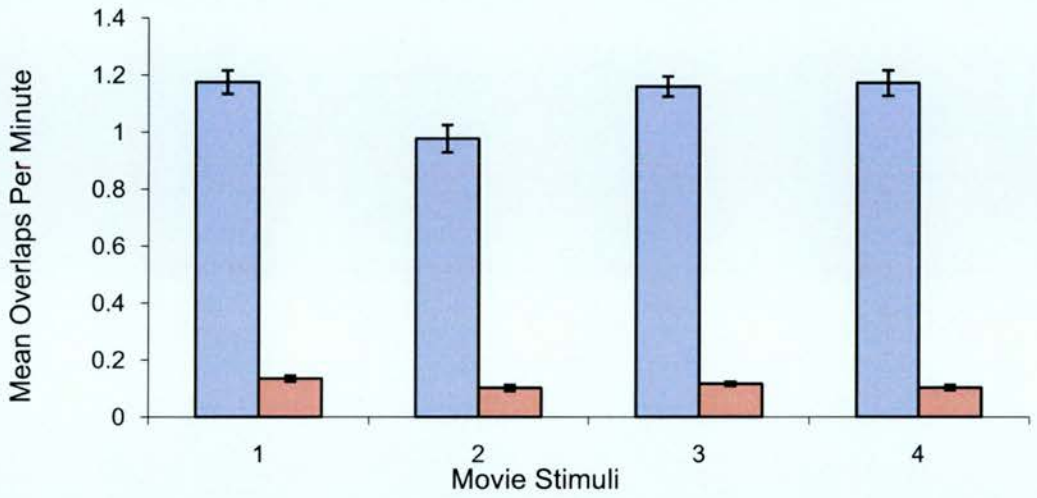

Figure 6-2: Mean number of overlap time-bins for recorded (purple) and randomly placed (blue) segmentations per minute are shown for each video; (1) doing the laundry, (2) making the bed, (3) planting plants and (4) washing the car. Error bars represent one standard error of the mean. For all four movies, significantly larger numbers of overlapping time-bins were recorded from participants marking coarse and fine event boundaries than would occur randomly.

T-test results for overlapping coarse- and fine-grain event perception

Activity	T-test result
Doing the laundry	[t(23) = -13.82; p < 0.001]
Making the bed	[t(23) = -10.92; p < 0.001]
Planting plants	[t(23) = -17.14; p < 0.001]
Washing the car	[t(23) = -13.72; p < 0.001]

Table 6-2: Resulting p-values from the two-tailed t-tests performed on each activity; clear differences are present between actual overlapping time bins recorded and those arising purely by chance.

Figure 6-3 shows the mean value of fine- before coarse-grain segmentations and coarse-before fine-grain segmentations. ANOVA with factors of condition (fine subsuming coarse/coarse subsuming fine) and

activity (doing the laundry, making the bed, planting plants and washing the car), revealed a main effect of condition [$F(1,23) = 16.1$; $p < 0.005$], reflecting the greater probability of participants using coarse-grain segmentation points to subsume fine-grain events. No interaction was revealed between condition and activity, reflecting the broadly similar strategy present across all movie stimuli. T-test results (reported in Table 6-3 reveal the pattern of coarse-grain event boundaries subsume fine-grain event parts across all movie stimuli. In summary, overall the behavioural results indicate that participants used coarse-grain event boundaries to group fine-grain event parts.

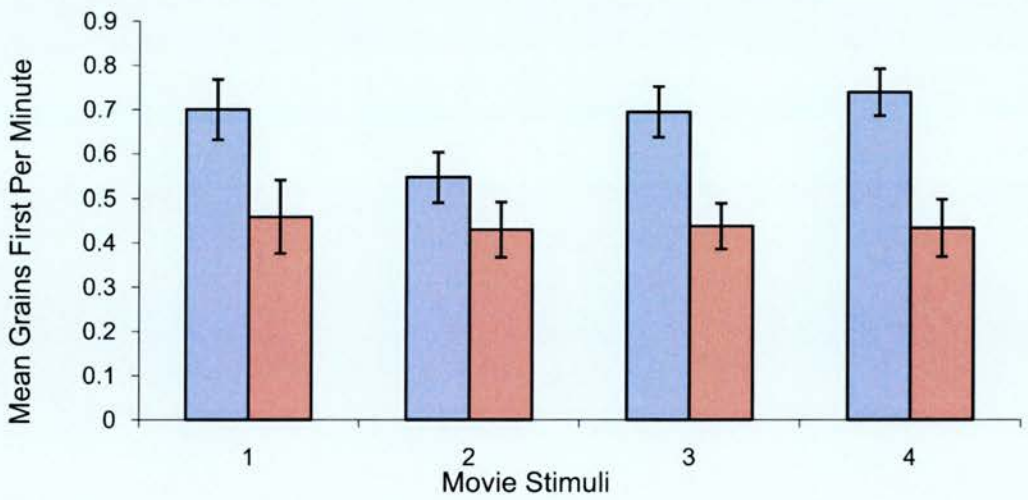

Figure 6-3: Mean number of fine- before coarse-grain segmentations (light blue), and coarse-before fine-grain segmentations (light red) per minute are shown for each video; (1) doing the laundry, (2) making the bed, (3) planting plants and (4) washing the car. Error bars represent one standard error of the mean. Movies three and four showed significantly larger numbers of fine- before coarse-grain segmentations than coarse- before fine-grain segmentations.

T-test results for coarse- subsuming fine-grain event perception

Activity	T-test result
Doing the laundry	[t(23) = 1.91; p < 0.1 (0.69)]
Making the bed	-
Planting plants	[t(23) = 3.08; p < 0.01]
Washing the car	[t(23) = 3.87; p < 0.005]

Table 6-3: Resulting p-values from the two-tailed t-tests performed on each activity analysing the use of coarse-grain boundaries to subsume fine-grain event parts. The results indicate a strong tendency for participants to automatically employ this strategy.

6.2.3 ERP Results

The following sections (6.2.3.1 to 6.2.3.3) describe the results of the ERP data collected during the current experiment of passive event segmentation described in this chapter. Subsequent sections compare the ERP results from the current experiment with those detailed in the previous chapter, which investigated directed event segmentation.

6.2.3.1 Investigating passive-coarse-grain segmentation

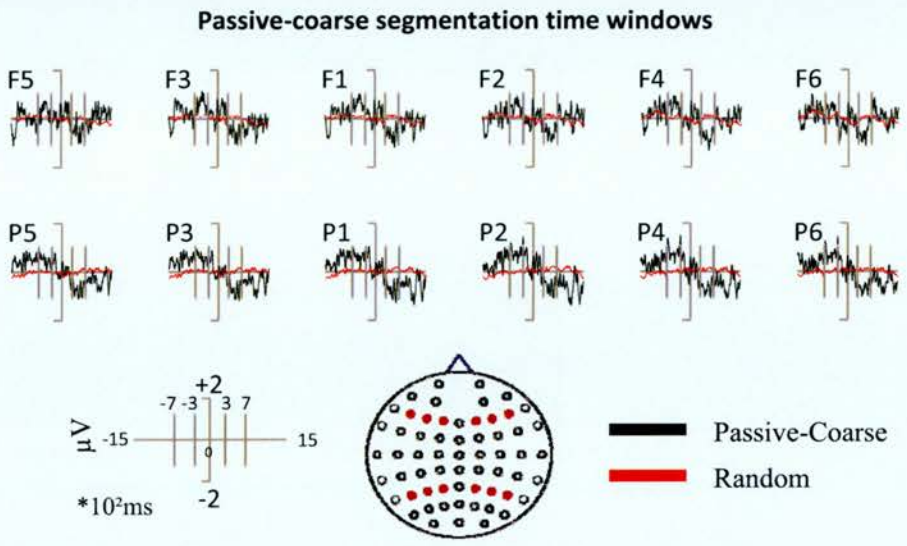

Figure 6-4: The pre-segmentation and post-segmentation time windows are illustrated.

6.2.3.1.1 Pre-segmentation time window (-700 to -300ms)

Following the steps outlined in the previous chapter (related overview tables are shown in Appendix A); a pre-segmentation time window of -700 to -300ms was selected. Figure 6-4 shows the grand average ERPs time-locked to passive-coarse and randomly-generated segmentation points over electrode sites selected for analysis. The mean number of trials (± SD) contributing to the ERPs was 25 (7) for passive-coarse.

ANOVA with factors of condition (passive-coarse/random), location (frontal/parietal), hemisphere (left/right) and site (superior/medial/inferior), revealed a marginal effect of condition [$F(1, 23) = 3.96$; $p < 0.1$ (0.059)], reflecting the weak nature of the effect, due to is

predominance over parietal electrodes only. However, an interaction between condition and site was revealed [$F(1.67, 38.48) = 7.21$; $p < 0.01$], reflecting the differences between passive-coarse and random conditions found over superior and medial electrode sites; present over frontal and parietal locations. To examine this pattern further, these data were subsequently subjected to a series of t-tests, examining each electrode individually (reported in Table 6-4). As is clear from the table, significant segmentation effects are predominantly present over parietal electrodes. Figure 6-5 shows the voltage magnitudes for the electrodes submitted to ANOVA over frontal and parietal locations. The magnitude analysis reflects the stronger effects for passive-coarse found superiorly and medially over frontal electrode sites, and across all parietal electrode sites.

T-test pairing results for passive-coarse and random (-700 to -300ms)

Left-Frontal Electrodes		Right-Frontal Electrodes	
F5	-	F6	-
F3	-	F4	-
F1	-	F2	-
Left-Parietal Electrodes		**Right-Parietal Electrodes**	
P5	[t(23) = 1.93; p < 0.1 (0.066)]	P6	[t(23) = 2.59; p < 0.05]
P3	[t(23) = 2.05; p < 0.1 (0.052)]	P4	[t(23) = 2.76; p < 0.05]
P1	[t(23) = 2.19; p < 0.05]	P2	[t(23) = 2.87; p < 0.01]

Table 6-4: T-test results for the passive-coarse and random pre-segmentation time window.

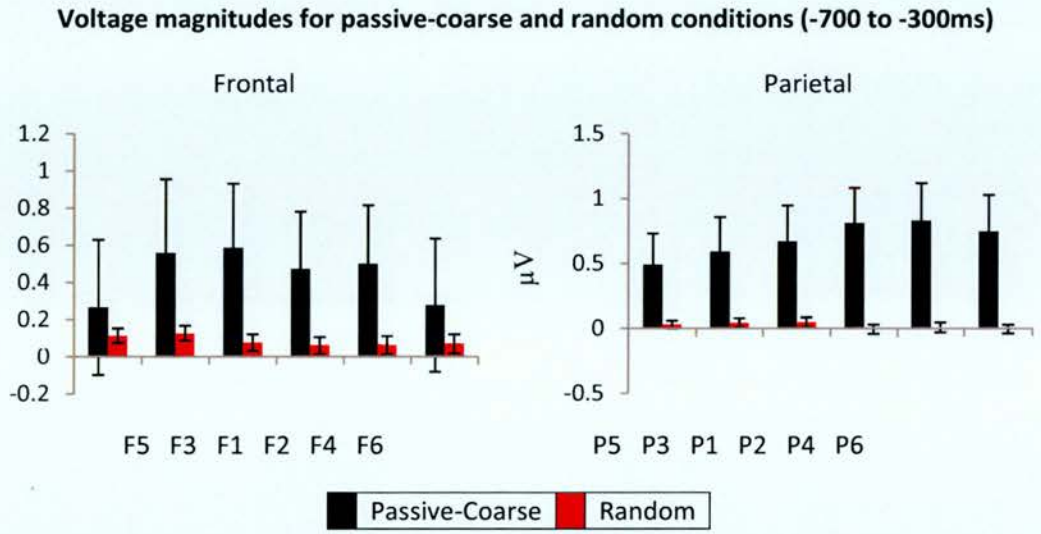

Figure 6-5: The magnitude of ERP effects from -700 to -300ms, shown as in Figure 5-7.

6.2.3.1.2 Post-segmentation time window (300 to 700ms)

A post-segmentation time window lasting from 300 to 700ms was identified for analysis. Grand average ERPs time-locked to passive-coarse and randomly-generated segmentation points are shown in Figure 6-4; ANOVA with factors of condition (passive-coarse/random), location (frontal/parietal), hemisphere (left/right) and site (superior/medial/inferior), revealed a only main effect of condition [$F(1, 23) = 4.68$; $p < 0.05$], which reflects a broad distribution of the differences in the ERP waveforms.

6.2.3.1.3 Topographic analysis

Figure 6-6 shows the scalp distributions of the differences between passive-coarse and random conditions for both pre and post segmentation time windows, illustrating a clear change in the pattern of effect over time.

ANOVA with factors of epoch (-700 to -300ms/300 to 700ms), location (frontal/parietal), hemisphere (left/right) and site (superior/medial/inferior), revealed a main effect of epoch [$F(1, 23) = 5.14$; $p < 0.05$], which reflects the broad differences between pre- and post-segmentation, notably the changing polarity of the effect over time. A further interaction between epoch and site [$(1.73, 39.88) = 3.95$; $p < 0.05$] reflects the superior-medial distribution of the effect found pre-segmentation, relative to the broad distribution found post-segmentation.

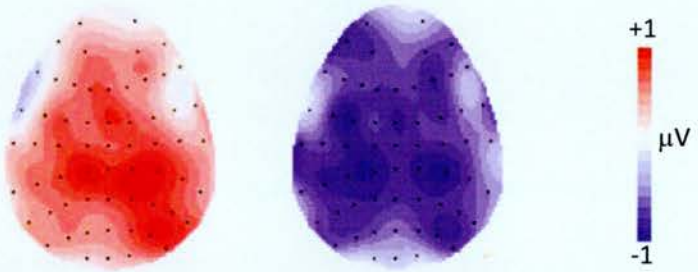

-700 to -300ms 300 to 700ms

Figure 6-6: Topographic distributions of the passive-coarse/random difference for the pre and post segmentations. Each cartoon shows the distribution of the difference between passive-coarse and randomly generated segmentations, averaged across a 400ms time period for the first time window (-700 to -300ms), and across 400ms for the second (300 to 700ms). The front of the head is at the top of each map, and the left hemisphere is on the left-hand side. Each dot represents a recording electrode. The scale bar indicates the range of activity (in microvolts). The effect in the first time window has a centro-right-lateralised and centro-posterior distribution; whereas the effect in the second time window exhibits bi-lateralised negativity over parietal electrodes.

6.2.3.2 Investigating passive-fine-grain segmentation

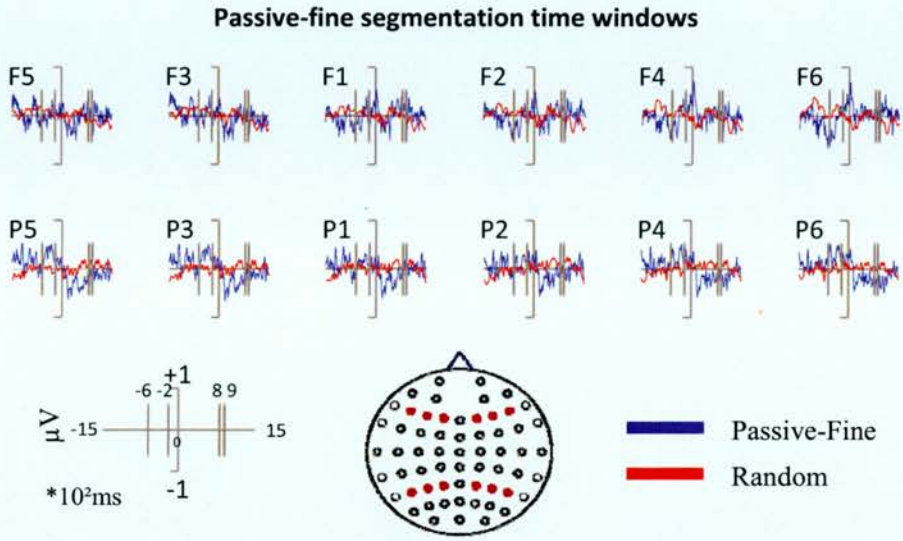

Figure 6-7: The pre-segmentation and post-segmentation time windows are illustrated.

6.2.3.2.1 Pre-segmentation time window (-600 to -200ms)

As previously a pre-segmentation time window was selected (related overview table available in Appendix A). Two pre-segmentation candidate time windows were initially identified; however, the period from -600ms to -200ms was favoured due to its closer temporal proximity to event boundary perception.

Figure 6-7 shows the grand average ERPs time-locked to passive-fine and randomly-generated segmentation points over electrode sites selected for analysis; the mean number of trials (± SD) contributing to the ERPs was 128 (70) for passive-fine. ANOVA with factors of condition (passive-fine/random), location (frontal/parietal), hemisphere (left/right) and site (superior/medial/inferior), revealed an interaction between condition and

location [F(1, 23) = 5.02; p < 0.05], reflecting the difference in ERPs fond over parietal sites, which are not found over frontal electrode sites.

T-test pairing results for passive-fine and random (-600 to -200ms)

Left-Frontal Electrodes		Right-Frontal Electrodes	
F5	-	F6	-
F3	-	F4	-
F1	-	F2	-
Left-Parietal Electrodes		**Right-Parietal Electrodes**	
P5	[t(23) = 4.01; p = 0.001]	P6	[t(23) = 3.09; p < 0.01]
P3	[t(23) = 3.13; p < 0.01]	P4	[t(23) = 2.16; p < 0.05]
P1	-	P2	-

Table 6-5: T-test results for the passive-fine and random pre-segmentation time window.

Voltage magnitudes for passive-fine and random conditions (-600 to -200ms)

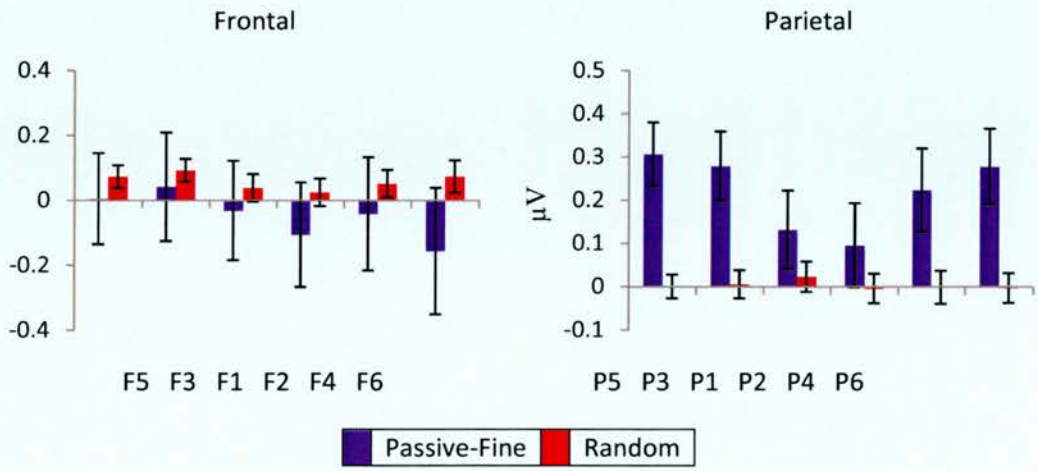

Figure 6-8: The magnitude of ERP effects from --600 to -200ms, shown as in Figure 5-7.

Finally, a 3-way interaction was revealed between condition, location and site [F(1.67, 38.45) = 4.28; p < 0.05], which reflects the relative inferior-medial nature of the effect found over parietal sites, when compared to the

broadly distributed nature of the effect found over frontal electrode sites (as shown in Figure 6-8). Successive t-tests are reported in Table 6-5; as is clear from the table, significant segmentation effects are predominantly present over medial and inferior parietal electrodes.

6.2.3.2.2 Post-segmentation time window (800 to 900ms)

The post-segmentation time window from 800 to 900ms was identified for analysis; Figure 6-7 shows the grand average ERPs time-locked to passive-fine and randomly-generated segmentation points over electrode sites selected for analysis. ANOVA with factors of condition (passive-fine/random), location (frontal/parietal), hemisphere (left/right) and site (superior/medial/inferior), revealed a 3-way interaction between condition, location and site [$F(1.72, 39.52) = 3.51$; $p < 0.05$], reflecting the inferior distribution of the effect, which is present only over parietal electrode locations, as illustrated in Figure 6-9. T-test results are shown in Table 6-6; significant segmentation effects are predominantly present over inferior parietal electrodes.

T-test pairing results for passive-coarse and random (800 to 900ms)

Left-Frontal Electrodes		Right-Frontal Electrodes	
F5	-	F6	-
F3	-	F4	-
F1	-	F2	-
Left-Parietal Electrodes		**Right-Parietal Electrodes**	
P5	[t(23) = -2.69; p < 0.05]	P6	[t(23) = -2.38; p < 0.05]
P3	-	P4	-
P1	-	P2	-

Table 6-6: T-test results for the passive-fine and random post-segmentation time window.

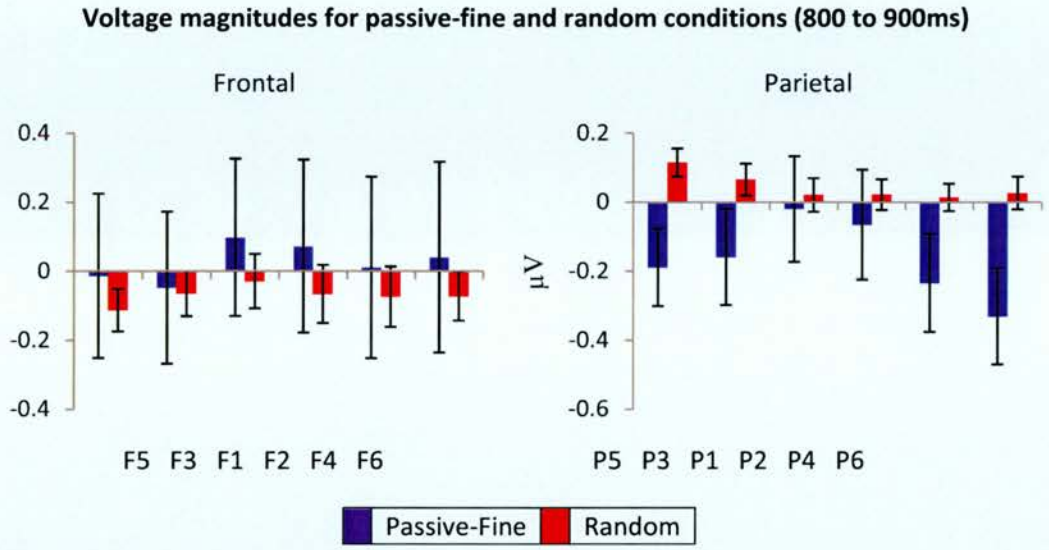

Figure 6-9: The magnitude of ERP effects from -800 to 900ms, shown as in Figure 5-7.

6.2.3.2.3 Topographic analysis

Figure 6-10 shows the scalp distributions of the differences between passive-coarse and random conditions for both pre and post segmentation time windows, illustrating a clear change in the pattern of effect over time. ANOVA with factors of epoch (-600 to -200ms/800 to 900ms), location (frontal/parietal), hemisphere (left/right) and site (superior/medial/inferior), revealed a 3-way interaction between epoch, location and site [$F(1.85, 42.57) = 4.98$; $p < 0.05$], reflecting the inferior posterioral greater than frontal differences present pre-segmentation, and the inferior frontal greater than inferior posterioral differences present post-segmentation.

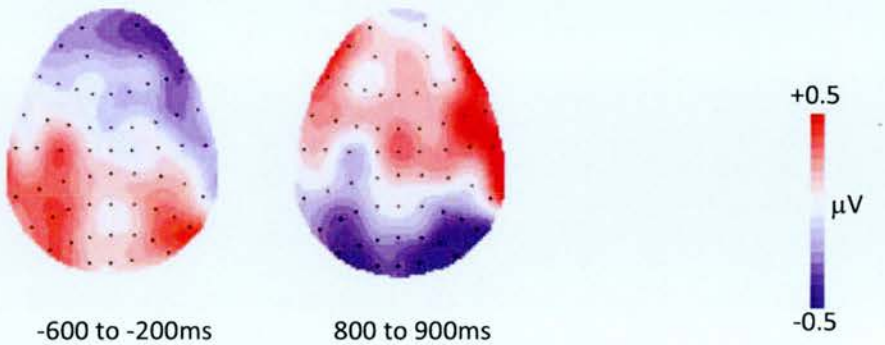

Figure 6-10: Topographic distributions of the passive-fine/random difference for the pre and post segmentations. Each cartoon shows the distribution of the difference between passive-coarse and randomly generated segmentations, averaged across a 400ms time period for the first time window (-600 to -200ms), and across 100ms for the second (800 to 900ms). The front of the head is at the top of each map, and the left hemisphere is on the left-hand side. Each dot represents a recording electrode. The scale bar indicates the range of activity (in microvolts). The effect in the first time window has fronto-right-lateralised negativity, and bi-lateral-posterior positivity distributed over inferiror electrodes; whereas the effect in the second time window exhibits a centro-right-lateralised positivity, and a bi-lateral negativity over parietal electrodes.

6.2.3.3 Comparing passive coarse- and fine-grain segmentation

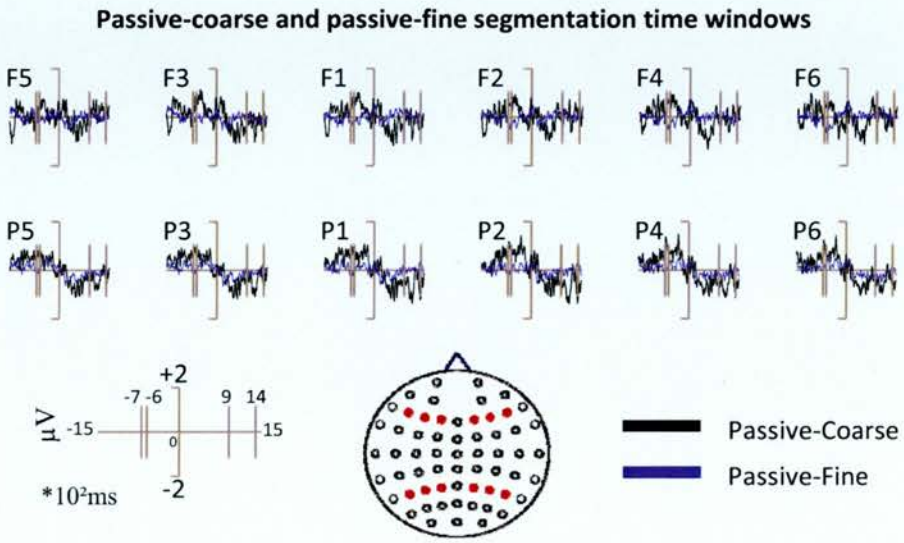

Figure 6-11: The pre-segmentation and post-segmentation time windows are illustrated.

6.2.3.3.1 Pre-breakpoint time window (-700 to -600ms)

The time window from -700 to -600ms was selected for focused analysis, due to the wider distribution of the effect when compared with the other candidate time windows (see Appendix A for overview table). Figure 6-11 shows the grand average ERPs time-locked to passive-coarse and passive-fine segmentation points over electrode sites selected for analysis.

ANOVA with factors of passive-coarse/passive-fine, location (frontal/parietal), hemisphere (left/right) and site (superior/medial/inferior), revealed an interaction between passive-coarse/passive-fine and site [$F(1.27, 29.17) = 5.35$; $p < 0.05$], which reflects the superior-medial nature of the differences between passive-coarse and passive-fine ERPs (as shown in Figure 6-12). T-test results are reported in Table 6-7, which shows significant segmentation effects are predominantly present over parietal electrodes.

T-test pairing results for passive-coarse and passive-fine (-700 to -600ms)

Left-Frontal Electrodes		Right-Frontal Electrodes	
F5	-	F6	-
F3	-	F4	-
F1	-	F2	-
Left-Parietal Electrodes		**Right-Parietal Electrodes**	
P5	[t(23) = 1.82; p < 0.1 (0.082)]	P6	-
P3	[t(23) = 2.17; p < 0.05]	P4	[t(23) = 2.28; p < 0.05]
P1	[t(23) = 2.26; p < 0.05]	P2	[t(23) = 2.62; p < 0.05]

Table 6-7: T-test results for the passive-coarse and passive-fine pre-segmentation time window.

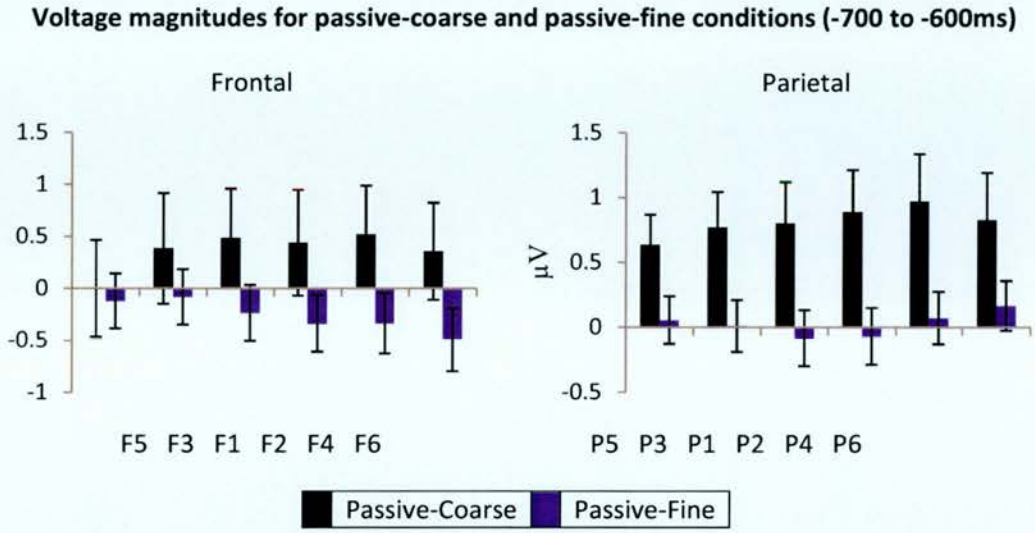

Figure 6-12: The magnitude of ERP effects from --700 to -600ms, shown as in Figure 5-7.

6.2.3.3.2 Post-breakpoint time window (900 to 1400ms)

Figure 6-11 shows the grand average ERPs time-locked to passive-coarse and passive-fine segmentation points over electrode sites selected for analysis of the 900-1400ms time window. ANOVA with factors of passive-coarse/passive-fine, location (frontal/parietal), hemisphere (left/right) and site (superior/medial/inferior), revealed an interaction between passive-coarse/passive-fine and site [$F(1.38, 31.62) = 4.4$; $p < 0.05$], which reflects the focus over superior electrode sites but not over medial or inferior electrode sites (illustrated in Figure 6-13). Surprisingly, no interaction was found between passive-coarse/passive-fine and location given the apparent parietal nature of the effect, which reflects the slight (non-significant) differences visible broadly across the ERPs. Subsidiary t-test results are reported in Table 6-8; significant segmentation effects are predominantly present over superior-parietal electrodes electrode sites.

T-test pairing results for passive-coarse and passive-fine (900 to 1400ms)

Left-Frontal Electrodes		Right-Frontal Electrodes	
F5	-	F6	-
F3	-	F4	-
F1	-	F2	-
Left-Parietal Electrodes		**Right-Parietal Electrodes**	
P5	-	P6	-
P3	-	P4	-
P1	[t(23) = -2.2; p < 0.05]	P2	[t(23) = -2.34; p < 0.05]

Table 6-8: T-test results for the passive-coarse and passive-fine post-segmentation time window.

Voltage magnitudes for passive-coarse and passive-fine conditions (900 to 1400ms)

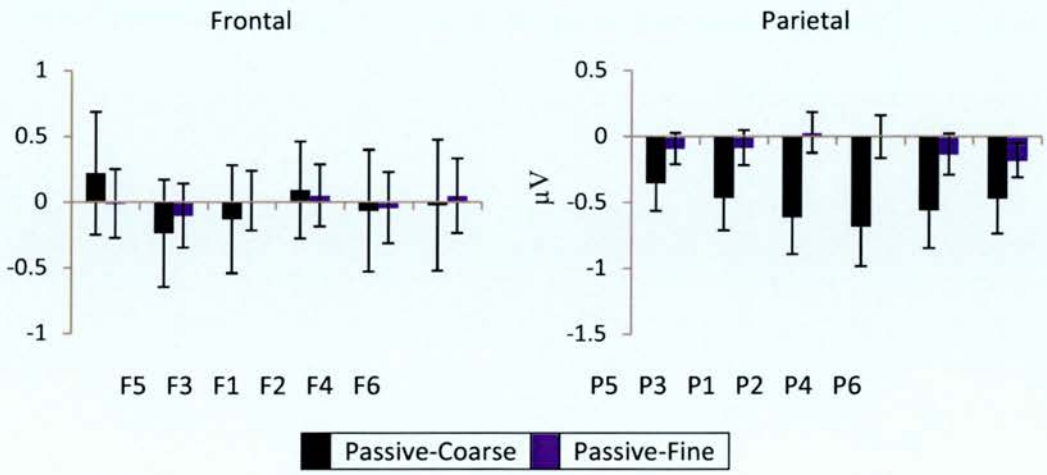

Figure 6-13: The magnitude of ERP effects from -900 to 1400ms, shown as in Figure 5-7.

6.2.3.3.3 Topographic Analysis

Figure 6-14 shows the scalp distributions of the differences between passive-coarse and random conditions, and between passive-fine and random, for both pre- and post-segmentation breakpoint time windows; with the effects

clearly changing polarity over time. ANOVA with factors of passive-coarse minus random/passive-fine minus random, epoch (-700 to -600ms/900 to 1400ms), location (frontal/parietal), hemisphere (left/right) and site (superior/medial/inferior), revealed a 3-way interaction between passive-coarse minus random/passive-fine minus random and epoch and site [$F(1.32, 30.24) = 4.84$; $p < 0.05$], reflecting the broad distribution of the effect during pre-segmentation time, when compared to the superior-medial nature of the effect post-segmentation. Focussed contrasts directly comparing locations, hemispheres and sites across passive-coarse and passive-fine event segmentation revealed a pre-segmentation interaction between passive-coarse minus random/passive-fine minus random and hemisphere [$F(1, 23) = 5.71$; $p < 0.05$], reflecting the right greater than left differences of the effect. A 3-way interaction was revealed between passive-coarse minus random/passive-fine minus random, location and hemisphere [$F(1, 23) = 4.41$; $p < 0.05$], which reflects the parietal greater than frontal and right greater than left differences of the effect. A further 4-way interaction was found between passive-coarse minus random/passive-fine minus random, location, hemisphere and site [$F(1.82, 41.93) = 6.07$; $p < 0.01$], reflecting the medial nature of the effect found over left-frontal electrode sites, when compared to the superior-medial nature of the effect found over parietal and right-frontal electrode sites. Analysis of the post-segmentation topographic data revealed only a marginal interaction (not reported).

Therefore, the topographic analyses confirm that the pattern of effects is distributionally different between passive-coarse/random and passive-fine/random ERPs, during pre-segmentation, however only marginally different post-segmentation. Additionally, the topographic analyses demonstrated differential pre- and post-segmentation distributions, inferring

the engagement of at least partially, if not wholly, different sets of neural generators.

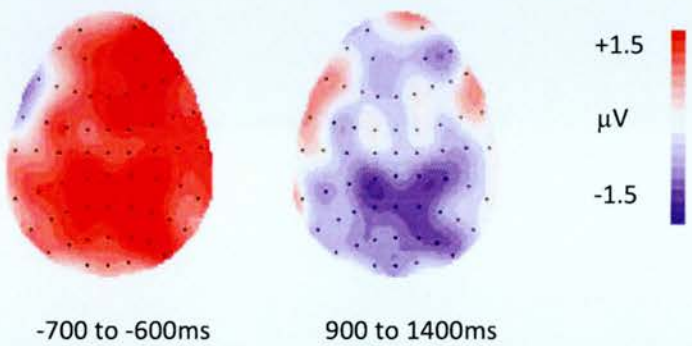

Figure 6-14: Topographic distributions of the passive-coarse/passive-fine difference for the pre and post segmentation breakpoints. Each cartoon shows the distribution of the difference between passive-coarse minus random and passive-fine minus random segmentation breakpoints, averaged across a 100ms time period for the first time window (-700 to -600ms), and across 500ms for the second (900 to 1400ms). The front of the head is at the top of each map, and the left hemisphere is on the left-hand side. Each dot represents a recording electrode. The scale bar indicates the range of activity (in microvolts). The effect in the first time window has a broad positive-going distribution; whereas the effect in the second time window exhibits centro and right-lateralised negativity over parietal electrode sites.

6.2.3.4 Active segmentation

Figure 6-15 shows the grand average ERPs for active-coarse and active-fine segmentation on electrode CZ; t-test examination revealed a clear difference in magnitude between active-coarse and active-fine segmentation [$t(23) = 2.08$; $p < 0.05$], with the ERPs for active-coarse more positive-going than those for active-fine.

The magnitude analysis and topographic distribution illustrated Figure 6-16 (a) and (b), respectively, may reflect a higher cognitive load present when participants mark coarse grain segmentation boundaries.

Similarly to the investigation in the previous chapter, the results are supportive and somewhat analogous to the coarse-greater-than-fine results reported in the Zacks et al. Study in 2001.

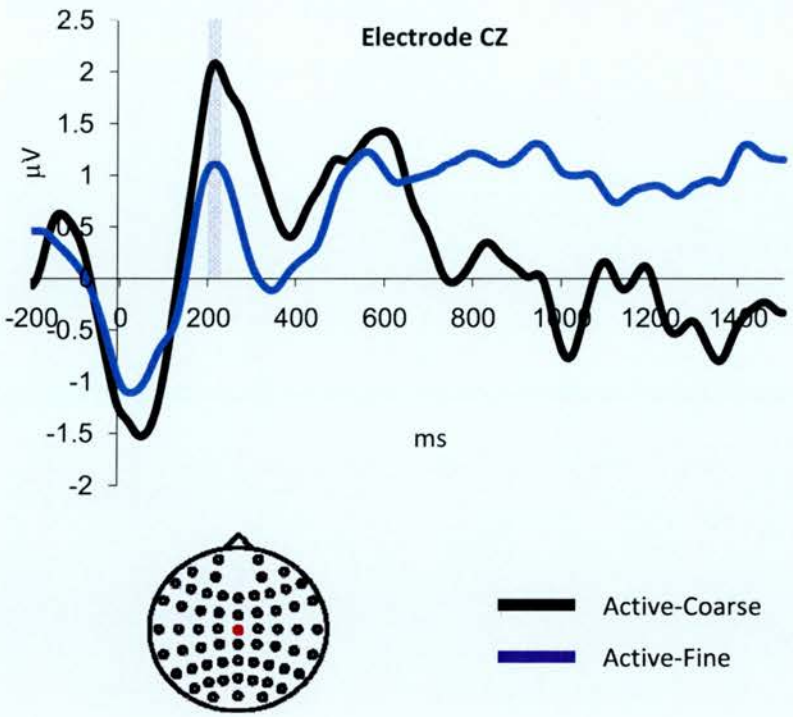

Figure 6-15: Grand average ERPs elicited for active-coarse (black) and active-fine (blue) on the electrode site CZ (shown as the red dot on the scalp map). More positive-going activity is present for active-coarse ERPs compared to active-fine ERPs during the 200 to 225ms time window (shaded grey).

6.2.4 Discussion

The aim of the experiment was to investigate whether the neural correlates of event segmentation could be elicited using ERPs, by employing replication of the paradigm set out by Newtson (1973) and employed by Zacks et al. (2001).

Crucially, by employing the paradigm used in the Zacks study, this experiment set out to investigate whether ERPs may be elicited that show clear pre- or post segmentation activity, and whether differences between coarse and fine grain segmentation will be present. In similarity with the previous experiment, a set of baseline ERPs was produced, which reflect background EEG activity, to compare the conditions.

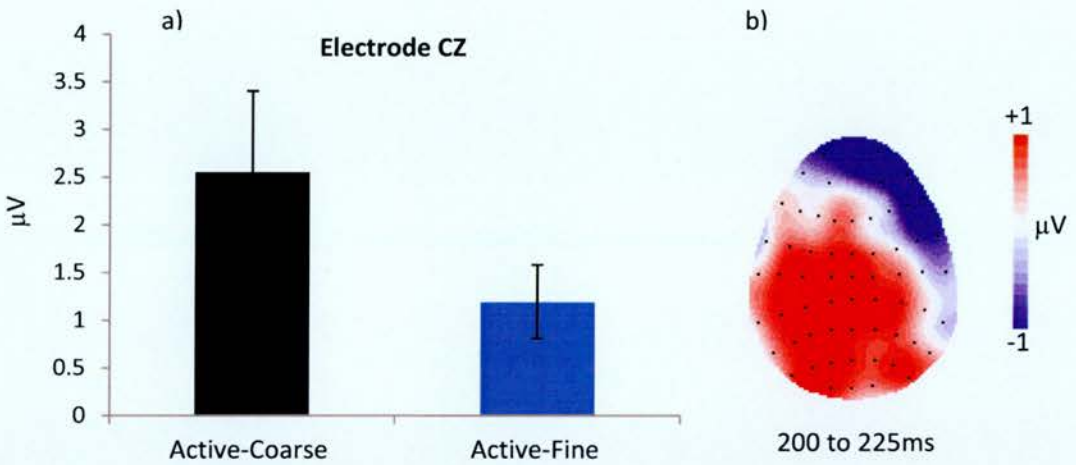

Figure 6-16: (a) Differences in effect sizes at electrode site CZ are shown for active-coarse (black) and active-fine (blue) segmentation points. Significantly larger effect sizes were present for active-coarse compared to active-fine segmentation points. (b) Topographic distribution of the active-coarse/active-fine difference averaged across a 25ms time period (200 to 225ms). The front of the head is at the top of the map, and the left hemisphere is on the left-hand side. Each dot represents a recording electrode. The scale bar indicates the range of activity (in microvolts). The effect is clearly distributed across the central electrodes, mostly likely reflecting the magnitude differences originating in the motor cortex. Additionally, the effect shows a centro-left-lateralised and centro-posterior distribution.

6.2.4.1 Summary and interpretation

ERPs for passive-coarse showed a pre-segmentation positive-going effect, present over parietal electrodes, when compared to the baseline ERPs. Additionally, when comparing the ERPs for passive-coarse and randomly generated segmentation points, a negative-going post-segmentation effect was found bi-laterally over posterior sites. Most notably, the effects found over parietal sites shift in polarity over time, more specifically they swap polarity at approximately the point of event segmentation (0ms). Topographic analyses revealed the engagement of differential neural generators over time, suggesting that at least partially, if not wholly, different psychological processes are engaged pre- and post passive-coarse segmentation.

In contrast with the ERPs for passive-coarse, ERPs for passive-fine showed the emergence of a slightly later effect present bi-laterally over medial and inferior parietal electrode sites pre-segmentation. Similarly, however, the pre-segmentation effects for both passive-coarse and passive-fine were found over parietal electrode sites, and exhibited the same polarity when compared to the baseline randomly generated ERPs. In correspondence with the ERPs for passive-coarse, the ERPs for passive-fine shift in polarity from positive-going to negative-going when compared with the baseline ERPs, at around the time of segmentation. Post-segmentation effects were also revealed when comparing passive-fine ERPs with baseline ERPs, which at least partially mirror the comparison of passive-coarse and baseline ERPs; both effects present over parietal electrode sites and are negative-going. In contrast with the ERPs for passive-coarse, the ERPs for passive-fine emerge later in the post-segmentation period and are not as long-lasting. Nonetheless, topographic analyses revealed corresponding

results with those performed on passive-coarse ERPs, with strong evidence indicating the engagement of different psychological processes, pre- and post-segmentation.

To summarise, the ERPs for passive-coarse and passive-fine share similarities, particularly over parietal electrode and occipital sites. Both exhibit positive-going pre-segmentation and negative-going post-segmentation effects when compared to the baseline ERPs over parietal sites, especially noticeable for coarse-grain segmentation. However, the ERPs for passive-coarse and passive-fine do also differ, notably with bi-lateralised frontal, central and centro-parietal effects found pre- and post-segmentation. Both sets of ERPs show reliable differences in the pattern of effects over time, and analysis confirmed the presence of differentially engaged neural generators, pre- and post-segmentation. Once again, given the problem of overlapping ERPs described in the previous chapter, it is perhaps unsurprising that similarities exist between passive-coarse and passive-fine ERP. Nevertheless, it is clear from the analyses that at least partially, if not wholly, different sets of neural generators are engaged during passive-coarse and passive-fine post-segmentation. Similarly with the previous study, the evidence gives rise to the suggestion that participants are capable of passively segmenting events on differing levels of granularity, and that different psychological processes are engaged when segmenting at different grains. Again in resemblance with the previous study, it may be inferred that different sets of psychological processes are engaged pre- and post-segmentation, when segmenting events at both a coarse and fine grain. Vitally, the data presented in this study once again support the hypothesis that the regions of the brain that respond to event segmentation are measurable with EEG. Considering the results from the previous study and

the data presented in this chapter, support for the hypothesis is demonstrated to be consistent.

6.2.4.2 Comparison with Zacks et al. (2001) study

The previous study demonstrated both similarities and striking neurological disparities with the fMRI study conducted by Zacks et al. in 2001. In line with the previous study, the results of this experiment display similar similarity and disparity. Again, pre- and post-segmentation responses were recorded during passive video viewings, and additionally during active segmentation. Differentially sensitive neural correlates were recorded for coarse- and fine-grain event segmentation, again during both passive and active segmentation. Once again considering the inverse problem and skull attenuation, only a tenuous link may be drawn between the bi-lateral activity noted during both coarse- and fine-grain segmentation recorded during this study, and the parietally located data reported by Zacks et al. in their 2001 fMRI study. In contrast with the previous study however, the link between right-frontally located neural activity reported in the Zacks study and the current study is less clear.

Once again in line with the previous study, evidence was reported pre-segmentation to support the claim that coarse-grain elicits greater responses than fine-grain passive-segmentation. Moreover, a greater magnitude for coarse-grain segmentation was reported during active segmentation. However, the pattern of weak passive and strong active evidence for coarse-fine differences is similar to the pattern reported in the Zacks study.

Nevertheless, in correspondence with the previous study, several differences exist between the current study and the Zacks study, not least the timing responses elicited for coarse compared to fine grain segmentation during passive viewing. As discussed in the previous chapter, the Zacks study reported stronger activity for coarse- than fine-grain segmentation only in posterior locations, and only after the segmentation. By contrast, and in similarity with the previous study, there is, however, evidence in this experiment for stronger responses occurring in passive-coarse grain segmentation as compared to passive-fine grain occurring pre-segmentation. In striking similarity with the previous study, data from the pre-segmentation time window (when comparing passive-coarse and passive-fine grain segmentation ERPs) exhibit a stronger effect for passive-coarse segmentation (more positive-going), but one again that is difficult to isolate to posterior electrodes; significant differences in magnitude were present over parietal locations at individual electrode sites, but no interaction with location was found when the data were analysed further. The pattern of effect found pre-segmentation and weak evidence for post-segmentation coarse-greater-than-fine differences found in this experiment, are in correspondence with results from the previous chapter.

Continuing the trend of comparable results with the previous study that are in conflict with the Zacks study, differential neural activity between pre- and post-segmentation was reported. The current and previous experiments indicate that pre- and post-segmentation activity is temporally distinct, and moreover, separated by a relatively non-active time period surrounding segmentation at 0ms. Moreover, both the previous and current studies confirm the engagement of sets of differential neural generators pre- and post-segmentation, in both passive-coarse- and passive-fine-grain

segmentation. This pattern emerging from EEG data is in direct conflict with the data produced in the Zacks study, which suggests that only a single set of neural generators were active once during a period of time that enveloped the segmentation point. In light of the emerging pattern, it may be postulated that the alternative neuroimaging technologies of EEG and fMRI record different underlying signals, revealing two equally valued views of the neural basis of event segmentation. Additionally, in light of the Zacks paradigm replication employed in the current study, the evidence suggests that the perception of an event boundary does reflect multiple cognitive functions engaged during information processing.

As postulated in the previous chapter, such psychological demands as prediction engineering and on-going event structuring may give rise to the engagement of multiple neural generators. Therefore, the ERP data from the current and the previous experiments may reflect the complex interaction of neural activity present during event segmentation. Again, regardless of the conservative analysis strategy, the data do provide sufficient evidence for the engagement of multiple neurological processes.

6.2.4.3 Comparison with event segmentation literature

As with the previous study and the Zacks study, participants were broadly found to agree over the perception of event boundaries (Figure 6-1); data which lends itself to the hypothesis that event segmentation is an automatic process (claimed most recently by Kurby and Zacks 2008). Furthermore, all three studies exhibit the common feature of hierarchical relationships being drawn between coarse and fine grain segmentation. However, the previous study failed to replicate the findings of Hard et al. (2001), which reported that coarse-grain event boundaries were perceived as occurring subsequent

to fine-grain boundaries. Supportively, however, the current study in which participants gained no prior knowledge of the experimental paradigm, replicated the findings of Hard et al. One possible source of the conflicting results reported in the previous study, may be the differences in task knowledge. The pattern if results suggest that the hierarchical grouping of sub-events may be sensitive to top-down factors such experimental paradigm. Given that the previous study reflected experimental task knowledge, the current positive result is hypothesised to significantly support the findings of Hard et al.

6.3 Conclusions

This chapter reported the results of an experiment that investigated the effects of event segmentation in both the behavioural and neural domains, which replicated the paradigm used in the Zacks et al. study of 2001. Evidence to suggest that the study is broadly in line with previous research in event segmentation was reported. Additionally, the replication of the Zacks paradigm produced more corresponding behavioural data than that of the previous study. Supportively, participant agreement was found over event boundaries and behavioural evidence for two measures of hierarchical structuring, demonstrated strong alignment with previous research. Moreover, neurophysiological data contained several comparable features with the Zacks study of 2001; firstly, neural responses to passive and active event segmentation; secondly, neural activity was found to present for both coarse- and fine-grain segmentation; and thirdly, the pattern of coarse-greater-than-fine segmentation (partially during passive- and wholly during active-segmentation), aligns with the Zacks et al. study. Conversely, the results of the previous study and the current study both yield evidence of

pre-segmentation coarse-greater-than-fine effects during passive segmentation, rather than the post-segmentation effects reported by the Zacks study.

Perhaps the most striking difference between the EEG studies and the fMRI study is the demonstration of differential neural generator engagement, pre- and post-segmentation. As discussed in the previous chapter, as part of ongoing everyday cognition, it is likely that many psychological processes such as cognitive schemata interaction, prediction engineering and sensory perceptual processing are all invoked. In light of the similarities between the EEG studies, it therefore appears more likely that the ERP data reflect a complex model of information processing; one which is sensitive to both top-down and bottom-up features on multiple levels of segmentation granularity. An alternative hypothesis was presented in the previous chapter; pre-segmentation responses reflect the perception of an event and point, and post-segmentation activity reflects the perception of a new event start point. However, considering again the multiple cognitive functions likely to be active during ongoing perception, it appears more probable that the EEG data reflect a temporally finer of measure of event segmentation; a measure which reflects the differential engagement of networks of brain regions that are tuned to perceptually salient event structures.

Given the success of the experiment reported in this chapter in demonstrating the neurophysiological correlates of event segmentation, the following experiments in this thesis may focus on investigating the nature of, and influences upon the, phenomenon of ongoing perception. The significant interaction of event segmentation with memory has been previously discussed in the introduction chapter; therefore the following study aims to investigate the influence of familiarity upon information processing.

7 Perception of familiar and unfamiliar events

7.1 Introduction

The experiment reported in the previous chapter further demonstrated that the neural correlates of event segmentation could be measured using scalp recorded EEG, but importantly, more closely replicated the paradigm used in the Zacks et al. study in 2001. Several findings were found to align with both the Zacks et al. study and with the first experiment, in which participants were directed to segment activity, for example firstly; that participants were found to encode activities in terms of their parts and constituent sub-parts, secondly; differential neural engagement was found when participants segmented activities into large and small parts, and thirdly; that at least during active segmentation, coarse-grain segmentation was found to elicit greater responses than for fine-grain event segmentation. By employing the paradigm used by Zacks et al. in 2001 more closely, the previous experiment refined the results found during the first experiment, for example, participants were found to use coarse-grain event boundaries to subsume fine-grain event boundaries; a result not found in the first experiment, but reported in previous studies of event segmentation (e.g. Hard et al., 2001). Importantly however, the neurological results reported in the previous experiment were more similar with the first investigation of directed event segmentation than with the Zacks et al. study. Notwithstanding activity reported during active event segmentation, passive event segmentation trials reported in the previous experiment once again failed to replicate the coarse-greater-than-fine neurological responses reported in the fMRI study performed by Zacks et al. Additionally, and perhaps most strikingly, the previous experiment aligned with the pilot EEG experiment in reporting

distinct neurological activity pre- and post-segmentation; a finding which is in direct contradiction with the Zacks et al. study. In summary, the previous experiment supported previously reported behavioural findings of hierarchically aligned part and sub-part event boundaries, and additionally confirmed the use of coarse-grain event boundaries to subsume fine-grain event boundaries when participants are not provided with paradigm knowledge. Moreover, the previous experiment refined the neurological findings of the pilot EEG study, perhaps suggesting that the finer temporal resolution offered by EEG is uniquely revealing the engagement of multiple neurological processes, when compared with the temporally weak resolution offered by fRMI. Finally, the previous experiment demonstrated that the neurological responses to event boundary perception were differentially sensitive to knowledge of the experimental task.

Given the success of the previous experiment, and the emerging pattern of differential neural generator engagement pre- and post-segmentation, the current experiment seeks to investigate more closely the underlying cognitive function of event boundary perception. As discussed in the introduction chapter, the perception of an event boundary is likely to involve interaction with cognitive schemata, and by supposition memory, as participants actively seek to base predications for the current activity on past experience. Invoking pre-existing cognitive schema to enable prediction is a hypothesis supported and extended by Event Segmentation Theory (EST), as discussed in the introduction chapter. EST proposes that as events become less familiar one has less knowledge on which to base accurate predictions, and in this scenario error feedback (unpredicted events) are fed back into an existing cognitive schema as one effectively learns an unfamiliar scenario. Therefore, the current experiment aims to extend the previously employed

paradigm to investigate the role of memory and activity familiarity upon the perception of an event boundary. More specifically, two groups of participants will comprise the current experiment, firstly; a group with no prior knowledge of suitably unfamiliar activities will be tested and compared with a second group; whose knowledge of the obscure activity is facilitated by a prior viewing. Although the two groups are summarily described in this chapter as activity *experts* and activity *naive* participants, they are more accurately interpreted as *recently-learned* obscure activity and *unfamiliar* activity population groups respectively. Based upon the hypotheses of cognitive schema interaction and an error-driven feedback system, it is hypothesised that the current experiment will reveal neurological correlates of event boundary perception that are differentially sensitive to activity knowledge. Additionally however, it is hypothesised that in correspondence with the previous two experiments, the differential engagement of neural generators will be found pre- and post-segmentation. A replication event boundary agreement and the emerging pattern of hierarchical structuring is also expected, however, given the sensitivity found in participants using coarse-grain event boundaries to subsume fine-grain event parts, it is hypothesised that only activity experts will replicate this phenomenon. Finally, as discussed in the introduction chapter, contradictory findings have been reported when investigating the segmentation of unfamiliar events; Hard, Tversky, & Lang (2006) found activities to be segmented into smaller parts when unfamiliar, which contradicts an earlier study (Zacks, Tversky, et al., 2001). Therefore, the current experiment seeks to clarify the previous studies by directly comparing the number of segments generated by activity expert and naive participants. Notwithstanding the Hard, Tversky, & Lang (2006) study, it is hypothesised that activity naive participants will fail to

segment the obscure activities into significantly greater numbers of sub-events, owing mainly to the broad agreement found previously over event boundary perception.

While the manipulation of familiarity proposed in this chapter is novel to the field of event segmentation, study and test methods are commonly used in ERP studies of memory. Typically, word lists or images presented during a study phase are mixed with additional stimuli during a test phase; participants are required to make judgements on whether they recognise previously studied stimuli (for overviews of ERP memory studies see Friedman & Johnson, 2000, or Rugg & Coles, 1995). Albeit that the proposed paradigm and stimuli vary from more typical ERP memory experiments, the widespread demonstration of participants memory for recently learned stimuli does, nevertheless, install confidence in this experiment.

To summarise, the key question of the current study is whether an effect of familiarity will give rise to differential neural correlates of event segmentation, and moreover, whether an effect of familiarity will elicit distinctive neural activity when compared with the segmentation of everyday events.

7.2 Experiment 3: Investigating the effect of familiarity on event segmentation using ERPs

7.2.1 Methods

The following sections detail the experimental methods followed in this experiment.

7.2.1.1 Stimuli

The videos used in this experiment were recorded using volunteer actors. Each video was a fixed shot, single scene recording of one actor performing an obscure task that would not be recognisable to participants. The four activities were erecting a clothes rail, constructing a table, setting up a confocal microscope and setting up electronic musical equipment.

7.2.1.2 Participants

Thirty-three participants took part in the experiment; the data from one participant was discarded due to behavioural non-compliance. Thirty-two participants remained in the group (13 male, age range 17-36).

7.2.1.3 Procedure

The current experiment employed two similar procedures based upon the paradigm employed by Zacks. In line with previous experiments, task-naive participants watched all four movies passively, before actively segmenting the activities into coarse- and fine-grain chunks. In contrast with the common procedure, task-expert participants viewed all four movies once before following the main procedure i.e. task-expert participants twice viewed the activities passively; active breakpoints were overlaid onto the second passive viewing run.

7.2.2 Behavioural results

The following section contains analysis of behavioural data collected from 32 participants as they performed the event segmentation experiment.

7.2.2.1 Investigating the concurrence of event perception

Participant agreement over boundary perception was investigated as per previous experiments; the results are illustrated in Figure 7-1 and Figure 7-2 for expert and naive participants, respectively. In line with the previous experiments, raster plot data suggest that participants shared a common perception of where segmentation points occur, perceiving many events in the same way, despite the presence of segmentation points that were unique to individuals.

In line with previous chapters, the relationship between participant responses and fine- and coarse-grain event boundary perceptions were examined; correlation results (listed in Table 7-1), for both groups of participants, clearly demonstrate a high-level of association between coarse- and fine-grain boundary perceptions across all activities. Therefore, the correlation analyses suggest that participants perceive separate levels of event segmentation to be interdependent, regardless of familiarity.

Correlation results for coarse- and fine-grain event perception

Activity	Familiar	Unfamiliar
Erecting a clothes rail	$r(425) = 0.481$; $p < 0.001$	$r(425) = 0.563$; $p < 0.001$
Constructing a table	$r(459) = 0.266$; $p < 0.001$	$r(459) = 0.416$; $p < 0.001$
Setting up a microscope	$r(344) = 0.364$; $p < 0.001$	$r(344) = 0.509$; $p < 0.001$
Setting up musical equipment	$r(311) = 0.343$; $p < 0.001$	$r(339) = 0.462$; $p < 0.001$

Table 7-1: Resulting p-values from the correlation tests performed on the temporal response distributions for coarse- with fine-grain segmentation

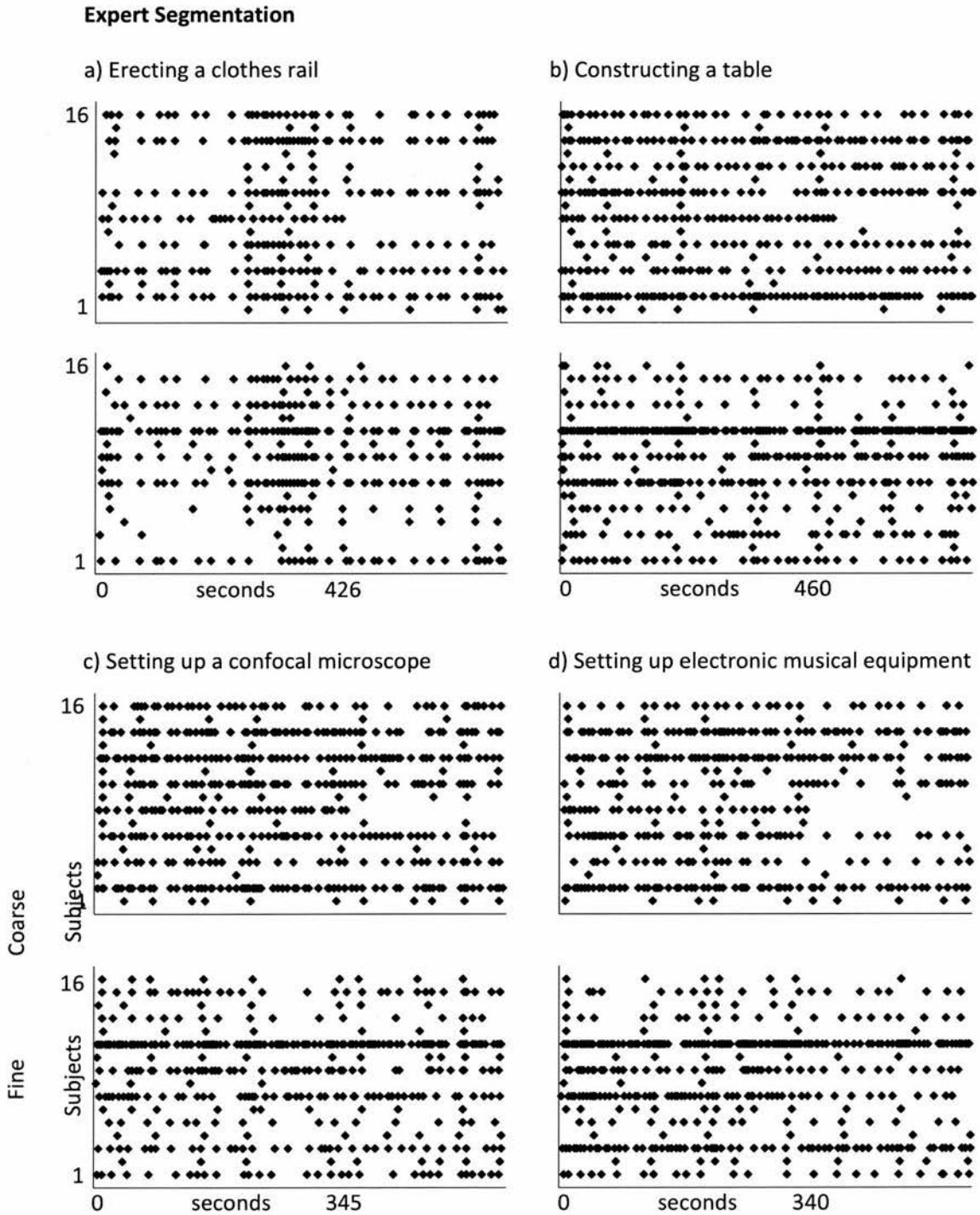

Figure 7-1: Raster plots of segmentation timings (x-plane) for each participant (y-plane), shown separately for each movie (a-d), for fine and coarse conditions. Each individual data point reflects a single segmentation response.

Naive Segmentation

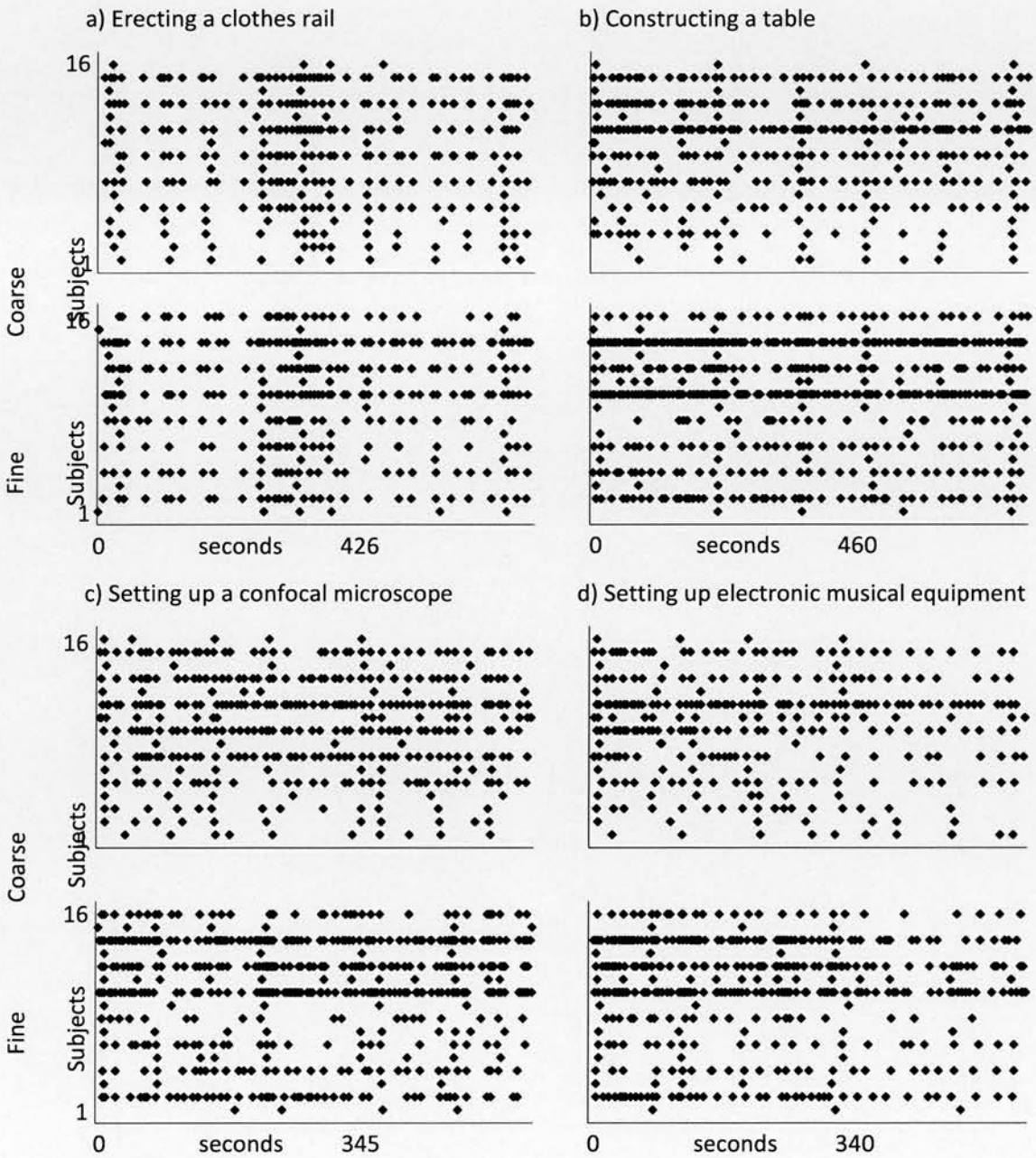

Figure 7-2: Raster plots of segmentation timings (x-plane) for each participant (y-plane), shown separately for each movie (a-d), for fine and coarse conditions. Each individual data point reflects a single segmentation response.

7.2.2.2 Investigating the hierarchical nature of event perception

Figure 7-3 shows the mean value of recorded and randomly placed overlap time-bins calculated for each activity, gathered from the activity-familiar (expert) and activity-naive groups of participants, respectively. An initial high-level analysis of the behavioural data failed to reveal any interaction between the expert and naive groups, indicating that familiarity does not significantly alter participant's tendency to segment activities hierarchically.

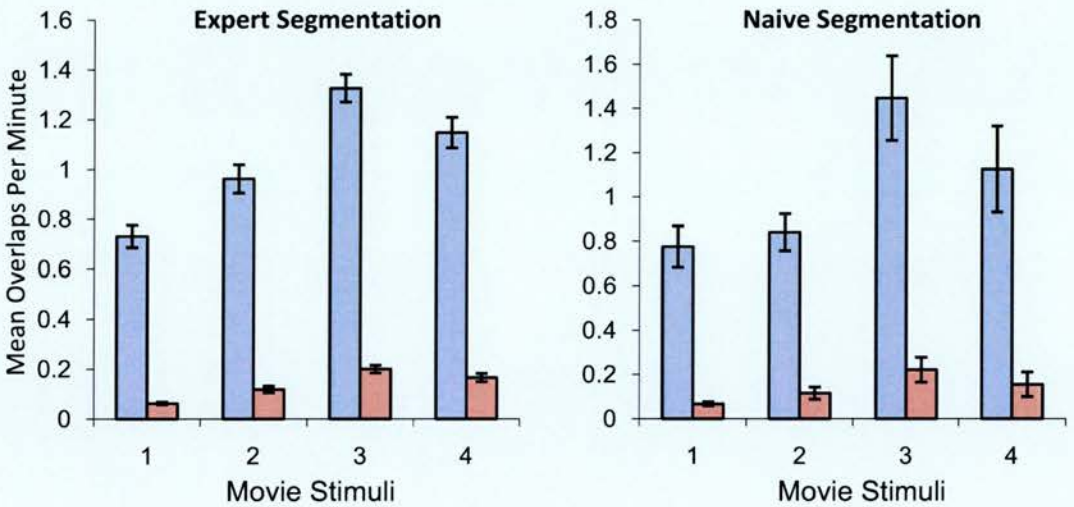

Figure 7-3: Mean number of overlap time-bins for recorded (purple) and randomly placed (blue) segmentations per minute are shown for each video; (1) erecting a clothes rail, (2) constructing a table, (3) setting up a confocal microscope and (4) setting up electronic musical equipment. Error bars represent one standard error of the mean. For all four movies, significantly larger number of overlapping time-bins was recorded from participants marking coarse and fine event boundaries than would occur randomly.

Nevertheless, each condition was subsequently subjected to a more focussed analysis to examine the pattern of recorded/randomly placed overlap time bin effects. ANOVA with factors of condition (recorded/randomly placed) and activity (erecting a clothes rail, constructing

a table, setting up a confocal microscope and setting up electronic musical equipment) revealed a main effect of condition overlap time-bins for experts [$F(1,15) = 105.47$; $p < 0.001$], and for naive participants [$F(1,15) = 127.36$; $p < 0.001$]. Additionally, interactions between condition overlap time-bins and activity were revealed for expert [$F(1.99,29.91) = 8.47$; $p < 0.005$], and naive [$F(2.55,38.24) = 11.69$; $p < 0.001$] groups, reflecting the different structures of the activities. To demonstrate that hierarchical performance was present for each movie, additional two-tailed paired sample t-tests were run on recorded and randomly placed overlap time bin mean values for each activity; t-tests results are listed in Table 7-2.

T-test results for overlapping coarse- and fine-grain event perception

Activity	Familiar	Unfamiliar
Erecting a clothes rail	[t(15) = -8.14; p < 0.001]	[t(15) = -8.14; p < 0.001]
Constructing a table	[t(15) = -10.97; p < 0.001]	[t(15) = -8.9; p < 0.001]
Setting up a microscope	[t(15) = -8.69; p < 0.001]	[t(15) = -11.81; p < 0.001]
Setting up musical equipment	[t(15) = -6.8; p < 0.001]	[t(15) = -9.5; p < 0.001]

Table 7-2: Resulting p-values from the two-tailed t-tests performed on each activity for both groups of participants. The results reflect the clear differences present between actual overlapping time bins recorded and those arising purely by chance, seemingly regardless of the level of familiarity one has with an activity.

Figure 7-4 shows the mean value of fine- before coarse-grain segmentations and coarse-before fine-grain segmentations for the expert and naive groups of participants respectively. High-level analyses of the behavioural data failed to reveal any interaction between the expert and naive groups, indicating that familiarity does not significantly alter

participant's tendency to use coarse-grain segments to subsume fine-grain events.

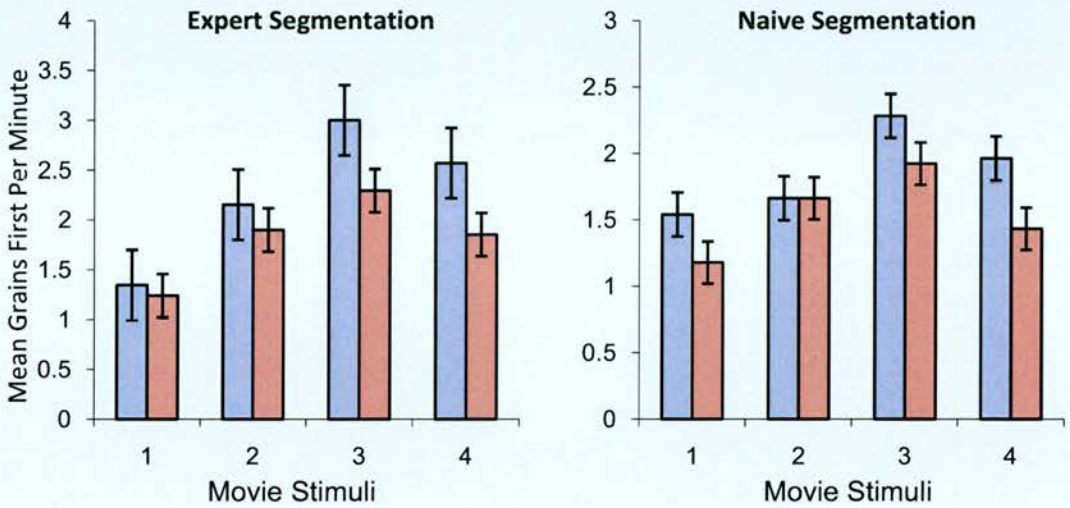

Figure 7-4: Mean number of fine- before coarse-grain segmentations (light blue), and coarse-before fine-grain segmentations (light red) per minute are shown for each video; (1) erecting a clothes rail, (2) constructing a table, (3) setting up a confocal microscope and (4) setting up electronic musical equipment. Error bars represent one standard error of the mean. Movies three and four showed significantly larger numbers of fine- before coarse-grain segmentations than coarse- before fine-grain segmentations.

ANOVA with factors of condition (fine subsuming coarse/coarse subsuming fine) and activity (erecting a clothes rail, constructing a table, setting up a confocal microscope and setting up electronic musical equipment) revealed a main effect of condition for expert participants [$F(1,15) = 5$; $p < 0.05$], but not for naive participants [$p>0.05$]. No interactions between condition and activity were revealed for either group, which reflects the lack of impact differing activity structures influenced participants tendency to mark coarse- slightly after fine-grain event boundaries. Table 7-3, which reports two-tailed paired sample t-tests for each activity, indicates

the stronger tendency for expert participants to use coarse-grain boundaries to subsume fine-grain parts when compared with naive participants.

T-test results for coarse- subsuming fine-grain event perception

Activity	Expert Segmentation	Naive Segmentation
Erecting a clothes rail	-	-
Constructing a table	-	-
Setting up a microscope	[t(15) = 2.84; p < 0.05]	[t(15) = 3.11; p < 0.01]
Setting up musical equipment	[t(15) = 2.26; p < 0.05]	-

Table 7-3: Resulting p-values from the two-tailed t-tests performed on each activity analysing the use of coarse-grain boundaries to subsume fine-grain event parts. The results indicate a stronger tendency for expert participants to automatically employ this strategy.

In summary, the behavioural results clearly indicate that activity-naive participants, in addition to activity-expert participants, encoded the activities in terms of hierarchical relationships between parts and sub-parts. By contrast, and regardless of the failure of a high-level analysis to reveal a main effect, focussed analyses clearly indicated that activity-expert participants did use coarse- to subsume fine-grain segments while activity-naive participants did not. Taken together, the results indicate that the influence of familiarity plays an important role not in how participants perceive overall structure in an activity, rather in how fine-grain event segments are grouped; activity-experts employ a strategy that is in line with previous experiments using everyday activities.

7.2.2.3 Investigating the influence of familiarity upon parsing rates

As discussed in the introduction chapter, some evidence exists to suggest that participants segment unfamiliar activities into smaller parts (Hard, Tversky, & Lang, 2006), thus resulting in a greater number of event segments. However, this effect has been contradicted (Zacks, Tversky, et al., 2001), and so given the nature of this experimental task, the parsing rates of recently learned (expert) and activity-naive participants are compared to investigate the discrepancies. Figure 7-5 illustrates participant activity parsing rates for activity expert and naive participants, for coarse- (a) and fine- (b) grain event segmentation.

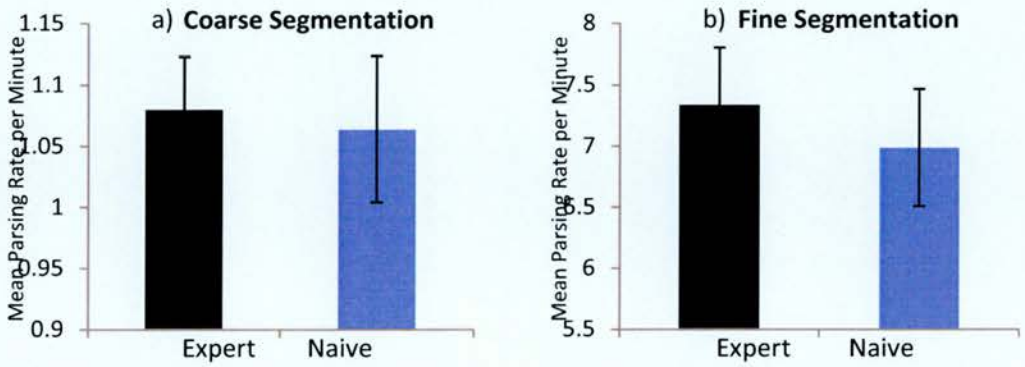

Figure 7-5: Mean parsing rates per minute for activity-expert (black) and activity-naive (blue) participants are compared during (a) coarse-grain event segmentation, and (b) fine-grain event segmentation. As the graphs indicate, no difference was found between the two groups for either coarse- or fine-grain segmentation.

These data were subjected to individual t-tests to measure the differences between participant groups. Analysis of the data failed to reveal any difference between the expert and naive participant groups during

coarse- or fine-grain event segmentation [p>0.1]. Therefore, the results of this experimental test concur with the original findings presented by Zacks, Tversky, et al. in 2001.

7.2.3 ERP results

The following section contains analysis of electrophysiological data collected from 32 participants as they performed the event segmentation experiment.

7.2.3.1 Investigating the differences between expert and naive event perception

7.2.3.1.1 Comparing expert- and naive-passive-coarse

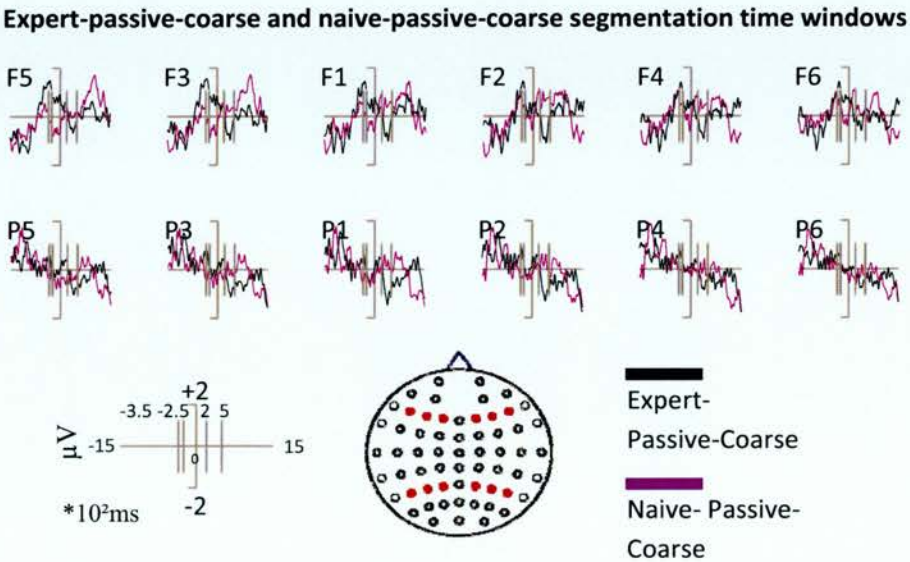

Figure 7-6: The pre-segmentation and post-segmentation time windows are illustrated.

7.2.3.1.1.1 Pre-segmentation time window (-350 to -250ms)

Following the procedures outlined in the General Methods chapter, the ERP results were characterised by selecting one time window from pre-segmentation time, and one from post-segmentation time based upon visual inspection of the grand average waveforms in Figure 7-6, and refined using the overview table (available in Appendix A). A pre-segmentation time window from -350 to -250ms was selected after repeated statistical analyses (supplemental data not presented), revealed the effect to be more robust over this period.

Figure 7-6 shows the grand average ERPs time-locked to expert-passive-coarse and naive-passive-coarse segmentation points, at electrodes chosen for statistical testing. The mean number of trials (± SD) contributing to the ERPs was 25 (9) for expert-passive-coarse and 26 (11) for naive-passive-coarse. ANOVA with factors of condition (expert-passive-coarse/naive-passive-coarse), location (frontal/parietal), hemisphere (left/right) and site (superior/medial/inferior), revealed a main effect of condition [$F(1, 15) = 7.67$; $p < 0.05$], indicating a that the effect is more broadly distributed than indicated in Figure 7-6.

7.2.3.1.1.2 Post-segmentation time window (200 to 500ms)

A post-segmentation time window of 200 to 500ms was selected for analysis (related overview data is available in Appendix A); ANOVA with factors of condition (expert-passive-coarse/naive-passive-coarse), location (frontal/parietal), hemisphere (left/right) and site (superior/medial/inferior), surprisingly, given the nature of the differences in waveforms reported in Figure 7-6, revealed a main effect of condition [$F(1, 15) = 6.05$; $p < 0.05$], revealing a widespread effect. A further interaction was revealed between condition and site [$F(1.75, 26.21) = 16.01$; $p < 0.001$], which reflects the superior distribution of the effect noted bi-laterally over parietal sites and right-laterally over frontal electrodes sites. Individual t-test results are reported in Table 7-4, which report significant segmentation effects present predominantly over superior parietal electrodes.

T-test pairing results for expert-passive-coarse and naive-passive-coarse (-200 to 500ms)

Left-Frontal Electrodes		Right-Frontal Electrodes	
F5	-	F6	-
F3	-	F4	-
F1	-	F2	[t(15) = -1.86; p < 0.1 (0.083)]
Left-Parietal Electrodes		**Right-Parietal Electrodes**	
P5	-	P6	-
P3	-	P4	-
P1	[t(15) = -2.66; p < 0.05]	P2	[t(15) = -3.01; p < 0.01]

Table 7-4: T-test results for the expert-passive-coarse and naive-passive-coarse post-segmentation time window.

For illustrative purposes, the voltage magnitudes for the electrodes submitted to ANOVA over frontal and parietal locations are shown in Figure 7-7. The magnitude analysis also support the data reported in Table 7-4, reflecting the stronger effects for expert-passive-fine located superiorly over right-frontal electrodes, and bi-laterally over superior parietal electrode sites.

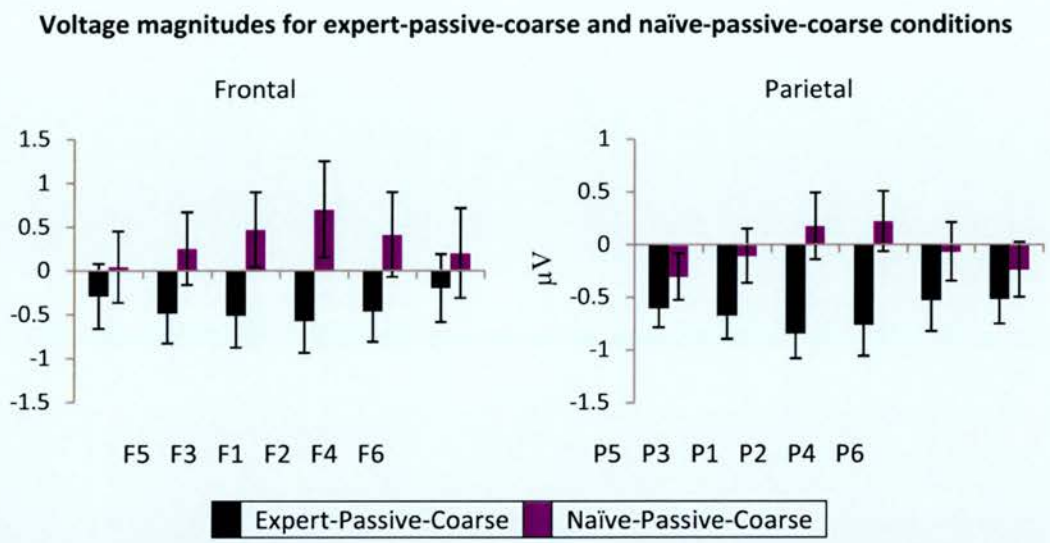

Figure 7-7: The magnitude of ERP effects from -200 to 500ms, shown as in Figure 5-7.

7.2.3.1.1.3 Topographic analysis

Figure 7-8 shows the scalp distributions of the differences between expert-passive-coarse and random conditions, and naive-passive-coarse and random, for both pre- and post-segmentation time windows. The figure illustrates a clear difference in the pattern of the effect between conditions, and additionally illustrates a change in the pattern of effect over time, most notably with the change in polarity. ANOVA with factors of expert-passive-coarse minus random/naive-passive-coarse minus random, epoch (-350 to -250ms/200 to 500ms), location (frontal/parietal), hemisphere (left/right) and

site (superior/medial/inferior), revealed a significant interaction between expert-passive-coarse minus random/naive-passive-coarse minus random and epoch [$F(1, 15) = 9.27$; $p < 0.01$], reflecting the positive-going differences in the conditions pre-segmentation, compared with the negative-going differences present post-segmentation. A further 3-way interaction between expert-passive-coarse minus random/naive-passive-coarse minus random, epoch and site [$F(1.17, 16.36) = 4.87$; $p < 0.05$] was revealed, which reflects the inferior-going-superior distribution of the differences in conditions pre-segmentation, compared with the superior-going-inferior distribution of the differences in conditions post-segmentation.

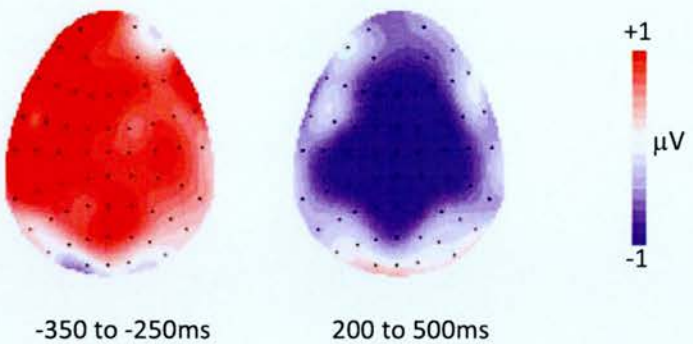

Figure 7-8: Topographic distributions of the expert-passive-coarse/naive-passive-coarse difference for the pre and post segmentation. Each cartoon shows the distribution of the difference between directed-passive-coarse and randomly generated segmentation, averaged across a 100ms time period for the first time window (-350 to -250ms), and across 300ms for the second (200 to 500ms). The front of the head is at the top of each map, and the left hemisphere is on the left-hand side. Each dot represents a recording electrode. The scale bar indicates the range of activity (in microvolts). The effect in the first time window has a centro-left-lateralised and centro-frontal distribution; whereas the effect in the second time window exhibits negativity over central electrodes.

Focussed contrasts directly comparing locations, hemispheres and sites across expert-passive-coarse and naive-passive-coarse pre-event segmentation revealed a 3-way interaction between expert-passive-coarse

minus random/naive-passive-coarse minus random, location and hemisphere [$F(1, 15) = 5.5$; $p < 0.05$], which reflects the broad distribution of the difference in conditions over frontal electrodes, compared with the left greater than right differences present over parietal electrode sites. Analysis of post-segmentation topographic data revealed a main effect of expert-passive-coarse minus random/naive-passive-coarse minus random [$F(1, 15) = 8.63$; $p < 0.05$], reflecting the widespread nature of the effect. A further 2-way interaction was revealed between expert-passive-coarse minus random/naive-passive-coarse minus random and site [$F(1.58, 22.12) = 13.44$; $p < 0.001$], which reflects the greatest differences in conditions present over superior electrode sites.

Therefore, the topographic analyses confirm that the pattern of effects is distributionally different between expert-passive-coarse/random and naive-passive-coarse/random ERPs, both during pre-segmentation and during post-segmentation, inferring the engagement of at least partially, if not wholly, different sets of neural generators. Additionally, the analyses confirm the differential engagement of neural generators pre- and post-segmentation.

7.2.3.1.2 Comparing expert- and naive-passive-fine

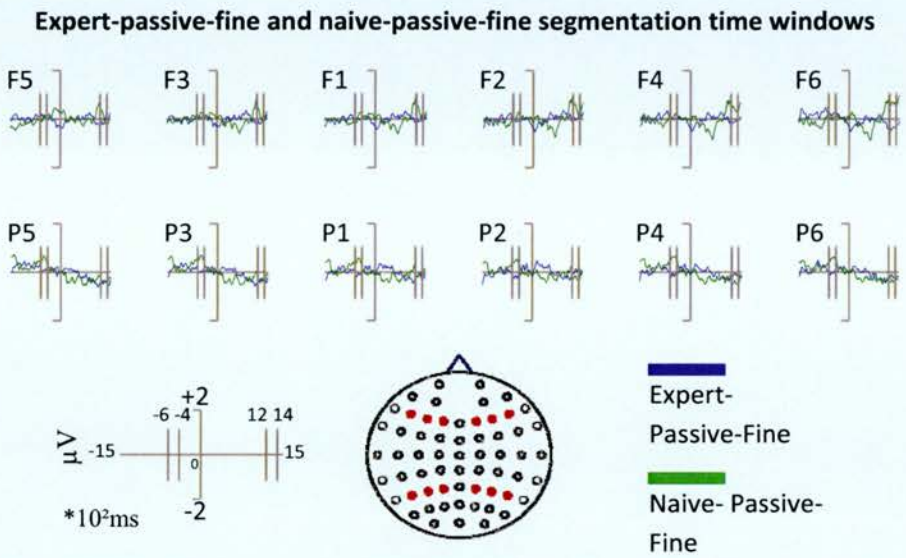

Figure 7-9: The pre-segmentation and post-segmentation time windows are illustrated.

7.2.3.1.2.1 Pre-segmentation time window (-600 to -400ms)

As previous, a pre-segmentation time of -600 to -400ms was selected for analysis (overview data available in Appendix A). Figure 7-9 shows the grand average ERPs time-locked to expert-passive-fine and naive-passive-fine segmentation points, at electrodes chosen for statistical testing; the mean number of trials (± SD) contributing to the ERPs was 26 (9) for expert-passive-fine and 171 (94) for naive-passive-fine.

ANOVA with factors of condition (expert-passive-fine/naive-passive-fine), location (frontal/parietal), hemisphere (left/right) and site (superior/medial/inferior), revealed a significant interaction between condition and site [$F(1.43, 21.44) = 4.12$; $p < 0.05$], reflecting the medially distributed nature of the effect, which follow-up t-tests (reported in Table

7-5) indicate is strongest over parietal electrode locations. Given that the data reported Table 7-5 show that the effect is strongest over parietal locations, it somewhat surprising that no interaction was found with location. Nevertheless, the data reported in Table 7-5 is supported by the illustration in Figure 7-10; greater magnitudes for expert-passive-coarse are present over the parietal electrodes, strongest over the medial electrode on left-lateralised electrodes, and broadly distributed over right-lateralised parietal electrode sites.

T-test pairing results for expert-passive-fine and naive-passive-fine (-600 to -400ms)

Left-Frontal Electrodes		Right-Frontal Electrodes	
F5	-	F6	-
F3	-	F4	-
F1	-	F2	-
Left-Parietal Electrodes		**Right-Parietal Electrodes**	
P5	[t(15) = -1.98; p < 0.1 (0.067)]	P6	[t(15) = -2.82; p < 0.05]
P3	[t(15) = -2.25; p < 0.05]	P4	[t(15) = -2.75; p < 0.05]
P1	[t(15) = -1.86; p < 0.1 (0.083)]	P2	[t(15) = -2.26; p < 0.05]

Table 7-5: T-test results for the expert-passive-coarse and naive-passive-coarse pre-segmentation time window.

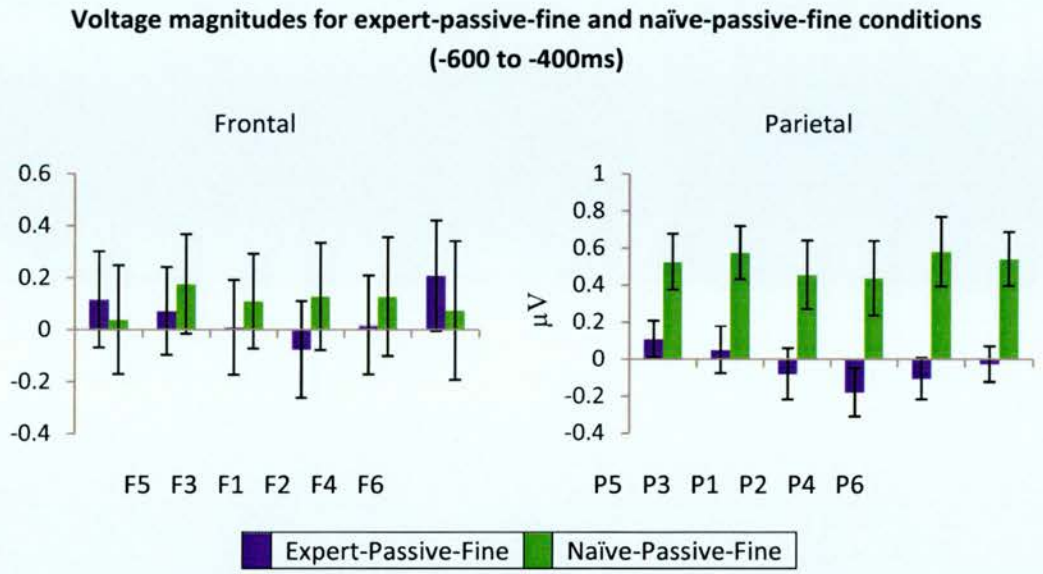

Figure 7-10: The magnitude of ERP effects from --600 to -400ms, shown as in Figure 5-7.

7.2.3.1.2.2 Post-segmentation time window (1200 to 1400ms)

A post-segmentation time window from -1200 to -1400ms was selected for further analysis; ANOVA with factors of condition (expert-passive-fine/naive-passive-fine), location (frontal/parietal), hemisphere (left/right) and site (superior/medial/inferior), revealed a significant interaction between condition and site [$F(1.79, 26.81) = 3.79$; $p < 0.05$], reflecting that the effect is strongest over inferior electrode sites. A further 3-way interaction between condition, location and hemisphere [$F(1, 15) = 12.76$; $p < 0.005$], reflects that the effect is strongest on the right over frontal electrode locations, and marginally stronger on the right over parietal electrode locations. Finally, a 3-way interaction was also revealed between condition, hemisphere and site [$F(1.56, 23.44) = 7.511$; $p < 0.01$], which reflects the effect being stronger inferiorly and medially over right-lateralised electrode sites, compared to a broad distribution found over left-lateralised sites (shown in Figure 7-11). Subsidiary t-tests reported in Table 7-6, indicate that significant

segmentation effects are localised to the right-lateralised frontal inferior electrode site.

T-test pairing results for expert-passive-fine and naive-passive-fine (1200 to -1400ms)

Left-Frontal Electrodes		Right-Frontal Electrodes	
F5	-	F6	[t(15) = -2.36; p < 0.05]
F3	-	F4	-
F1	-	F2	-
Left-Parietal Electrodes		**Right-Parietal Electrodes**	
P5	-	P6	-
P3	-	P4	[t(15) = 1.82; p < 0.1 (0.09)]
P1	-	P2	-

Table 7-6: T-test results for the expert-passive-coarse and naive-passive-coarse post-segmentation time window.

Voltage magnitudes for expert-passive-fine and naïve-passive-fine conditions

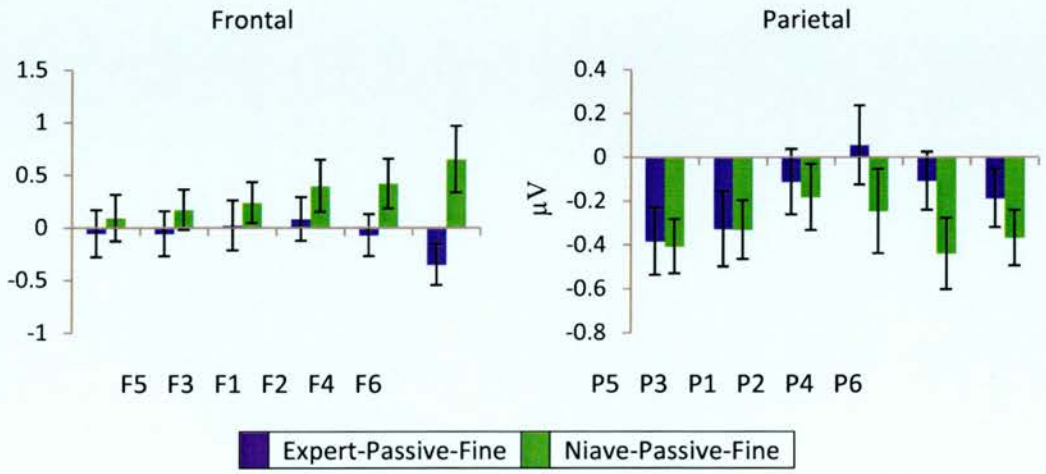

Figure 7-11: The magnitude of ERP effects from -1200 to 1400ms, shown as in Figure 5-7.

7.2.3.1.2.3 Topographic analysis

Figure 7-12 illustrates a clear difference in the pattern of the effect between conditions, and additionally illustrates a change in the pattern of effect over time, most notably with the changing polarity over time present across parietal and right-frontal electrode sites.

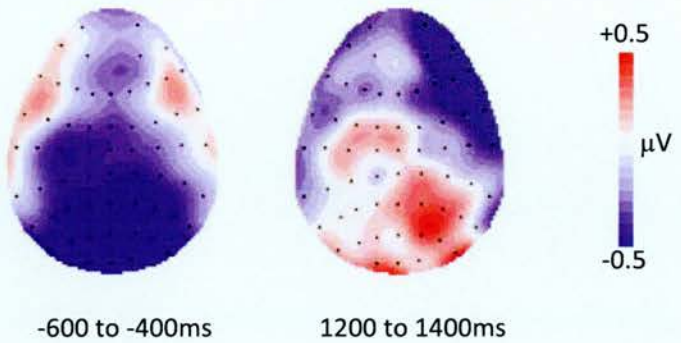

Figure 7-12: Topographic distributions of the expert-passive-fine/navie-passive-fine difference for the pre and post segmentation. Each cartoon shows the distribution of the difference between directed-passive-coarse and randomly generated segmentation, averaged across a 200ms time period for the first time window (-600 to -400ms), and across 200ms for the second (1200 to 1400ms). The front of the head is at the top of each map, and the left hemisphere is on the left-hand side. Each dot represents a recording electrode. The scale bar indicates the range of activity (in microvolts). The effect in the first time window has a centro-posterior and bi-lateral posterior distribution; whereas the effect in the second time window exhibits right-lateralised negativity over frontal electrodes, and a right-lateralised positivity over posterior electrodes.

ANOVA with factors of expert-passive-fine minus random/naive-passive-fine minus random, epoch (-600 to -400ms/1200 to 1400ms), location (frontal/parietal), hemisphere (left/right) and site (superior/medial/inferior), revealed a 3-way interaction between expert-passive-fine minus random/naive-passive-fine minus random, epoch and site [$F(1.83, 25.68) = 7.91$; $p < 0.01$], reflecting the positive differences between conditions present over inferior sites during pre-segmentation, compared

with the positive differences between conditions located over superior electrode sites. A 4-way interaction revealed between expert-passive-fine minus random/naive-passive-fine minus random, epoch, location and hemisphere [$F(1, 15) = 6.8$; $p < 0.05$], is reflective of the front greater than parietal pre-segmentation effect, compared with the parietal greater than frontal, right greater than left parietal distribution and the left greater than right fontal post-segmentation distributions. An additional 4-way interaction was revealed between expert-passive-fine minus random/naive-passive-fine minus random, epoch, hemisphere and site [$F(1.56, 21.79) = 4.03$; $p < 0.05$], which reflects the positive differences in waveforms present bi-laterally during pre-segmentation over inferior electrodes, compared with the right lateralised superior and left lateralised and broadly distributed effect present post-segmentation.

Focussed contrasts directly comparing locations, hemispheres and sites across expert-passive-fine and naive-passive-fine event segmentation revealed an interaction between expert-passive-fine minus random/naive-passive-fine minus random and site [$F(1.42, 19.87) = 4.86$; $p < 0.05$], which reflects positive differences in the waveforms overlying inferior electrode sites. Analysis of post-segmentation topographic data revealed a 2-way interaction between expert-passive-fine minus random/naive-passive-fine minus random and site [$F(1.75, 24.45) = 5.61$; $p < 0.05$], which reflects positive differences in the waveforms overlying superior electrode sites. A 3-way interaction was revealed between expert-passive-fine minus random/naive-passive-fine minus random, location and hemisphere [$F(1, 15) = 9.88$; $p < 0.01$], reflecting the right greater than left differences over parietal electrodes, compared with the left greater than right differences present over frontal electrodes. An additional 3-way interaction was revealed between expert-

passive-fine minus random/naive-passive-fine minus random, hemisphere and site [$F(1.97, 27.57) = 9.2$; $p < 0.01$], reflecting the right-lateralised differences which are strongest over superior electrodes, compared with the broad distribution of left-lateralised differences over electrode sites.

Therefore, the topographic analyses confirm that the pattern of effects is distributionally different between expert-passive-fine/random and naive-passive-fine/random ERPs, marginally pre-segmentation and significantly post-segmentation, inferring the engagement of at least partially, if not wholly, different sets of neural generators. Additionally, the analyses confirm the differential engagement of neural generators pre- and post-segmentation.

7.2.3.2 Active segmentation

7.2.3.2.1 Comparing expert-active-coarse and fine

Grand average ERPs for expert-active-coarse and expert-active-fine segmentation on electrode CZ are illustrated in Figure 7-13; maximal positive-going ERP activity is notably earlier than in the previous two investigations reported in previous chapters. For this reason, two time-windows were selected for analyses; the time surrounding maximal positivity (175 to 200ms), and the same time-window used in the previous chapters (200 to 225ms). Once again the data were subjected to a t-test analysis.

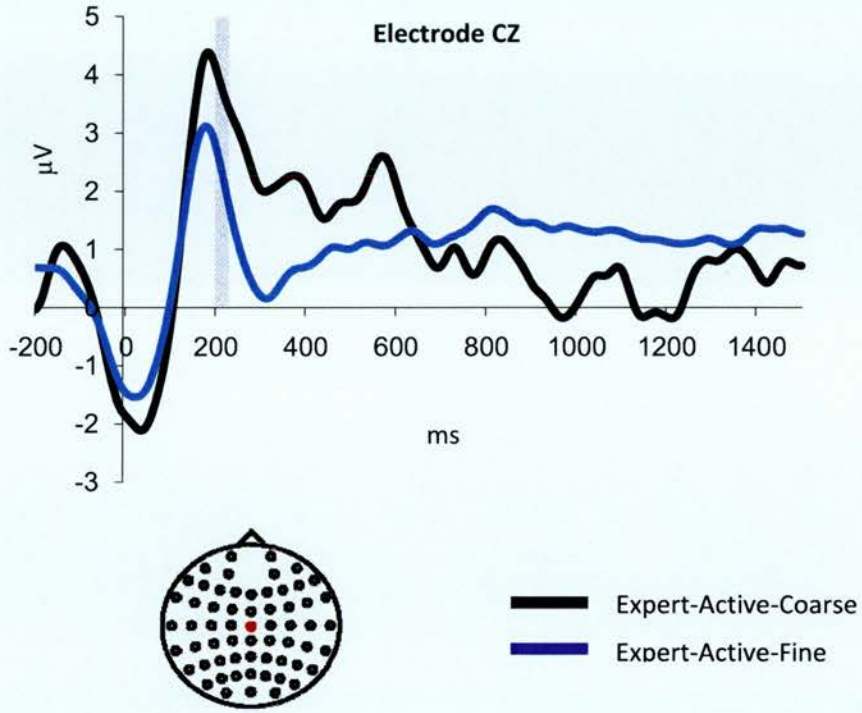

Figure 7-13: Grand average ERPs elicited for expert-active-coarse (black) and expert-active-fine (blue) on the electrode site CZ (shown as the red dot on the scalp map). More positive-going activity is present for active-coarse ERPs compared to active-fine ERPs during the 200 to 225ms time window (shaded grey).

Notwithstanding the additional time window analysis, no effect of magnitude was found between expert-active-coarse and expert-active-fine, with only the second time-window (200 to 225ms) yielding marginally significant result [$t(15) = 1.93$; $p < 0.1$ (0.072)]. For illustrative purposes, the magnitude analysis and topographic distribution from the second time-window are illustrated Figure 7-14 (a) and (b) respectively.

In summary, the results failed to demonstrate a significantly greater magnitude for expert-active-coarse segmentation when compared to expert-active-fine segmentation, perhaps indicating that participants who have recently learned an activity, fail to place the same emphasis on coarse-grain boundaries as participants watching everyday tasks as reported in the

previous chapters. Although the waveforms are analogous in morphology to the results of the Zacks et al. (2001) study, they differ in that coarse-grain responses are not significantly greater than fine-grain responses for recently learned obscure activities.

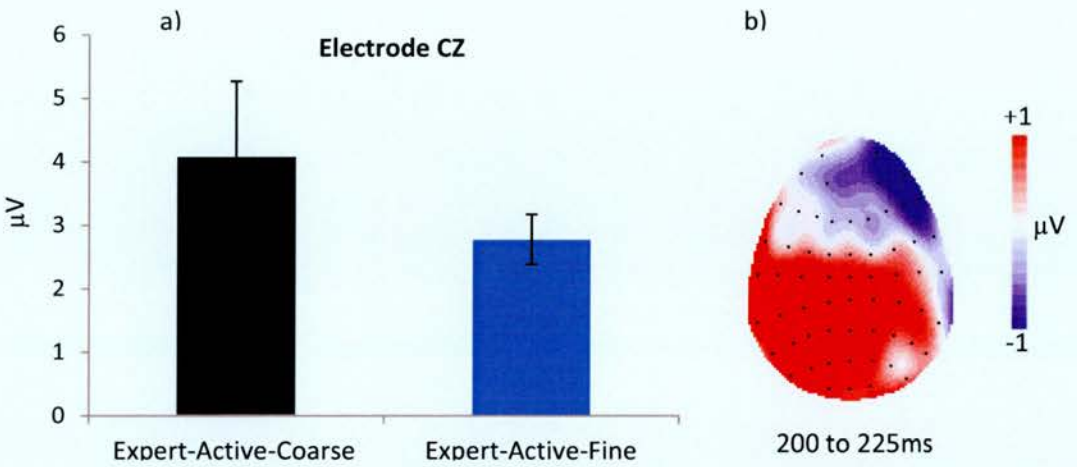

Figure 7-14: (a) Differences in effect sizes at electrode site CZ are shown for expert-active-coarse (black) and expert-active-fine (blue) segmentation points. Only marginally significant larger effect sizes were present for expert-active-coarse compared to expert-active-fine segmentation points. (b) Topographic distribution of the expert-active-coarse/ expert-active-fine difference averaged across a 25ms time period (200 to 225ms). The front of the head is at the top of the map, and the left hemisphere is on the left-hand side. Each dot represents a recording electrode. The scale bar indicates the range of activity (in microvolts). The effect is clearly distributed across the central electrodes, mostly likely reflecting the magnitude differences originating in the motor cortex. Additionally, the effect shows a centro-left-lateralised and centro-posterior distribution.

7.2.3.2.2 Comparing naive-active-coarse and fine

As previous, data from electrode CZ (see Figure 7-15) were subjected to a t-test examination; revealing a clear difference in magnitude between naive-active-coarse and naive-active-fine segmentation [$t(13) = 3.99$; $p < 0.01$], with

the ERPs for naive-active-coarse more positive-going than those for naive-active-fine. For illustrative purposes, the magnitude analysis and topographic distribution are illustrated Figure 7-16 (a) and (b) respectively.

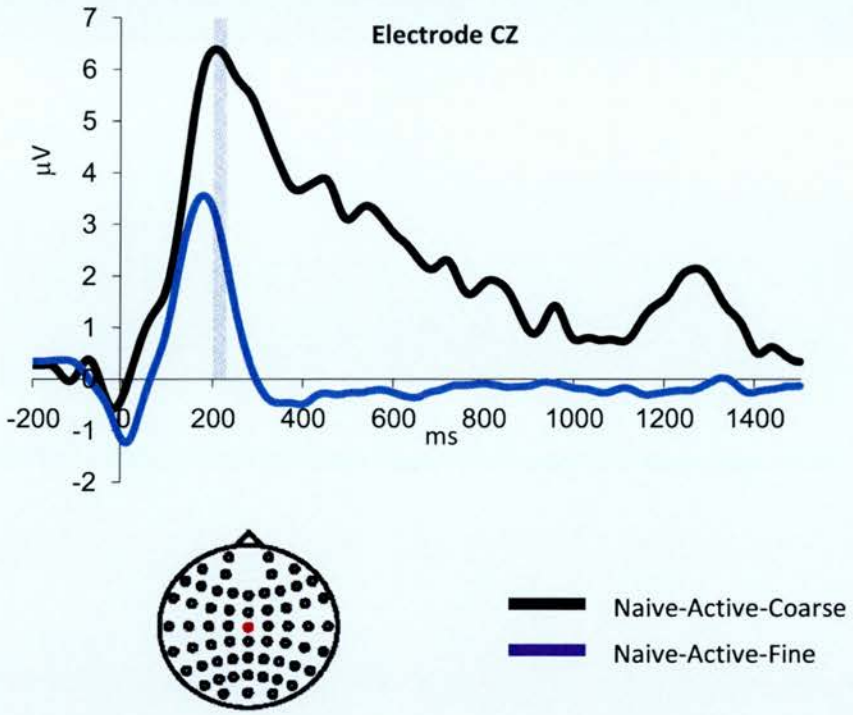

Figure 7-15: Grand average ERPs elicited for naive-active-coarse (black) and naive-active-fine (blue) on the electrode site CZ (shown as the red dot on the scalp map). More positive-going activity is present for active-coarse ERPs compared to active-fine ERPs during the 200 to 225ms time window (shaded grey).

In summary, the results reveal a somewhat surprising alignment with analyses conducted in the previous two chapters; greater voltage magnitudes for naive-active-coarse segmentation were found when compared to naive-active-fine segmentation. The result is interesting because the previous two studies used everyday activities for testing, while the current participant group had no knowledge of the obscure activities displayed prior to testing.

Although not overwhelmingly surprising on its own, when compared against the activity expert participant group who failed to display a significant difference in magnitudes, the result does give rise to questions such as: why would activity expert participants fail to demonstrate the same effect?

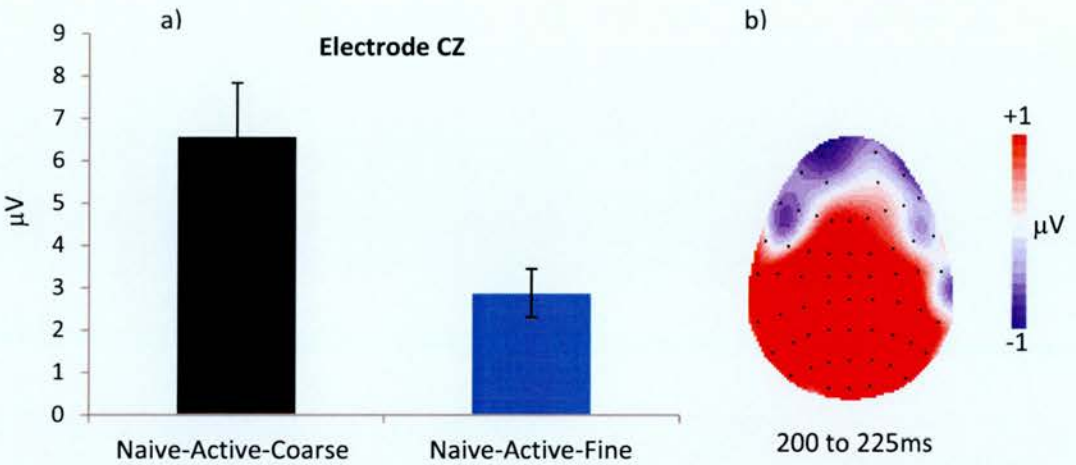

Figure 7-16: (a) Differences in effect sizes at electrode site CZ are shown for naive-active-coarse (black) and naive-active-fine (blue) segmentation points. Significantly larger effect sizes were present for naive-active-coarse compared to naive-active-fine segmentation points. (b) Topographic distribution of the naive-active-coarse/ naive-active-fine difference averaged across a 25ms time period (200 to 225ms). The front of the head is at the top of the map, and the left hemisphere is on the left-hand side. Each dot represents a recording electrode. The scale bar indicates the range of activity (in microvolts). The effect is clearly distributed across the central electrodes, mostly likely reflecting the magnitude differences originating in the motor cortex. Additionally, the effect shows a bi-lateralised distribution over parietal electrodes.

One clear disparity between the groups that match the pattern of results is the number of stimulus viewings; expert participants actively marked segmentation points on the third viewing of the activities, compared with all the other groups who actively marked boundaries on only the

second viewing. This pattern may reflect the structural updating of a cognitive schema, which has been somewhat satisfied by the third viewing of an activity. The results also suggest that cognitive schema updating is likely to occur for even everyday activities as participants match the structure in the activities with their own, pre-existing, schema structure.

7.2.4 Discussion

The aim of the experiment was to investigate whether familiarity with an activity gave rise to differential neural correlates of event segmentation. The experiment also investigated how familiarity affected behavioural activity in relation to the perception of everyday events.

7.2.4.1 Summary and interpretation

The ERPs for expert- and naive-passive-coarse appear broadly similar in morphology, particularly over parietal electrodes where pre-segmentation activity is positive-going before switching polarity, developing into negative-going post-segmentation activity. Nevertheless, clear divergences in the waveforms are present, most notably present post-segmentation over centralised electrode sites. Furthermore, magnitude analyses revealed more positive-going pre-segmentation activity for expert-passive-coarse ERPs over left-frontal electrodes. Notably, post-segmentation divergences displayed inversely proportional activity, with expert-passive-coarse ERPs more negative-going; conversely, however, waveform divergences were present over parietal electrode sites. Indeed, topographic analyses confirmed that differences between expert-passive-coarse and naive-passive-coarse ERPs were a result of the differential engagement of neural generators, both pre-

and post-segmentation. Moreover, the topographic analyses present evidence for the activation of different neural generators pre- and post-segmentation.

In contrast with the comparison of expert- and naive-passive-coarse ERPs, the ERPs for expert-passive-fine and naive-passive-fine share little commonality in their morphologies. Correspondingly, however, the comparison of expert-passive-fine and naive-passive-fine ERPs revealed pre- and post-segmentation divergences; naive-passive-fine ERPs were more positive bi-laterally pre-segmentation, and more positive right-frontally post-segmentation. Additionally, topographic analyses demonstrated the activation of differing neural generators pre-, post- and between pre- and post-segmentation, in similarity with the comparison of expert-passive-coarse and naive-passive-coarse ERPs.

To summarise, the ERPs for expert-passive-coarse and naive-passive-fine share broadly similar characteristics, particularly early pre-segmentation over frontal electrode sites, and late pre-segmentation over parietal sites. Both appear to exhibit positive-going pre-segmentation and negative-going post-segmentation effects over parietal sites, which is in correspondence with the previous two ERP studies. Nevertheless, the ERPs for expert -passive-coarse and naive passive-fine do also exhibit differences; a late pre-segmentation effect is demonstrated over left-frontal electrodes, and an early post-segmentation effect is present over central and centro-parietal electrodes. Similarly, the ERPs for expert-passive-fine and naive-passive-fine also exhibit positive-going pre- and negative-going post-segmentation activity over parietal electrode sites, but also clearly exhibit divergences. Furthermore, topographic analyses confirm the differential engagement of neural generators pre- and post-segmentation for both the comparison of expert- and naive-passive-coarse- and passive-fine segmentation. Therefore,

the results clearly demonstrate a neurophysiological effect of familiarity upon passive event segmentation at both a coarse- and fine-level.

Interestingly, greater responses for naive-passive-fine ERPs rather than expert-passive-fine ERPs were noted pre- and post-segmentation, indicating that more emphasis is placed upon processing fine-grain event boundaries when activities are unfamiliar. Following this elucidation, it could be hypothesised that task expert participants focus more on top-down structuring during their second stimulus viewing, having previously studied the unfamiliar objects and actions. Hence, the larger response revealed for task naive participants during fine-grain segmentation is reflective of the greater attention paid to bottom-up cues when processing unfamiliar events; perhaps suggesting that participants learn bottom-up features of unfamiliar tasks first, before assimilating this information into a cognitive structure.

The aforementioned interpretation also goes someway to explaining the somewhat surprising result that familiarity was shown to have an effect upon active event segmentation. The summation is not surprising, more the pattern of effect uncovered; activity naive participants were shown to align with previous data by demonstrating larger magnitudes elicited for coarse- than fine-grain segmentation, while participants whom had recently learned the obscure activity did not. Why then should active unfamiliar and everyday activity segmentation align with each other in terms of magnitude differences elicited for coarse- and fine-grain segmentation, yet mutually conflict with the magnitudes elicited during active segmentation of a recently-learned activity? One possible interpretation may be that segmenting an everyday activity represents the norm, e.g. that greater psychological emphasis is placed upon coarse-grain event boundaries. Therefore, the conflict potentially arises owing to the fact that participants

who are unfamiliar with an activity attempt to process information by the only means they know how: segmenting events normally, perhaps even implying a hierarchical structure as best they can (yet differently as per the Hard et al. 2006 comparisons).

Taken together, it could be suggested that having just learned a new activity one is attempting to reinforce newly generated cognitive schema, by perhaps focussing less on the finer-grain event parts and more on refining a new internal structure. The interpretation could lead to the conclusion that different schemata-related neurological processes are active having just learned a new activity, compared to processing an everyday activity with a pre-existing cognitive schema, or when processing an activity with no cognitive schema by employing automatic event segmentation.

7.2.4.2 Comparison with event segmentation literature

In correspondence with the previous ERP studies, behavioural measures were recorded in this experiment to facilitate a comparison with existing event segmentation literature. Generally, the behavioural data correspond with the previous two ERP studies and the results of previous event segmentation investigations. Specifically, participants were found to segment activities in terms of their parts and sub-parts, so forming a hierarchical relationship between coarse- and fine-grain segmentation (Zacks, Tversky, et al., 2001; Zacks et al. (2001). Moreover, the raster plots shown in Figure 7-1 and Figure 7-2 suggest that there is common agreement between participants over the perception of event breakpoints, a characteristic exhibited for both expert and naive groups, respectively. This finding aligns with previous research (e.g. Newtson, 1973a; Zacks & Tversky, 2001; Bower et al., 1979). It may be interpreted from these results that familiarity has no effect on how a

participant defines an event boundary, and additionally has no influence over the tendency to align coarse- with fine-grain event boundaries. Conversely, the comparison of expert and naive participant's use of coarse-grain boundaries to subsume fine-grain events did reveal an effect of familiarity. In line with the previous experiment investigating the segmentation of everyday events, activity experts were found to subsume small segments with large segment boundaries. However this trend was not observed in activity naive participants. The pattern of results reveals an interesting effect; when activities are unfamiliar, participants fail to group event sub-parts by large segment boundaries. It is possible, that the lack of existing schemata upon which to base accurate predictions of event relation is reflected in the results.

The experiment also sought to investigate conflicts in event segmentation literature; namely, the claim that participants who are unfamiliar with an activity perceive more event parts than those who are familiar with the activity (Hard, Tversky, & Lang, 2006), and an opposing claim (Zacks, Tversky, et al., 2001). No effect of familiarity was found during the investigation of segmentation rates, demonstrated clearly in section 7.2.2.4. Therefore, the results of this experiment support the earlier findings of Zacks, Tversky, et al. (2001), concluding that the occurrence of event sub-part boundary perception is unaffected by the level of familiarity one has with an activity.

7.3 Conclusions

The chapter reported an experiment that investigated the effects of familiarity upon event segmentation in both the behavioural and neural

domains. In similarity with the previous ERP studies, there was evidence to suggest that the study is broadly in line with previous research in event segmentation. Again, participants agreed over the perception of event boundaries, and behavioural evidence for hierarchical structuring demonstrated consistency with the literature. Additionally, however, the use of coarse-grain event boundaries to subsume fine-grain event parts was shown to be sensitive to level of familiarity one has with an activity. Neural data also contained several comparable features with the Zacks et al. study of 2001, including neural responses to passive and active event segmentation, present for both coarse- and fine-grain segmentation in activity expert and naive groups. However, analysis of active segmentation data revealed a coarse-greater-than-fine magnitude effect present only in activity naive participants. Additionally, a greater response was elicited from task naive participants than for task exert participants during fine-grain segmentation. When taken together, these two findings led to the claim that participants who have recently learned an activity focus less on comprehending unfamiliar objects and tasks, but more on refining a hierarchical structure. Nevertheless, a clear pattern of expected effects were demonstrated during passive segmentation. Specifically, greater differences were present between the ERPs for unfamiliar segmentation compared with everyday and recently-learned ERPs. Moreover, the ERPs for everyday and recently-learned activity segmentation failed to differ significantly post-segmentation (see Appendices). In sum, the pattern perhaps reflects the retrieval of pre-existing cognitive schema versus a failed retrieval when events are unfamiliar.

In the grander scheme, it appears satisfactory that this experiment should successfully demonstrate differential neural correlates of information processing that are sensitive to familiarity. Certainly, one would expect the

differential engagement of cognitive-schema based upon existing knowledge structure to elicit varying neurological activity. Importantly, however, the current experiment demonstrates an effect of familiarity within the realms of event segmentation theory. The results clearly show that event segmentation is sensitive to the expected disparities in processing activities with varying levels of familiarity. Moreover, the experiment revealed the sensitivity of hierarchical structuring to the familiarity one has with an activity. Significantly, the experiment also demonstrated the differential engagement of neural generators pre- and post-segmentation, supporting the previous hypothesis that EEG data more closely reflect the multiple cognitive functions likely to be active when processing information.

Given the success of the experiment in demonstrating a clear interdependence between event segmentation and memory, the following study will focus again on the influences on event segmentation. Specifically, in light of the demonstration of top-down influence upon coarse- and fine-grain segmentation, bottom-up influences will be investigated in the following chapter. Additionally, the influence of structure and goal-directness upon event segmentation will be further investigated.

8 Segmenting abstract events

8.1 Introduction

Thus far, the experiments reported in this thesis have consistently demonstrated that the neural correlates of event segmentation may be measured using EEG. Moreover, in a somewhat surprising finding given the results of the fMRI study (Zacks et al., 2001), a pattern is emerging of differentially engaged neural generators pre- and post-segmentation. In similarity however with previous studies, the behavioural correlates of event segmentation have demonstrated a robust effect of hierarchical structuring. Additionally, the previous experiments have shown that the use of coarse-grain event boundaries to subsume fine-grain event parts is sensitive to both experiment task knowledge and activity familiarity. The previous experiment in particular, demonstrated that in support of Event Segmentation Theory (EST), event boundary perception was neurophysiologically sensitive to a participant's familiarity with an activity, perhaps reflecting the differential engagement of cognitive schemata in response to error prediction.

In a further extension of the experimental paradigm employed in previous studies of event segmentation, the current experiment seeks to investigate top-down and bottom-up influences upon event boundary perception. Firstly; top-down knowledge of an activity is removed by presenting abstract movie stimuli (geometric shapes), thus allowing a test of the hypothesis that participants will rely more heavily upon the bottom-up physical characteristics of the activity, and secondly; by introducing a subtle manipulation of top-down knowledge whereby one participant group will believe the abstract movie stimuli represent a goal-directed activity, whilst a

second group of participants will believe the same shape movements to be random. The experimental manipulations allow two distinct hypotheses to be generated, firstly; that the removal of top-down knowledge will elicit neurologically distinguishable correlates of event segmentation compared with processing of everyday events as participants rely more heavily on the bottom-up features of the activity, and secondly; that the neural correlates of event segmentation will be sensitive to the inference of goal-directedness. As discussed in Section 4.1.2.4, the movie stimulus presented in the current experiment are not goal-directed; the movements of the geometric shapes are generated randomly, but importantly, a study group of participants identified the movements in the movies to most represent a real-life objective e.g. one shape chasing the other (see Zacks, 2004).

Owing to the robust effect of hierarchical structuring found in all previous experiments, it is hypothesised that this phenomenon will be unaffected by the manipulation of activity abstraction or the inference of goal-directedness. However, given the sensitivity of coarse-grain boundaries subsuming fine-grain events effect demonstrated in the thesis thus far, the affect the top-down manipulations will have in the current experiment is less clear; it is tentatively hypothesised that participants perceiving the activities as reflecting a *game*, will subsume fine-grain events with coarse-grain boundaries, whilst participants perceiving the activities as reflecting *random* actions will not. Finally, the previous experiment failed to demonstrate an effect of familiarity upon the number of event segments perceived, however in face of contradictory studies (e.g. Hard et al., 2001 and Zacks, Tversky, et al. 2001), the hypothesis is investigated further by comparing the number of event boundary perceptions between groups of varying inferred top-down knowledge. Owing mainly to the failure in the previous study, it is

hypothesised that the inference of goal-directedness will fail to significantly alter the number of perceived event parts.

The critical question to be addressed in the current study is whether the mere inference of structure and goal-directedness will elicit differential neural correlates of event segmentation. Additionally, this experiment will address the question of whether top-down knowledge and activity abstraction elicit distinguishing ERP correlates of event segmentation, when compared with the event segmentation of everyday events.

8.2 Experiment 4: Investigating the effect of coaching on event segmentation using ERPs

8.2.1 Methods

The following sections detail the experimental methods followed in this experiment.

8.2.1.1 Stimuli

As previously discussed, video stimuli employed in this experiment were previously generated and used by Zacks in his 2004 study. Four activities were depicted; shapes fighting, shapes chasing, shapes courting and shapes playing.

8.2.1.2 Participants

Thirty-three participants took part in the experiment; data from one participant was discarded due to behavioural non-compliance, leaving thirty-two participants in the group (10 male, age range 17-32).

8.2.1.3 Procedure

Principally, the procedure used in this experiment replicates the methods outlined in the General Methods chapter, and the Zack et al. study in 2001. Distinguishingly, however, participants in this experiment were subjected to a subtle manipulation; one group was informed that shape movements reflected only a randomly generated pattern, whereas a second group was informed that shape movements reflected a game being played by two students, e.g. circle chases square.

8.2.2 Behavioural results

The following section contains analysis of behavioural data collected from 32 participants as they performed the event segmentation experiment.

8.2.2.1 Investigating the concurrence of event perception

As in the previous experiment the automaticity of event segmentation was investigated by examining participant agreement, illustrated in Figure 8-1 and Figure 8-2. In line with the findings from the previous studies, visual inspection of the raster plots clearly indicates a common perception of event boundaries in time, particularly for the coarse conditions.

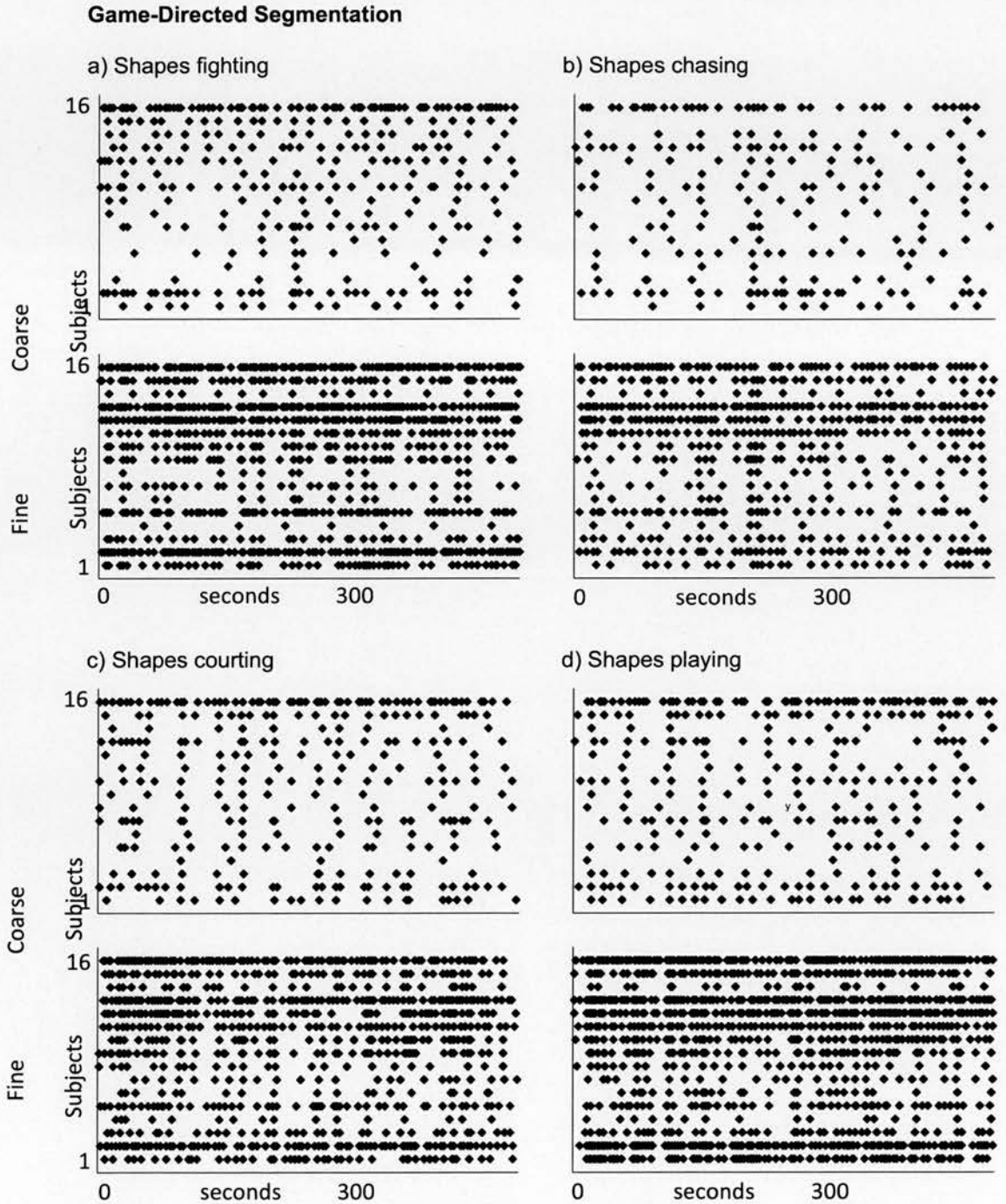

Figure 8-1: Raster plots of segmentation timings (x-plane) for each participant (y-plane), shown separately for each movie (a-d), for fine and coarse conditions. Each individual data point reflects a single segmentation response.

Figure 8-2: Raster plots of segmentation timings (x-plane) for each participant (y-plane), shown separately for each movie (a-d), for fine and coarse conditions. Each individual data point reflects a single segmentation response.

Correlation results for coarse- and fine-grain event perception

Activity	Game-Directed	Random-Directed
Shapes chasing	$r(298) = 0.394$; $p < 0.001$	$r(298) = 0.389$; $p < 0.001$
Shapes courting	$r(298) = 0.353$; $p < 0.001$	$r(298) = 0.31$; $p < 0.001$
Shapes fighting	$r(298) = 0.326$; $p < 0.001$	$r(298) = 0.207$; $p < 0.001$
Shapes playing	$r(298) = 0.446$; $p < 0.001$	$r(298) = 0.241$; $p < 0.001$

Table 8-1: Resulting p-values from the correlation tests performed on the temporal response distributions for coarse- with fine-grain segmentation

As previously, Temporal Response Distributions (TDRs) were formed for participant responses to examine the relationship between fine- and coarse-grain event boundary perceptions; correlation results (listed in Table 8-1) for both groups of participants, which clearly demonstrate a high-level of association between coarse- and fine-grain boundary perceptions across all activities. The results indicate that participants share a common strategy across coarse- and fine-grain event segmentation independent of the implication of structure.

8.2.2.2 Investigating the hierarchical nature of event perception

Figure 8-3 shows the mean value of recorded and randomly placed overlap time-bins calculated for each activity, recorded from the game-directed and random-directed segmentation groups of participants.

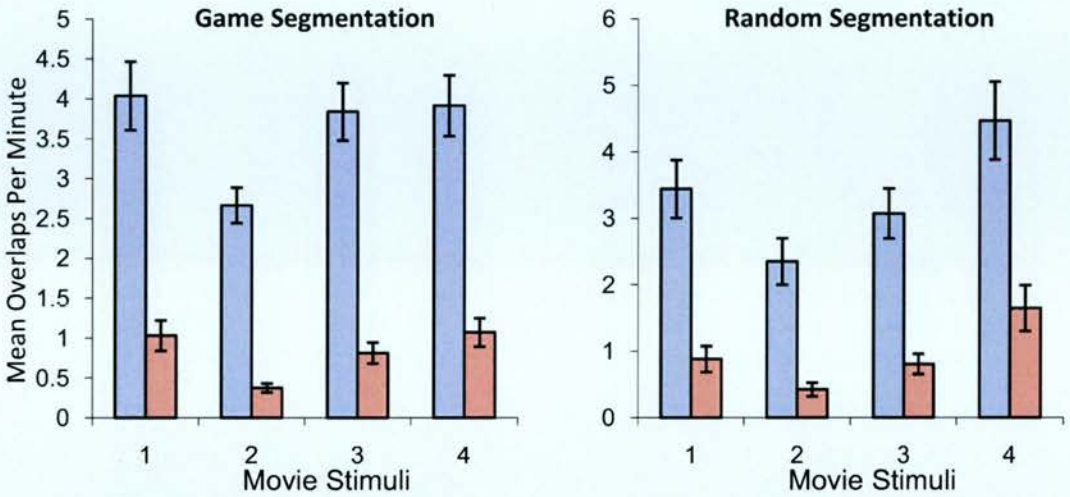

Figure 8-3: Mean number of overlap time-bins for recorded (purple) and randomly placed (blue) segmentations per minute are shown for each video; (1) shapes fighting, (2) shapes chasing, (3) shapes courting and (4) shapes playing. Error bars represent one standard error of the mean. For all four movies, significantly larger numbers of overlapping time-bins were recorded from participants marking coarse and fine event boundaries than would occur randomly.

Despite an initial high-level analysis failing to demonstrate an effect of direction, each group was submitted to ANOVA with factors of condition (recorded/randomly placed) and activity (shapes fighting, shapes chasing, shapes courting and shapes playing). In line with the previous experiments, both the game-directed [$F(1,15) = 48.34$; $p < 0.001$] and random-directed [$F(1,15) = 77.31$; $p < 0.001$] groups demonstrated main effects of condition overlap time-bins. Two-tailed paired sample t-tests results (reported in Table 8-2), demonstrate that hierarchical performance was present for each movie, for both groups of participants. In summary, the behavioural results clearly indicate that participants encoded the activity in terms of hierarchical relationships between parts and sub-parts, regardless of structure inference.

T-test results for overlapping coarse- and fine-grain event perception

Activity	Game Directed	Random Directed
Shapes fighting	[t(15) = -5.92; p < 0.001]	[t(15) = -7.56; p < 0.001]
Shapes chasing	[t(15) = -6.64; p < 0.001]	[t(15) = -6.85; p < 0.001]
Shapes courting	[t(15) = -6.49; p < 0.001]	[t(15) = -8.3; p < 0.001]
Shapes playing	[t(15) = -6.54; p < 0.001]	[t(15) = -8.47; p < 0.001]

Table 8-2: Resulting p-values from the two-tailed t-tests performed on each activity for both groups of participants; clear differences are present between actual overlapping time bins recorded and those arising purely by chance, seemingly regardless of the level of the influence of structure.

Albeit in the absence of any effect of inference found when comparing fine- before coarse-grain/coarse-before fine-grain segmentations for the game and random participants (as illustrated in Figure 8-4), ANOVA with factors of condition (fine subsuming coarse/coarse subsuming fine) and activity (shapes fighting, shapes chasing, shapes courting and shapes playing), demonstrated a main effect of condition for the game-directed group [$F(1,15) = 7.27$; $p < 0.05$], but not for the random-directed group [$p>0.05$]. T-test results run on each activity for both groups of participants, revealed only one significant result for game-directed participants segmenting the 'shapes chasing' stimulus [$t(15) = 2.26$; $p < 0.05$]. Nevertheless, the comparison of each group's ANOVA results leads to the conclusion that one may only attempt to hierarchically group seemingly random events, when one believes an ongoing activity reflects goal-orientated behaviour.

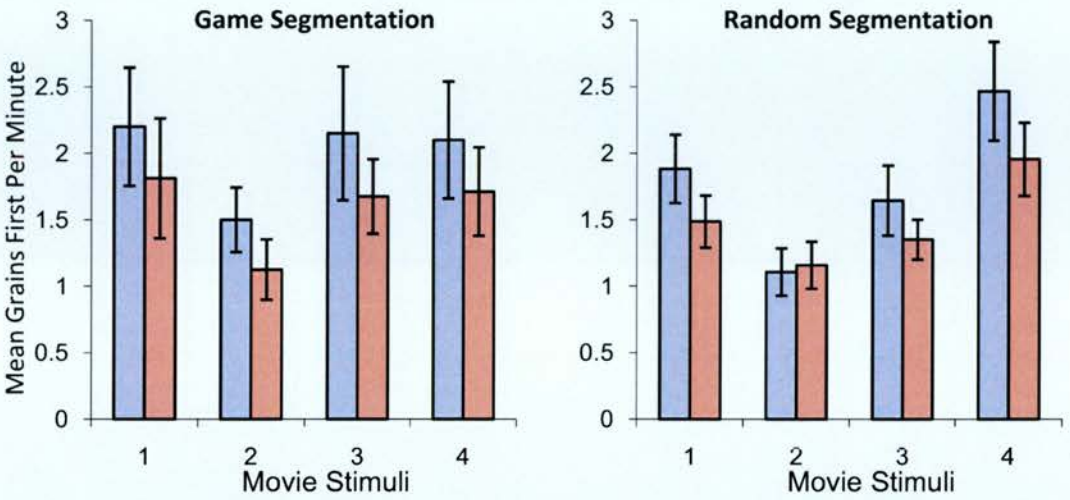

Figure 8-4: Mean number of fine- before coarse-grain segmentations (light blue), and coarse-before fine-grain segmentations (light red) per minute are shown for each video; (1) shapes fighting, (2) shapes chasing, (3) shapes courting and (4) shapes playing. Error bars represent one standard error of the mean. Movie three showed significantly larger numbers of fine- before coarse-grain segmentations than coarse- before fine-grain segmentations.

8.2.2.3 Investigating the influence of structural inference upon parsing rates

As discussed in the introduction chapter, and investigated in Chapter 7, contradictory evidence exists to support the hypothesis that participants segment unfamiliar activities into smaller parts. The results reported in Chapter 7 failed to support the hypothesis; nevertheless, the influence of activity structure inference upon parsing rates is investigated. For illustrative purposes, participant parsing rates for activity game- and random-directed participants are shown in Figure 8-5, (a) coarse-grain segmentation and (b) fine-grain event segmentation. T-test results failed to reveal any difference between the game- and random-directed participant groups during coarse- or fine-grain event segmentation, suggesting that parsing rates are unaffected by the inference of structure upon an activity.

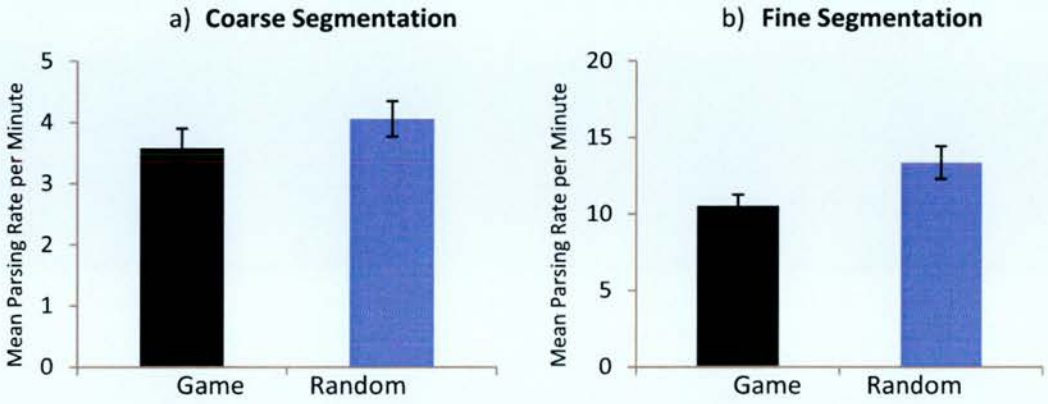

Figure 8-5: Mean parsing rates per minute for game-directed (black) and random-directed (blue) participants are compared during (a) coarse-grain event segmentation, and (b) fine-grain event segmentation. As the graphs indicate, no difference was found between the two groups for either coarse- or fine-grain segmentation.

8.2.3 ERP results

8.2.3.1 Investigating the differences between game-orientated and random event perception

8.2.3.1.1 Comparing game- and random-passive-coarse

8.2.3.1.1.1 Pre-segmentation time window (-1000 to -800ms)

As per the procedures outlined previously, a pre-segmentation time window from -1000 to -800ms was selected for analysis (overview data available in Appendix A). Figure 8-6 shows the grand average ERPs time-locked to game-passive-coarse and random-passive-coarse segmentation points, at electrodes chosen for statistical testing; the mean number of trials (± SD) contributing to the ERPs was 70 (53) for game-passive-coarse and 86 (43) for random-passive-coarse.

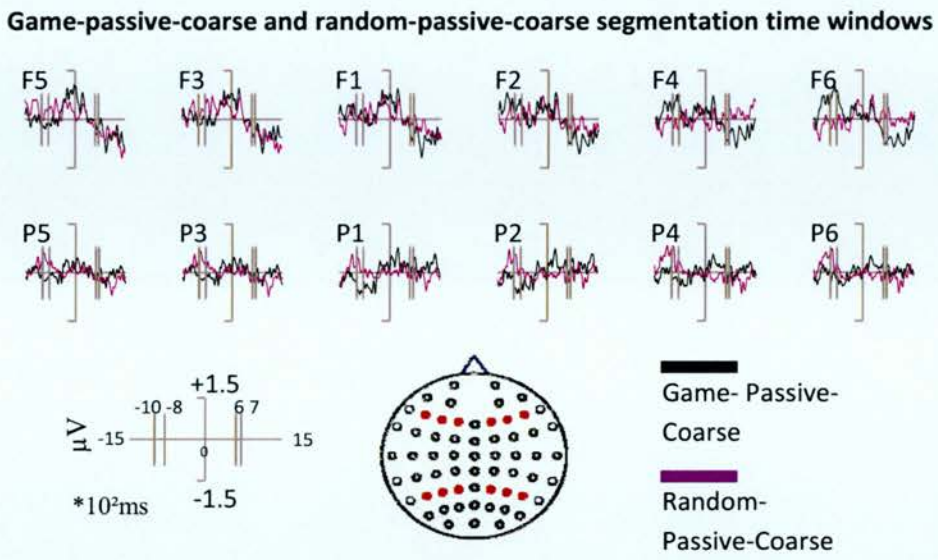

Figure 8-6: The pre-segmentation and post-segmentation time windows are illustrated.

ANOVA with factors of condition (game-passive-coarse/random-passive-coarse), location (frontal/parietal), hemisphere (left/right) and site (superior/medial/inferior), revealed a significant interaction between condition and location [$F(1, 15) = 5.43$; $p < 0.05$], which reflects parietal greater than frontal distribution of the effect. A further 3-way interaction between condition, location and hemisphere [$F(1, 15) = 6.89$; $p < 0.05$], reflects the right greater than left differences over frontal electrodes, when compared to the broad bi-lateral distribution over parietal electrode sites (illustrated in Figure 8-7). The data were subsequently subjected to a series of individual t-test results (reported in Table 8-3); significant segmentation effects present predominantly over parietal electrodes.

T-test pairing results for game-passive-coarse and random-passive-coarse (-1000 to -800ms)

Left-Frontal Electrodes		Right-Frontal Electrodes	
F5	-	F6	[t(15) = 1.96; p < 0.1 (0.069)]
F3	-	F4	-
F1	-	F2	-
Left-Parietal Electrodes		**Right-Parietal Electrodes**	
P5	[t(15) = -2.05; p < 0.1 (0.059)]	P6	[t(15) = -1.8; p < 0.1 (0.093)]
P3	[t(15) = -1.98; p < 0.1 (0.067)]	P4	[t(15) = -2.27; p < 0.05]
P1	[t(15) = -2.02; p < 0.1 (0.062)]	P2	[t(15) = -2.11; p < 0.1 (0.052)]

Table 8-3: T-test results for the game-passive-coarse and random-passive-coarse post-segmentation time window.

Voltage magnitudes for game-passive-coarse and random-passive-coarse conditions

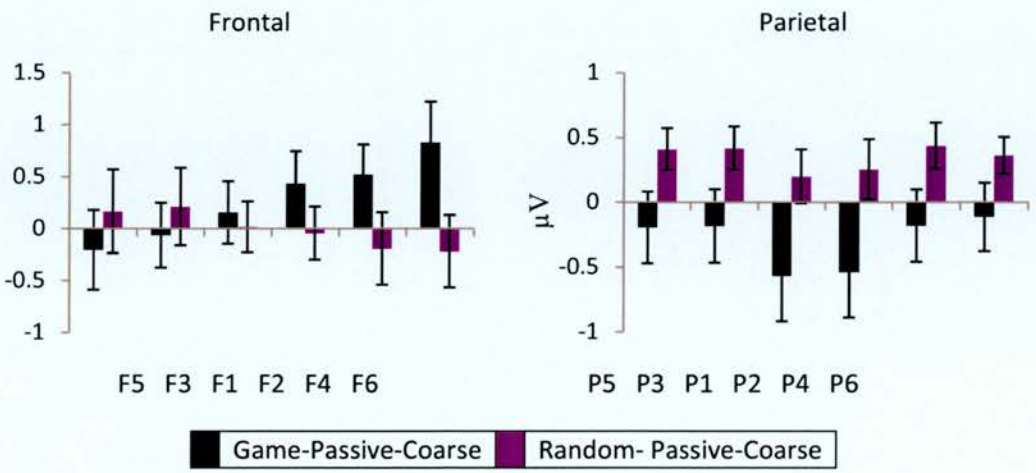

Figure 8-7: The magnitude of ERP effects from --1000 to -800ms, shown as in Figure 5-7.

8.2.3.1.1.2 Post-segmentation time window (600 to 700ms)

Despite the lack of data presented in the overview table, visual inspection of the waveforms in Figure 8-6 clearly indicate a bi-lateral divergence present

over parietal electrode sites. Therefore, a series of time windows were statistically analysed (data not presented), with the effect found most robust between 600 and 700ms. The analysis of the time window 600 to 700ms is therefore presented below.

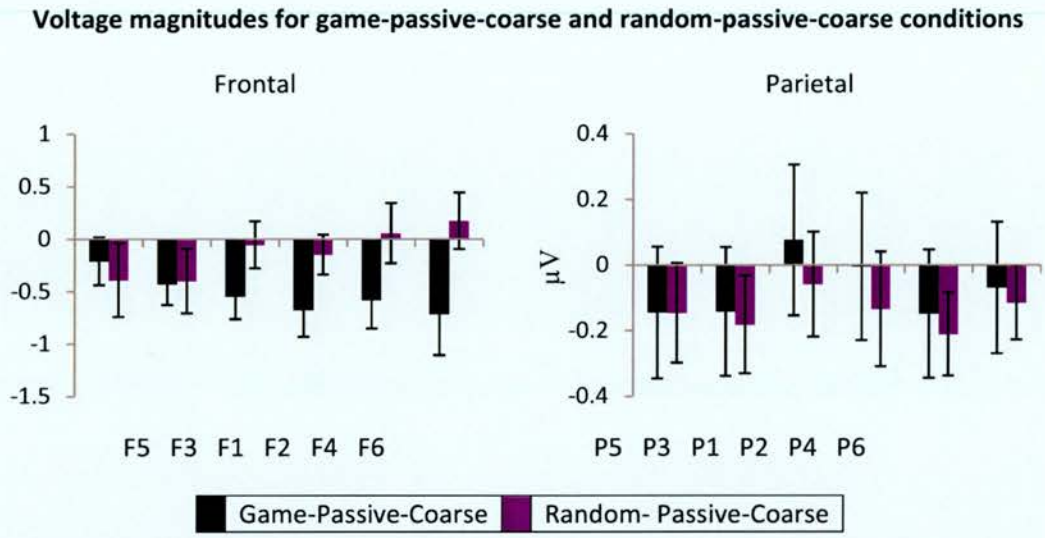

Figure 8-8: The magnitude of ERP effects from -600 to 700ms, shown as in Figure 5-7.

The data from 600 to 700ms were submitted to ANOVA to examine the pattern of game-passive-coarse/random-passive-coarse effects, with factors of condition (game-passive-coarse/random-passive-coarse), location (frontal/parietal), hemisphere (left/right) and site (superior/medial/inferior). Analysis of the data from 600 to 700ms revealed a significant 4-way interaction between condition, location, hemisphere and site [$F(1.39, 20.79) = 4.07$; $p < 0.05$], which reflects left greater than right distribution of the effect found on superior frontal electrodes, when compared to parietal electrodes, and the front greater than parietal distribution of the effect found over left-lateralised superior electrode sites

(shown in Figure 8-8). Successive t-test analyses of electrodes failed to produce a positive result.

8.2.3.1.1.3 Topographic analysis

Figure 8-9 illustrates a clear difference in the pattern of the effect between conditions and a changing polarity over time. ANOVA with factors of game-passive-coarse minus random/random-passive-coarse minus random, epoch (-1000 to -800ms/600 to 700ms), location (frontal/parietal), hemisphere (left/right) and site (superior/medial/inferior), failed to reveal significant interactions (two marginally significant interactions not reported). Similarly, focused analysis of pre-segmentation data also revealed only marginal interactions (not reported). Nonetheless, analysis of post-segmentation topographic data revealed a significant 4-way interaction between game-passive-coarse minus random/random-passive-coarse minus random, location, hemisphere and site [$F(1.4, 19.62) = 4.57$; $p < 0.05$], the left-lateralised inferior distribution over frontal electrodes and superior distribution over partial electrodes, when compared with the broad distribution of the effect over right-lateralised electrodes.

The pattern of effects is only marginally distributionally different between game-passive-coarse/random and random-passive-coarse/random ERPs during pre-segmentation, and between pre- and post-segmentation. Therefore, the topographic analyses only confirm that the pattern of effects is distributionally different between game-passive-coarse/random and random-passive-coarse/random ERPs during post-segmentation, inferring the engagement of at least partially, if not wholly, different sets of neural generators.

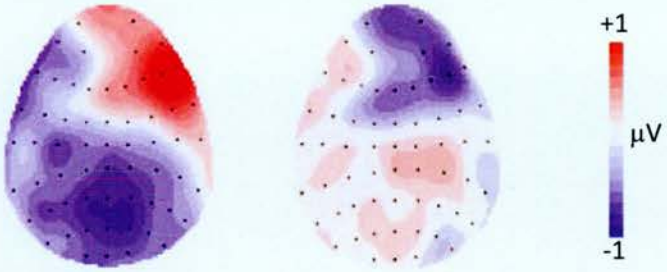

Figure 8-9: Topographic distributions of the game-passive-coarse/passive-coarse difference for the pre- and post-segmentations. Each cartoon shows the distribution of the difference between game-passive-coarse and passive-coarse segmentations, averaged across a 200ms period for the first time window (-1000 to -800ms), and across 100ms for the second (600 to 700ms). The front of the head is at the top of each map, and the left hemisphere is on the left-hand side. Each dot represents a recording electrode. The scale bar indicates the range of activity (in microvolts). The effect in the first time window shows centro-left-lateralised and centro-posterior negativity, and a right-frontal positive-going distribution; whereas the effect in the second time window exhibits right-lateralised negativity over fontal electrodes and a centro-right-lateralised positivity over parietal electrode sites.

8.2.3.1.2 Comparing game- and random-passive-fine

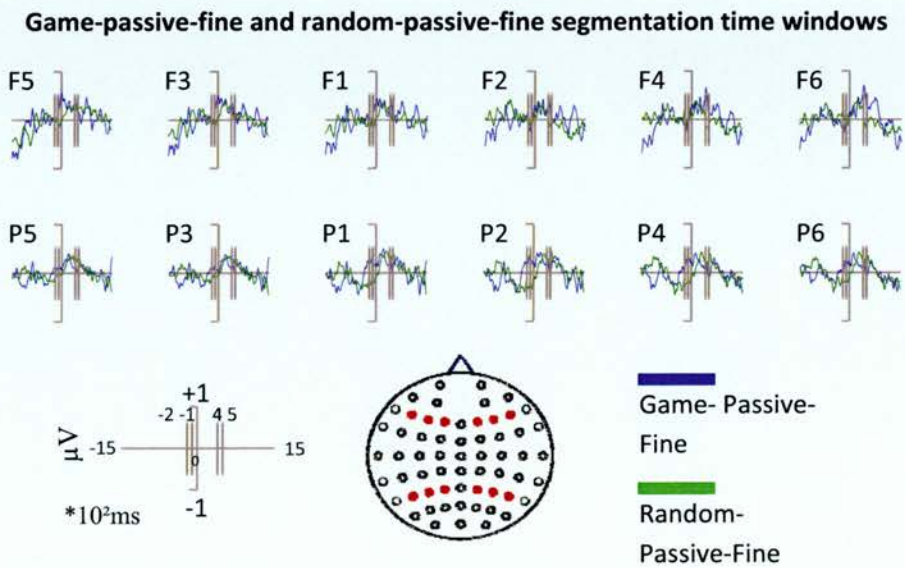

Figure 8-10: The pre-segmentation and post-segmentation time windows are illustrated.

8.2.3.1.2.1 Pre-segmentation time window (-200 to -100ms)

A pre-segmentation time window lasting from -200 to -100ms, which captures a divergence present over right-parietal electrodes locations, was selected for analysis (for overview data see Appendix A). Figure 8-10 shows the grand average ERPs time-locked to game-passive-fine and random-passive-fine segmentation points, at electrodes chosen for statistical testing; the mean number of trials (± SD) contributing to the ERPs was 208 (121) for game-passive-fine and 286 (165) for random-passive-fine. ANOVA with factors of condition (game-passive-fine/random-passive-fine), location (frontal/parietal), hemisphere (left/right) and site (superior/medial/inferior), revealed a significant 3-way interaction between condition, location and hemisphere [$F(1, 15) = 6.37$; $p < 0.05$], reflecting the right greater than left distribution of the effect over parietal electrodes, when compared to the bi-lateral distribution over frontal electrode sites (see Figure 8-11). T-test results (reported in Table 8-4) reveal significant segmentation effects present principally over right-parietal electrodes.

T-test pairing results for game-passive-fine and random-passive-fine (-200 to -100ms)

Left-Frontal Electrodes		Right-Frontal Electrodes	
F5	-	F6	-
F3	-	F4	-
F1	-	F2	-
Left-Parietal Electrodes		**Right-Parietal Electrodes**	
P5		P6	[$t(15) = 2.147$; $p < 0.05$]
P3		P4	[$t(15) = 2.351$; $p < 0.05$]
P1	[$t(15) = 1.878$; $p < 0.1$ (0.08)]	P2	[$t(15) = 2.802$; $p < 0.05$]

Table 8-4: T-test results for the game-passive-coarse and random-passive-coarse post-segmentation time window.

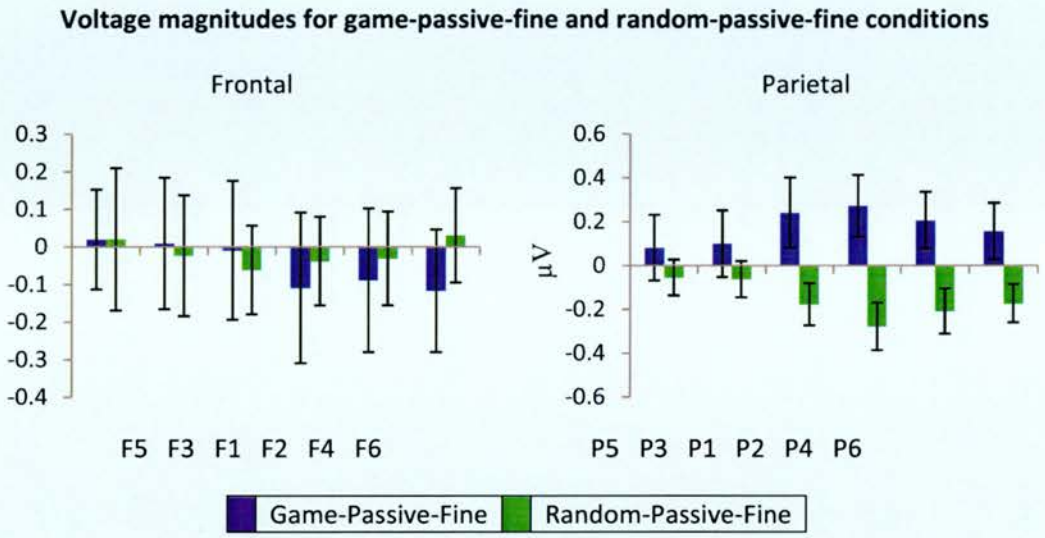

Figure 8-11: The magnitude of ERP effects from --200 to -100ms, shown as in Figure 5-7.

8.2.3.1.2.2 Post-segmentation time window (400 to 500ms)

As previous, a post-segmentation time window lasting from 400 to 500ms was selected for analysis; ANOVA with factors of condition (game-passive-fine/random-passive-fine), location (frontal/parietal), hemisphere (left/right) and site (superior/medial/inferior), revealed a significant interaction between condition and location [$F(1, 15) = 5.51$; $p < 0.05$], which reflects the right greater than left distribution of the effect, as shown in Figure 8-12. A series of t-tests (reported in Table 8-5) show significant segmentation effects predominantly present over right-frontal electrodes.

T-test pairing results for game-passive-fine and random-passive-fine (400 to 500ms)

Left-Frontal Electrodes		Right-Frontal Electrodes	
F5	-	F6	[t(15) = 2.82; p < 0.05]
F3	-	F4	[t(15) = 3.09; p < 0.01]
F1	-	F2	[t(15) = 1.85; p < 0.1 (0.084)]
Left-Parietal Electrodes		**Right-Parietal Electrodes**	
P5	-	P6	-
P3	-	P4	-
P1	-	P2	-

Table 8-5: T-test results for the game-passive-coarse and random-passive-coarse post-segmentation time window.

Voltage magnitudes for game-passive-fine and random-passive-fine conditions

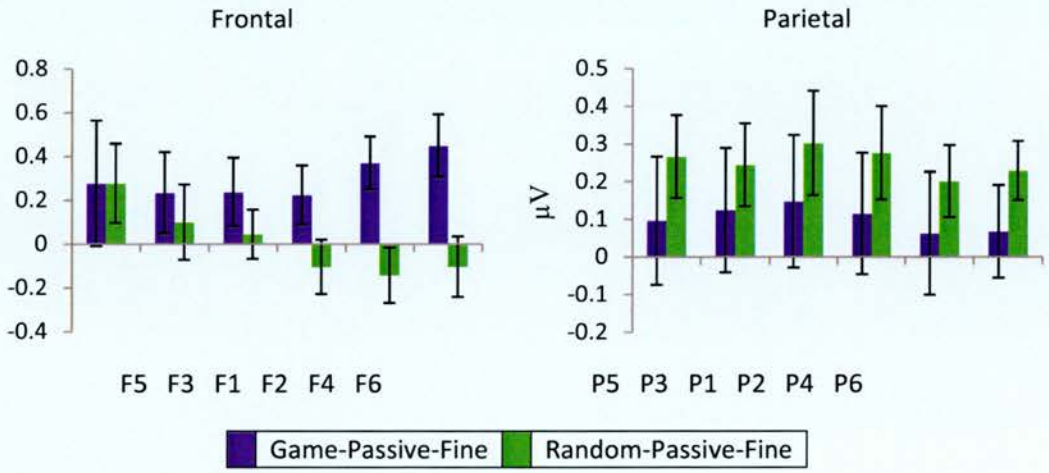

Figure 8-12: The magnitude of ERP effects from -400 to 500ms, shown as in Figure 5-7.

8.2.3.1.2.3 Topographic analysis

Figure 8-13 illustrates a clear difference in the pattern of the effect between conditions, and additionally illustrates a change in the pattern of effect over time, most notably with the changing polarity over time. ANOVA with

factors of game-passive-fine minus random/random-passive-fine minus random, epoch (-200 to -100ms/400 to 500ms), location (frontal/parietal), hemisphere (left/right) and site (superior/medial/inferior), revealed a 3-way interaction between game-passive-fine minus random/random-passive-fine minus random, epoch and location [$F(1, 15) = 7.86$; $p < 0.05$], reflecting the parietal greater than frontal distribution pre-segmentation, compared with the frontal greater than parietal distribution of the effect post-segmentation.

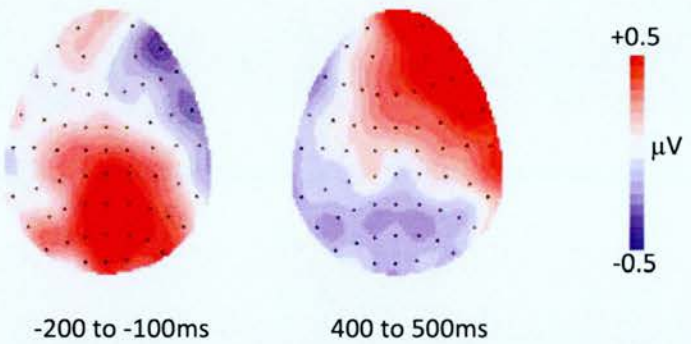

Figure 8-13: Topographic distributions of the directed-passive-coarse/random difference for the pre and post segmentations. Each cartoon shows the distribution of the difference between directed-passive-coarse and randomly generated segmentations, averaged across a 100ms time period for the first time window (-200 to -100ms), and across 100ms for the second (400 to 500ms). The front of the head is at the top of each map, and the left hemisphere is on the left-hand side. Each dot represents a recording electrode. The scale bar indicates the range of activity (in microvolts). The effect in the first time window shows a centro-bi-lateralised and centro-posterior positive-going distribution, and right-lateralised negativity over frontal electrodes; whereas the effect in the second time window exhibits right-lateralised negativity over frontal electrodes, and a centro-parietal distribution of negativity.

A further 4-way interaction was revealed between game-passive-fine minus random/random-passive-fine minus random, epoch, location and hemisphere [$F(1, 15) = 5.1$; $p < 0.05$], which reflects the left greater than right distribution over frontal electrodes and right greater than left distribution

over parietal electrodes pre-segmentation, compared with the right greater than left distribution over frontal electrodes and the broad distribution over parietal electrode s post-segmentation.

Focussed contrasts directly comparing locations, hemispheres and sites across game-passive-fine and random-passive-fine event segmentation revealed a 3-way interaction between game-passive-fine minus random/random-passive-fine minus random, location and hemisphere [$F(1, 15) = 6.9$; $p < 0.05$], reflecting the left greater than right distribution of the effect over frontal electrodes, compared with the right greater than left distribution over parietal electrodes. Analysis of post-segmentation topographic data revealed a significant interaction between game-passive-fine minus random/random-passive-fine minus random and location [$F(1, 15) = 7.85$; $p < 0.05$], which reflects the frontal greater than parietal distribution of the effect. Consequently, the topographic analyses substantiate that the pattern of effects is distributionally different between game-passive-fine/random and random-passive-fine/random ERPs, both during pre-segmentation and post-segmentation, inferring the engagement of at least partially, if not wholly, different sets of neural generators. Additionally, the analyses confirm the differential engagement of neural generators pre- and post-segmentation.

8.2.3.2 Active segmentation

8.2.3.2.1 Comparing game-active-coarse and fine

In line with previous chapters, activity surrounding the maximal positive-going deflections on electrode CZ (illustrated in Figure 8-14) was subjected to

a t-test examination; a clear difference in magnitude between game-active-coarse and game-active-fine segmentation [$t(15) = 3.99$; $p < 0.01$] reflects the greater magnitude present for end-active-coarse ERPs. The magnitude differences are also reflected in Figure 8-15 (a), with the topographic distribution shown in (b).

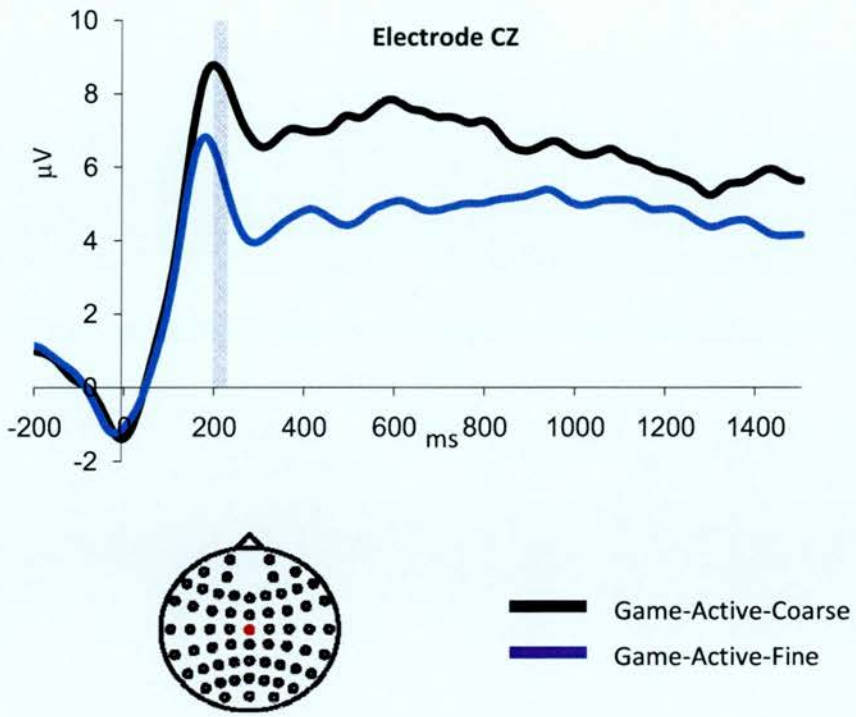

Figure 8-14: Grand average ERPs elicited for game-active-coarse (black) and game-active-fine (blue) on the electrode site CZ (shown as the red dot on the scalp map). More positive-going activity is present for game-active-coarse ERPs compared to game-active-fine ERPs during the 200 to 225ms time window (shaded grey).

In summary, the results clearly demonstrate greater voltage magnitude for game-active-coarse segmentation when compared to game-active-fine segmentation. Similarly to previous magnitude analyses, participants appear to place more emphasis upon coarse grain segmentation

boundaries. However, in contrast with previous analyses, the current participant are only implying a structure, rather than matching a familiar activity with a familiar activity.

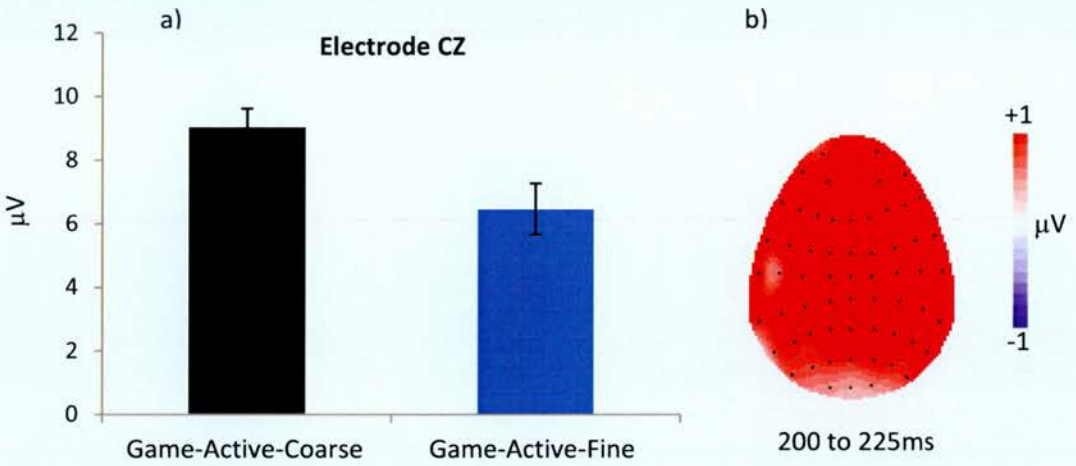

Figure 8-15: (a) Differences in effect sizes at electrode site CZ are shown for game-active-coarse (black) and game-active-fine (blue) segmentation points. Significantly larger effect sizes were present for game-active-coarse compared to game-active-fine segmentation points. (b) Topographic distribution of the game-active-coarse/ game-active-fine difference averaged across a 25ms time period (200 to 225ms). The front of the head is at the top of the map, and the left hemisphere is on the left-hand side. Each dot represents a recording electrode. The scale bar indicates the range of activity (in microvolts). The effect is broadly distributed across the entire scalp, with central electrodes mostly likely reflecting the magnitude differences originating in the motor cortex.

8.2.3.2.2 Comparing random-active-coarse and fine

Again, activity surrounding the maximal positive-going deflections in the waveforms (shown in Figure 8-16) was selected for magnitude analysis (200 to 225ms). Conversely, however, the onset of active-fine positive-going activity occurs prior to the onset of active-coarse positive-going activity; notwithstanding the differing onsets of positive-going activity, analysis of

the data revealed a clear difference in magnitude between random-active-coarse and random-active-fine segmentation [$t(11) = 3.31$; $p < 0.01$], with the ERPs for random-active-coarse more positive-going than those for random-active-fine. The magnitude analysis and topographic distribution are illustrated Figure 8-17 (a) and (b) respectively.

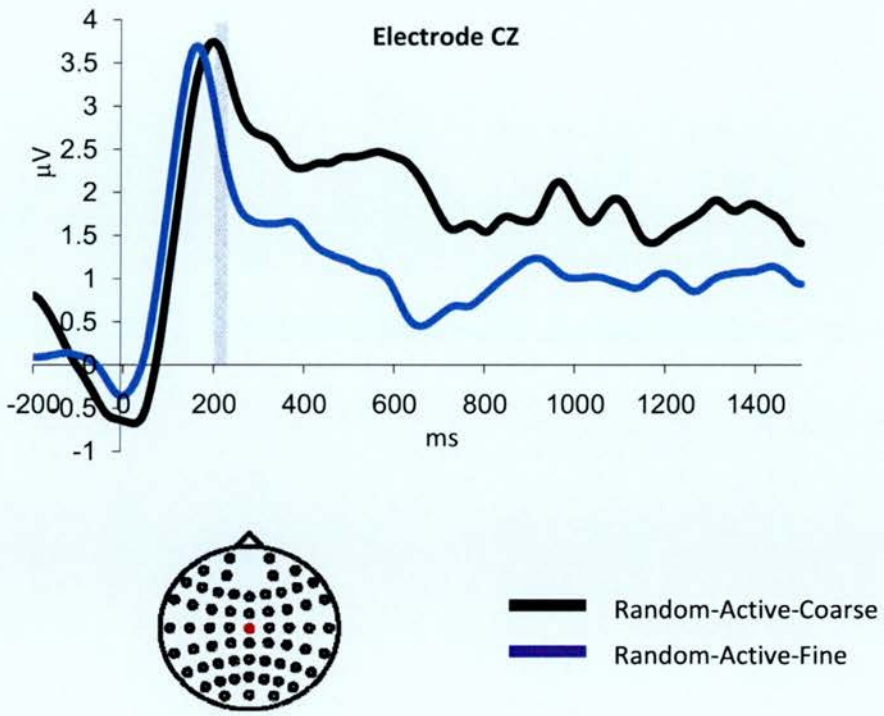

Figure 8-16: Grand average ERPs elicited for random-active-coarse (black) and random-active-fine (blue) on the electrode site CZ (shown as the red dot on the scalp map). More positive-going activity is present for random-active-coarse ERPs compared to random-active-fine ERPs during the 200 to 225ms time window (shaded grey).

In summary, the results clearly demonstrate greater voltage magnitude for active-coarse segmentation when compared to active-fine segmentation, in line with previous analyses, indicating that participants place higher significance upon coarse grain segmentation boundaries.

Distinctively, the results are surprising as participants are instructed to segment seemingly random activity, and therefore, it appears as though a greater emphasis is again placed upon coarse grain segments even when no pre-existing or easily recognised cognitive schema may be in operation.

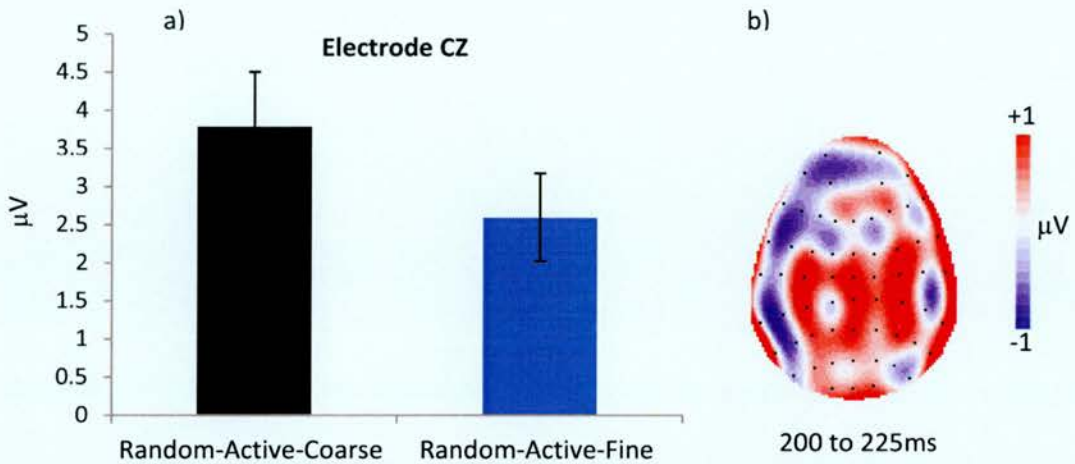

Figure 8-17: (a) Differences in effect sizes at electrode site CZ are shown for random-active-coarse (black) and random-active-fine (blue) segmentation points. Significantly larger effect sizes were present for random-active-coarse compared to random-active-fine segmentation points. (b) Topographic distribution of the random-active-coarse/ random-active-fine difference averaged across a 25ms time period (200 to 225ms). The front of the head is at the top of the map, and the left hemisphere is on the left-hand side. Each dot represents a recording electrode. The scale bar indicates the range of activity (in microvolts). The effect is clearly not localised across the central electrodes, nevertheless, activity present on electrode CZ mostly likely reflects the magnitude differences originating in the motor cortex.

8.2.4 Discussion

The aim of the experiment was to investigate whether the influence of top-down knowledge, even that which is inferred, affected the perception of event boundaries. The experiment also sought to address the question of whether top-down knowledge manipulation and activity abstraction elicited

distinctive neural correlates of event segmentation, when compared with the perception of everyday events.

8.2.4.1 Summary and interpretation

Despite the broadly similar waveform morphologies visible when comparing game-passive-coarse and random-passive-coarse ERPs, clear divergences are nonetheless evident. An early, robust effect over right-parietal electrode sites was revealed pre-segmentation, in addition to a later and shorter-lasting post-segmentation effect. Topographic analysis demonstrated that the post-segmentation effect was the result of the differential engagement of neural generators. However, only marginally different generators were reported pre-segmentation, and additionally between pre- and post-segmentation.

In comparing the ERPs for game-passive-fine and random-passive-fine, a later and shorter-lasting pre-segmentation effect was revealed than in the abovementioned comparison. In contrast with the general findings of experiments two and three, a further post-segmentation effect failed to display the same inverse polarity pre-and post-segmentation. Correspondingly, the emergence of the post-segmentation effect occurred in comparative temporal alignment with the comparison of game-passive-coarse and random-passive-coarse ERPs. In discord with the previous comparison however, topographic analysis demonstrated the differential activation of neural generators pre-, post- and between pre- and post-segmentation divergences.

As might be expected when comparing similar experimental tasks, the ERPs for game-passive-coarse and random-passive-coarse are broadly similar, notwithstanding an early pre-segmentation divergence over parietal

electrodes. However, the experiment did produce an interesting and powerful result; the inference of structure and goal-directness yielded significant differences in magnitude between game- and random-passive-coarse ERPs. Although the topographic analysis failed to demonstrate the differential engagement of neural generators pre-segmentation, differences in post-segmentation activity may be attributed to separate neural generators. An effect of structure and goal-directness inference is further supported and more strongly demonstrated, when comparing the ERPs for game-passive-fine and random-passive-fine. Both pre- and post-segmentation differences were revealed in the ERPs, and moreover, both results were attributable to the engagement of different sets of neural generators. It is perhaps surprising when considering the model proposed by Zacks (2004), that fine-grain segmentation shows greater sensitivity to top-down manipulation. Nevertheless, the results of the current study facilitate a powerful interpretation; that as perhaps may be expected, the neural correlates of event segmentation are differentially sensitive to even the implication of structure and activity goal. Additionally, the neurological results appear to uniquely demonstrate that fine-grain event segmentation is more sensitive to top-down influence than coarse-grain segmentation, engaging different neural generators both pre- and post-segmentation. Unlike the passive segmentation data, analysis of active segmentation data for both groups of participants failed to yield an effect of implied structure, with a coarse-greater-than-fine difference in magnitude found in game-active and random-active ERPs.

8.2.4.2 Comparison with event segmentation literature

Regardless of the abstraction of the activities presented to participants, the current experiment shared many common characteristics with previous studies of event segmentation. Although less clear than with the previous studies reported in this thesis, Figure 8-1 and Figure 8-2 agreement over the perception of an event boundary. In particular, agreement over fine-grain event boundary perception is difficult to elicit, most likely owing to the greater number of boundary perceptions when compared with the previous EEG studies. Interestingly, the so far robust phenomenon of aligning coarse- with fine-grain event boundaries in time, is further strengthened by the failure of the current study to reveal an effect of structure inference. Once again however, the Hard et al. (2001) measure of coarse- subsuming fine-grain grain event boundaries was shown to be sensitive to top-down knowledge. Specifically, those participants who inferred a structure and activity goal used coarse-grain boundaries to subsume fine-grain parts, while those who assumed the activities to be random, failed to do so. The pattern of effect is in accordance with the sensitivity shown thus far by the previous EEG experiments; participants who are more closely aligned with the automatic perception of structured and familiar events, exhibit the coarse-subsuming fine-grain effect.

The previous experiment failed to demonstrate any effect of familiarity upon the number of event segments that were defined. However, given the conflicting results in the literature discussed in the previous and introduction chapter, the hypothesised phenomenon was once again investigated. The current study compared the parsing rates of implied structure and structure-less participants, but also failed to reveal any sensitivity to top-down knowledge. Considering the results of the previous

and current experiment together, the hypothesis proposed by Zacks, Tversky, et al. (2001) is again supported.

8.3 Conclusions

The experiment reported in this chapter investigated the effects of top-down knowledge and bottom-up influence upon event segmentation in both the behavioural and neural domains. Behavioural evidence suggested that the study is broadly in line with previous research in event segmentation. Specifically, participant agreement over event boundaries was concurrent, and partial behavioural evidence for hierarchical structuring followed the results reported in previous experiments and the literature. In further similarity with the previous study, the use of coarse-grain boundaries to subsume fine-grain parts was shown to be sensitive to top-down knowledge; removing the inference of structure and goal-directness suppressed the phenomenon. Neural data was also broadly in line with the previous experiments, and comparable with the Zacks et al. (2001) fMRI study. Namely, responses were elicited for coarse- and fine-grain segmentation form both participants groups, significantly, during pre- and post-segmentation. There was little evidence to support the claims made by Zacks et al. (2001) that coarse-grain segmentation elicits greater responses than fine-grain event segmentation during passive segmentation, although a similar effect was noted in both groups during active segmentation.

Perhaps the most striking finding of the current experiment is the clear demonstration of differences in neurological activity that result from the manipulation of event structure and goal-directedness inference. Given that both participant groups viewed the same set of movie stimuli and

simply had their top-down perception of the activities manipulated, the finding is even more striking, yet perhaps unsurprising. As part of ongoing everyday perception, one would expect cognitive function to be sensitive to the inference of structure and activity goal, especially when compared with an activity upon which no structure is implied. The differences in neurological magnitude and neural generator engagement may reflect the subtle engagement of related cognitive schema by the structure inferred group, compared with no attempt to retrieve cognitive schema when participants were instructed that the activity was structure-less and goalless.

Doubtlessly, the most surprising implication of the current experiment is that during passive viewing, fine-gain event segmentation is more sensitive to top-down manipulation than coarse-grain. This finding goes somewhat against the model proposed by Zacks (2004), which suggests that fine-grain event segmentation would be more likely influenced by the bottom-up characteristics of an activity. However, the implication is further supported when considering that structure inferred and everyday perception (in which structure is also applied), failed to demonstrate differential neural generator engagement during fine-grain segmentation. A finding which is in stark contrast with the clear neurological and generator engagement differences found between the two applied structure and structure-less participant group. In sum, the results suggest that a common set of generators is active when processing fine-grain events that appear to reflect a structure.

All of the experiments reported in this thesis have thus far focussed on measuring the neural correlates of event boundary perception, and additionally the influence of top-down and bottom-up activity features. However, as discussed in the introduction chapter, the exact structure of

activities and events in real life is likely to be far more complex than continuous stream of clearly defined events which all temporally align. Moreover, previous chapters have alluded to the fact that pre- and post-segmentation might reflect the perception of an event end and start points, respectively. Therefore, the following study will investigate the very nature of event structure by manipulating the well used experimental paradigm; participants will be asked to mark event start and end points instead of breakpoints between two events.

9 Defining event boundaries

9.1 Introduction

The experiments reported in this thesis have so far have investigated the influence of top-down and bottom-up knowledge upon event boundary perception. More specifically, the previous experiments demonstrated that event boundary perception is sensitive to activity familiarity, experimental task knowledge, and to the inference of goal-directedness and structure. Additionally, the robust nature of hierarchical structuring and the sensitivity of coarse-grain event parts subsuming fine-grain parts have been confirmed.

Nevertheless, all of the previous experiments have followed and extended the breakpoint paradigm set out by Newtson in 1973, and followed by the fMRI study conducted by Zacks et al. in 2001. Yet, as discussed in the introduction chapter, the definition of an event in terms of how one perceives its structure and constituent sub-parts is not clear. Moreover, it is likely that our cognitive schemata are comprised of a mixture of partonomic and taxonomic structures, so facilitating bridges between perception and function or behaviour (Tversky & Hemenway, 1984). Notwithstanding the complexity of events and their structures, the current experiment again focuses on the perception of partonomic goal-orientatied activities. Nonetheless, the current study differs from its predecessors by investigating the structure of partonomic activities; whether an activity may be represented by a continuous sequence of sub-events, or whether the sub-parts of an activity each have their own discrete beginnings and endings, is an important question for the research of event segmentation. For example, when considering the goal-directed task of making a cup of tea, after one places the tea-bag in the cup, there may be a pause in activity until the kettle boils and

pouring can begin. Therefore, can the final act of placing a tea-bag in the cup be reasonably considered as the beginning of the act of pouring in the water? Or conversely, could one consider the wait on the kettle boiling to be a sub-event, neatly fitting between the two acts of placing a tea-bag in the cup and pouring from the kettle? Considering that one may reach for the kettle slightly before it has finished boiling so amalgamating sub-events, the representation of the real-world by continuous structure appears less likely. In light of this philosophical contradiction, the current study manipulates the original experimental paradigm to investigate another method of segmenting activities; participants are asked to define the starts and ends of sub-events, rather than define the boundaries between two temporally aligned sub-events. In order that the investigation may be compared with the perception of event boundaries, the same movie stimuli are used that were employed by the second experiment, in which participants segmented everyday activities without any experimental task knowledge. Owing to the argument that events may be interpreted as having discrete beginnings and endings, it is hypothesised that the current experiment will elicit neurologically distinct correlates of event segmentation when compared with the perception of event boundaries. Furthermore, it is hypothesised that the perception of an event beginning and ending will differentially engage neural generators, owing to the psychological differences in considering the start and end of an event.

Behaviourally, it is hypothesised that the robust effect of hierarchal structure will be present both when defining the start and the end of an event, as sub-events may still be interpreted as comprising larger event parts independent of their definition. Conversely, an effect of starts versus ends is expected to be found when comparing the use of coarse-grain events to

subsume fine-grain events. As one might expect, if the aforementioned effect is true, only the definition of event end points will demonstrate the use of coarse-grain events to subsume fine-grain parts e.g. the definition of a coarse-grain event start point is likely to occur before or in temporal alignment with the definition of a fine-grain event start point.

In summary, the critical question to be addressed in the current study is whether the definition of event start and end points elicit ERP correlates, and moreover, whether any potential effect differs from the neural correlates of event boundary perceptions.

9.2 Experiment 5: Investigating the effect of coaching on event segmentation using ERPs

9.2.1 Methods

The following sections detail the experimental methods followed in this experiment.

9.2.1.1 Stimuli

Video stimuli used in this experiment were as per Chapter 6 and discussed in the General Methods chapter.

9.2.1.2 Participants

Twenty-seven participants took part in the experiment; data from three participants was discarded due to behavioural non-compliance, leaving twenty-four participants in the group (12 male, age range 17-35).

9.2.1.3 Procedure

Once again, participants viewed all videos passively before actively segmenting the activities on subsequent viewings. In contrast with previous experiments, however, participants in this experiment were instructed to mark the start and end points of meaningful event segments, rather than define the customary breakpoints between events. Participants were informed that there was no set method they should follow, for example, events may freely be perceived as overlapping or having no delay between the end of one event and the start of the next.

9.2.2 Behavioural results

The following section contains analysis of behavioural data collected from 24 participants as they performed the event segmentation experiment.

9.2.2.1 Investigating the concurrence of event perception

As in the previous experiments, the automaticity of event segmentation was investigated by examining participant agreement, and is illustrated in Figure 9-1 and Figure 9-2. In line with the findings from the previous experiments, visual inspection of the raster plots clearly indicates a common perception of event boundaries in time, particularly for the coarse conditions. As in

previous chapters, coarse- and fine-grain correlation results (listed in Table 9-1), demonstrated a high-level of association between coarse- and fine-grain boundary perceptions across all activities.

Correlation results for coarse- and fine-grain event perception

Activity	Starts	Ends
Doing the laundry	$r(299) = 0.216$; $p < 0.001$	$r(299) = 0.171$; $p < 0.01$
Making the bed	$r(311) = 0.496$; $p < 0.001$	$r(311) = 0.358$ $p < 0.001$
Planting plants	$r(353) = 0.503$; $p < 0.001$	$r(353) = 0.383$; $p < 0.001$
Washing the car	$r(430) = 0.51$; $p < 0.001$	$r(430) = 0.526$; $p < 0.001$

Table 9-1: Resulting p-values from the correlation tests performed on the temporal response distributions for coarse- with fine-grain segmentation.

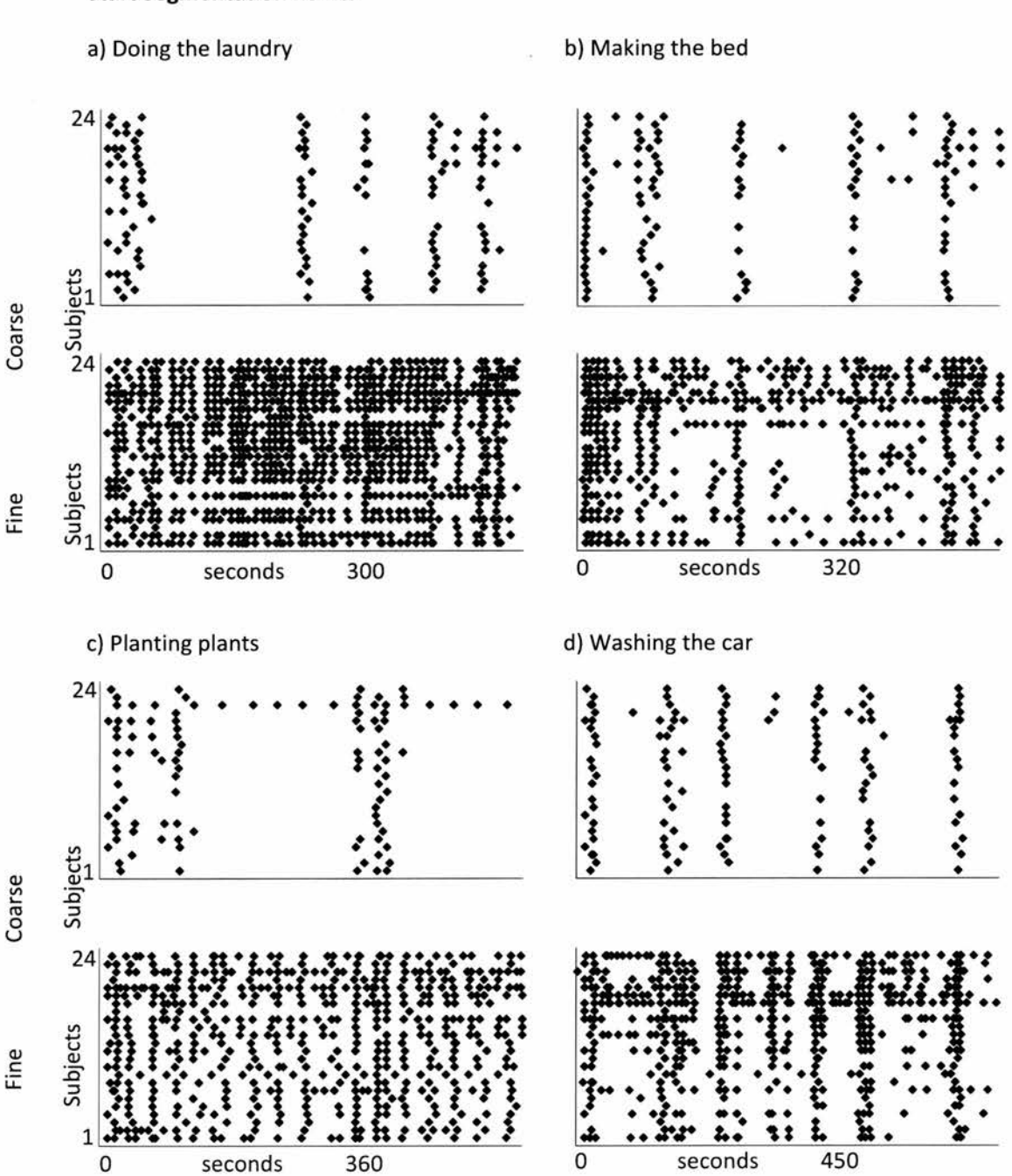

Figure 9-1: Raster plots of segmentation timings (x-plane) for each participant (y-plane), shown separately for each movie (a-d), for fine and coarse conditions. Each individual data point reflects a single segmentation response.

Figure 9-2: Raster plots of segmentation timings (x-plane) for each participant (y-plane), shown separately for each movie (a-d), for fine and coarse conditions. Each individual data point reflects a single segmentation response.

9.2.2.2 Investigating the hierarchical nature of event perception

As previous, participants behavioural responses were analysed for hierarchical structure; the mean value of recorded and randomly placed overlap time-bins, as illustrated in Figure 9-3. No effect of start- and end-segmentation breakpoints was found in a high-level analysis, however, ANOVA with factors of condition (recorded/randomly placed) and activity (doing the laundry, making the bed, planting plants and washing the car), revealed main effects of condition overlap time-bins for both starts [$F(1,23) = 148$; $p < 0.001$], and ends [$F(1,23) = 133.03$; $p < 0.001$].

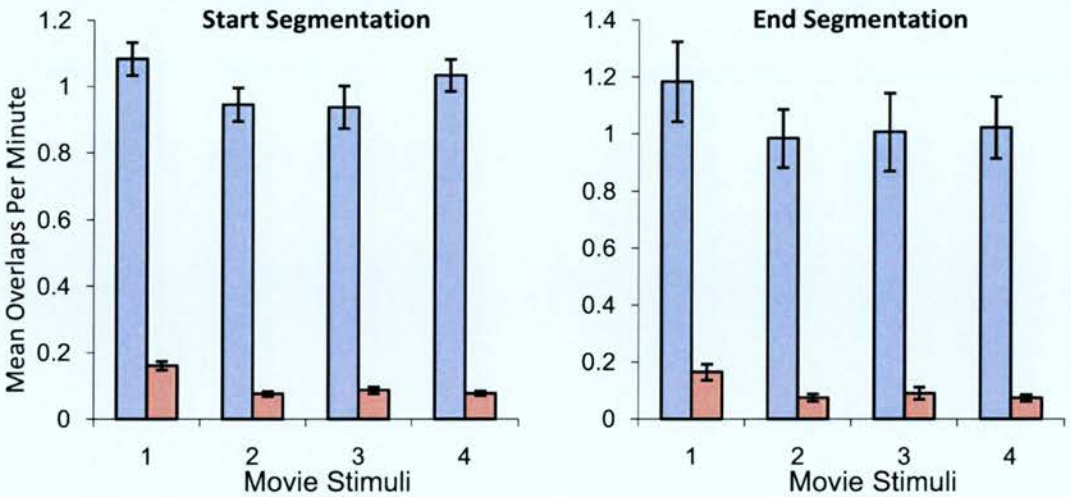

Figure 9-3: Mean number of overlap time-bins for recorded (purple) and randomly placed (blue) breakpoints per minute are shown for each video; (1) doing the laundry, (2) making the bed, (3) planting plants and (4) washing the car. Error bars represent one standard error of the mean. For all four movies, significantly larger number of overlapping time-bins were recorded from participants marking coarse and fine event boundaries than would occur randomly.

Table 9-2 lists t-test results for each activity for both event boundary types; significant results are reported universally, demonstrating that both start and

end event points are temporally grouped by granularity, suggesting hierarchical relationships between parts and sub-parts.

T-test results for overlapping coarse- and fine-grain event perception

Activity	Starts	Ends
Doing the laundry	[t(23) = -12.17; p < 0.001]	[t(23) = -8.8; p < 0.001]
Making the bed	[t(23) = -9.8; p < 0.001]	[t(23) = -9.99; p < 0.001]
Planting plants	[t(23) = -7.76; p < 0.001]	[t(23) = -7.9; p < 0.001]
Washing the car	[t(23) = -10.9; p < 0.001]	[t(23) = -9.5; p < 0.001]

Table 9-2: Resulting p-values from the two-tailed t-tests performed on each activity for both types of event boundary. The results reflect the clear differences present between actual overlapping time bins recorded and those arising purely by chance, regardless whether start or end event points are defined.

The mean value of fine- before coarse-grain segmentations and coarse-before fine-grain segmentations for the start and end breakpoints are illustrated in Figure 9-4; ANOVA with factors of condition (fine subsuming coarse/coarse subsuming fine), breakpoint (start-points/end-points) and activity (doing the laundry, making the bed, planting plants and washing the car), revealed an interaction between condition and breakpoint [$F(1,15) = 22.07$; $p < 0.001$], reflecting the strong tendency of participants to use coarse-grain end-points to subsume fine-grained event segments. More focussed analyses failed to reveal any effect when participants marked the starts of event segments, however, ANOVA with factors of condition (fine subsuming coarse/coarse subsuming fine) and activity (doing the laundry, making the bed, planting plants and washing the car), revealed a main effect of condition [$F(1,23) = 82.02$; $p < 0.001$] for event end points. T-test results (reported in

Table 9-3 show coarse-grain event boundaries subsuming fine-grain event parts present only for event end point perceptions. Although the results are reflective of what one might expect (e.g. coarse-grain end-points subsuming fine-grain end points), it is interesting to note that coarse-grain start-points neither precede nor follow fine-grain points; for example, one might expect coarse-grain start-points to precede fine-grain start-points if coarse-grain units subsume fine-grain event parts. This result may reflect a psychological corollary of event segmentation; fine-grain event parts are grouped and stored only once one judges a natural breakpoint between groups of fine-grain parts. Moreover, the data support the hypothesis that once a new group of fine-grain event parts commences, this perception consequently invokes the perception of a coarse grain boundary i.e. the start of a new group of fine-grain event parts.

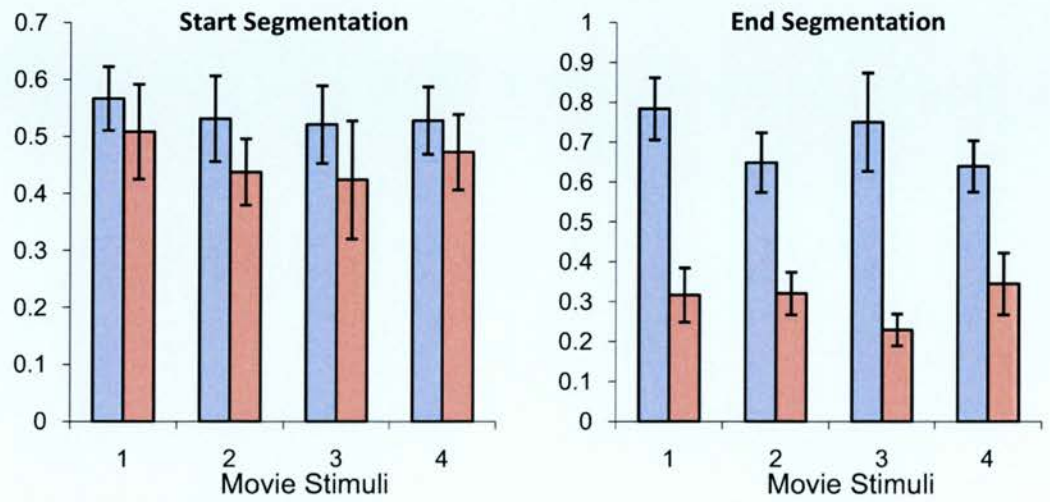

Figure 9-4: Mean number of fine- before coarse-grain segmentations (light blue), and coarse-before fine-grain segmentations (light red) per minute are shown for each video; (1) doing the laundry, (2) making the bed, (3) planting plants and (4) washing the car. Error bars represent one standard error of the mean. Movie three showed significantly larger

numbers of fine- before coarse-grain segmentations than coarse- before fine-grain segmentations.

T-test results for coarse- subsuming fine-grain event perception

Activity	Starts	Ends
Doing the laundry	-	[t(23) = 4.98; p < 0.001]
Making the bed	-	[t(23) = 3.88; p < 0.005]
Planting plants	-	[t(23) = 4.24; p < 0.001]
Washing the car	-	[t(23) = 2.82; p < 0.05]

Table 9-3: Resulting p-values from the two-tailed t-tests performed on each activity analysing the use of coarse-grain boundaries to subsume fine-grain event parts. The results clearly demonstrates participant to automatically employing this strategy when perceiving event end-points.

9.2.3 ERP results

Thus far, the proceeding experiments have all employed data epochs of 3 seconds, with a number of effects identified within this period. Similarly, the current chapter employs the same range of data epoch based upon the following rationale; (a), the previous experiments have failed to demonstrate consistency in the timing of effects that may guide time window selection; (b), the start/end paradigm is unique to the field of event segmentation and so requires full exploration; and (c), previously selected time windows have been found to lie in close proximity to the ends of the epoch. While it is inopportune not to have revealed a common time window across the previous experiments, it is perhaps unsurprising given the variety of experimental tasks undertaken by participants e.g. comparing familiar with unfamiliar segmentation and comparing top-down manipulations on the

segmentation of abstract events. Consequently, and particularly given the novel experimental procedure, this chapter will continue to select time windows guided by visual inspection of the ERP waveforms and refined using the overview tables.

9.2.3.1 Investigating the differences between event start and end perception

9.2.3.1.1 Comparing start- and end-passive-coarse

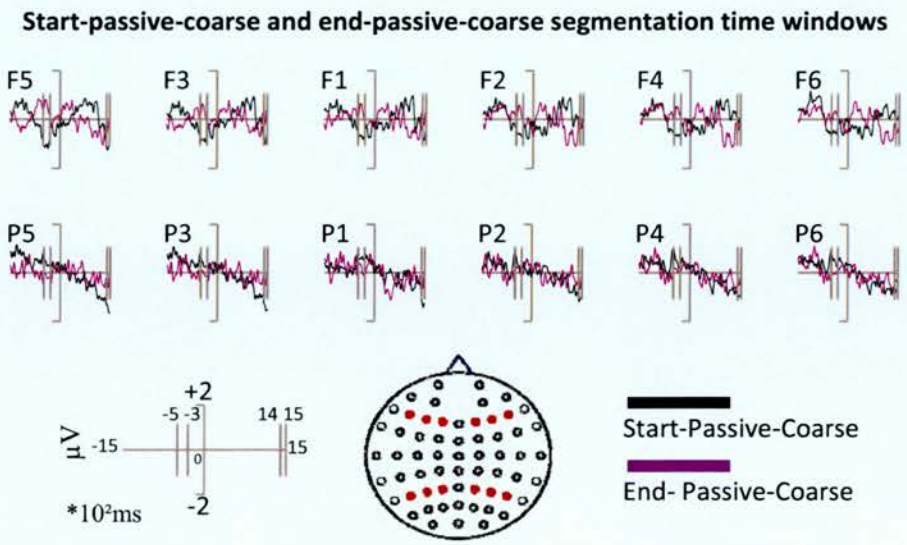

Figure 9-5: The pre-segmentation and post-segmentation time windows are illustrated.

9.2.3.1.1.1 Pre-segmentation time window (-500 to -300ms)

Following the procedures outlined in previous chapters, a pre-segmentation time window from -500 to -300ms was selected for analysis (for overview table see Appendix A); Figure 9-5 shows the grand average ERPs time-locked

to start-passive-coarse and end-passive-coarse segmentation points, at electrodes chosen for statistical testing. The mean number of trials (± SD) contributing to the ERPs was 27 (11) for start-passive-coarse and 27 (10) for end-passive-coarse. ANOVA with factors of condition (start-passive-coarse/end-passive-coarse), location (frontal/parietal), hemisphere (left/right) and site (superior/medial/inferior), revealed a significant interaction between condition and location [$F(1, 23) = 8.02$; $p < 0.01$], reflecting front greater than parietal distribution of the effect (illustrated in Figure 9-6). These data were subsequently subjected to a series of t-tests (reported in Table 9-4); significant segmentation effects are predominantly present over the left-frontal inferior electrode site.

T-test pairing results for start-passive-coarse and end-passive-coarse (-500 to -300ms)

Left-Frontal Electrodes		Right-Frontal Electrodes	
F5	[$t(23) = -2.56$; $p < 0.05$]	F6	-
F3	-	F4	-
F1	-	F2	-
Left-Parietal Electrodes		**Right-Parietal Electrodes**	
P5	-	P6	-
P3	-	P4	-
P1	-	P2	-

Table 9-4: T-test results for the start-passive-coarse and end-passive-coarse post-segmentation time window.

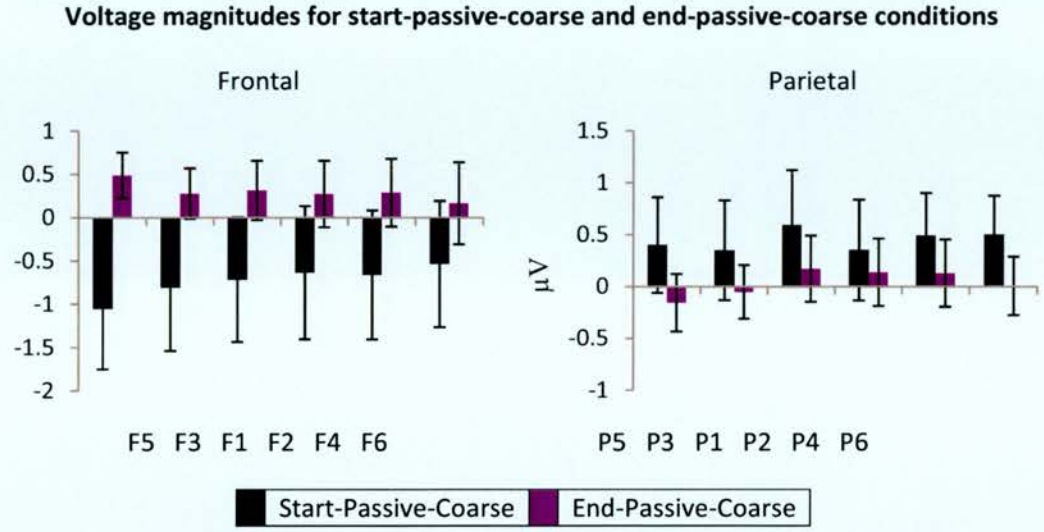

Figure 9-6: The magnitude of ERP effects from --500 to -300ms, shown as in Figure 5-7.

Given the pattern of data reported in Table 9-4, it is surprising to find no interactions between condition and hemisphere, suggesting that the effect is more widespread over frontal electrode sites than indicated by Table 9-4. Furthermore, it is also surprising that no interaction was found involving condition and site, again suggesting that the effect is more widespread than indicted by the pattern of data in Table 9-4.

9.2.3.1.1.2 Post-segmentation time window (1400 to 1500ms)

The post-segmentation period from 1400 to 1500ms was selected for further analysis (overview data available in Appendix A); ANOVA with factors of condition (start-passive-coarse/end-passive-coarse), location (frontal/parietal), hemisphere (left/right) and site (superior/medial/inferior), revealed a significant interaction between condition and hemisphere [$F(1, 23) = 8.91$; $p < 0.01$], which reflects the left greater than right distribution of the effect (illustrated in Figure 9-7). Follow-

up t-test results reported in Table 9-5 demonstrate significant segmentation effects present predominantly over left-lateralised parietal electrodes. Surprisingly, given the pattern of data reported in Table 9-5, no interaction was found between condition and location, suggesting that the effect is more widespread than is indicated in Table 9-5.

T-test pairing results for start-passive-coarse and end-passive-coarse (1400 to 1500ms)

Left-Frontal Electrodes		Right-Frontal Electrodes	
F5	-	F6	-
F3	-	F4	-
F1	-	F2	-
Left-Parietal Electrodes		**Right-Parietal Electrodes**	
P5	[t(23) = -2.8; p = 0.01]	P6	-
P3	[t(23) = -2.74; p < 0.05]	P4	-
P1	-	P2	-

Table 9-5: T-test results for the start-passive-coarse and end-passive-coarse post-segmentation time window.

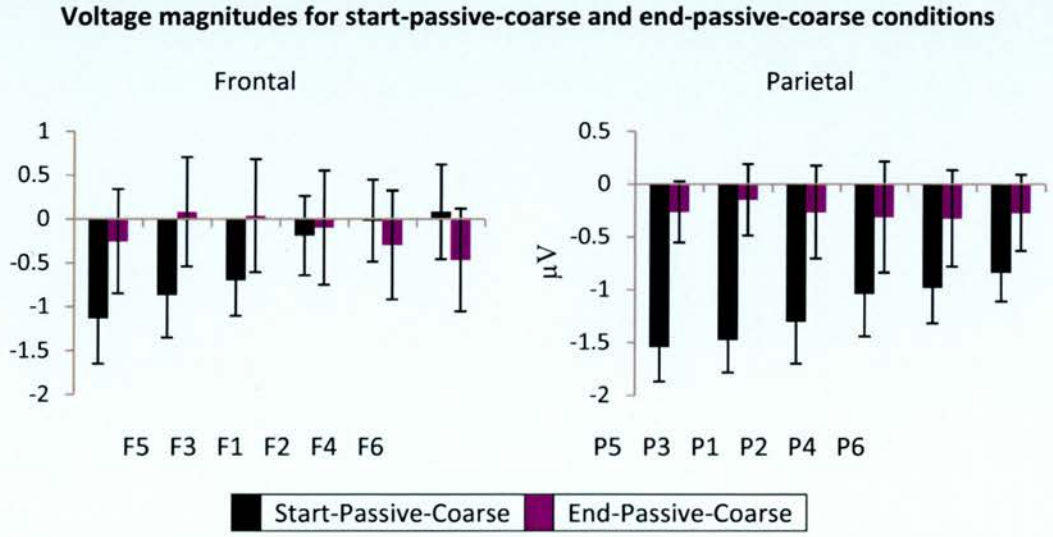

Figure 9-7: The magnitude of ERP effects from -1400 to 1500ms, shown as in Figure 5-7.

9.2.3.1.1.3 Topographic analysis

Figure 9-8 illustrates a clear difference in the pattern of the effect between conditions, and additionally illustrates a change in the pattern of effect over time. ANOVA with factors of start-passive-coarse minus random/end-passive-coarse minus random, epoch (-500 to -300ms/1400 to 1500ms), location (frontal/parietal), hemisphere (left/right) and site (superior/medial/inferior), revealed only a marginally significant interaction between start-passive-coarse minus random/end-passive-coarse minus random, epoch and location [$F(1, 23) = 3.42$; $p < 0.1$ (0.078)], reflecting the weak nature of the parietal greater than frontal distribution pre-segmentation when compared with the frontal greater than parietal distribution of the effect post-segmentation. Nonetheless, focussed contrasts directly comparing locations, hemispheres and sites across start-passive-coarse and end-passive-coarse event segmentation revealed a significant interaction between start-passive-coarse minus random/end-passive-coarse minus random and location [$F(1, 23) = 5.8$; $p < 0.05$], reflecting the parietal greater than frontal distribution of the effect. Analysis of post-segmentation topographic data also revealed a significant interaction between start-passive-coarse minus random/end-passive-coarse minus random and hemisphere [$F(1, 23) = 4.29$; $p = 0.05$], reflecting the right greater than left distribution of the effect. Therefore, the topographic analyses confirm that the pattern of effects is distributionally different between start-passive-coarse/random and end-passive-coarse/random ERPs, both during pre-segmentation and post-segmentation, inferring the engagement of at least partially, if not wholly, different sets of neural generators. However, the analyses failed to confirm the differential engagement of neural generators pre- and post-segmentation, revealing only a marginal interaction.

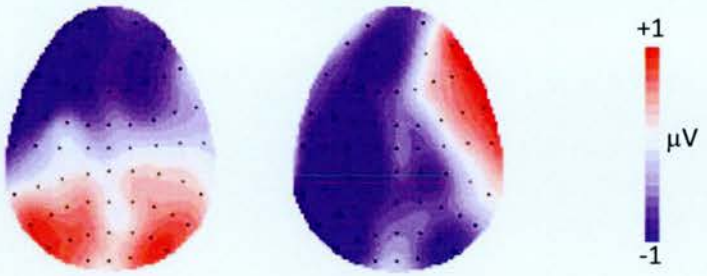

Figure 9-8: Topographic distributions of the directed-passive-coarse/random difference for the pre and post segmentation. Each cartoon shows the distribution of the difference between directed-passive-coarse and randomly generated segmentation, averaged across a 200ms time period for the first time window (-500 to -300ms), and across 100ms for the second (1400 to 1500ms). The front of the head is at the top of each map, and the left hemisphere is on the left-hand side. Each dot represents a recording electrode. The scale bar indicates the range of activity (in microvolts). The effect in the first time window has a centro-left-lateralised and centro-frontal negative-going distribution, and a bi-lateral positive-going destruction over parietal electrodes; whereas the effect in the second time window exhibits left-lateralised negativity over frontal and parietal electrodes, and a right-lateralised positivity over frontal electrodes and negativity over parietal electrodes.

9.2.3.1.2 Comparing start- and end-passive-fine

9.2.3.1.2.1 Pre-segmentation time window (-900 to -200ms)

As previously, a pre-segmentation time window lasting from -900 to -200ms was selected to best characterise the widespread pre-segmentation divergences in the waveforms. Figure 9-9 shows the grand average ERPs time-locked to start-passive-fine and end-passive-fine segmentation points. The mean number of trials (± SD) contributing to the ERPs was 128 (44) for start-passive-fine and 127 (44) for end-passive-fine.

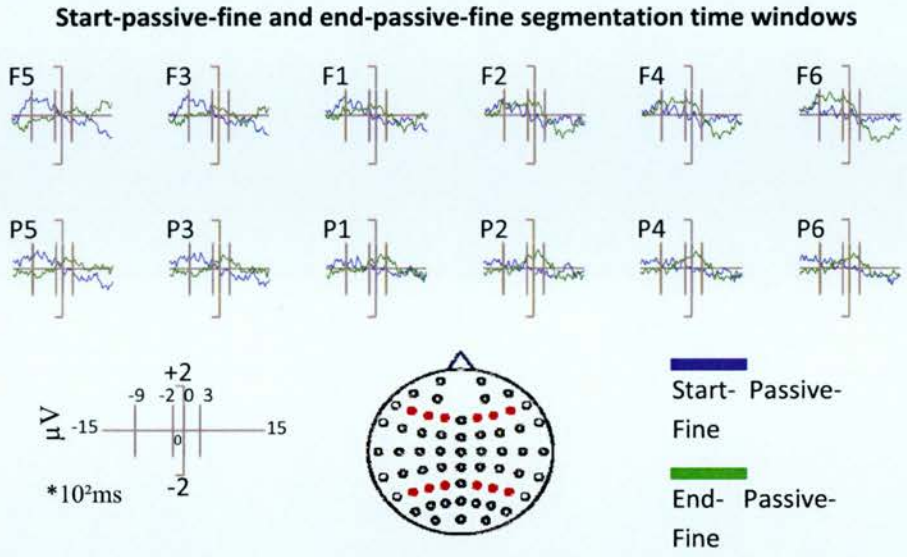

Figure 9-9: The pre-segmentation and post-segmentation time windows are illustrated.

ANOVA with factors of condition (start-passive-fine/end-passive-fine), location (frontal/parietal), hemisphere (left/right) and site (superior/medial/inferior), revealed a significant interaction between condition and hemisphere [$F(1, 23) = 44.1$; $p < 0.001$], reflecting the left greater than right distribution of the effect. A further 2-way interaction was revealed between condition and site [$F(1.29, 29.67) = 5.84$; $p < 0.05$], which reflects the medial-inferior nature of the effect. A 3-way interaction revealed between condition location and hemisphere [$F(1, 23) = 16.71$; $p < 0.001$], reflects the left greater than right distribution of the effect, when compared to the bi-lateral distribution over frontal electrode sites. A further 3-way interaction between condition, location and site [$F(1.4, 32.24) = 4.05$; $p < 0.05$] reflects the stronger medial-inferior distribution of the effect over frontal electrodes, when compared to the more broadly distributed effect present over parietal electrodes. An additional 3-way interaction revealed between condition, hemisphere and site [$F(1.17, 27) = 18.9$; $p < 0.001$], reflects the

medial- inferior distribution of the effect over left-lateralised electrodes, when compared to the more broadly distributed effect found over right-lateralised electrode locations. Finally, a 4-way interaction revealed between condition, location, hemisphere and site [$F(1.39, 31.92) = 8.83$; $p < 0.01$] was revealed, which reflects the nature of the left inferior-medial greater than right inferior when compared with the inferior frontal greater than broad distribution of parietal electrodes.

Following the proceeding analysis, subsidiary t-test results are reported in Table 9-6; significant segmentation effects predominantly are present over left-lateralised electrodes. Figure 9-10 shows the voltage magnitudes for the electrodes submitted to ANOVA over frontal and parietal locations. The magnitude analysis reflects the stronger effects for start-passive-fine inferior-medially over left frontal and inferiorly over right-frontal electrodes, and inferior-medially over left-parietal with broad distribution over right-parietal electrode sites.

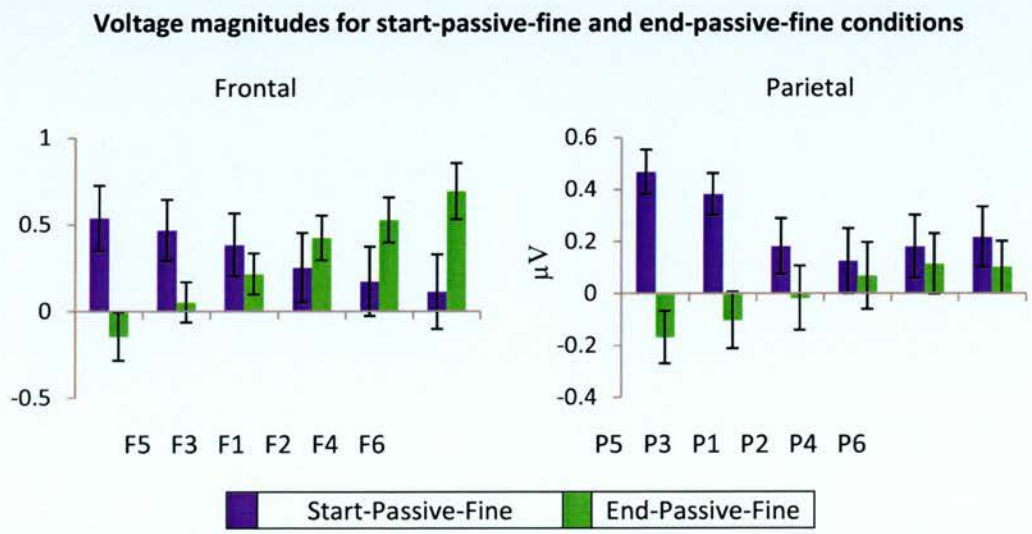

Figure 9-10: The magnitude of ERP effects from --900 to -200ms, shown as in Figure 5-7.

T-test pairing results for start-passive-fine and end-passive-fine (-900 to -200ms)

Left-Frontal Electrodes		Right-Frontal Electrodes	
F5	[t(23) = 3.26; p < 0.01]	F6	[t(23) = -2.73; p < 0.05]
F3	[t(23) = 2.46; p < 0.05]	F4	[t(23) = -1.85; p < 0.1 (0.078)]
F1	-	F2	-
Left-Parietal Electrodes		**Right-Parietal Electrodes**	
P5	[t(23) = 4.84; p < 0.001]	P6	-
P3	[t(23) = 3.85; p = 0.001]	P4	-
P1	-	P2	-

Table 9-6: T-test results for the start-passive-coarse and end-passive-coarse post-segmentation time window.

9.2.3.1.2.2 Post-segmentation time window (0 to 300ms)

A post-segmentation time period from 0ms segmentation to 300ms was selected to capture an early widespread and robust effect in close temporal proximity to segmentation. ANOVA with factors of condition (start-passive-fine/end-passive-fine), location (frontal/parietal), hemisphere (left/right) and site (superior/medial/inferior), revealed a main effect of condition [$F(1, 23) = 9.961$; $p < 0.01$], reflecting the broadly distribution nature of the effect. A further 2-way interaction was revealed between condition and site[$F(1.332, 30.639) = 4.425$; $p < 0.05$], which reflects the strongest point of the differences in the waveforms visible over superior electrodes, weakening as the effect spreads over medial and inferior electrode sites, as shown in Figure 9-11. Individual t-tests performed on electrodes chosen for statistical testing revealed that significant segmentation effects are predominantly present over parietal electrodes (see Table 9-7).

T-test pairing results for start-passive-fine and end-passive-fine (0 to 300ms)

Left-Frontal Electrodes		Right-Frontal Electrodes	
F5	-	F6	-
F3	[t(23) = -1.91; p < 0.1 (0.069)]	F4	[t(23) = -2.29; p < 0.05]
F1	[t(23) = -2.12; p < 0.05]	F2	[t(23) = -2.52; p < 0.05]
Left-Parietal Electrodes		**Right-Parietal Electrodes**	
P5	[t(23) = -2.53; p < 0.05]	P6	[t(23) = -3.91; p = 0.001]
P3	[t(23) = -2.77; p < 0.05]	P4	[t(23) = -4.2; p < 0.001
P1	[t(23) = -2.14; p < 0.05]	P2	[t(23) = -3.81; p = 0.001]

Table 9-7: T-test results for the start-passive-coarse and end-passive-coarse post-segmentation time window.

Voltage magnitudes for start-passive-fine and end-passive-fine conditions

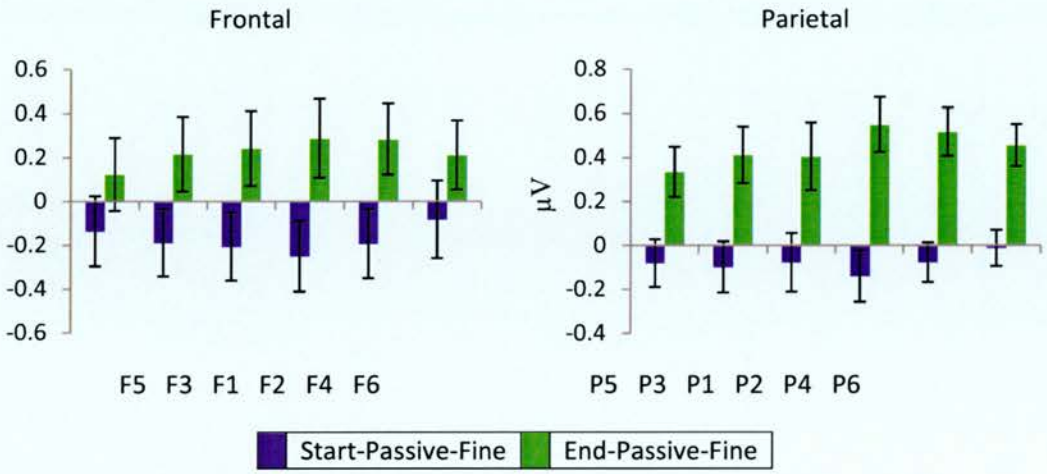

Figure 9-11: The magnitude of ERP effects from -0 to 300ms, shown as in Figure 5-7.

9.2.3.1.2.3 Topographic analysis

Figure 9-12 illustrates a clear difference in the pattern of the effect between conditions with a changing polarity over time. ANOVA with factors of start-passive-fine minus random/end-passive-fine minus random, epoch (-900 to -

200ms/0 to 300ms), location (frontal/parietal), hemisphere (left/right) and site (superior/medial/inferior), revealed an interaction between start-passive-fine minus random/end-passive-fine minus random and epoch [$F(1, 23) = 10.46$; $p < 0.005$], reflecting the broad differences present in the conditions when comparing pre- and post-segmentation time windows. A 3-way interaction between start-passive-fine minus random/end-passive-fine minus random, epoch and hemisphere [$F(1, 23) = 9.31$; $p < 0.01$] was revealed, which reflects the left greater than right distribution pre-segmentation, when compared with the broad distribution of the effect post-segmentation. Additionally, a 4-way interaction was revealed between start-passive-fine minus random/end-passive-fine minus random, epoch, location and hemisphere [$F(1, 23) = 7.89$; $p < 0.05$], reflecting the left greater than right and front greater than parietal distribution pre-segmentation, when compared with the bi-lateral frontal greater than parietal distribution of the effect post-segmentation. Finally, an additional 4-way interaction between start-passive-fine minus random/end-passive-fine minus random, epoch, hemisphere and site [$F(1.17, 26.99) = 8.92$; $p < 0.01$] was revealed, which reflects the inferiorly left greater than superiorly right electrode site distribution pre-segmentation, when compared with the bi-lateral inferior distribution of the effect post-segmentation.

Focussed contrasts directly comparing locations, hemispheres and sites across start-passive-fine and end-passive-fine event segmentation revealed a significant interaction between start-passive-fine minus random/end-passive-fine minus random and hemisphere [$F(1, 23) = 38.88$; $p < 0.001$], reflecting the left greater than right distribution of the effect. An additional 2-way interaction was revealed between start-passive-fine minus random/end-passive-fine minus random and site [$F(1.30, 29.86) = 5.82$; $p <$

0.05], reflecting the greatest differences between conditions distributed over inferior electrode sites locations. A 3-way interaction between start-passive-fine minus random/end-passive-fine minus random, location and hemisphere $F(1, 23) = 14.599$; $p < 0.005$], reflects frontal greater than parietal destruction when compared with the left greater than right destruction of the effect.

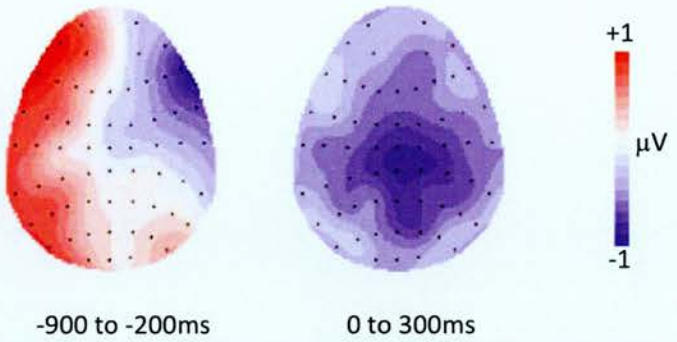

Figure 9-12: Topographic distributions of the directed-passive-coarse/random difference for the pre and post segmentation. Each cartoon shows the distribution of the difference between directed-passive-coarse and randomly generated segmentation, averaged across a 700ms time period for the first time window (-900 to -200ms), and across 300ms for the second (0 to 300ms). The front of the head is at the top of each map, and the left hemisphere is on the left-hand side. Each dot represents a recording electrode. The scale bar indicates the range of activity (in microvolts). The effect in the first time window has a left-lateralised positive-going distribution and exhibits right-lateralised and centro-frontal negativity; whereas the effect in the second time window exhibits and centro-posterior negativity.

Additionally, a 3-way interaction between start-passive-fine minus random/end-passive-fine minus random, location and site was revealed [$F(1.33, 30.63) = 4.6$; $p < 0.05$], which reflects broad distribution across summed frontal electrode sites, compared with the bi-laterally inferior destruction present over parietal electrode sites. A further 3-way interaction was revealed between start-passive-fine minus random/end-passive-fine minus random, hemisphere and site [$F(1.18, 27.03) = 17.17$; $p < 0.001$], which

is reflective of the left-lateralised inferior destruction, compared with the right-lateralised superior distribution of the effect. Finally, a 4-way interaction between start-passive-fine minus random/end-passive-fine minus random, location, hemisphere and site [$F(1.38, 31.67) = 7.16$; $p < 0.01$], reflects the left-lateralised inferior distribution of the effect, when compared with the frontal-superior and parietal-inferior destruction over right-lateralised electrode sites.

Analysis of post-segmentation topographic data revealed a main effect of start-passive-fine minus random/end-passive-fine minus random [$F(1, 23) = 8.5$; $p < 0.01$], reflecting the broadly distributed differences between conditions. Additionally, a 2-way interaction between start-passive-fine minus random/end-passive-fine minus random and site [$F(1.33, 30.59) = 4.38$; $p < 0.05$] was revealed, reflecting the greatest differences between conditions being distributed over superior electrodes.

Therefore, the topographic analyses confirm that the pattern of effects is distributionally different between start-passive-fine/random and end-passive-fine/random ERPs, both during pre-segmentation and post-segmentation, inferring the engagement of at least partially, if not wholly, different sets of neural generators. Additionally, the analyses confirm the differential engagement of neural generators pre- and post-segmentation.

9.2.3.2 Active segmentation

9.2.3.2.1 Comparing active-coarse and fine

Corresponding with previous chapters, start-active-coarse- and start-active-fine-grain motor cortex activation were analysed; Figure 9-13 shows the grand average ERPs on electrode CZ. Analysis of the data revealed a clear

difference in magnitude between start-active-coarse and start-active-fine segmentation [$t(21) = 2.99$; $p < 0.01$], with the ERPs for start-active-coarse more positive-going than those for start-active-fine, as illustrated in Figure 9-14 (a) and (b) respectively. However, no differences were found when comparing end-active-coarse and end-active-fine [$p > 0.1$].

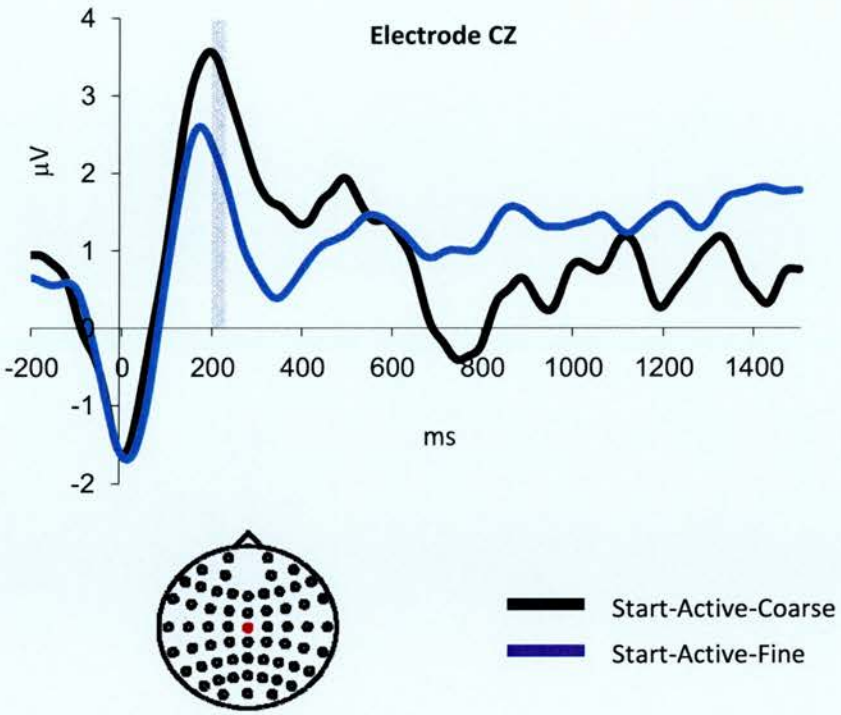

Figure 9-13: Grand average ERPs elicited for start-active-coarse (black) and start-active-fine (blue) on the electrode site CZ (shown as the red dot on the scalp map). More positive-going activity is present for start-active-coarse ERPs compared to start-active-fine ERPs during the 200 to 225ms time window (shaded grey).

In summary, the results clearly demonstrate greater voltage magnitude for start-active-coarse segmentation when compared to start-active-fine segmentation, perhaps reflecting the higher significance participants may place upon the start of coarse grain event segments. Once

again, these results are analogous and supportive of the coarse-greater-than-fine results reported in the Zacks et al. (2001) study, despite the paradigm manipulation used in the current experiment.

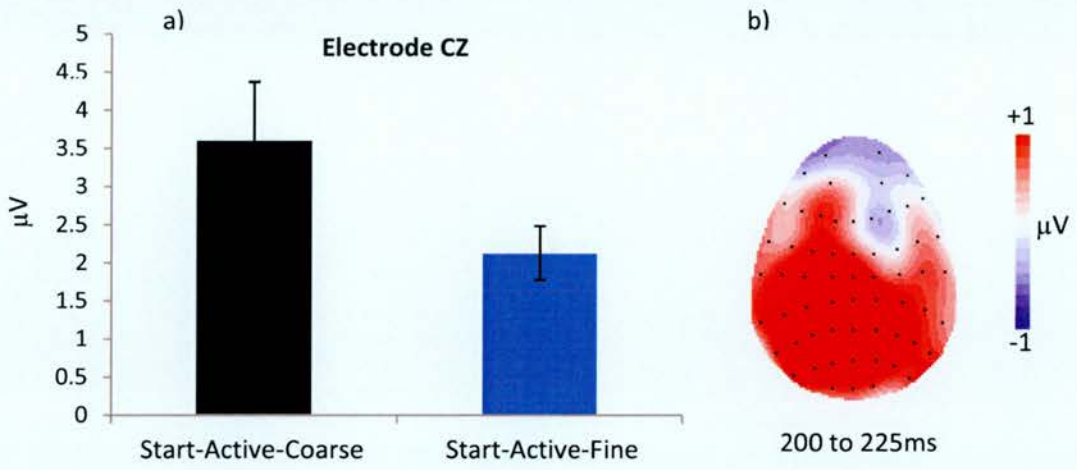

Figure 9-14: (a) Differences in effect sizes at electrode site CZ are shown for start-active-coarse (black) and start-active-fine (blue) segmentation points. Significantly larger effect sizes were present for start-active-coarse compared to start-active-fine segmentation points. (b) Topographic distribution of the start-active-coarse/ start-active-fine difference averaged across a 25ms time period (200 to 225ms). The front of the head is at the top of the map, and the left hemisphere is on the left-hand side. Each dot represents a recording electrode. The scale bar indicates the range of activity (in microvolts). The effect is clearly distributed across the central electrodes, mostly likely reflecting the magnitude differences originating in the motor cortex. Additionally, the effect shows a bi-lateralised distribution over parietal electrodes.

9.2.4 Discussion

The aim of the experiment was to investigate whether the perception of event start or end points elicited ERP correlates of event segmentation. Additionally, the experiment sought to investigate whether the perception of event start and end points differed from the perception of event boundary perceptions.

9.2.4.1 Summary and interpretation

Although the ERPs for start-passive-coarse and end- start-passive-coarse share broadly similar waveform morphologies across parietal and centralised electrode sites, clear divergences in the waveforms are apparent. Left-frontal sites in particular demonstrate more positive-going activity for start-passive-coarse ERPs pre-segmentation, whereas post-segmentation, the ERPs for start-passive-coarse show more negative-going activity over left-parietal sites; the switch in polarity is in accordance with the trend found in all previous experiments. Topographic analysis failed to demonstrate the differential engagement of neural generators between pre- and post-segmentation. Nonetheless, differential neural generators were found to be active in both pre- and post-segmentation time windows.

In summary, the comparison of perceived start and end points reveal two clear findings; firstly, on both coarse- and fine-grain levels, differential neural activity pre- and post-segmentation is a result of the engagement on different sets of neural generators; and secondly, that pre- and post-segmentation neural activity does not, as previously postulated, reflect the perception of an event's start and end point. Conversely, the data align with the previously discussed hypothesis that multiple neural generators are active during event segmentation, as the pre- and post-segmentation responses suggest. Interestingly, the analysis of active segmentation data revealed that only the perception of an event start point elicited stronger responses for coarse- than fine-grain segmentation. This pattern of result perhaps suggests that the perception of an event boundary more closely relates to the perception of a segment of activity beginning, rather than ending.

9.2.4.2 Comparison with event segmentation literature

Perhaps unsurprisingly, given the strong agreement over boundary perception in line with the literature reported thus far, Figure 9-1 and Figure 9-2 illustrate that participants are in broad agreement over the perception of event start and end points. Again, the current study replicates a robust finding reported in the previous EEG and Zacks fMRI studies; participants segmented the activities in terms of parts and sub-parts forming a hierarchical relationship between coarse- and fine-grain segmentation. This phenomenon was similarly recorded for both event start and end point definitions, suggesting that regardless of how one defines event segments, structuring segments hierarchically is a key element of how one processes ongoing activity. As discussed in previous chapter and the introduction, Hard et al. (2001) demonstrated that coarse-grain event boundaries were used to subsume fine-grain event parts. In terms of event start and end points, one would expect coarse-grain event end points to subsume fine-grain event end points, if the grouping of sub-events is an automatic phenomenon. The results reported in the current chapter support this hypothesis i.e. coarse-grain start points were found not to subsume fine-grain start points, while end point organisation yielded a positive result.

9.3 Conclusions

The chapter reported an experiment that deliberately manipulated the well used experimental paradigm to investigate the nature of event structure in perception. Principally, the experiment demonstrated that neural activity is sensitive to how events were parsed e.g. coarse- and fine-grain segmentation was shown to differ in magnitude and generator engagement pre- and post-

segmentation between a perceived segment start and end point. Notwithstanding the lack of differential neural generator engagement found post-segmentation between end-passive-coarse and breakpoint-passive-coarse ERPs, the same pattern of effect was found when comparing start and end point with breakpoint perception. Overall, the experiment demonstrates that perceiving events as continuous blocks of activity or as temporally independent discrete packets each with its own start and end point, elicits differential neural activity. Each view appears to be equally valid given the similar pattern of effects present during the perception; pre- and post-event definition responses are present across experiments. This finding also lends weight to the hypothesis that the EEG data are reflecting multiple cognitive processes active during event perception.

During everyday perception, it is likely that event structures will differ subtly as each is encountered. Some activities may be best represented by a continuous stream of sub-parts whose boundaries align in temporal space; however, the current experiment suggests that it is equally valid to represent activities as containing temporally distinct sub-parts, each with its own start and end point. The findings of the current experiment suggest that this is possible even when structuring the same activity differently. Therefore, this chapter confirms that, as expected, segmenting activity in manageable chunks is more complex than the traditional experimental paradigm attempts to reveal. Investigating how exactly one accurately represents activity structure in cognitive schemata, including possible combinations of event definitions, appears to be a valid topic for future research.

10 General Discussion

This thesis has presented a number of experiments that investigated event segmentation, a psychological process found to active as a part of ongoing perception. After firstly, establishing that the neural correlates of event segmentation may be measured using breakpoint-locked ERPs (Experiments 1-2); the thesis secondly, assessed the psychological mechanism of event segmentation (Experiments 3-5). In this chapter the main findings will be summarised, interpretations of the data will be presented and future areas of research will be suggested.

10.1 Critical analysis

Adopting the paradigm used by Zacks et al. (2001) for the ERP studies presented in this thesis raises a number of key methodological questions. Crucially, the 'trial' structure of the experiment is defined by participant's responses that are recorded after the passive viewing EEG data are collected; a method at odds with traditional ERP studies in which the trial structure is defined by the experimentalist e.g. Rugg (1985). However, in addition to the Zacks fMRI study, self-paced designs have been applied successfully in studies of binocular rivalry (Lumer et al. 1998; Lumer & Rees, 1999; Tong et al., 1998). Fundamentally, the studies presented in this thesis indicate that self-paced ERP designs are a valid means of recording perceptual experience, and furthermore, allow for quantitative analyses of these data.

Another key concern is for the quality of the EEG data given a number of inherent paradigm factors, such as the use of video clips as stimuli. Typically, participants are asked to minimise eye movement during ERP

studies, thus allowing a participant to freely scan the video screen is likely to induce a greater amount of eye muscle artefact in the EEG data. Furthermore, as the numbers of trials are defined by participant's perceptions, coarse-grain segmentation ERPs may have suffered from a lack of statistical power; often, the number of coarse-grain event perceptions was close to the minimum of 16 trials required for statistical strength. Lastly, the problem of overlapping coarse- and fine-grain ERPs is likely to weaken the statistical strengths owing to cross-contamination. Notwithstanding such concerns, the ERP studies have consistently demonstrated statistically significant results in each experiment, indicating that self-paced ERP designs are a valid method of investigating event segmentation.

10.2 Summary of main findings

The summary of findings is divided into three sections; firstly, the results of the baseline studies are discussed (Experiments 1-2); secondly, results from the investigation into the psychological mechanism of event segmentation will be examined (Experiments 3-5); and thirdly, the results are incorporated with evidence from the wider literature.

10.2.1 Summary: Experiments 1-2

The primary aim of Experiments 1-2 was to establish a baseline event segmentation ERP effect; in Experiment 1, participants were directed to segment the ongoing activity during passive viewing; whereas in Experiment 2, participants had no prior knowledge of the event segmentation paradigm. Examination of coarse- and fine-grain segmentation-locked ERPs across both studies revealed a clear pattern of effect (illustrated in Figure 10-1); relative

to a randomly generated waveform, both experiments showed pre-segmentation positive-going waveforms and post-segmentation negative-going waveforms over parietal electrode locations.

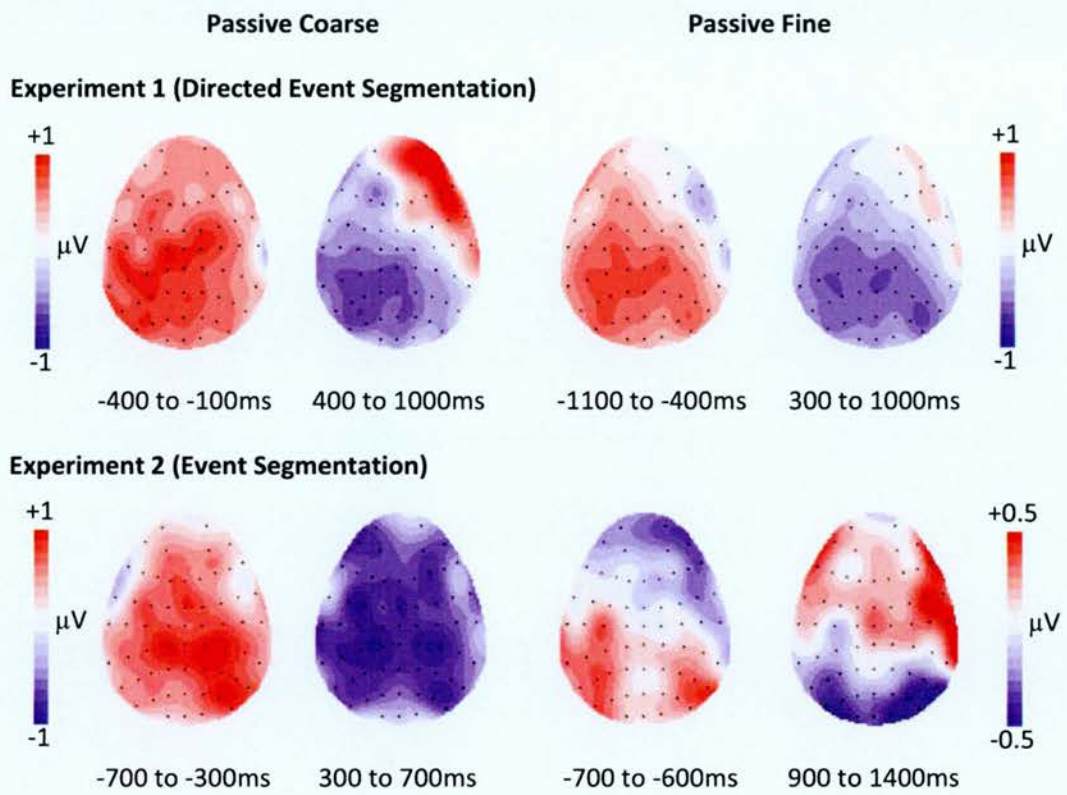

Figure 10-1: Topographic distributions of the passive-coarse/random and passive-fine/random differences for the pre and post segmentations taken from Experiment 1 and Experiment 2. The front of the head is at the top of each map, and the left hemisphere is on the left-hand side. Each dot represents a recording electrode. The scale bar indicates the range of activity (in microvolts).

Notwithstanding the difference in experimental paradigm knowledge, pre-segmentation posterior positivity for passive-coarse in Experiment 1 (400 to -100ms) and Experiment 2 (-700 to -300ms), were found to overlap in

temporal space, as were post-segmentation effects in Experiment 1 (400 to 1000ms) and Experiment 2 (300 to 700ms). Similarly, pre-segmentation effects found in passive-fine ERPs were found to overlap in time when comparing Experiment 1 (-1100 to -400ms) with Experiment 2 (-700 to -600ms). Finally, albeit to a lesser extent, passive-fine post-segmentation effects were found to overlap from Experiment 1 (300 to 1000ms) and Experiment 2 (900 to 1400ms). Whilst the manipulation of experimental paradigm knowledge across the baseline studies clearly alters the exact timings of the effects, the effects do share temporal space, in addition to sharing pre-segmentation positivity and post-segmentation negativity located over parietal electrodes.

Importantly, pre- and post-segmentation effects were shown to be topographically dissociable in the baseline experiments, for both passive-coarse and passive-fine segmentation. This trend demonstrates the differential engagement of psychological processes before and after the perception of an event boundary. Taken together, consistencies in the results could be interpreted as providing strong evidence for the biphasic pattern of effect to be considered a neural correlate of event segmentation. Nonetheless, it is crucial to note that, as would be expected of differing experimental tasks, sufficient variance in the onset, duration and scalp distribution of the effects lead to the conclusion that the components are not identical. Further, cross-experiment comparison data (see Appendix D) report divergences during passive-coarse and passive-fine event segmentation, with dissociable topographical distributions also noted. Therefore, while the pattern of effect across the experiments is strikingly similar, it cannot be assumed that entirely common components are engaged.

Notwithstanding such concerns, the comparison of coarse- and fine-grain event segmentation ERPs from within each experiment revealed clear

divergences during pre- and post-segmentation time. Moreover, coarse- and fine-grain ERPs were found to significantly vary during both passive and active segmentation, providing robust evidence to support existing theories that events are simultaneously tracked on multiple time scales (Zacks, Tversky, et al., 2001; Speer et al., 2007; Kurby & Zacks, 2008).

10.2.2 Summary: Experiments 3-5

After establishing an event segmentation ERP pattern of effect, two experiments (topographic summaries illustrated in Figure 10-2) investigated potential influences upon the event segmentation mechanism (Experiments 3-4), and a third investigated event structure perception (Experiment 5).

Event segmentation effects were associated with familiarity of ongoing events in Experiment 3, pre-segmentation during both passive-coarse (-350 to -250ms) and passive-fine segmentation (-600 to -400ms), and post-segmentation for passive-coarse (200 to 500ms) and passive-fine (1200 to 1400ms). Most importantly, quantative differences between the segmentation of familiar and unfamiliar events were consistently found to be topographically dissociable. These data provide robust evidence to support the hypothesis that differential processes associated with event segmentation are engaged depending upon the level of familiarity with an event. Additionally, pre- and post-segmentation familiar/unfamiliar effects mirrored the pattern shown in the baseline studies; neural generators were differentially engaged before and after the perception of an event boundary, during the segmentation of either familiar or unfamiliar events.

Experiment 4 investigated the affect of goal-directedness upon event segmentation; ERPs demonstrated that pre- and post-segmentation neural

activations were a modulated by the inference of goal-directedness. These data support the prevailing view that the goal of an activity plays an important role in how ongoing activity is internally conceptualised (e.g. Zacks & Tversky, 2001), and add weight to the hypothesis that existing cognitive schemata are retrieved in order to 'best fit' ongoing events.

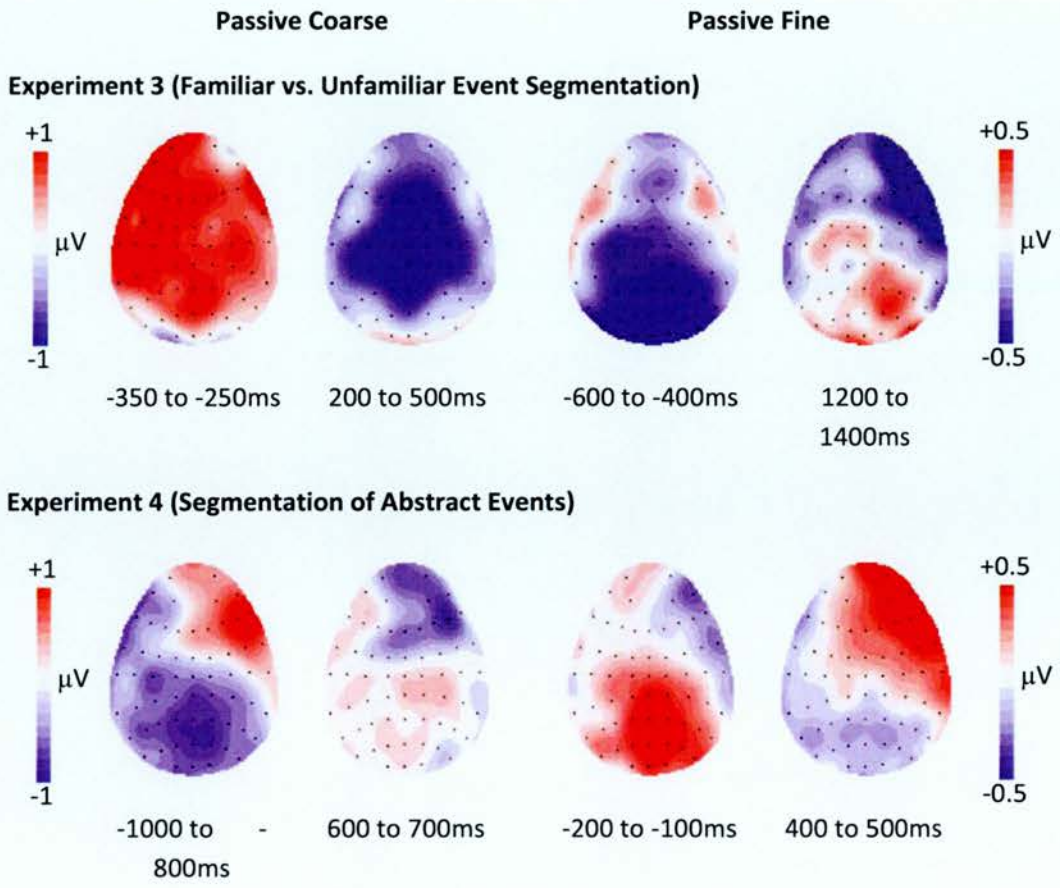

Figure 10-2: Topographic distributions of the passive-coarse/random and passive-fine/random differences for the pre and post segmentations taken from Experiment 3 and Experiment 4. The front of the head is at the top of each map, and the left hemisphere is on the left-hand side. Each dot represents a recording electrode. The scale bar indicates the range of activity (in microvolts).

Finally, examination of ERPs time-locked to the perception of event start and end points (Experiment 5), demonstrated pre- and post-segmentation effects associated with the perception of event unit structure. Moreover, the perception of event start and end boundaries were shown to differ from the perception of a single breakpoint between events pre- and post-segmentation; this effect is found during the unitisation of events at a coarse- and fine-grain level. The results support the hypothesis that complex event structures may be represented by cognitive schemata, accounting for the many and varied events present in everyday life.

10.3 Theoretical implications

The results of the studies described in this thesis have several important theoretical implications. Most importantly, the results support an event segmentation view of how the human mind processes information, while also providing new information about the identification and validation of neural correlates of event segmentation. The question of the extent to which goal-direction, familiarity and unit structure has upon event segmentation will be also be discussed.

10.3.1 The neural correlates of event segmentation

First and foremost, the baseline ERP experiments demonstrated that neural activation in response to the perception of event boundaries is measurable with the electroencephalograph. Particularly, the effects shown in ERPs time-locked to event boundaries during *passive* viewing represent a major finding of theoretical and methodical significance. Firstly, the unique set of neurophysiological data support the prevailing view that event segmentation

is active as a part of ongoing perception (e.g. Zacks, Tversky, et al., 2001), and secondly, the experiments demonstrate that ERP investigations of event segmentation are feasible using a self-paced paradigm.

Most strikingly, ERPs formed time-located to event perceptions exhibited pre-segmentation positivity and post-segmentation negativity. This finding is in contrast with the Zacks et al. (2001) fMRI study, which indicated a single response was present over a network of cortical regions. This finding is perhaps unsurprising, however, given the difference in time scales used to sample neurological data; the fMRI time course of 36 seconds would smear together the two effects shown in the ERP data, which are separated by approximately one or two seconds. As discussed previously (see Chapter 2), ERP data exposes temporally-finer cognitive processes compared to fMRI data, thus, the biphasic ERP response represents a unique view of the neural correlates of event segmentation.

Significantly, effects noted pre- and post-segmentation were found to be, in general, topographically dissociable across all studies and experimental conditions. This finding infers the differential engagement of neural generators pre- and post-segmentation, again in contrast with the Zacks fMRI study. As to what these neural generators might be, is currently a matter of supposition; however, the literature does provide some compelling arguments. Perhaps most relevantly, Sitnikova et al. (2008) conducted an ERP study which investigated how the human mind represents events by concluding video stimuli of everyday activities with incongruent endings. Sitnikova describes two effects; firstly, a N400 component which has been shown previously to be modulated by context (e.g., Bentin, McCarthy, & Wood, 1985); and secondly, a parietally located P600 component that was found to be sensitive to the appearance of incongruous objects in video

scenes. In summary, Sitnikova et al. conclude that the processing of everyday events may involve two distinct neural mechanisms; the first mechanism which is reflected by the N400, maps incoming information onto a cognitive schema; and the second, reflected by the P600, assesses the relevance of the information given the perceived goal of the task. Furthermore, Sitnikova and colleagues suggest that these two cognitive mechanisms may be differentially invoked depending upon the familiarity of the ongoing activity. It is important to note, however, that both processes identified by Sitnikova et al. temporally lie in what would be in effect, post-segmentation time. Albeit that the suggested mechanisms would occur after the perception of an event, the distinction and order of cognitive mechanisms proposed by Sitnikova proposes are of interest given the neurophysioligcally distinct features revealed across studies in this thesis.

Another view of cognitive event processing is proposed by Event Segmentation Theory (EST); as previously discussed (see section 1.7.1), EST suggests that pre-existing cognitive schemas (or event models) are retrieved to best fit the current activity, and that this schema is updated when predictions fail to meet actual events. Liberally applying this theorem to the perception-encompassing, biphasic responses reported in this thesis, would suggest that pre-segmentation evoked responses reflect error monitoring, and post-segmentation responses reflect cognitive schema updating. Interestingly, it could be argued that the Sitnikova study suggests something similar when applied to the results of this thesis i.e. contextual referencing occurs prior to schematic assessment and updating.

Whilst it is highly likely that invoking and updating cognitive schemata is routed within the realms of memory function, it is clear that higher-level cognitive mechanisms are required to mediate these processes.

Moreover, just as the data presented in this thesis suggest, cognitive processing surrounding the perception of an event is likely to invoke many distinguishable psychological operations. In summary, the neural correlates of event segmentation presented in this thesis are likely to reflect memory indexing and higher-level cognitive processes. Arguably, pre-segmentation responses could be seen to reflect schematic integration of low-level cues based on activity relevance, whereas post-segmentation activity reflects the mediating and updating of cognitive schema.

10.3.2 Cognitive processing of ongoing activity

The results of the experiments presented in this thesis, overwhelmingly support the prevailing view that event segmentation is an automatic process. Firstly, as would be expected, the behavioural responses from all studies reported positive correlations between coarse- and fine-grain boundary perceptions. Secondly, visual inspection of raster plots used to represent behavioural responses across participants, in the main, indicated good agreement over where event boundaries are perceived. This result could be interpreted to again suggest that event segmentation is an automatic process, given the common agreement over where event boundaries lie.

All experiments produced a large and robust effect of hierarchical segmentation, indicating that small and large event parts may be mentally represented in hierarchical structures e.g. a cognitive schema. Further analysis of behavioural responses led to, on the whole, the conclusion that coarse-grain event boundaries are used to subsume fine-grain event parts, thus strengthening the argument for a hierarchical representation of events. Interestingly, the enclosure effect was not found when participants were

directed to segment (Experiment 1), when ongoing activity was unfamiliar (Experiment 3: naive group), and when no inference of goal-directedness is present (Experiment 4: random group). In other words, the enclosure effect was only demonstrated when activities were familiar and goal-directed. Although the data are weak, the finding indicates that coarse-grain event boundaries may only be used to group fine-grain event parts when a pre-existing, goal-orientated, cognitive schema exists in memory.

Two experiments (3-4), specifically investigated possible influences upon event segmentation, such as activity familiarity. The results reported in this thesis clearly demonstrate that differential psychological processes are engaged, depending on the level of knowledge one has of an activity. Considering the propositions of EST and the Sitnikova et al. (2008) study, it may be considered that these results support an account of semantic and scematic integration. Further, neurological differences shown between the segmentation of familiar and unfamiliar events may reflect the updating of an existing cognitive schema, versus the formation of an almost entirely new schema when an unfamiliar activity is first studied. Moreover, neurophysiologically distinctive processes were shown to be active when comparing the segmentation of goal-orientated and goalless activity; clearly indicating the importance of goal perception when attempting to process ongoing events. Therefore, it could be argued that these results reflect the differential engagement of cognitive schemata, depending on whether the activity is perceived to be goal-orientated or not.

10.4 Future Directions

Given that the research presented in this thesis suggests self-paced ERP studies are a valid method of investigating event segmentation, a series of

future ERP experiments is clearly justified. Whilst the baseline studies, for example, provided novel insight into the neural correlates of event segmentation, further replications of existing fMRI-based studies could similarly reveal new findings, e.g. the Sridharan et al. (2007) study of segmentation in music, or a study of narrative comprehension e.g. Speer et al. (2007). Additionally, further ERP studies may shed more light upon the top-down and bottom-up influences on event segmentation, and in particular, the psychological processes that underlie event segmentation e.g. the role of cognitive schemata.

Following the investigation of event start and end point perceptions (Experiment 5), this novel paradigm could be used to drive an important new direction; researching how the human mind deals with multiple overlapping structures, or what the mind might be doing between the end of one event and the start of the next, could provide new valuable information on the perception and internal representation of complex events.

One of the problems when attempting to compare fMRI and EEG data is the lack of spatial resolution offered by electroencephalogram recordings. However, by employing computational methods such as Principal or Independent Component Analysis (PCA/ICA), which attempt to recover sources from mixed signals, measured estimates can be as to the sources of EEG activity. Primarily, these tools could be of use when comparing similar EEG and fMRI experiments, and could further, reveal neural generators undetectable with current fMRI methods.

10.5 Conclusions

The mental processing of ongoing activity is supported by multiple cognitive operations, each of which is engaged under different circumstances. Sense is made of complex, real-world events by breaking the world around us into manageable chunks for comprehension, communication and learning. It is likely that cognitive schemata are retrieved from memory to facilitate prediction during processing, and that when faced with an unfamiliar or seemingly goalless activity, more attention is paid to updating schemata in order to facilitate learning. Furthermore, well-formed cognitive schemas are internally represented as hierarchical structures, just as events are tracked simultaneously on multiple timescales during normal perception.

The series of experiments reported in the thesis was the first attempt at a systematic investigation of event segmentation in the electrophysiological domain. The novel approach used ERPs to identify distinctive pre- and post-segmentation neural generator engagements, and to assess the role of familiarity and goal-directedness in event segmentation. The experiments support an account of event segmentation, active as a part of normal perception.

Bibliography

Abbott, V., Black, J. H., & Smith, E. E. (1985). The representation of scripts in memory. *Journal of Memory and Language, 24*, 179-199.

Avrahami, J., & Kareev, Y. (1994). The emergence of events. *Cognition*, 53, 239-261.

Bauer, P. J., & Mandler, J. M. (1989). One thing follows another: effects of temporal structure on 1-to-2-year-olds' recall of events. *Dev. Psychol.*, 25, 197-206.

Beatty, J., & Lucero-Wagoner, B. (2000). The pupillary system. . *In Handbook of Psychophysiology (Cacioppo, J.T. et al., eds)*, pp. 142-162, Cambridge University Press.

Boltz, M. G. (1992). Temporal accent structure and the remembering of filmed narratives. *J. Exp. Psychol. Hum. Percept. Perform.*, 18, 90-105.

Bower, G. (1982). Plans and goals in understanding episodes. *In A. Flammer & W. Kintsch (Eds.), Discourse Processing (pp. 2-15). Amsterdam: North-Holland Publishing Company.*

Bower, G. H., Black, J. B., & Turner, T. J. (1979). Scripts in memory for text. *Cognitive Psychology*, 11, 177-220.

Bower, G. H., & Rinck, M. (2001). Selecting oneamongmany referents in spatial situation models. . *J. Exp. Psychol. Learn. Mem. Cogn.*, 27, 81-98.

Byrne, R. W. (2002). Seeing actions as hierarchically organized structures: great ape manual skills. *In The Imitative Mind: Development, Evolution, and Brain Bases (Meltzoff, A. and Prinz, W., eds)*, pp. 122-142, Cambridge University Press.

Carpenter, G. A., & Grossberg, S. (2003). Adaptive resonance theory. *In M. A. Arbib (Ed.), The handbook of brain theory and neural networks*, (2nd ed., pp. 87-90). Cambridge, MA: MIT Press.

Corbetta, M., E. Akbudak, et al. (1998). "A common network of functional areas for attention and eye movements." *Neuron*: 21, 761–773.

Elman, J. L. (1990). Finding structure in time. *Cognitive Science*, 14, 179-211.

Friedman D., & Johnson Jr R. (2000). Event-related potential (ERP) studies of memory encoding and retrieval: a selective review. *Microsc Res Tech 2000;51:6±28.*

Fuster, J. M. (1991). The prefrontal cortex and its relation to behavior. *Progress in Brain Research*, 87, 201-211.

Gernsbacher, M. A. (1985). Surface information loss in comprehension. *Cognit. Psychol.*, 17, 324-363.

Gernsbacher, M. A. (1990). Language Comprehension as Structure Building. *Earlbaum*.

Glenberg, A. M., & Kaschak, M. P. (1987). Mental models contribute to foregrounding during text comprehension. *J. Mem. Lang.*, 26, 69-83.

Gobet, F., Lane, P. C., Croker, S., Cheng, P. C., Jones, G., Oliver, I., et al. (2001). Chunking mechanisms in human learning. *Trends Cogn. Sci.*, 5, 236-243.

Graesser, A., & Clark, L. (1985). Structure and Procedures of Implicit Knowledge. *Ablex. Norwood, NJ*.

Hanson, C., & Hanson, S. J. (1996). Development of schemata during event parsing: Neisser's perceptual cycle as a recurrent connectionist network. *Journal of Cognitive Neuroscience*, 8, 119-134.

Hard, B. M., Lozano, S. C., & Tversky, B. (2006). Hierarchical encoding of behavior: translating perception into action. *J. Exp. Psychol. Gen.*, 135, 588-608.

Hard, B. M., Tversky, B., & Lang, D. S. (2006). Making sense of abstract events: Building event schemas. *Mem. Cognit.*, 34, 1221-1235.

Hudson, J. A. (1988). Children's memory for atypical actions in scriptbased stories: Evidence for a disruption effect. *Journal of Experimental Child Psychology*, 46, 159-173.

Jordan, M. I., & Rumelhart, D. E. (1992). Forward models: Supervised learning with a distal teacher. *Cognitive Science*, 16, 307-354.

Kurby, C. A., & Zacks, J. M. (2008). Segmentation in the perception and memory of events. *Trends in Cognitive Science*, 12, 72-19.

Lichtenstein, E. D., & Brewer, W. F. (1980). Memory for goal-directed events. *Cognit. Psychol.*, 12, 412-445.

Lumer, E. D., Friston, K. J. & Rees, G. Neural correlates of perceptual rivalry in the human brain. *Science* 280, 1930–1934 (1998).

Lumer, E. D. & Rees, G. Covariation of activity in visual and prefrontal cortex associated with subjective visual perception. *Proc. Natl. Acad. Sci. USA* 96, 1669–1673 (1999).

Mandler, J. M., & Johnson, N. S. (1977). Remembrance of things parsed: Story structure and recall. *Cognitive Psychology, 15*, 513-532.

Michelon, P., A. Z. Snyder, et al. (2003). "Neural correlates of incongruous visual information. An event-related fMRI study." *Neuroimage*: 19, 1612-26.

Morrow, D. G., Bower, G. H., & Greenspan, S. L. (1989). Updating situation models during narrative comprehension. *J. Mem. Lang.*, 28, 292-312.

Neisser, U. (1967). Cognitive psychology. *New York: Appleton-Century-Crofts.*

Nelson, K., & Gruendel, J. (1986). Children's scripts. In K. Nelson (Ed.), Event Knowledge: Structure and Function in Development. *Hillsdale, NJ: Lawrence Erlbaum Associates.*, 21-46.

Newtson, D. (1973). Attribution and the unit of perception of ongoing behavior. *Journal of Personality and Social Psychology*, 28, 28-38.

Newtson, D. (1976). Foundations of attribution: the perception of ongoing behavior. *In New Directions in Attribution Research Harvey, J.H. et al., eds,*, pp. 223-248, Erlbaum.

Newtson, D., & Engquist, G. (1976). The perceptual organization of ongoing behavior. *Journal of Experimental Social Psychology*, 12, 436-450.

Newtson, D., Engquist, G., & Bois, J. (1977). Objective basis of behavior units. *J. Pers. Soc. Psychol.*, 12, 847-862.

Radvansky, G. A., & Copeland, D. E. (2006). Walking through doorways causes forgetting: situation models and experienced space. *Mem. Cognit.*, 34, 1150-1156.

Rinck, M., & Bower, G. (2000). Temporal and spatial distance in situation models. *Mem. Cognit.*, 28, 1310-1320.

Rinck, M., & Weber, U. (2003). Who when where: an experimental test of the event-indexing model. *Mem. Cognit.*, 31, 1284-1292.

Rumelhart, D. E. (1977). Understanding and summarizing brief stories. *In Basic Processes in Reading: Perception and Comprehension Laberge, D. and Samuels, S.J., eds, ,* pp. 265-303, Erlbaum.

Rugg, M. D. (1985). The effects of semantic priming and word repetition on eventrelated potentials. *Psychophysiology,* 22, 642-647.

Rugg M.D., & Coles M.G.H. (1995). ERP studies of memory. In: Electrophysiology of Mind: Event-related Brain Potentials and Cognition. *New York: Oxford University Press, pp 132–170.*

Schank, R. C., & Abelson, R. P. (1977). Scripts, plans, goals, and understanding: An inquiry into human knowledge structures. *Hillsdale, NJ: Erlbaum.*

Schwan, S., & Garsoffky, B. (2004). The cognitive representation of filmic event summaries. *Appl. Cognit. Psychol.,* 18, 37-55.

Sekuler, R., S. N. J. Watamaniuk, et al. (2002). "Perception of visual motion." In Steven's handbook of experimental psychology: Sensation and perception: *Vol. 1, 3rd edn Pashler, H. and Yantis, S., eds In pp.* 121-176, John Wiley & Sons.

Sitnikova, T., P. J. Holcomb, et al. (2008). "Two Neurocognitive Mechanisms of Semantic Integration during the Comprehension of Visual Real-world Events." *Journal of Cognitive Neuroscience.*

Sitnikova, T., G. Kuperberg, et al. (2003). "Semantic integration in videos of real-world events: an electrophysiological investigation." *Psychophysiology*: 40(1): p. 160-4.

Speer, N. K., Swallow, K. M., & Zacks, J. M. (2003). Activation of human motion processing areas during event perception. *Cognitive, Affective, & Behavioral Neuroscience*, 3 (4), 335-345.

Speer, N. K., & Zacks, J. M. (2005). Temporal changes as event boundaries: processing and memory consequences of narrative time shifts. *J. Mem. Lang.*, 53, 125-140.

Speer, N. K., Zacks, J. M., & Reynolds, J. R. (2007). Human brain activity time-locked to narrative event boundaries. *Psychol. Sci.*, 18, 449-455.

Squire, L. R., & Zola-Morgan, S. (1991). The medial temporal lobe memory system. *Science*, 253, 1380-1386.

Sridharan, D., D. J. Levitin, et al. (2007). "Neural dynamics of event segmentation in music: Converging evidence for dissociable ventral and dorsal networks." *Neuron*: 55, 521-532.

Swallow, K. M., & Zacks, J. M. (2004). Hierarchical grouping of events revealed by eye movements. *Abstr. Psychon. Soc.*, 9, 81.

Swallow, K. M., Zacks, J. M., & Abrams, R. A. (2007). Perceptual events may be the "episodes" in episodic memory. *Abstr. Psychon. Soc.*, 12, 25.

Thorndyke, P. W. (1977). Cognitive structures in comprehension and memory of narrative discourse. *Cognitive Psychology, 9*, 77-110.

Tong, F., Nakayama, K., Vaughan, J. T. & Kanwisher, N. Binocular rivalry and visual awareness in human extrastriate cortex. *Neuron* 21, 753–759 (1998).

Trabasso, T., & van den Broek, P. (1985). Causal thinking and the representation of narrative events. *Journal of memory and language*, 24, 612-630.

Travis, L. L. (1997). Goal-based organization of event memory in toddlers. *In Developmental Spans on Event Comprehension and Representation: Bridging Fictional and Actual Events van den Broek, P.W. et al., eds*, 111-139, LEA.

Tversky, B., & Hemenway, K. (1984). Objects, parts, and categories. *Journal of Experimental Psychology: General*, 113, 169-193.

van den Broek, P., Lorch, E. P., & Thurlow, R. (1996). Children's and adults' memory for television stories: The role of causal factors, story-grammar categories, and hierarchical level. *Child Development*, 67, 3010-3028.

van Dijk, T. A., & Kintsch, W. (1983). Strategies of discourse comprehension. *New York: Academic Press.*

Wynn, K. (1996). Infants' individuation and enumeration of actions. *Psychological Science*, 7, 164-169.

Zacks, J. M. (2004). Using movement and intentions to understand simple events. *Cognit. Sci.*, 28, 979-1008.

Zacks, J. M., Braver, T. S., Sheridan, M. A., Donaldson, D. I., Snyder, A. Z., Ollinger, J. M., et al. (2001). Human brain activity time-locked to perceptual event boundaries. *Nature Neuroscience*, 4, 651-655.

Zacks, J. M., Speer, N. K., Swallow, K. M., Braver, T. S., & Reynolds, J. R. (2007). Event perception: A mind/brain perspective. *Psychol. Bull.*, 133, 273-293.

Zacks, J. M., Speer, N. K., Vettel, J. M., & Jacoby, L. L. (2006). Event understanding and memory in healthy aging and dementia of the Alzheimer type. *Psychol. Aging*, 21, 466-482.

Zacks, J. M., & Tversky, B. (2001). Event structure in perception and conception. *Psychol. Bull.*, 127, 123-121.

Zacks, J. M., & Tversky, B. (2003). Structuring information interfaces for procedural learning. *J. Exp. Psychol. Appl.*, 9, 88-100.

Zacks, J. M., Tversky, B., & Iyer, G. (2001). Perceiving, remembering, and communicating structure in events. *J. Exp. Psychol. Gen.*, 130, 129-158.

Zacks, J. M., K. M. Swallow, et al. (2006). "Visual movement and the neural correlates of event perception." *Brain Res.*: 1076, 150-162.

Zacks, J. M. et. al. (2006). "The human brain's response to change in cinema." *Abstr. Psychon. Soc.*: 11, 9.

Zwaan, R. A., Langston, M. C., & Graesser, A. C. (1995). The construction of situation models in narrative comprehension: An event-indexing model. *Psychol. Sci.*, 6, 292-297.

Zwaan, R. A., Magliano, J. P., & Graesser, A. C. (1995). Dimensions of situation model construction in narrative comprehension. *J. Exp. Psychol. Learn. Mem. Cogn.*, 21, 386-397.

Zwaan, R. A., Radvansky, G. A., Hilliard, A. E., & Curiel, J. M. (1998). Constructing multidimensional situation models during reading. *Sci. Stud. Read.*, 2, 199-220.

Appendix A: Summary Tables

EPT2

Passive-Coarse versus Random

Time window (*10²ms)	-15	-14	-13	-12	-11	-10	-9	-8	-7	-6	-5	-4	-3	-2	-1	0	1	2	3	4	5	6	7	8	9	10	11	12	13	14
Left Frontal																														
Right Frontal	•				•				•	•	•	•							•	•				•		•				
Right Parietal					•				•	•			•							•	•	•					•	•		
Left Parietal									•	•																				
									Segmentation																					

Passive-Fine versus Random

Time window (*10²ms)	-15	-14	-13	-12	-11	-10	-9	-8	-7	-6	-5	-4	-3	-2	-1	0	1	2	3	4	5	6	7	8	9	10	11	12	13	14
Left Frontal																														
Right Frontal	•		•							•			•			•				•			•	•	•					
Right Parietal	•	•	•								•	•	•								•	•	•	•						
Left Parietal																														
																Segmentation														

Passive-Coarse versus Passive-Fine

Time window (*10²ms)	-15	-14	-13	-12	-11	-10	-9	-8	-7	-6	-5	-4	-3	-2	-1	0	1	2	3	4	5	6	7	8	9	10	11	12	13	14
Left Frontal																														
Right Frontal					•				•		•														•	•		•		
Right Parietal									•																•	•	•			
Left Parietal																											•			
																Segmentation														

EPT2 (comparison)

Directed-Passive-Coarse versus Passive-Coarse

Time window	-15	-14	-13	-12	-11	-10	-9	-8	-7	-6	-5	-4	-3	-2	-1	0	1	2	3	4	5	6	7	8	9	10	11	12	13	14
Left Frontal																														
Right Frontal																			•	•										
Right Parietal																														
Left Parietal																														

Segmentation

Directed-Passive-Fine versus Passive-Fine

Time window	-15	-14	-13	-12	-11	-10	-9	-8	-7	-6	-5	-4	-3	-2	-1	0	1	2	3	4	5	6	7	8	9	10	11	12	13	14
Left Frontal																														
Right Frontal					•																									
Right Parietal				•							•										•	•								
Left Parietal				•				•																						

Segmentation

EPT3

Expert-Passive-Coarse versus Naive-Passive-Coarse

Time window (*10²ms)	-15	-14	-13	-12	-11	-10	-9	-8	-7	-6	-5	-4	-3	-2	-1	0	1	2	3	4	5	6	7	8	9	10	11	12	13	14
Left Frontal												•						•												
Right Frontal																		•	•											
Right Parietal																		•	•											
Left Parietal	•																													
	Segmentation																													

Expert-Passve-Fine versus Naive-Passive-Five

Time window (*10²ms)	-15	-14	-13	-12	-11	-10	-9	-8	-7	-6	-5	-4	-3	-2	-1	0	1	2	3	4	5	6	7	8	9	10	11	12	13	14
Left Frontal																														
Right Frontal										•												•					•	•	•	
Right Parietal										•	•																			
Left Parietal																		•	•											
	Segmentation																													

Expert-Passive-Coarse versus Expert-Passive-Fine

Time window (*10²ms)	-15	-14	-13	-12	-11	-10	-9	-8	-7	-6	-5	-4	-3	-2	-1	0	1	2	3	4	5	6	7	8	9	10	11	12	13	14
Left Frontal																														
Right Frontal																			•	•									•	
Right Parietal																			•	•									•	
Left Parietal	•																												•	
	Segmentation																													

Naive-Passve-Coarse versus Naive-Passive-Five

Time window (*10²ms)	-15	-14	-13	-12	-11	-10	-9	-8	-7	-6	-5	-4	-3	-2	-1	0	1	2	3	4	5	6	7	8	9	10	11	12	13	14
Left Frontal																						•	•							
Right Frontal		•	•				•															•			•					
Right Parietal																									•	•				
Left Parietal																						•	•							
	Segmentation																													

EPT3 (comparison)

Expert-Passive-Coarse versus Passive-Coarse

Time window (*10²ms)	-15	-14	-13	-12	-11	-10	-9	-8	-7	-6	-5	-4	-3	-2	-1	0	1	2	3	4	5	6	7	8	9	10	11	12	13	14
Left Frontal																														
Right Frontal												•																		
Right Parietal																														
Left Parietal																														
Segmentation																														

Naive-Passive-Coarse versus Passive-Coarse

Time window (*10²ms)	-15	-14	-13	-12	-11	-10	-9	-8	-7	-6	-5	-4	-3	-2	-1	0	1	2	3	4	5	6	7	8	9	10	11	12	13	14
Left Frontal																														
Right Frontal				•								•										•						•		
Right Parietal												•										•								
Left Parietal																														
Segmentation																														

Expert-Passive-Fine versus Passive-Fine

Time window (*10²ms)	-15	-14	-13	-12	-11	-10	-9	-8	-7	-6	-5	-4	-3	-2	-1	0	1	2	3	4	5	6	7	8	9	10	11	12	13	14
Left Frontal																														
Right Frontal																•														
Right Parietal										•																				
Left Parietal																														
Segmentation																														

Naive-Passive-Fine versis Passive-Fine

Time window (*10²ms)	-15	-14	-13	-12	-11	-10	-9	-8	-7	-6	-5	-4	-3	-2	-1	0	1	2	3	4	5	6	7	8	9	10	11	12	13	14
Left Frontal																														
Right Frontal																					•	•								
Right Parietal											•																			
Left Parietal																														
Segmentation																														

EPTS

Passive-Coarse-Game versus Passive-Coarse-Random

Time window (*10²ms)	-15	-14	-13	-12	-11	-10	-9	-8	-7	-6	-5	-4	-3	-2	-1	0	1	2	3	4	5	6	7	8	9	10	11	12	13	14
Left Frontal																														
Right Frontal							•																							
Right Parietal						•																								
Left Parietal																														

Segmentation

Passive-Fine-Game versus Passive-Fine-Random

Time window (*10²ms)	-15	-14	-13	-12	-11	-10	-9	-8	-7	-6	-5	-4	-3	-2	-1	0	1	2	3	4	5	6	7	8	9	10	11	12	13	14
Left Frontal																														
Right Frontal				•	•																•									
Right Parietal				•										•																
Left Parietal																														

Segmentation

Passive-Coarse-Game versus Passive-Fine-Game

Time window (*10²ms)	-15	-14	-13	-12	-11	-10	-9	-8	-7	-6	-5	-4	-3	-2	-1	0	1	2	3	4	5	6	7	8	9	10	11	12	13	14
Left Frontal	•																													
Right Frontal		•																				•								
Right Parietal																									•					
Left Parietal																														

Segmentation

Passive-Coarse-Random versus Passive-Fine-Random

Time window (*10²ms)	-15	-14	-13	-12	-11	-10	-9	-8	-7	-6	-5	-4	-3	-2	-1	0	1	2	3	4	5	6	7	8	9	10	11	12	13	14
Left Frontal																								•						
Right Frontal				•																•										
Right Parietal				•		•														•										
Left Parietal				•		•																								

Segmentation

EPT5 (comparison)

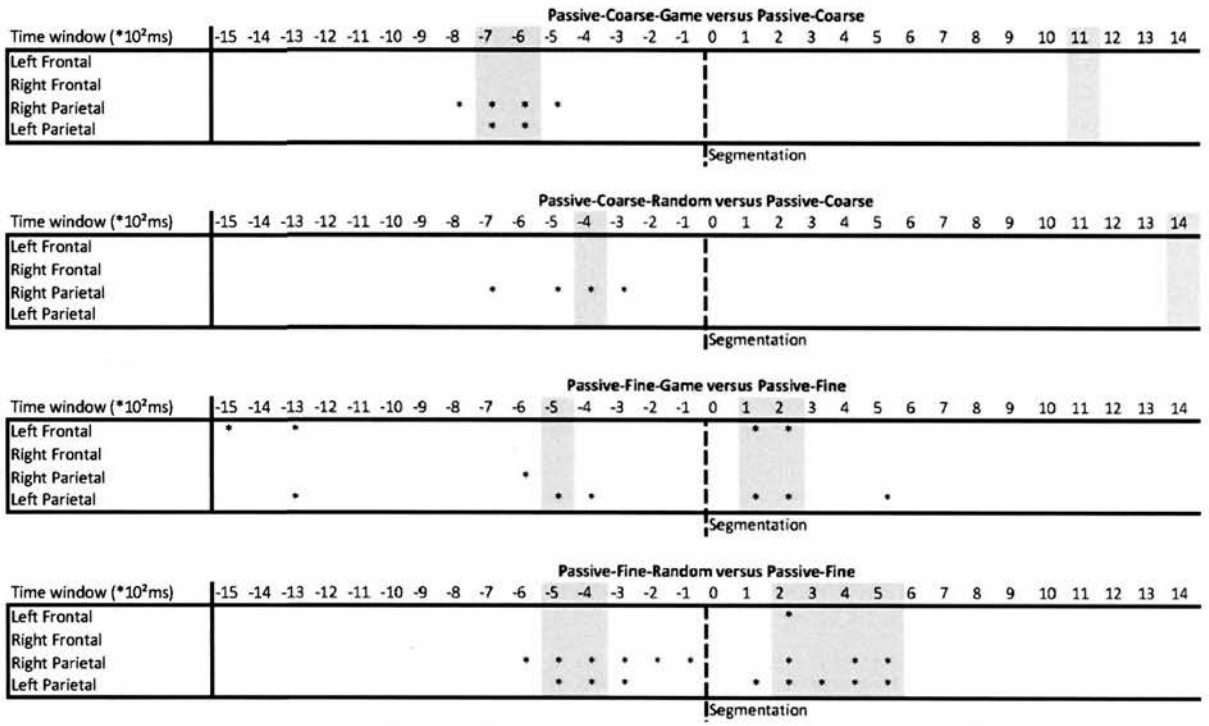

EPT4

Passive-Coarse-Start versus Passive-Coarse-End

Time window (*10²ms)	-15	-14	-13	-12	-11	-10	-9	-8	-7	-6	-5	-4	-3	-2	-1	0	1	2	3	4	5	6	7	8	9	10	11	12	13	14
Left Frontal																														
Right Frontal																														
Right Parietal																														
Left Parietal																														
Segmentation																														

Passive-Fine-Start versus Passive-Fine-End

Time window (*10²ms)	-15	-14	-13	-12	-11	-10	-9	-8	-7	-6	-5	-4	-3	-2	-1	0	1	2	3	4	5	6	7	8	9	10	11	12	13	14
Left Frontal																														
Right Frontal																														
Right Parietal																														
Left Parietal																														
Segmentation																														

Passive-Coarse-Start versus Passive-Fine-Start

Time window (*10²ms)	-15	-14	-13	-12	-11	-10	-9	-8	-7	-6	-5	-4	-3	-2	-1	0	1	2	3	4	5	6	7	8	9	10	11	12	13	14
Left Frontal																														
Right Frontal																														
Right Parietal																														
Left Parietal																														
Segmentation																														

Passive-Coarse-End versus Passive-Fine-End

Time window (*10²ms)	-15	-14	-13	-12	-11	-10	-9	-8	-7	-6	-5	-4	-3	-2	-1	0	1	2	3	4	5	6	7	8	9	10	11	12	13	14
Left Frontal																														
Right Frontal																														
Right Parietal																														
Left Parietal																														
Segmentation																														

EPT4 (comparison)

Passive-Coarse-Start versus Passive-Coarse

Time window (*10²ms)	-15	-14	-13	-12	-11	-10	-9	-8	-7	-6	-5	-4	-3	-2	-1	0	1	2	3	4	5	6	7	8	9	10	11	12	13	14
Left Frontal																														
Right Frontal																														
Right Parietal																														
Left Parietal																											•	•	•	
Segmentation																														

Passive-Coarse-End versus Passive-Coarse

Time window (*10²ms)	-15	-14	-13	-12	-11	-10	-9	-8	-7	-6	-5	-4	-3	-2	-1	0	1	2	3	4	5	6	7	8	9	10	11	12	13	14
Left Frontal																														
Right Frontal									•			•																		
Right Parietal																														
Left Parietal																					•	•								
Segmentation																														

Passive-Fine-Start versus Passive-Fine

Time window (*10²ms)	-15	-14	-13	-12	-11	-10	-9	-8	-7	-6	-5	-4	-3	-2	-1	0	1	2	3	4	5	6	7	8	9	10	11	12	13	14
Left Frontal				•	•				•	•	•																			
Right Frontal										•																				
Right Parietal								•																						
Left Parietal																														
Segmentation																														

Passive-Fine-End versus Passive-Fine

Time window (*10²ms)	-15	-14	-13	-12	-11	-10	-9	-8	-7	-6	-5	-4	-3	-2	-1	0	1	2	3	4	5	6	7	8	9	10	11	12	13	14
Left Frontal																														
Right Frontal						•	•	•	•	•	•	•	•	•							•	•	•	•	•	•	•			
Right Parietal															•	•														
Left Parietal	•					•					•	•				•	•	•	•	•	•									
Segmentation																														

Appendix B: Grand Average ERPs

Perception of everyday events

Inter-Experiment

Passive-Coarse

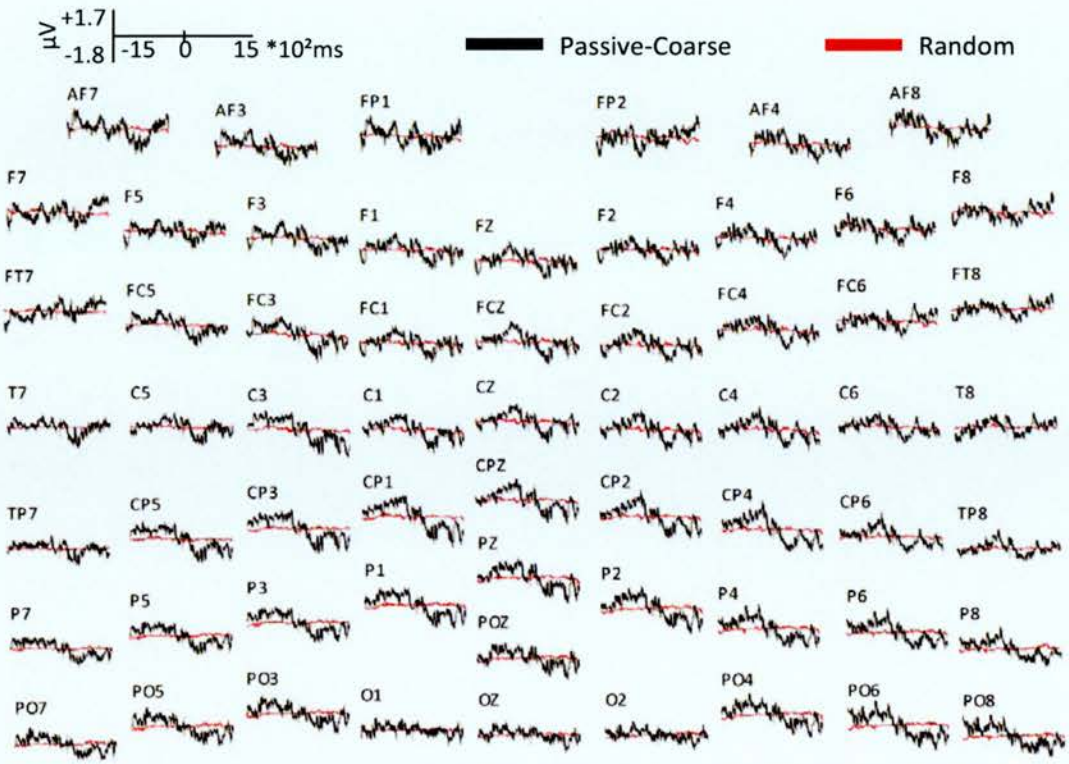

Passive-Fine

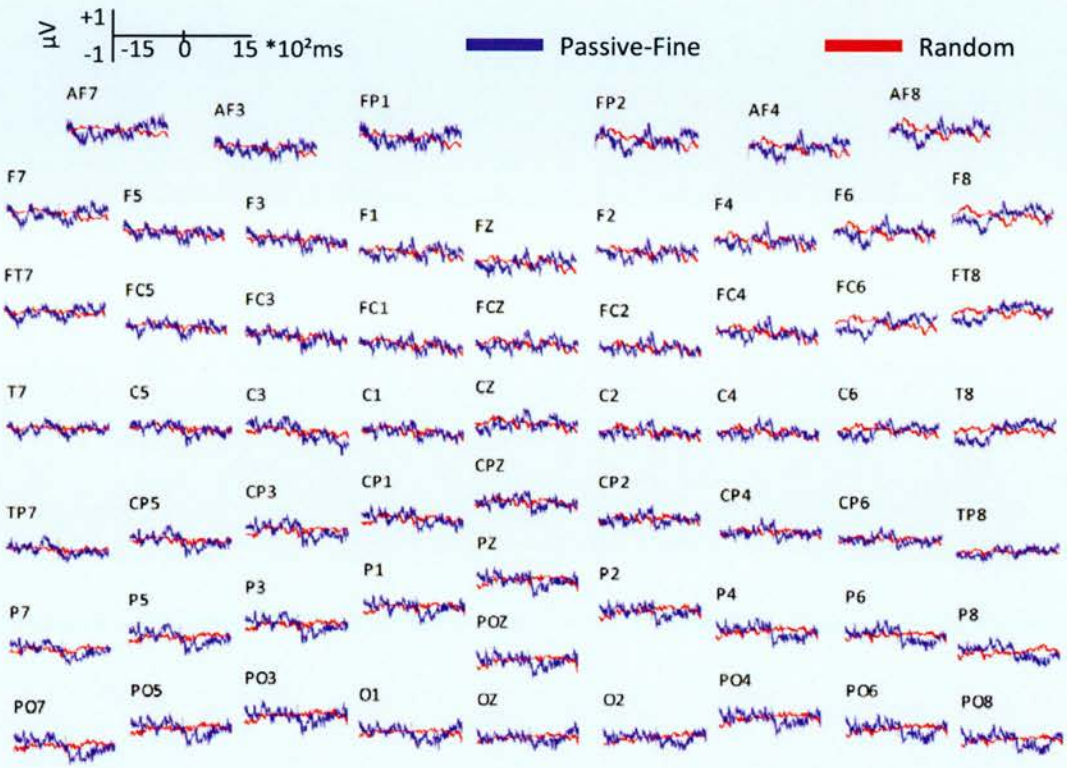

Coarse vs. Fine

Passive-Coarse vs. Passive-Fine

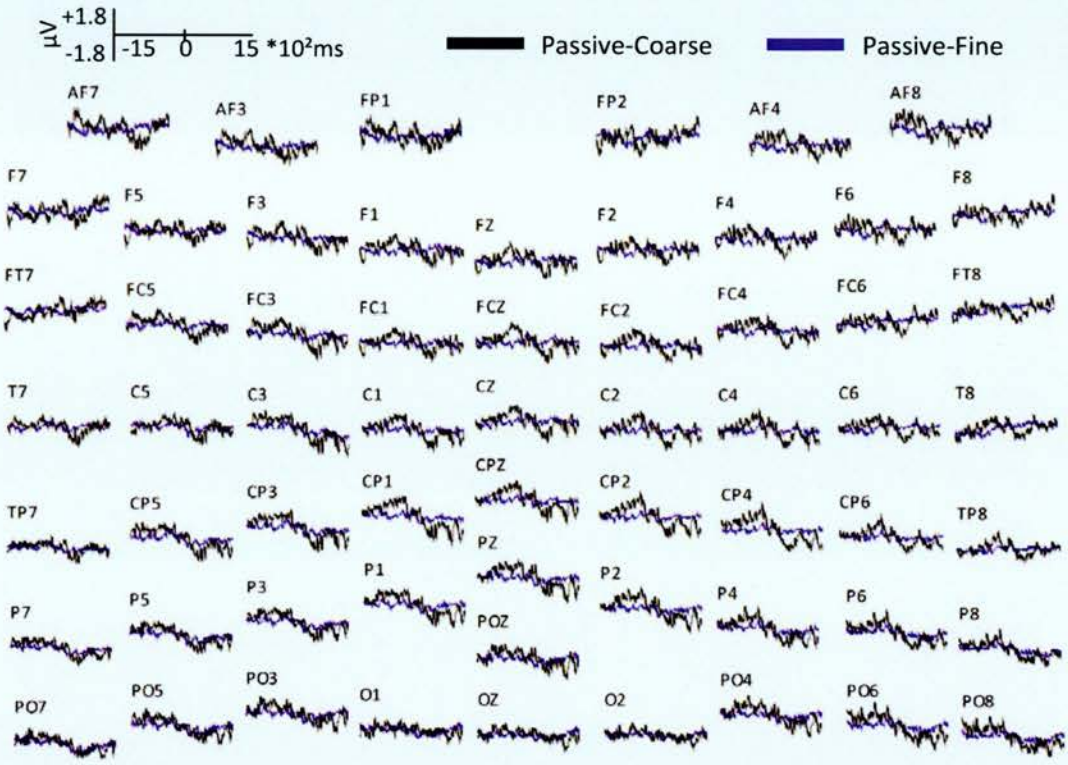

Cross-Experiment

Passive-Coarse vs. Directed-Passive-Coarse

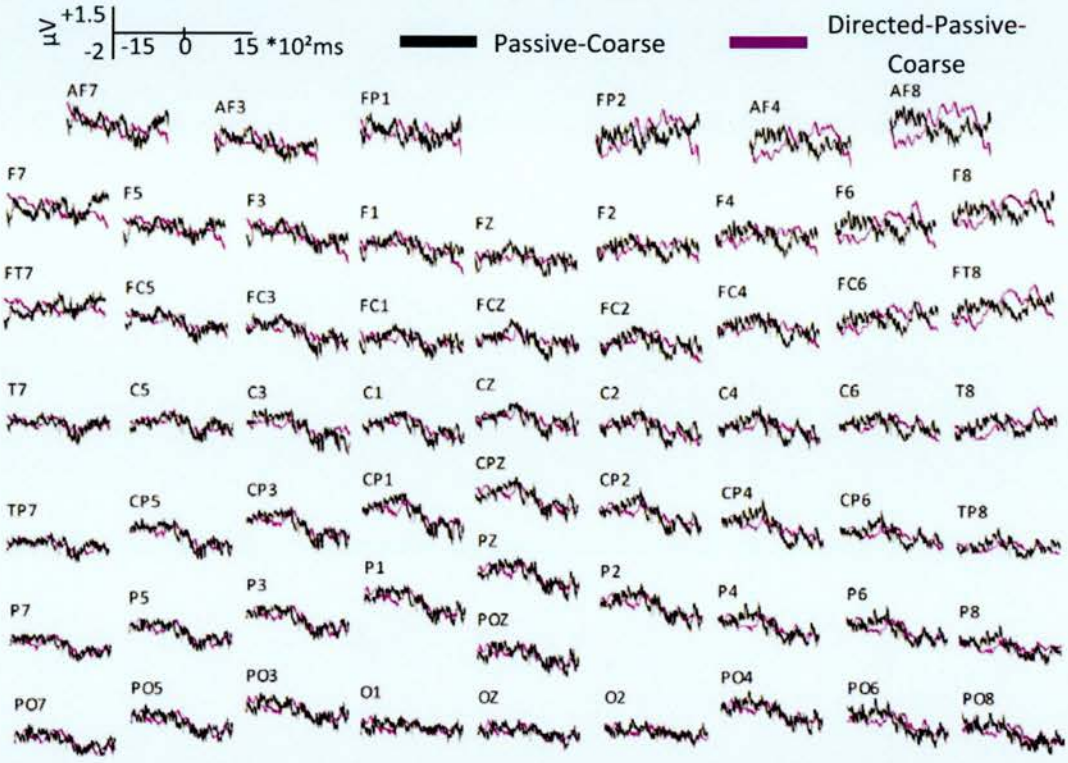

Appendix B: Grand Average ERPs

Passive-Fine vs. Directed-Passive-Fine

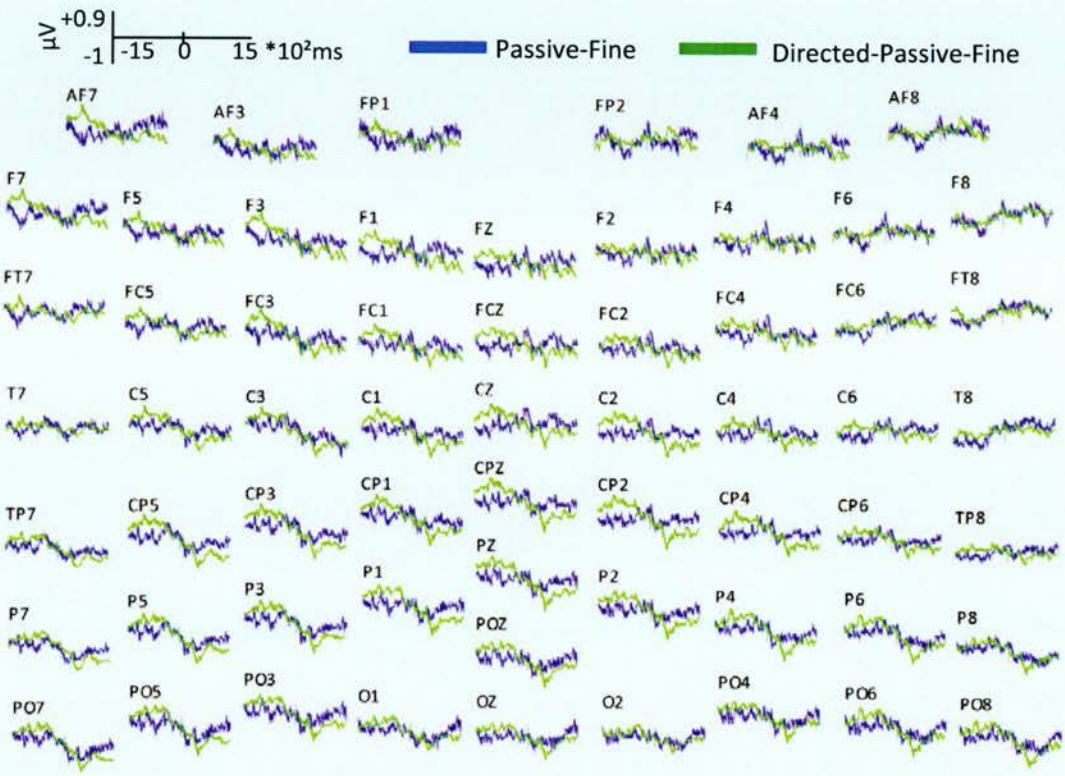

Expert vs. Naive

Inter-Experiment

Expert vs. Naive Passive-Coarse

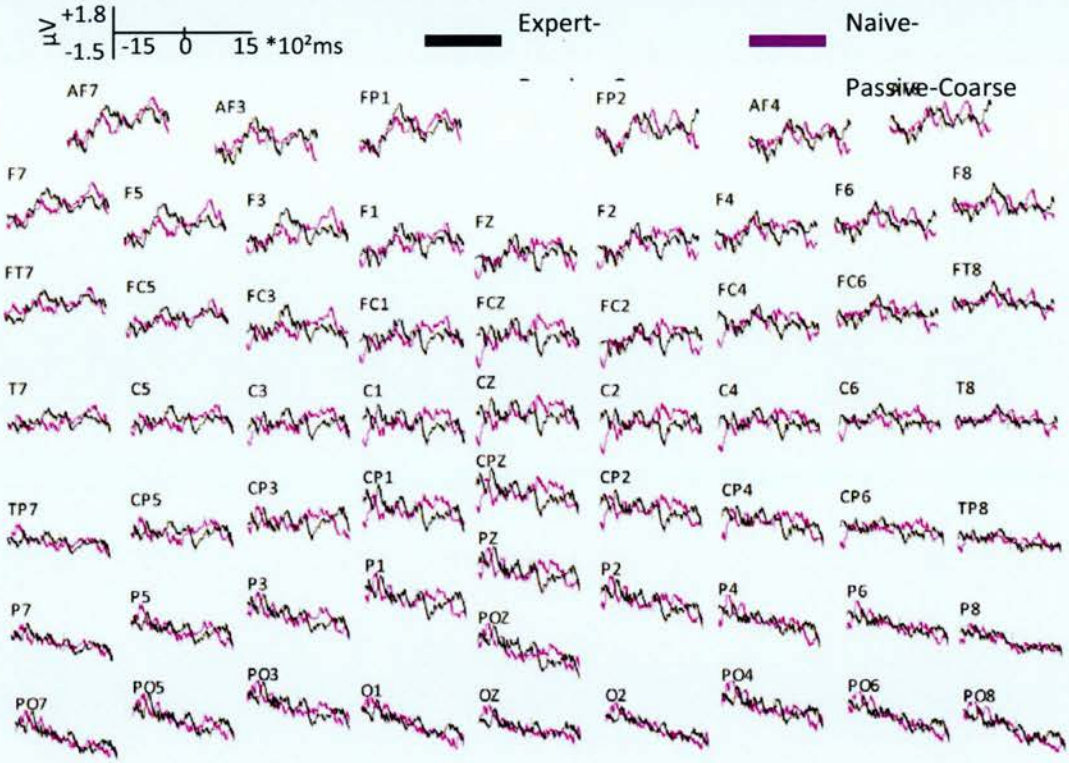

Expert vs. Naive Passive-Fine

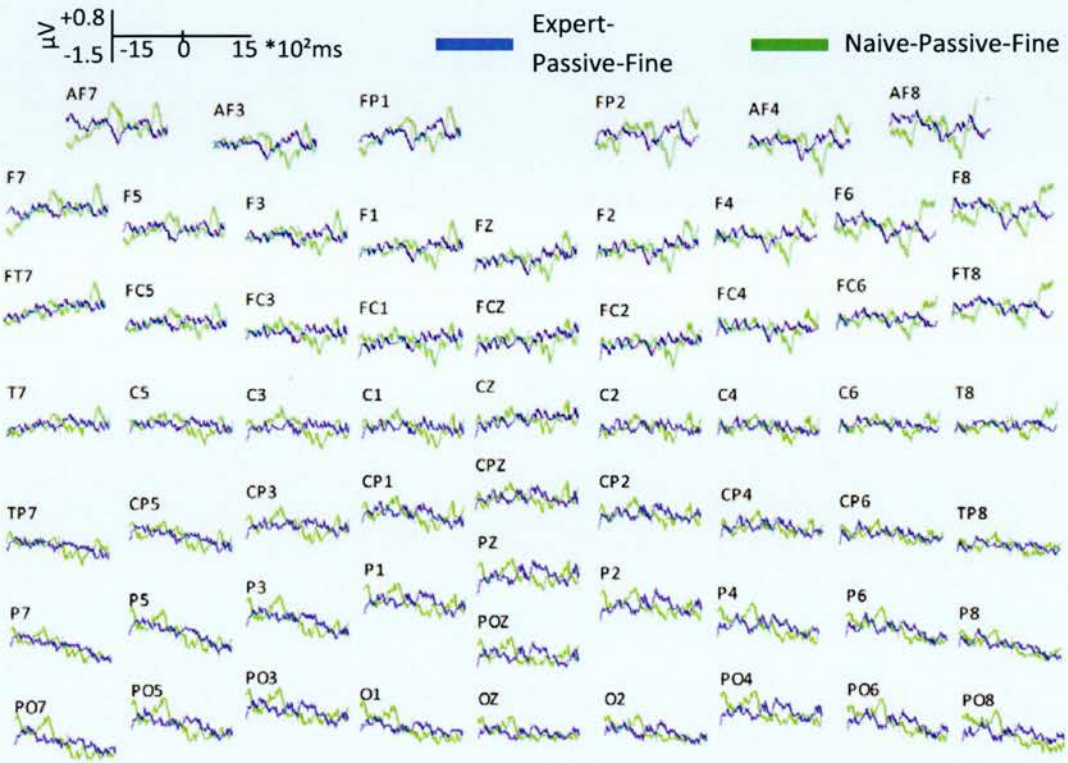

Coarse vs. Fine

Expert Passive-Coarse vs. Passive-Fine

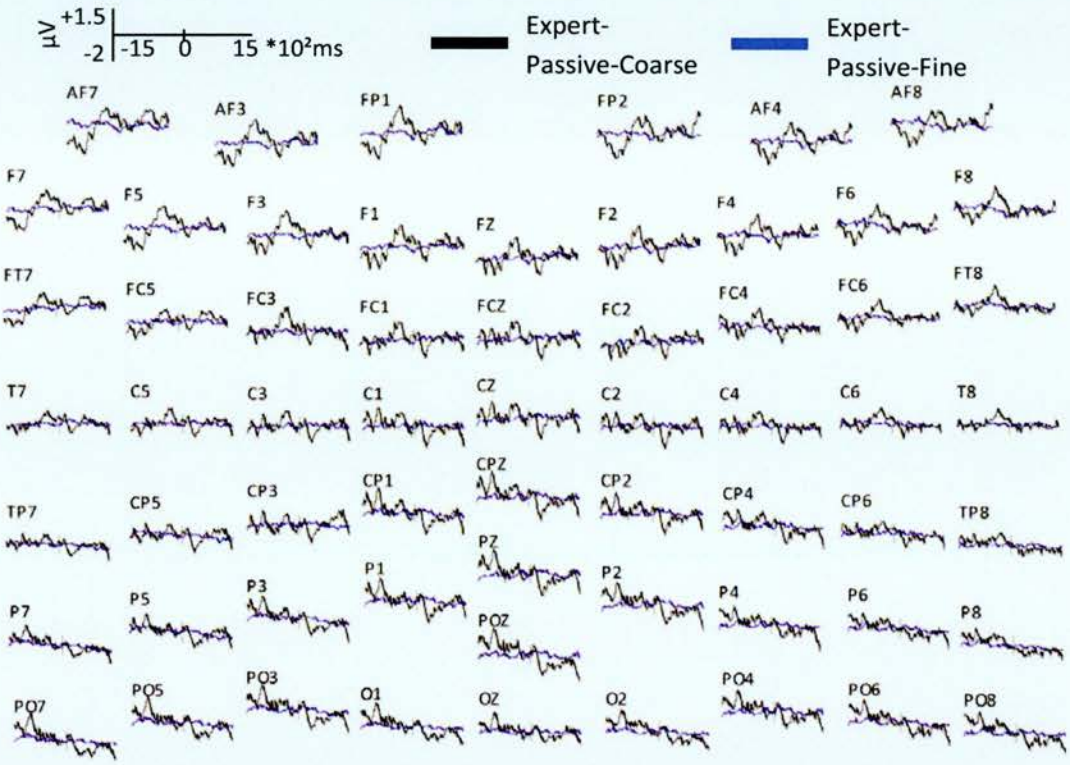

Appendix B: Grand Average ERPs

Naive Passive-Coarse vs. Passive-Fine

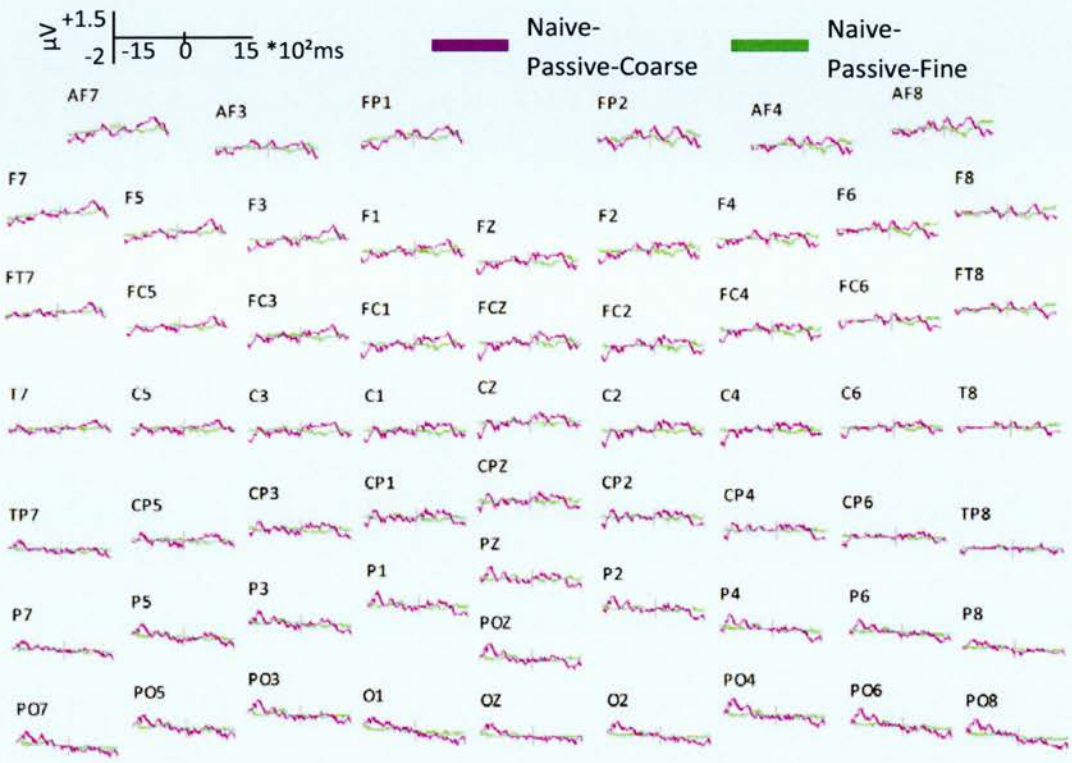

Cross-Experiment

Expert vs. Passive-Coarse

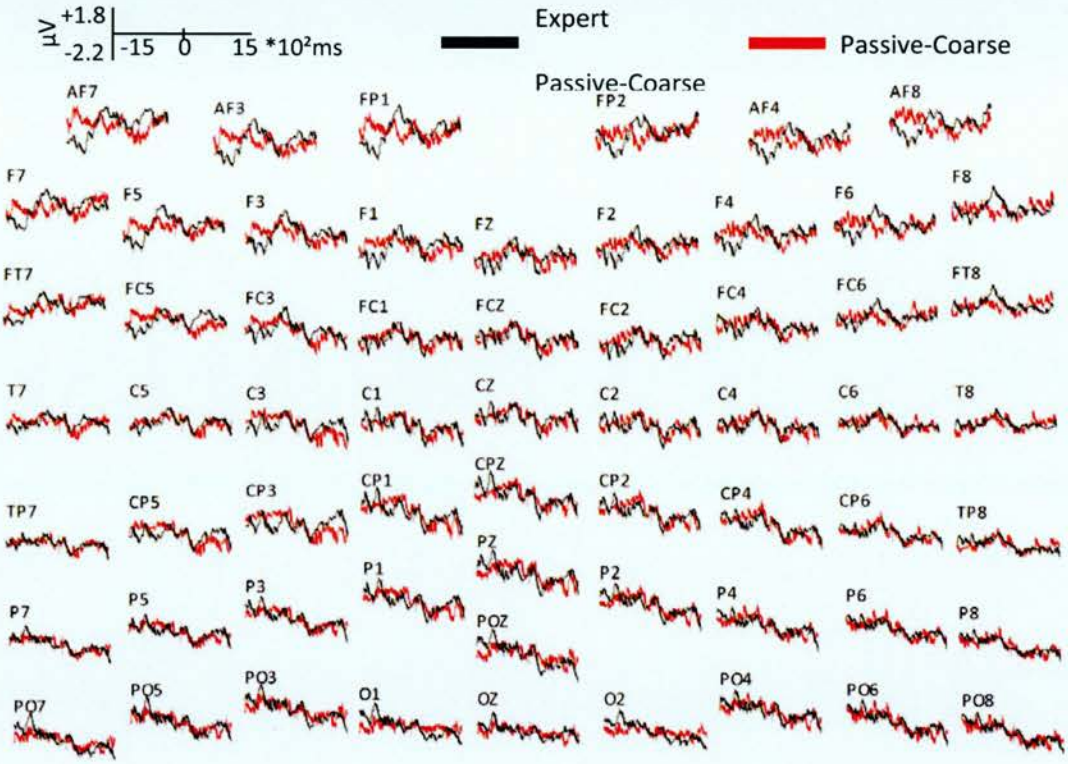

Appendix B: Grand Average ERPs

Expert vs. Passive-Fine

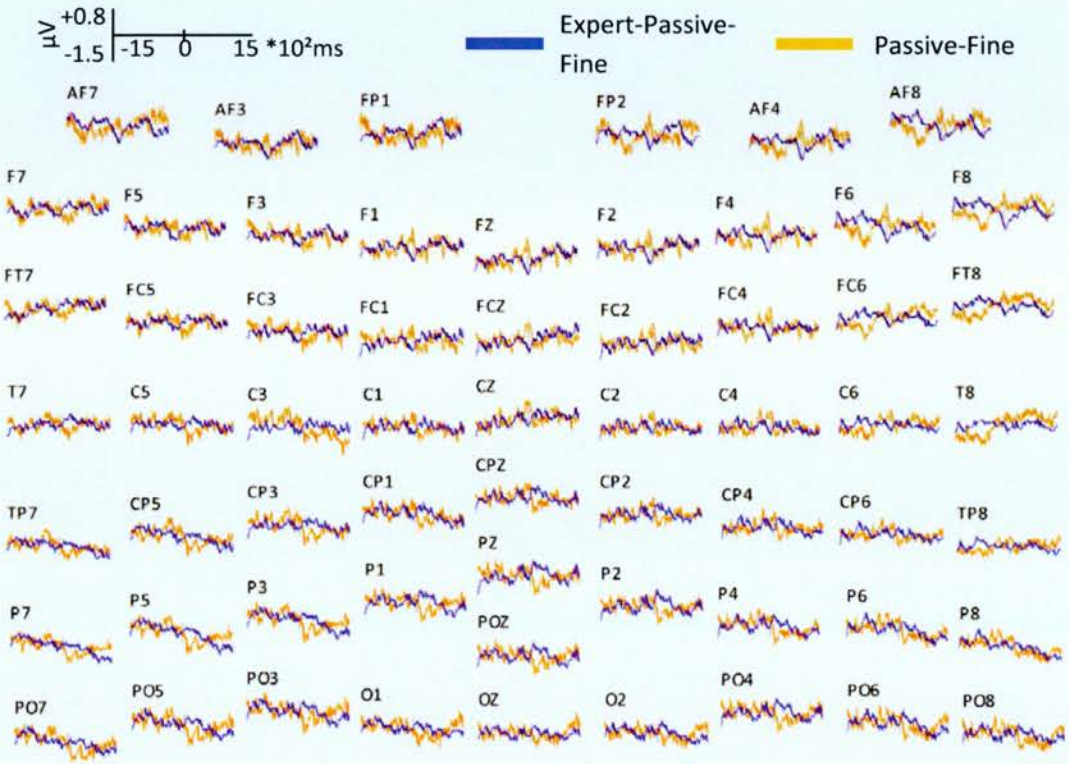

Naive vs. Passive-Coarse

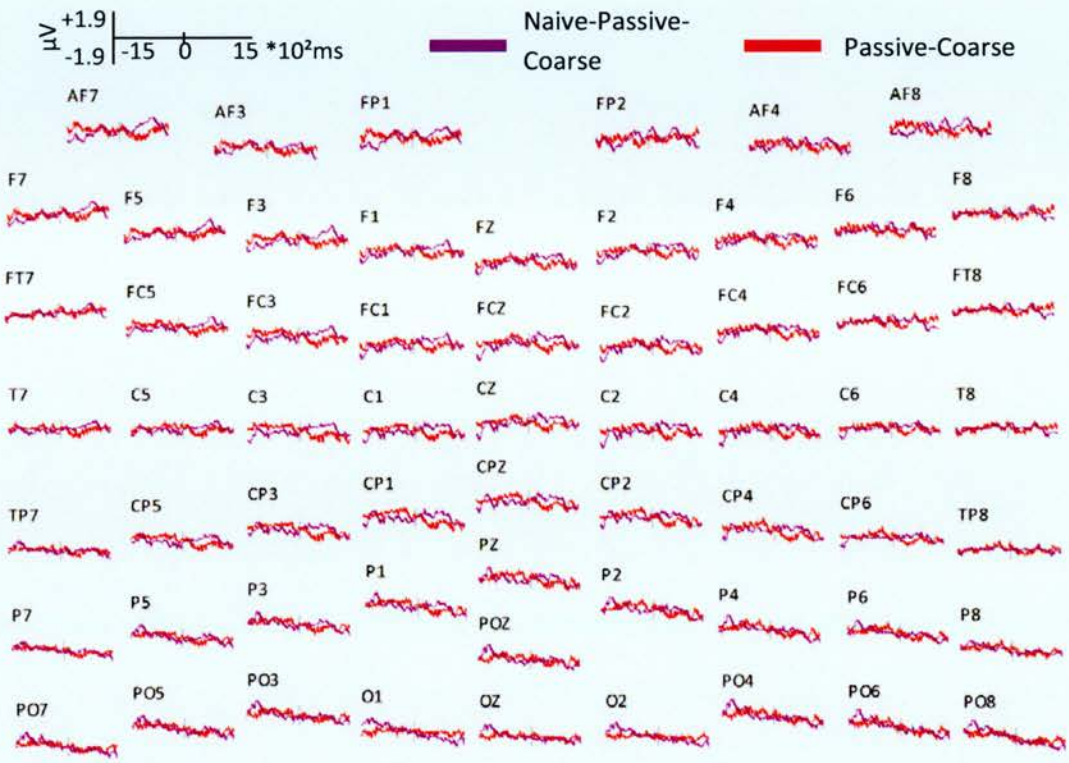

Appendix B: Grand Average ERPs

Naive vs. Passive-Fine

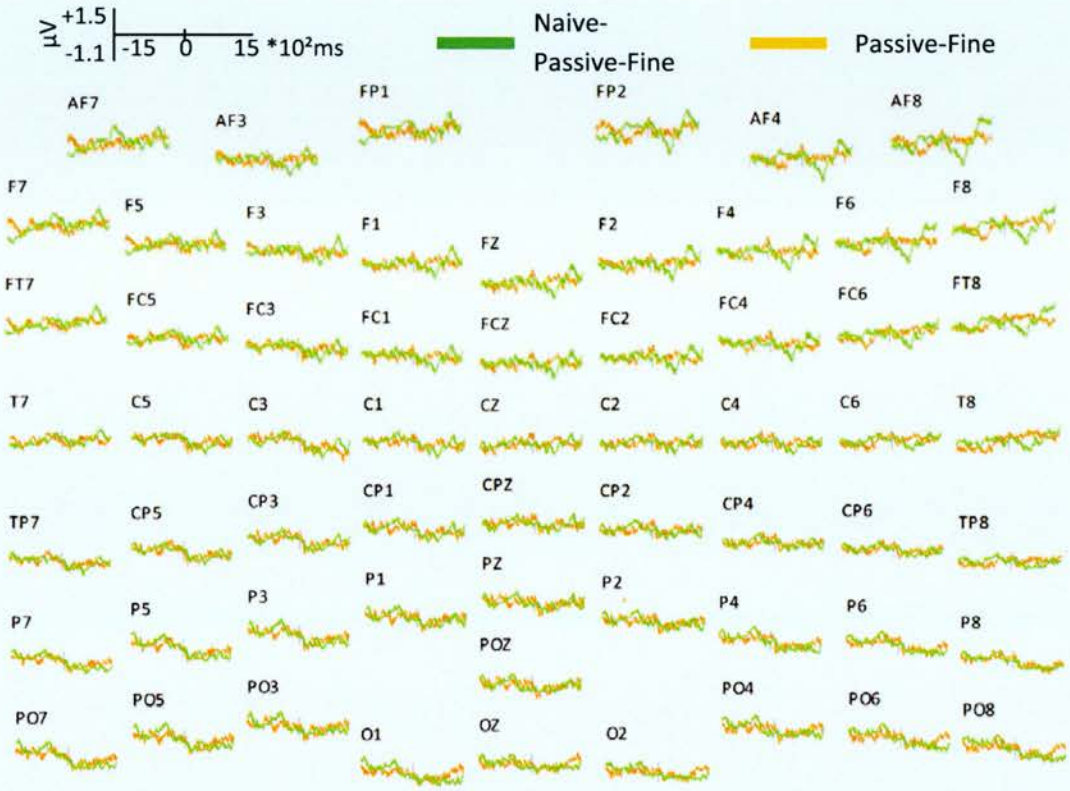

Game vs. Random

Inter-Experiment

Game vs. Random Passive-Coarse

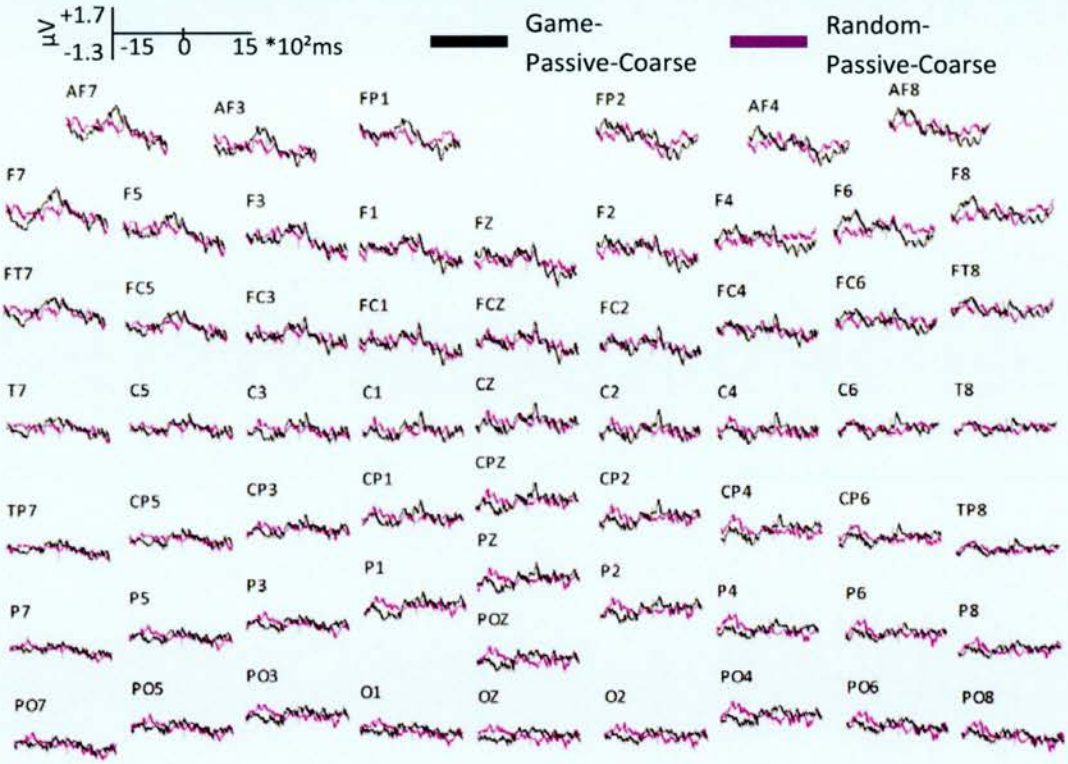

Game vs. Random Passive-Fine

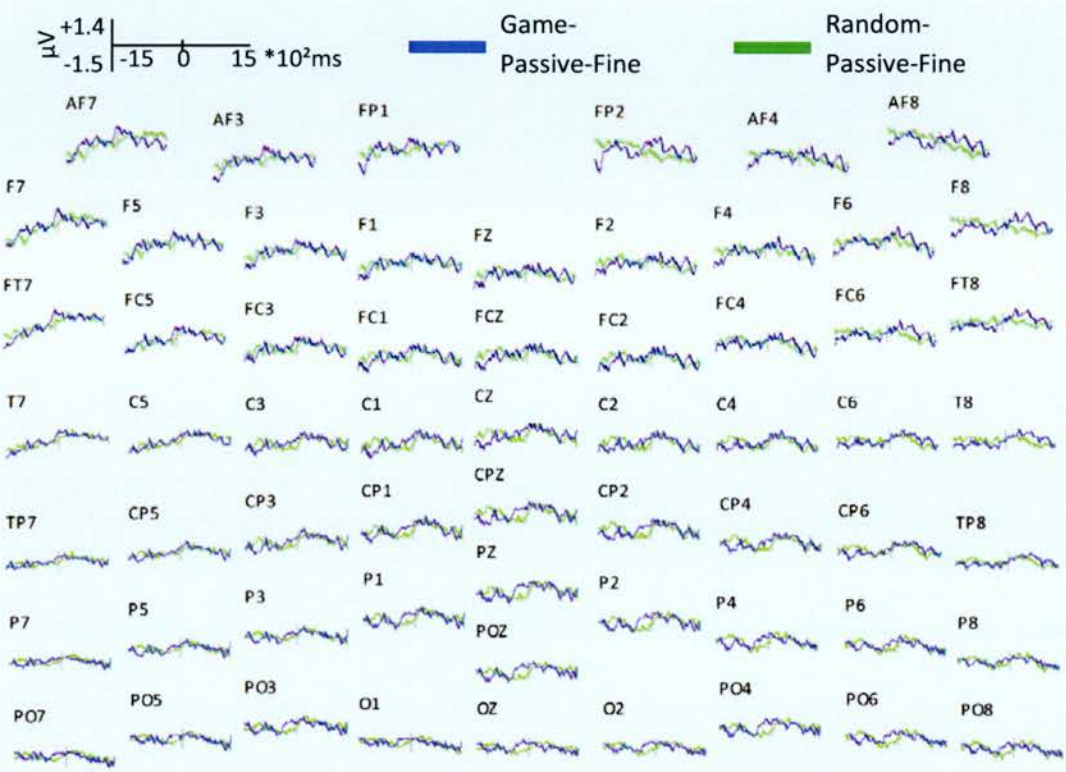

Coarse vs. Fine

Game Passive-Coarse vs. Passive-Fine

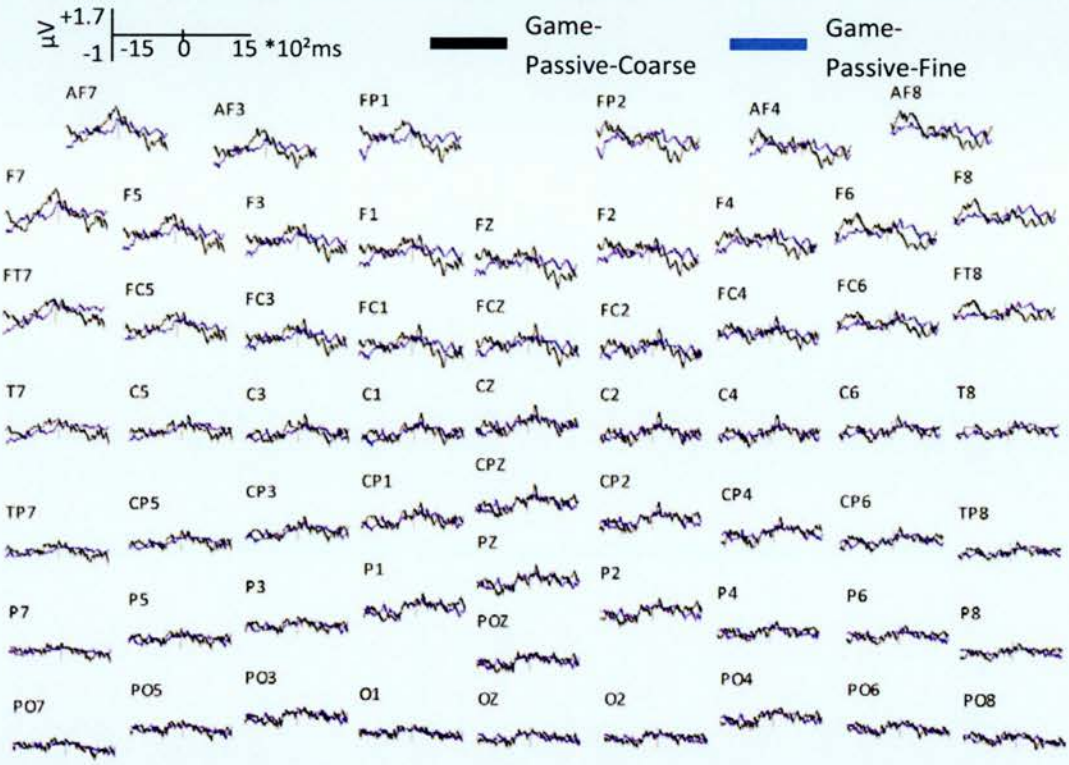

Appendix B: Grand Average ERPs

Random Passive-Coarse vs. Passive-Fine

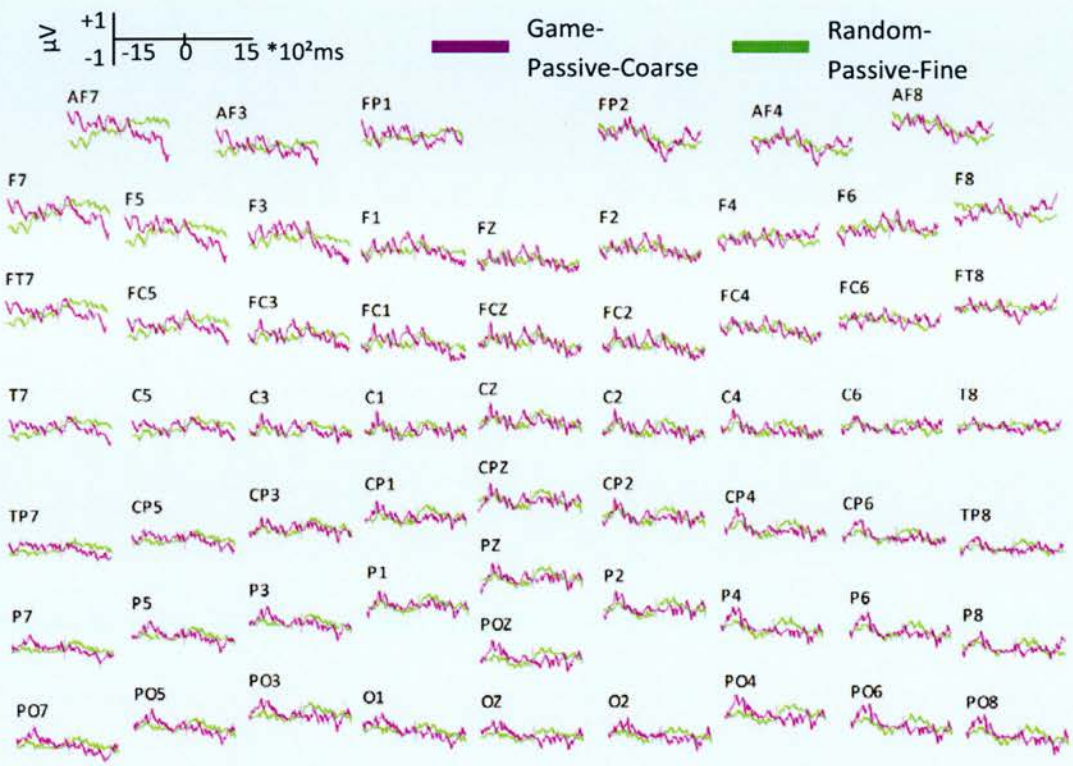

Cross-Experiment

Game vs. Passive-Coarse

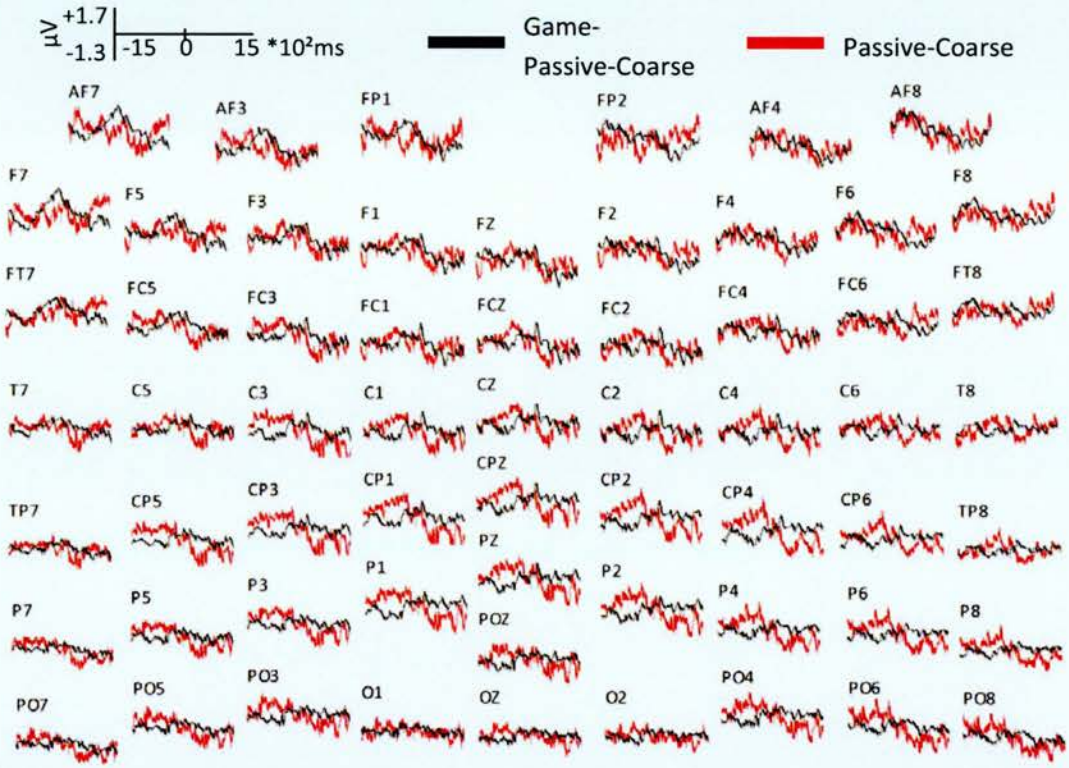

Appendix B: Grand Average ERPs

Game vs. Passive-Fine

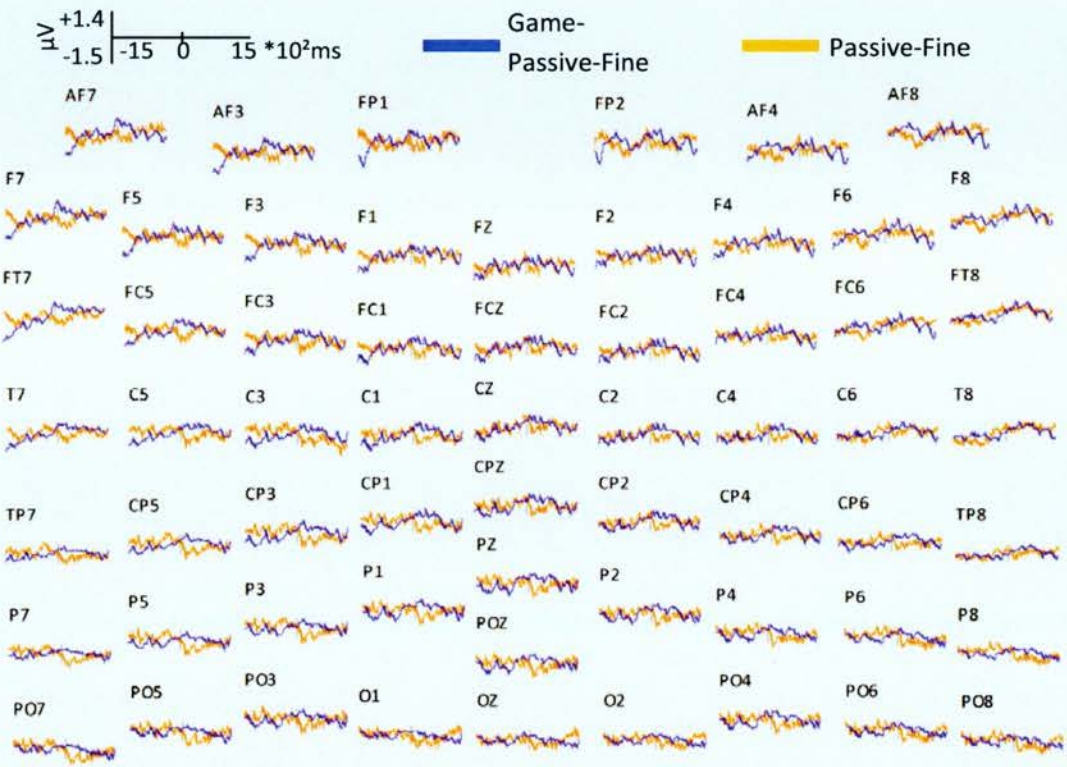

Random vs. Passive-Coarse

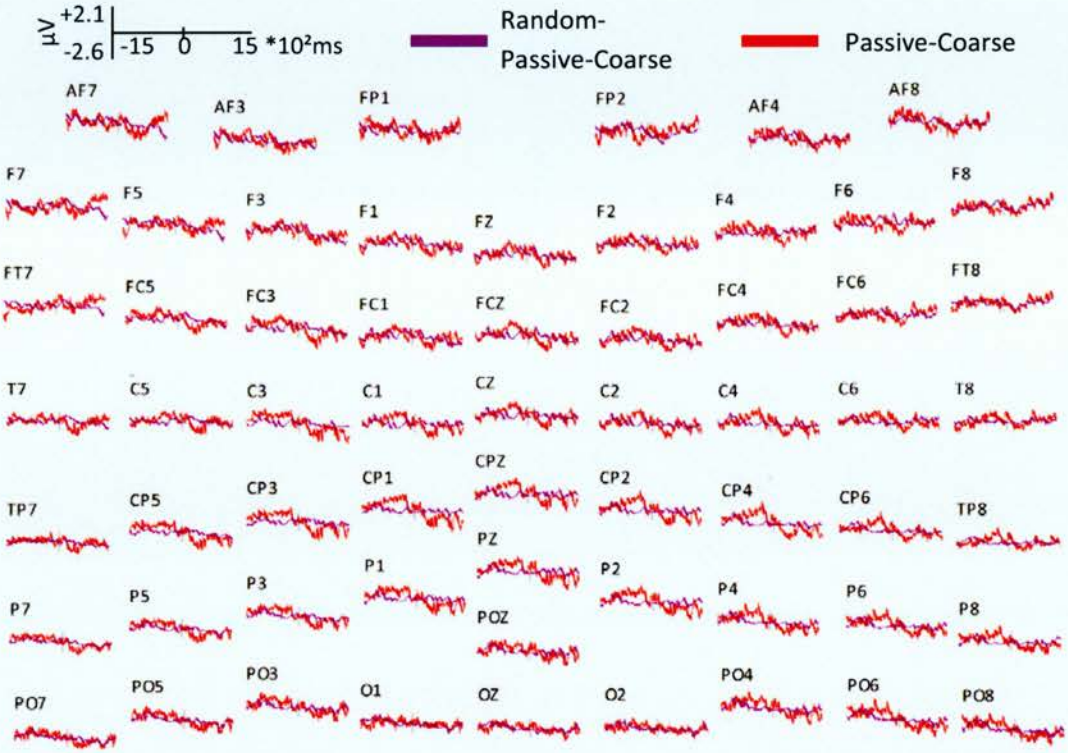

Random vs. Passive-Fine

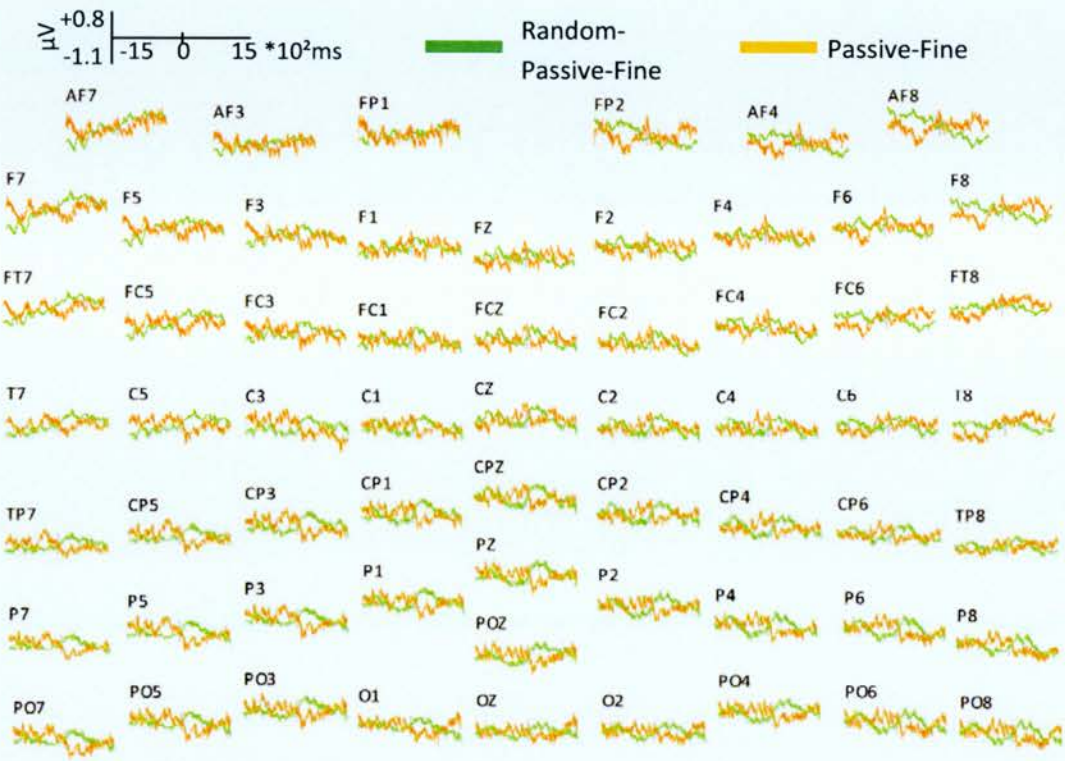

Starts vs. Ends

Inter-Experiment

Starts vs. Ends Passive-Coarse

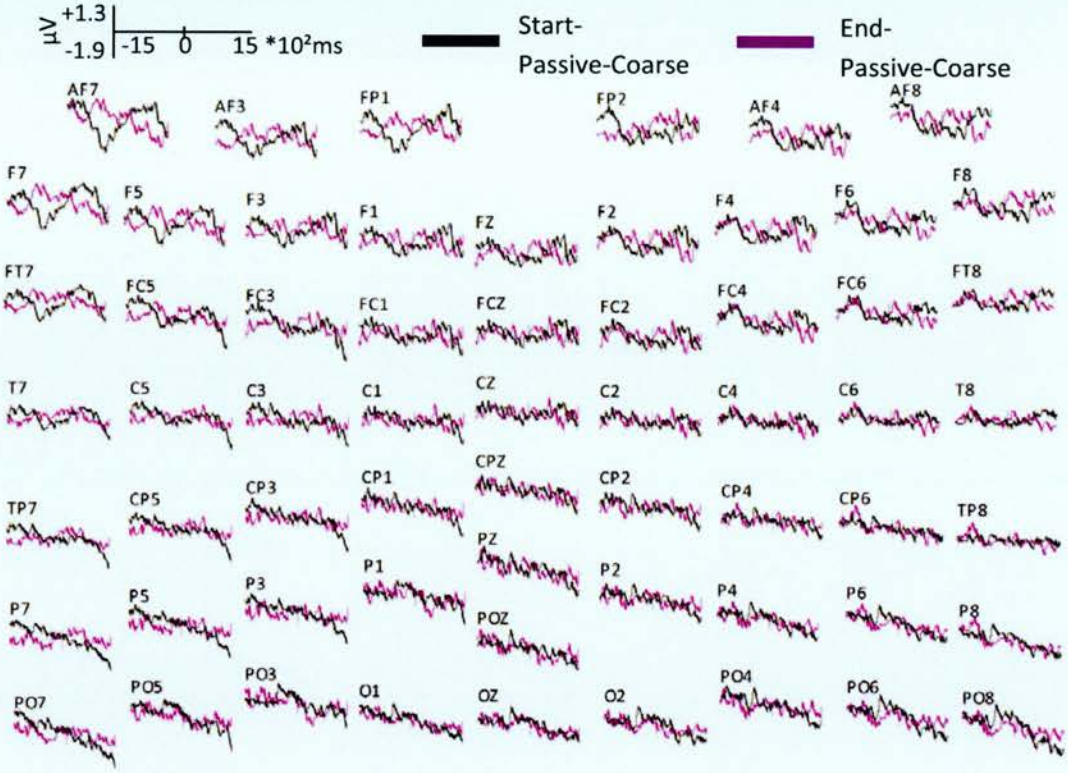

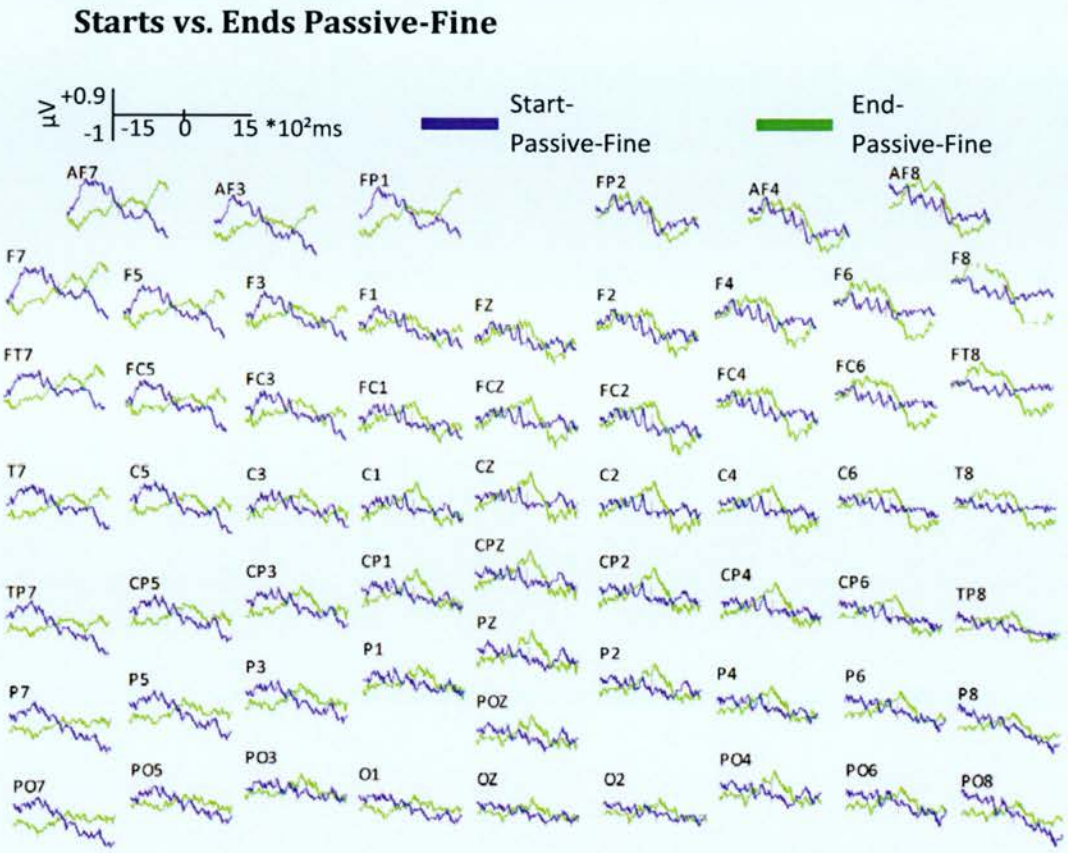
Starts vs. Ends Passive-Fine
μV
+0.9
-1
-15
0
15 *10²ms
Start-
Passive-Fine
End-
Passive-Fine
AF7
AF3
FP1
FP2
AF4
AF8
F7
F5
F3
F1
FZ
F2
F4
F6
F8
FT7
FC5
FC3
FC1
FCZ
FC2
FC4
FC6
FT8
T7
C5
C3
C1
CZ
C2
C4
C6
T8
TP7
CP5
CP3
CP1
CPZ
CP2
CP4
CP6
TP8
P7
P5
P3
P1
PZ
P2
P4
P6
P8
PO7
PO5
PO3
O1
POZ
OZ
O2
PO4
PO6
PO8

Coarse vs. Fine

Starts Passive-Coarse vs. Passive-Fine

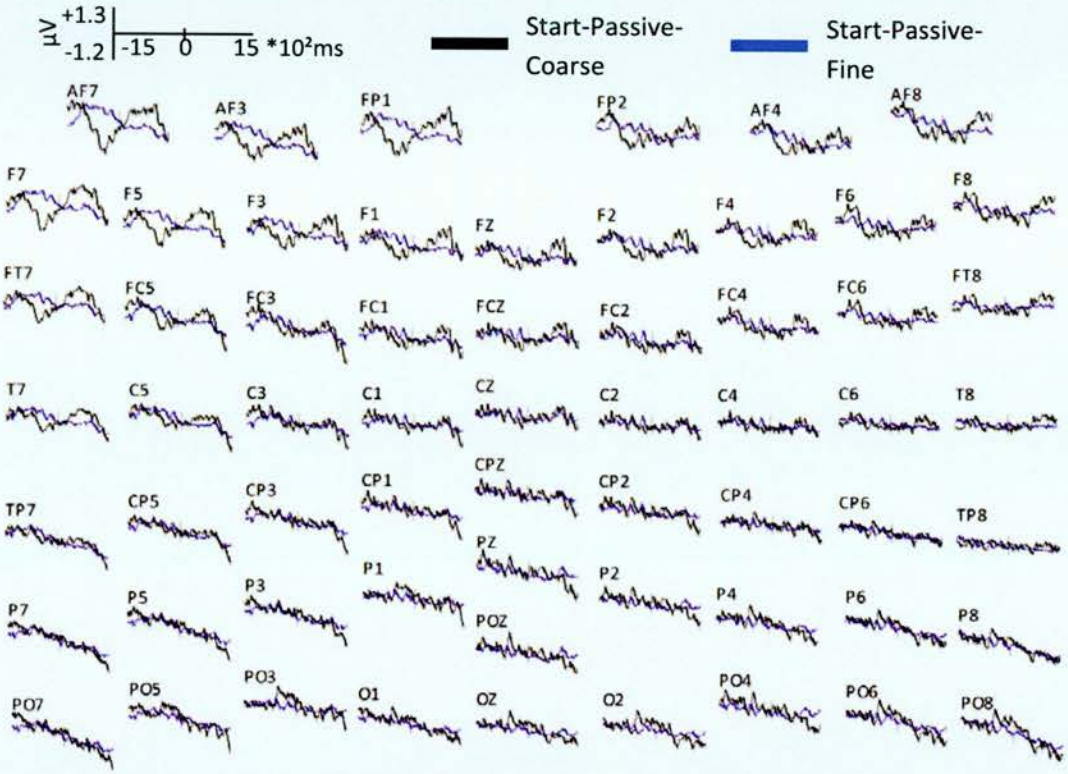

Ends Passive-Coarse vs. Passive-Fine

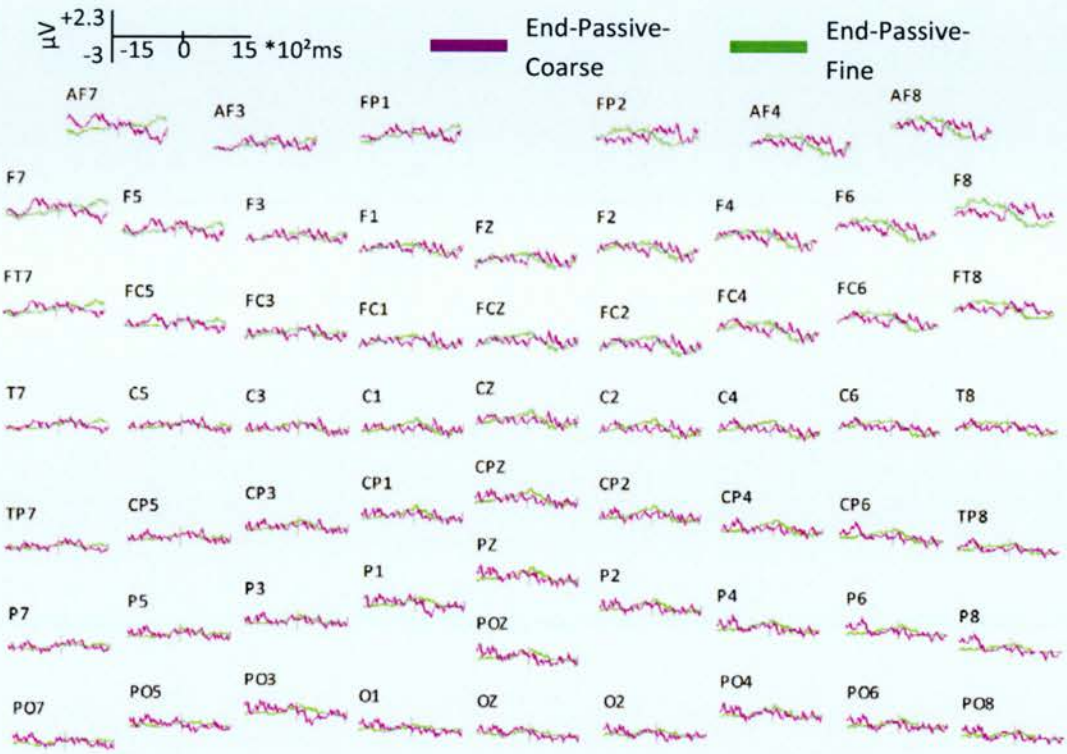

Cross-Experiment

Starts vs. Passive-Coarse

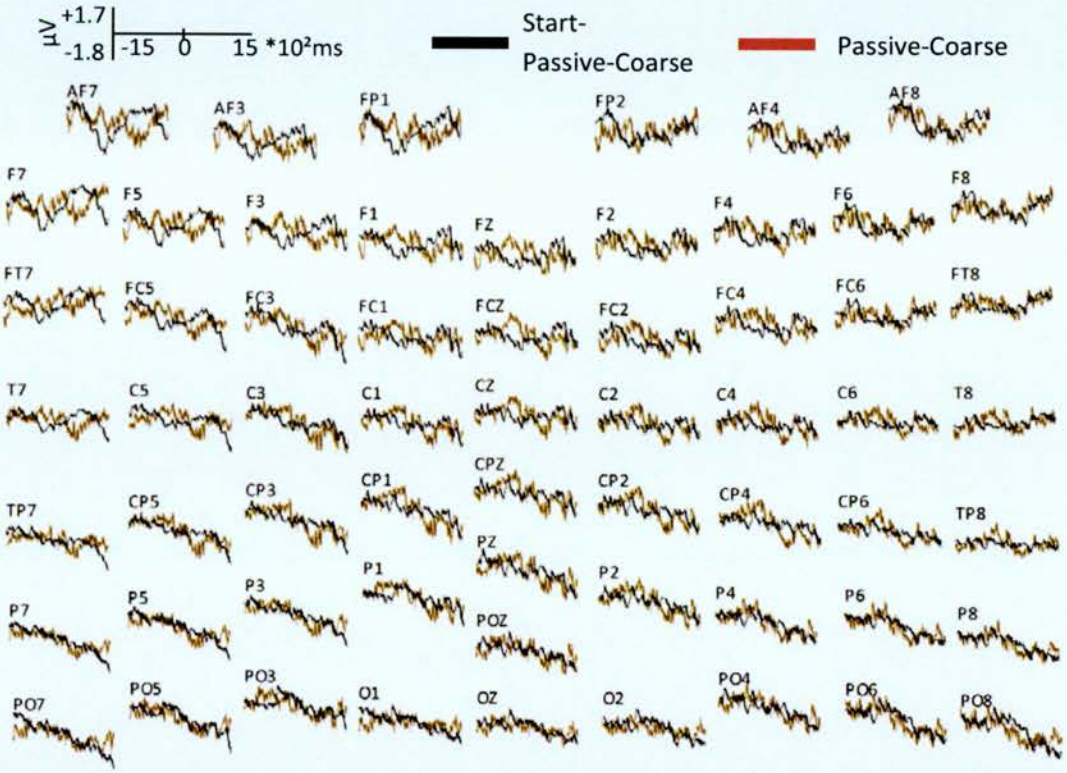

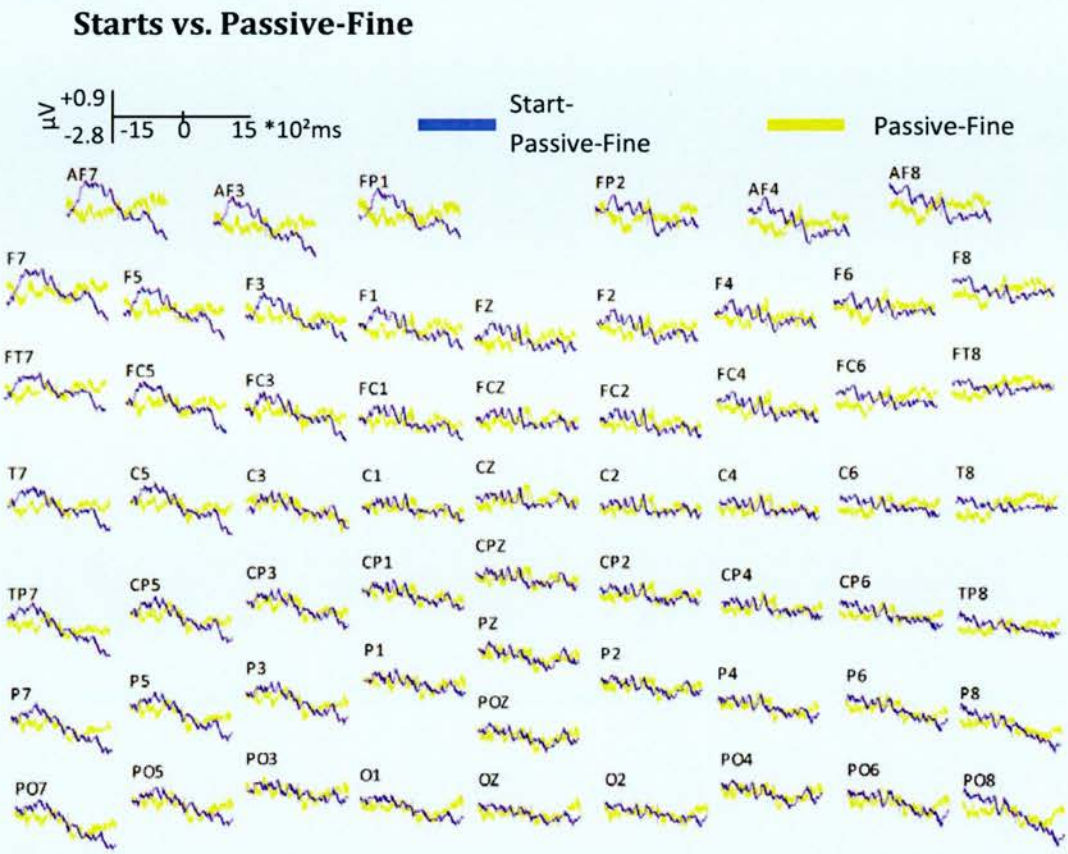
Starts vs. Passive-Fine
μV
+0.9
-2.8
-15
0
15 *10²ms
Start-Passive-Fine
Passive-Fine
AF7
AF3
FP1
FP2
AF4
AF8
F7
F5
F3
F1
FZ
F2
F4
F6
F8
FT7
FC5
FC3
FC1
FCZ
FC2
FC4
FC6
FT8
T7
C5
C3
C1
CZ
C2
C4
C6
T8
TP7
CP5
CP3
CP1
CPZ
CP2
CP4
CP6
TP8
P7
P5
P3
P1
PZ
P2
P4
P6
P8
PO7
PO5
PO3
O1
POZ
OZ
O2
PO4
PO6
PO8

Ends vs. Passive-Coarse

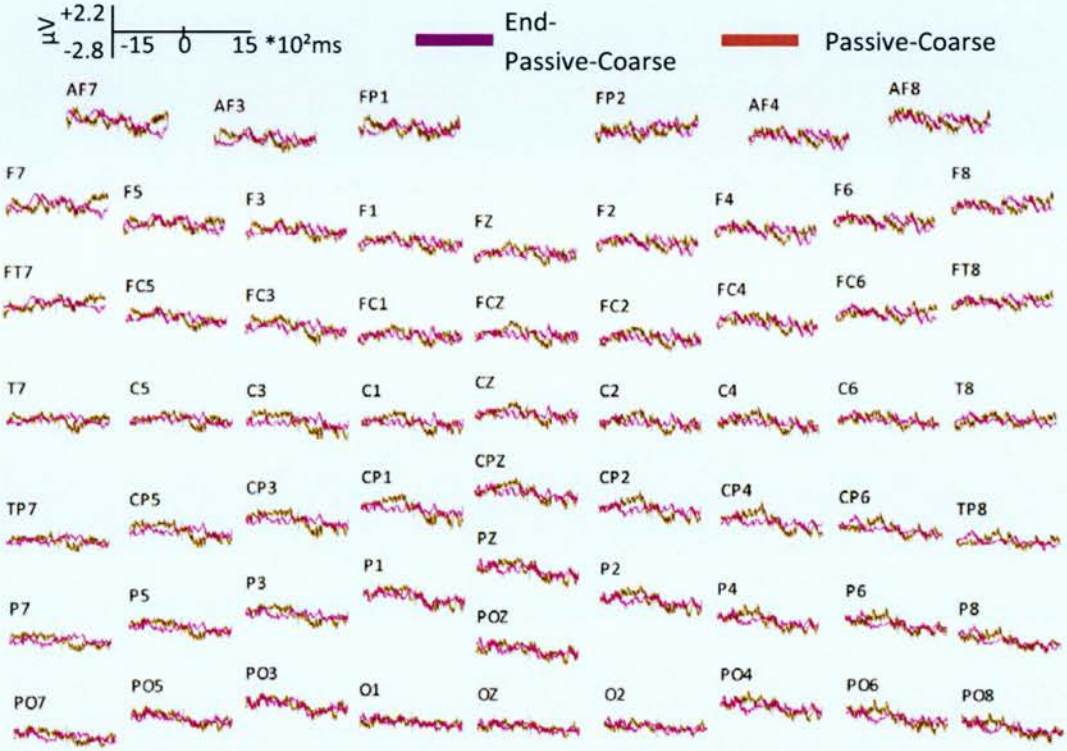

Appendix B: Grand Average ERPs

Ends vs. Passive-Fine

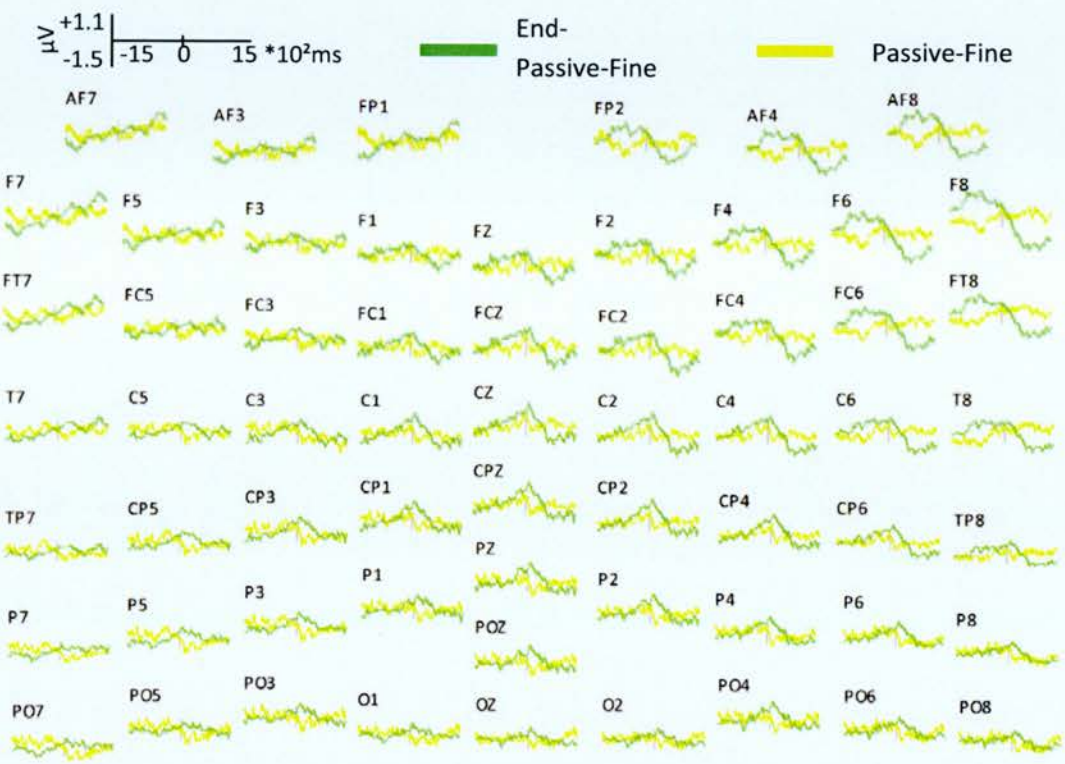

Appendix C: Coarse versus Fine Results

Comparing expert-passive-coarse and expert-passive-fine

Pre-breakpoint time window (-1050 to -950ms)

ANOVA Result	Interaction
[F(1, 15) = 10.97; p < 0.01]	condition*location

T-test pairing results

Left-Frontal Electrodes		Right-Frontal Electrodes	
F5	[t(15) = -2.106; p < 0.1 (0.052)]	F6	-
F3	-	F4	-
F1	-	F2	-
Left-Parietal Electrodes		**Right-Parietal Electrodes**	
P5	-	P6	-
P3	[t(15) = 1.985; p < 0.1 (0.066)]	P4	-
P1	[t(15) = 2.011; p < 0.1 (0.063)]	P2	[t(15) = 1.865; p < 0.1 (0.082)]

Post-breakpoint time window (300 to 500ms)

ANOVA Result	Interaction
[F(1, 15) = 4.636; p < 0.05]	condition
[F(1.560, 23.404) = 5.501; p < 0.05]	condition*site

T-test pairing results

Left-Frontal Electrodes		Right-Frontal Electrodes	
F5	-	F6	-
F3	-	F4	-
F1	-	F2	-
Left-Parietal Electrodes		**Right-Parietal Electrodes**	
P5	[t(15) = -2.917; p < 0.05]	P6	[t(15) = -1.922; p < 0.1 (0.074)]
P3	[t(15) = -2.933; p = 0.01]	P4	[t(15) = -2.044; p < 0.1 (0.059)]
P1	[t(15) = -3.462; p < 0.01]	P2	-

Topographic Analysis

ANOVA Result	**Interaction**
Pre- vs. Post-Segmentation	
[F(1.22, 17.01) = 5.696; p < 0.05]	condition. epoch and site
Pre-Segmentation	
[F(1.26, 17.69) = 4.212; p < 0.05]	condition and site
Post-Segmentation	
[F(1, 14) = 4.864; p < 0.05]	condition
[F(1.19, 16.65) = 4.451; p < 0.05]	condition and site

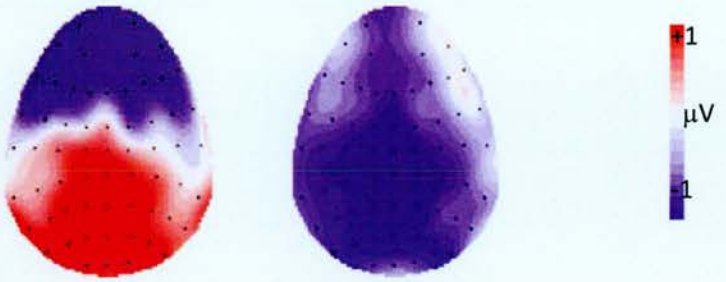

-1100 to -700ms 500 to 700ms

Topographic distributions for the pre- and post-segmentations.

Comparing naive-passive-coarse and naive-passive-fine

Pre-breakpoint time window (-1300 to -1100ms)

ANOVA Result	Interaction
[F(1, 15) = 3.865; p < 0.1 (0.068)]	condition*location

T-test pairing results

T-test pairing results for passive-coarse and random (-700 to -300ms)

Left-Frontal Electrodes		Right-Frontal Electrodes	
F5	-	F6	-
F3	-	F4	-
F1	-	F2	-
Left-Parietal Electrodes		**Right-Parietal Electrodes**	
P5	[t(15) = 1.862; p < 0.1 (0.082)]	P6	[t(15) = 2.157; p < 0.05]
P3	-	P4	[t(15) = 2.326; p < 0.05]
P1	[t(15) = 1.987; p < 0.1 (0.065)]	P2	[t(15) = 2.376; p < 0.05]

1.1.1 Post-breakpoint time window (600 to 800ms)

ANOVA Result	Interaction
[F(1, 15) = 8.852; p < 0.01]	condition

T-test pairing results

Left-Frontal Electrodes		Right-Frontal Electrodes	
F5	-	F6	[t(15) = 1.789; p < 0.1 (0.094)]
F3	[t(15) = 2.651; p < 0.05]	F4	[t(15) = 2.622; p < 0.05]
F1	[t(15) = 2.237; p < 0.05]	F2	[t(15) = 2.574; p < 0.05]
Left-Parietal Electrodes		**Right-Parietal Electrodes**	
P5	[t(15) = 2.819; p < 0.05]	P6	-
P3	[t(15) = 2.645; p < 0.05]	P4	-
P1	[t(15) = 2.148; p < 0.05]	P2	[t(15) = 1.783; p < 0.1 (0.095)]

Topographic Analysis

ANOVA Result	Interaction
Pre- vs. Post-Segmentation	
[F(1, 15) = 3.338; p < 0.1 (0.088)]	condition*epoch
[F(1.65, 24.78) = 3.482; p < 0.1 (0.054)]	condition*epoch*location*site
Pre-Segmentation	
[F(1.43, 21.43) = 3.074; p < 0.1 (0.081)]	condition*location*site
Post-Segmentation	
[F(1, 15) = 3.85; p < 0.1 (0.069)]	condition*location*hemisphere

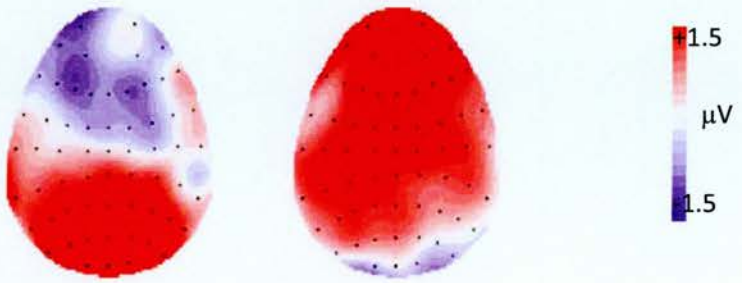

-1100 to -700ms 500 to 700ms

Topographic distributions for the pre- and post-segmentations.

Comparing game-passive-coarse and game-passive-fine

Pre-breakpoint time window (-1300 to -1200ms)

ANOVA Result	Interaction
[F(1, 15) = 6.902; p < 0.05]	condition

T-test pairing results

Left-Frontal Electrodes		Right-Frontal Electrodes	
F5	-	F6	[t(15) = 2.288; p < 0.05]
F3	[t(15) = 2.054; p < 0.1 (0.058)]	F4	[t(15) = 2.472; p < 0.05]
F1	[t(15) = 2.944; p = 0.01]	F2	[t(15) = 2.886; p < 0.05]
Left-Parietal Electrodes		**Right-Parietal Electrodes**	
P5	[t(15) = 2.043; p < 0.1 (0.059)]	P6	-
P3	[t(15) = 1.990; p < 0.1 (0.065)]	P4	-
P1	-	P2	-

1.1.2 Post-breakpoint time window (900 to 1000ms)

ANOVA Result	Interaction
[F(1, 15) = 6.884; p < 0.05]	condition*location
[F(1.277, 19.162) = 4.097; p < 0.05]	condition*location*site

T-test pairing results

Left-Frontal Electrodes		Right-Frontal Electrodes	
F5	[t(15) = -2.178; p < 0.05]	F6	[t(15) = -1.986; p < 0.1 (0.066)]
F3	[t(15) = -2.177; p < 0.05]	F4	-
F1	[t(15) = -2.894; p < 0.05]	F2	-
Left-Parietal Electrodes		**Right-Parietal Electrodes**	
P5	-	P6	-
P3	-	P4	-
P1	-	P2	-

Topographic Analysis

ANOVA Result	Interaction
Pre- vs. Post-Segmentation	
[F(1, 14) = 6.03; p < 0.05]	condition, epoch and location
[F(1.52, 21.3) = 7.152; p < 0.01]	condition, epoch, location and site
Pre-Segmentation	
[F(1, 14) = 4.357; p < 0.1 (0.056)]	condition and location
Post-Segmentation	
[F(1.37, 19.16) = 4.637; p < 0.05]	condition, location and site

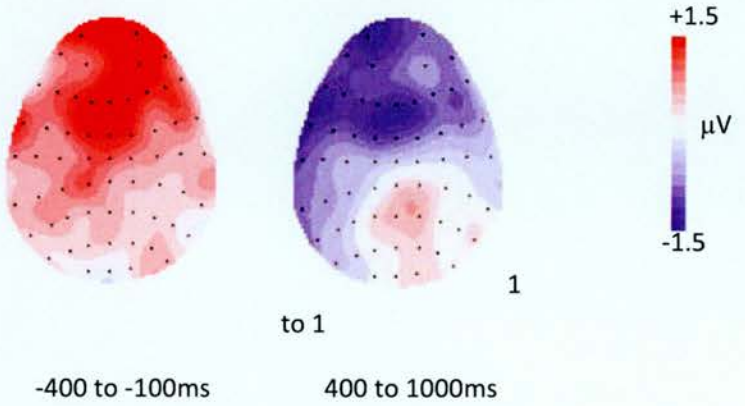

Topographic distributions for the pre- and post-segmentations.

Comparing random-passive-coarse and random-passive-fine

Pre-breakpoint time window (-12500 to -1150ms)

ANOVA Result	Interaction
[F(1, 15) = 5.439; p < 0.05]	condition*location*hemisphere
[F(1.488, 22.316) = 5.305; p < 0.05]	condition*location*hemisphere*site

T-test pairing results

Left-Frontal Electrodes		Right-Frontal Electrodes	
F5	[t(15) = 1.989; p < 0.1 (0.065)]	F6	-
F3	[t(15) = 1.771; p < 0.1 (0.097)]	F4	-
F1	-	F2	-
Left-Parietal Electrodes		**Right-Parietal Electrodes**	
P5	-	P6	[t(15) = 2.230; p < 0.05]
P3	-	P4	-
P1	-	P2	-

1.1.3 Post-breakpoint time window (800 to 900ms)

ANOVA Result	Interaction
[F(1, 15) = 5.060; p < 0.05]	condition*hemisphere
[F(1, 15) = 6.381; p < 0.05]	condition*location*hemisphere
[F(1.465, 21.976) = 4.236; p < 0.05]	condition*hemisphere*site

T-test pairing results

Left-Frontal Electrodes		Right-Frontal Electrodes	
F5	[t(15) = -2.200; p < 0.05]	F6	-
F3	[t(15) = -1.973; p < 0.1 (0.067)]	F4	-
F1	-	F2	-
Left-Parietal Electrodes		**Right-Parietal Electrodes**	
P5	-	P6	-
P3	-	P4	-
P1	-	P2	-

Topographic Analysis

ANOVA Result	Interaction
Pre- vs. Post-Segmentation	
[F(1, 14) = 10.838; p < 0.01]	condition, epoch, location and hemisphere
[F(1.67, 23.34) = 5.884; p < 0.05]	condition, epoch, location, hemisphere and site
Pre-Segmentation	
[F(1, 14) = 5.653; p < 0.05]	condition, location and hemisphere
[F(1.5, 20.95) = 4.754; p < 0.05]	condition, location, hemisphere and site
Post-Segmentation	
[F(1, 14) = 5.674; p < 0.05]	condition
[F(1, 14) = 5.763; p < 0.05]	condition and hemisphere
[F(1, 14) = 6.879; p < 0.05]	condition, location and hemisphere

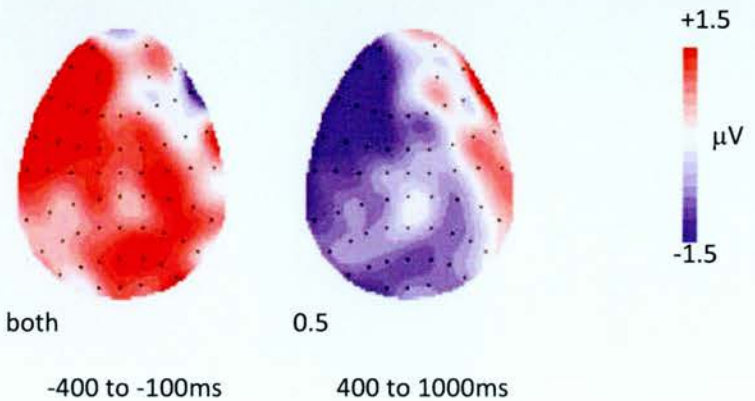

Topographic distributions for the pre- and post-segmentations.

Comparing start-passive-coarse and start-passive-passive fine

Pre-breakpoint time window (-525 to -425ms)

ANOVA Result	Interaction
[F(1, 23) = 9.270; p < 0.01]	condition*location
[F(1, 23) = 13.131; p < 0.005]	condition*hemisphere
[F(1.349, 31.038) = 5.535; p < 0.05]	condition*hemisphere*site

T-test pairing results

Left-Frontal Electrodes		Right-Frontal Electrodes	
F5	[t(23) = -2.060; p < 0.1 (0.051)]	F6	-
F3	-	F4	-
F1	-	F2	-
Left-Parietal Electrodes		**Right-Parietal Electrodes**	
P5	-	P6	[t(23) = 1.729; p < 0.1 (0.097)]
P3	-	P4	-
P1	-	P2	-

Post-breakpoint time window (650 to 750ms)

ANOVA Result	Interaction
[F(1, 23) = 5.147; p < 0.05]	condition*hemisphere
[F(1.180, 27.143) = 5.333; p < 0.05]	condition*hemisphere*site

Topographic Analysis

ANOVA Result	Interaction
Pre- vs. Post-Segmentation	
[F(1, 22) = 11.437; p < 0.01]	condition, epoch and hemisphere
[F(1.2, 26.39) = 5.786; p < 0.05]	condition, epoch, hemisphere and site
Pre-Segmentation	
[F(1, 22) = 7.615; p < 0.05]	condition and location
[F(1, 22) = 18.16; p < 0.001]	condition and hemisphere
[F(1.26, 27.64) = 7.415; p < 0.01]	condition, hemisphere and site
Post-Segmentation	
[F(1, 22) = 4.37; p < 0.05]	condition and hemisphere

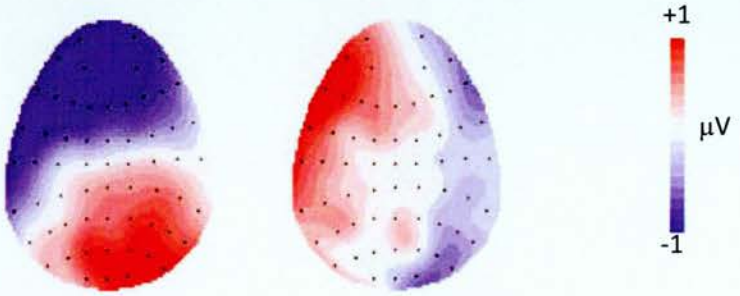

-400 to -100ms 400 to 1000ms

Topographic distributions for the pre- and post-segmentations.

Comparing end-passive-coarse and end-passive-passive-fine

Pre-breakpoint time window (-200 to 0ms)

ANOVA Result	Interaction
[F(1, 23) = 8.850; p < 0.01]	condition*hemisphere

T-test pairing results

Left-Frontal Electrodes		Right-Frontal Electrodes	
F5	-	F6	[t(23) = -2.760; p < 0.05]
F3	-	F4	[t(23) = -2.427; p < 0.05]
F1	-	F2	[t(23) = -2.125; p < 0.05]
Left-Parietal Electrodes		**Right-Parietal Electrodes**	
P5	-	P6	-
P3	-	P4	-
P1	-	P2	-

1.1.4 Post-breakpoint time window (1100 to 1400ms)

ANOVA Result	Interaction
[F(1.201, 27.616) = 4.812; p < 0.05]	condition*hemisphere*site
[F(1.237, 28.462) = 4.064; p < 0.05]	condition*location*hemisphere*site

T-test pairing results

Left-Frontal Electrodes		Right-Frontal Electrodes	
F5	[t(23) = -2.658; p < 0.05]	F6	-
F3	-	F4	-
F1	-	F2	-
Left-Parietal Electrodes		**Right-Parietal Electrodes**	
P5	-	P6	-
P3	-	P4	-
P1	-	P2	-

Topographic Analysis

ANOVA Result	Interaction
Pre- vs. Post-Segmentation	
[F(1, 23) = 4.549; p < 0.05]	condition*epoch*hemisphere
[F(1.21, 27.84) = 4.439; p < 0.05]	condition*epoch*hemisphere*site
[F(1.23, 28.21) = 4.609; p < 0.05]	condition*epoch*location*hemisphere *site
Pre-Segmentation	
[F(1, 23) = 7.928; p < 0.05]	condition*hemisphere
Post-Segmentation	
[F(1.19, 27.38) = 4.143; p < 0.05]	condition*hemisphere*site

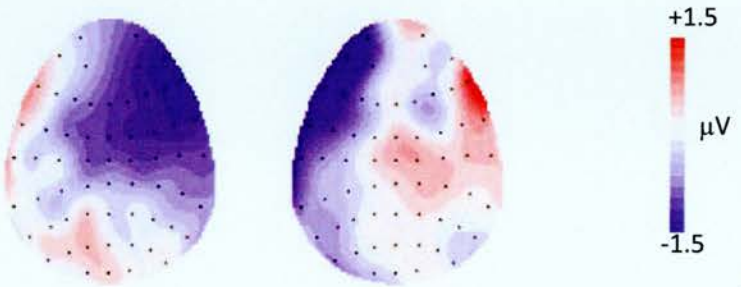

-400 to -100ms 400 to 1000ms

Topographic distributions for the pre- and post-segmentations.

Appendix D: Cross-experiment Results

Comparing passive-coarse and directed-passive-coarse-grain segmentation

Pre-segmentation time window (none)
Post-segmentation time window (300 to 500ms)

ANOVA Result	Interaction
[F(1.46, 61.23) = 4.67; p < 0.05]	condition*hemisphere*site

T-test pairing results

Left-Frontal Electrodes		Right-Frontal Electrodes	
F5	-	F6	[t(42) = 2.84; p < 0.01]
F3	-	F4	[t(42) = 1.89; p < 0.1 (0.066)]
F1	-	F2	-

Left-Parietal Electrodes		Right-Parietal Electrodes	
P5	-	P6	-
P3	-	P4	-
P1	-	P2	-

Topographic analysis

ANOVA Result	Interaction
Post-Segmentation	
[F(1.39, 58.32) = 3.24; p < 0.1 (0.063)]	condition*hemisphere and site

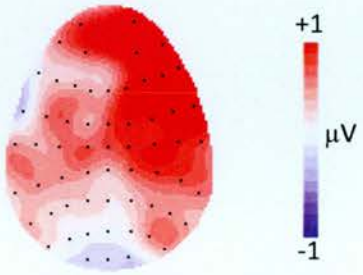

300 to 500ms

Topographic distributions for post-segmentation.

Comparing passive-fine and directed-passive-fine-grain segmentation

Pre-segmentation time window (-1100 to -1000ms)

ANOVA Result	Interaction
[F(1, 42) = 6.48; p < 0.05]	condition*location*hemisphere

T-test pairing results

Left-Frontal Electrodes		Right-Frontal Electrodes	
F5	[t(42) = 1.81; p < 0.1 (0.077)]	F6	-
F3	[t(42) = 2.2; p < 0.05]	F4	-
F1	[t(42) = 1.91; p < 0.1 (0.063)]	F2	-

Left-Parietal Electrodes		Right-Parietal Electrodes	
P5	[t(42) = 1.9; p < 0.1 (0.065)]	P6	[t(42) = 2.68; p < 0.05]
P3	[t(42) = 2.17; p < 0.05]	P4	[t(42) = 2.42; p < 0.05]
P1	[t(42) = 1.99; p < 0.1 (0.053)]	P2	[t(42) = 2.08; p < 0.05]

Post-segmentation time window (500 to 700ms)

ANOVA Result	Interaction
[F(1, 42) = 8.83; p < 0.01]	condition* location and hemisphere

T-test pairing results

Left-Frontal Electrodes		Right-Frontal Electrodes	
F5	-	F6	-
F3	[t(42) = -1.74; p < 0.1 (0.09)]	F4	-
F1	[t(42) = -1.73; p < 0.1 (0.09)]	F2	-

Left-Parietal Electrodes		Right-Parietal Electrodes	
P5	[t(42) = -1.87; p < 0.1 (0.068)]	P6	[t(42) = -2.46; p < 0.05]
P3	[t(42) = -2.09; p < 0.05]	P4	[t(42) = -2.57; p < 0.05]
P1	[t(42) = -2.3; p < 0.05]	P2	[t(42) = -2.66; p < 0.05]

Topographic analysis

ANOVA Result	Interaction
Pre- vs. Post-Segmentation	
[F(1, 42) = 5.92; p < 0.05]	condition*epoch, location and hemisphere
Pre-Segmentation	
-	-
Post-Segmentation	

[F(1, 42) = 5.45; p < 0.05]	condition*location and hemisphere

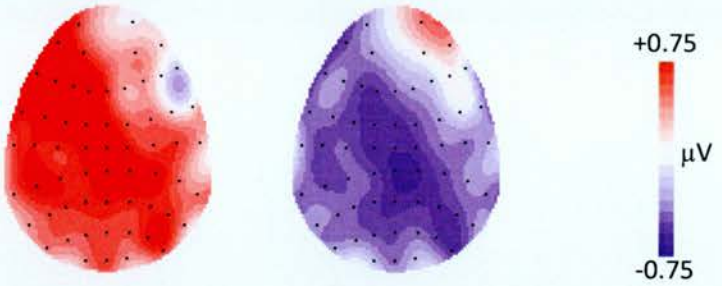

-1100 to -1000ms 500 to 700ms

Topographic distributions for the pre- and post-segmentations.

Comparing expert-passive-coarse and passive-coarse

Pre-segmentation time window (-400 to -300ms)

ANOVA Result	Interaction
[F(1, 38) = 5.24; p < 0.05]	condition*location

T-test pairing results

Left-Frontal Electrodes		Right-Frontal Electrodes	
F5	[t(38) = 2.13; p < 0.05]	F6	-
F3	[t(38) = 1.77; p < 0.1 (0.084)]	F4	-
F1	-	F2	-
Left-Parietal Electrodes		**Right-Parietal Electrodes**	
P5	-	P6	-
P3	-	P4	-
P1	-	P2	-

Post-segmentation time window (none)
Topographic analysis

ANOVA Result	Interaction
Pre-Segmentation	
[F(1, 38) = 5.23; p < 0.05]	condition*location

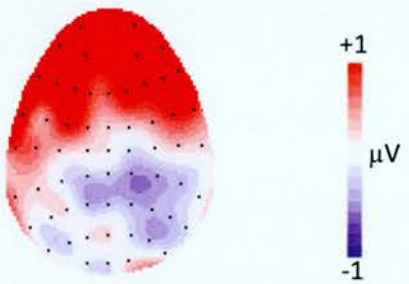

-400 to -300ms

Topographic distributions for the post-segmentation.

Comparing expert-passive-fine and passive-fine

Pre-segmentation time window (-600 to -500ms)

ANOVA Result	Interaction
[F(1, 38) = 4.32; p < 0.05]	condition*location
[F(1.75, 66.5) = 3.28; p = 0.05]	condition*location*site
[F(1.55, 58.73) = 5.66; p < 0.05]	condition*hemisphere*location*site

T-test pairing results

Left-Frontal Electrodes		Right-Frontal Electrodes	
F5	-	F6	-
F3	-	F4	-
F1	-	F2	-
Left-Parietal Electrodes		**Right-Parietal Electrodes**	
P5	-	P6	[t(38) = -2.11; p < 0.05]
P3	-	P4	[t(38) = -1.92; p < 0.1 (0.062)]
P1	-	P2	-

Post-segmentation time window (200 to 300ms)

ANOVA Result	**Interaction**
[F(1, 38) = 5.14; p < 0.05]	condition and location

T-test pairing results

Left-Frontal Electrodes		Right-Frontal Electrodes	
F5	-	F6	-
F3	-	F4	-
F1	-	F2	-
Left-Parietal Electrodes		**Right-Parietal Electrodes**	
P5	[t(38) = 2.49; p < 0.05]	P6	-
P3	[t(38) = 2.15; p < 0.05]	P4	[t(38) = 1.76; p < 0.1 (0.086)]
P1	[t(38) = 2.02; p = 0.05]	P2	[t(38) = 1.97; p < 0.1 (0.057)]

Topographic analysis

ANOVA Result	Interaction
Pre- vs. Post-Segmentation	
[F(1, 38) = 8.03; p < 0.01]	condition*epoch and location
[F(1.49, 56.62) = 4.48; p < 0.05]	condition*epoch and site
[F(1, 38) = 5.46; p < 0.05]	condition*epoch, location and hemisphere
[F(1.69, 64.14) = 5.47; p < 0.01]	condition*epoch, hemisphere, location and site
Pre-Segmentation	
[F(1.53, 58.31) = 5.51; p < 0.05]	condition*location, hemisphere and site
Post-Segmentation	
[F(1, 38) = 5.57; p < 0.05]	condition*location

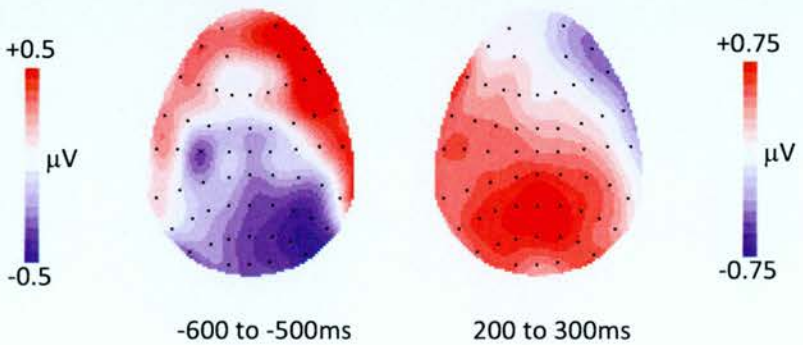

Topographic distributions for the pre- and post-segmentations.

Comparing naive-passive-coarse and passive-coarse

Pre-segmentation time window (-400 to -300ms)

ANOVA Result	Interaction
[F(1, 38) = 4.78; p < 0.05]	condition and location
[F(1, 38) = 3.57; p < 0.1 (0.067)]	condition, hemisphere and location

T-test pairing results

Left-Frontal Electrodes		Right-Frontal Electrodes	
F5	-	F6	-
F3	-	F4	-
F1	-	F2	-
Left-Parietal Electrodes		**Right-Parietal Electrodes**	
P5	[t(38) = -1.75; p < 0.1 (0.088)]	P6	[t(38) = -1.78; p < 0.1 (0.082)]
P3	[t(38) = -1.87; p < 0.1 (0.069)]	P4	[t(38) = -2; p < 0.1 (0.053)]
P1	[t(38) = -2.04; p < 0.05]	P2	[t(38) = -2.47; p < 0.05]

Post-segmentation time window (1200 to 1300ms)

ANOVA Result	Interaction
[F(1, 38) = 5.91; p < 0.05]	condition and hemisphere

T-test pairing results

Left-Frontal Electrodes		Right-Frontal Electrodes	
F5	-	F6	-
F3	-	F4	-
F1	-	F2	-
Left-Parietal Electrodes		**Right-Parietal Electrodes**	
P5	[t(38) = -1.85; p < 0.1 (0.073)]	P6	[t(38) = -2.26; p < 0.05]
P3	[t(38) = -1.84; p < 0.1 (0.073)]	P4	[t(38) = -2.75; p < 0.01]
P1	[t(38) = -1.84; p < 0.1 (0.074)]	P2	[t(38) = -2.12; p < 0.05]

Topographic analysis

ANOVA Result	Interaction
Pre- vs. Post-Segmentation	
-	-
Pre-Segmentation	
[F(1.37, 49.18) = 2.85; p < 0.1 (0.86)]	condition*site
Post-Segmentation	
[F(1, 36) = 2.87; p < 0.1 (0.99	condition*hemisphere

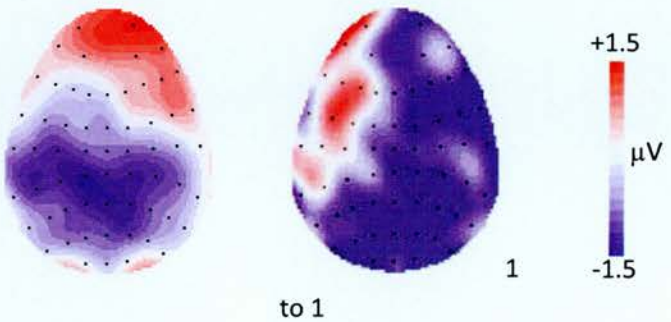

Topographic distributions for the pre- and post-segmentations.

Comparing naive-passive-fine and passive-fine

Pre-segmentation time window (-500 to -400ms)

ANOVA Result	Interaction
[F(1, 38) = 2.96; p < 0.1 (0.094)]	condition and hemisphere

T-test pairing results

Left-Frontal Electrodes		Right-Frontal Electrodes	
F5	-	F6	-
F3	-	F4	-
F1	-	F2	-
Left-Parietal Electrodes		**Right-Parietal Electrodes**	
P5	-	P6	[t(38) = 2.3; p < 0.05]
P3	-	P4	[t(38) = 2.3; p < 0.05]
P1	-	P2	[t(38) = 2.07; p < 0.05]

Post-segmentation time window (500 to 700ms)

ANOVA Result	Interaction
[F(1, 38) = 5.52; p < 0.05]	condition and hemisphere
[F(1.34, 50.72) = 4.03; p < 0.05]	condition, hemisphere and site

T-test pairing results

Left-Frontal Electrodes		Right-Frontal Electrodes	
F5	-	F6	[t(38) = -2.33; p < 0.05]
F3	-	F4	[t(38) = -2.14; p < 0.05]
F1	[t(38) = -1.78; p < 0.1 (0.083)]	F2	[t(38) = -1.86; p < 0.1 (0.071)]
Left-Parietal Electrodes		**Right-Parietal Electrodes**	
P5	-	P6	-
P3	-	P4	-
P1	-	P2	-

Topographic analysis

ANOVA Result	**Interaction**
Pre- vs. Post-Segmentation	
[F(1, 38) = 4.72; p < 0.05]	condition*epoch and hemisphere
Pre-Segmentation	
-	-
Post-Segmentation	
-	-

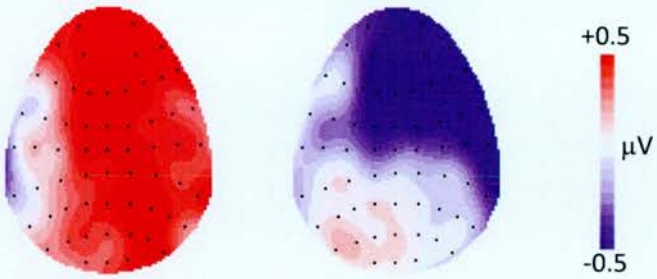

-500 to -400ms 500 to 700ms

Topographic distributions for the pre- and post-segmentations.

Comparing game-passive-coarse and passive-coarse

Pre-segmentation time window (-700 to -500ms)

ANOVA Result	Interaction
[F(1.54, 58.36) = 4.45; p < 0.05]	condition and site

T-test pairing results

Left-Frontal Electrodes		Right-Frontal Electrodes	
F5	-	F6	-
F3	-	F4	-
F1	-	F2	-
Left-Parietal Electrodes		**Right-Parietal Electrodes**	
P5	[t(38) = -2.2; p < 0.05]	P6	[t(38) = -2.42; p < 0.05]
P3	[t(38) = -2.38; p < 0.05]	P4	[t(38) = -2.65; p < 0.05]
P1	[t(38) = -2.68; p < 0.05]	P2	[t(38) = -2.78; p < 0.01]

Post-segmentation time window (1075 to 1175ms)

ANOVA Result	Interaction
[F(1, 38) = 4.57; p < 0.05]	condition and location

T-test pairing results)

Left-Frontal Electrodes		Right-Frontal Electrodes	
F5	-	F6	-
F3	-	F4	-
F1	-	F2	-
Left-Parietal Electrodes		**Right-Parietal Electrodes**	
P5		P6	-
P3	[t(38) = 1.72; p < 0.1 (0.094)]	P4	[t(38) = 1.86; p < 0.1 (0.07)]
P1	[t(38) = 2.1; p < 0.05]	P2	[t(38) = 2.15; p < 0.05]

Topographic analysis

ANOVA Result	Interaction
Pre- vs. Post-Segmentation	
[F(1.4, 50.55) = 3.79; p < 0.05]	condition, epoch and site
Pre-Segmentation	
[F(1.52, 54.77) = 3.91; p < 0.05]	condition*site
Post-Segmentation	
[F(1, 36) = 4.26; p < 0.05]	condition*location

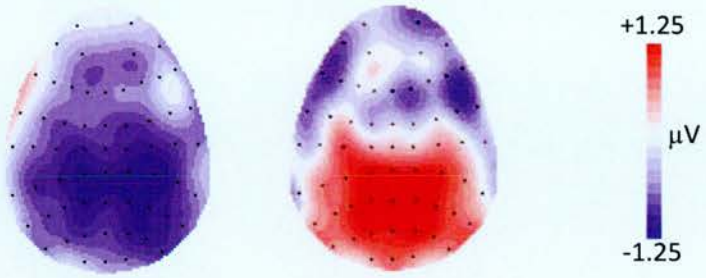

-700 to -500ms 1075 to 1175ms

Topographic distributions for the pre- and post-segmentations.

Comparing game-passive-fine and passive-fine

Pre-segmentation time window (-550 to -450ms)

ANOVA Result	Interaction
[F(1, 38) = 4.91; p < 0.05]	condition and location

T-test pairing results

Left-Frontal Electrodes		Right-Frontal Electrodes	
F5	-	F6	-
F3	-	F4	-
F1	-	F2	-
Left-Parietal Electrodes		**Right-Parietal Electrodes**	
P5	[t(38) = -2.77; p < 0.01]	P6	[t(38) = -2.22; p < 0.05]
P3	[t(38) = -2.36; p < 0.05]	P4	[t(38) = -2.14; p < 0.05]
P1	[t(38) = -2.06; p < 0.05]	P2	[t(38) = -1.87; p < 0.1 (0.069)]

Post-segmentation time window (100 to 300ms)

ANOVA Result	Interaction
-	-

T-test pairing results

Left-Frontal Electrodes		Right-Frontal Electrodes	
F5	[t(38) = 1.77; p < 0.1 (0.085)]	F6	-
F3	[t(38) = 2.53; p < 0.05]	F4	-
F1	[t(38) = 1.8; p < 0.1 (0.079)]	F2	-
Left-Parietal Electrodes		**Right-Parietal Electrodes**	
P5	[t(38) = 2.95; p < 0.01]	P6	[t(38) = 1.91; p < 0.1 (0.064)]
P3	[t(38) = 2.55; p < 0.05]	P4	[t(38) = 1.97; p < 0.1 (0.056)]
P1	[t(38) = 2.32; p < 0.05]	P2	[t(38) = 2.05; p < 0.05]

Topographic analysis

ANOVA Result	Interaction
Pre- vs. Post-Segmentation	
-	-
Pre-Segmentation	
-	-
Post-Segmentation	
-	-

Comparing random-passive-coarse and passive-coarse

Pre-segmentation time window (-500 to -200ms)

T-test pairing results

Left-Frontal Electrodes		Right-Frontal Electrodes	
F5	-	F6	-
F3	-	F4	-
F1	-	F2	-
Left-Parietal Electrodes		**Right-Parietal Electrodes**	
P5	-	P6	[t(38) = -2.59; p < 0.05]
P3	-	P4	[t(38) = -2.33; p < 0.05]
P1	[t(38) = -1.92; p < 0.1 (0.062)]	P2	[t(38) = -2.59; p < 0.05]

Post-segmentation time window (1400 to 1500ms)

ANOVA Result	**Interaction**
[F(1, 38) = 4.69; p < 0.05]	condition*hemisphere

Topographic analysis

ANOVA Result	**Interaction**
Pre- vs. Post-Segmentation	
[F(1, 36) = 4.97; p < 0.05]	condition* epoch and hemisphere
Pre-Segmentation	
[F(1, 36) = 4.26; p < 0.05]	condition*location
Post-Segmentation	
[F(1, 36) = 6.26; p < 0.05]	hemisphere

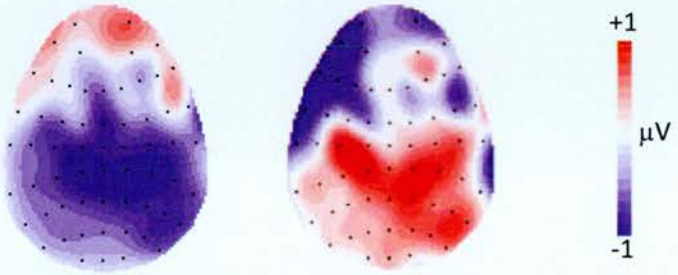

-500 to -200ms 1400 to 1500ms

Topographic distributions for the pre- and post-segmentations.

Comparing random-passive-fine and passive-fine

Pre-segmentation time window (-500 to -300ms)

ANOVA Result	Interaction
[F(1, 38) = 8.26; p < 0.01]	condition*location

T-test pairing results

Left-Frontal Electrodes		Right-Frontal Electrodes	
F5	-	F6	-
F3	-	F4	-
F1	-	F2	-
Left-Parietal Electrodes		**Right-Parietal Electrodes**	
P5	[t(38) = -4.49; p < 0.001]	P6	[t(38) = -3.1; p < 0.01]
P3	[t(38) = -3.74; p < 0.005]	P4	[t(38) = -2.97; p < 0.01]
P1	[t(38) = -2.85; p < 0.01]	P2	[t(38) = -2.45; p < 0.05]

Post-segmentation time window (200 to 600ms)

ANOVA Result	Interaction
[F(1, 38) = 4.8; p < 0.05]	condition*location

T-test pairing results

Left-Frontal Electrodes		Right-Frontal Electrodes	
F5	-	F6	-
F3	-	F4	-
F1	-	F2	-
Left-Parietal Electrodes		**Right-Parietal Electrodes**	
P5	[t(38) = 3.65; p = 0.001]	P6	[t(38) = 2.98; p < 0.01]
P3	[t(38) = 3.06; p < 0.01]	P4	[t(38) = 2.79; p < 0.01]
P1	[t(38) = 2.75; p < 0.01]	P2	[t(38) = 2.6; p < 0.05]

Topographic analysis

ANOVA Result	Interaction
Pre- vs. Post-Segmentation	
[F(1, 38) = 6.14; p < 0.05]	condition* epoch
[F(1, 38) = 12; p < 0.005]	condition*epoch and location
Pre-Segmentation	
[F(1, 38) = 15.83; p < 0.01]	condition*location
Post-Segmentation	
[F(1, 38) = 4.86; p < 0.05]	condition*location

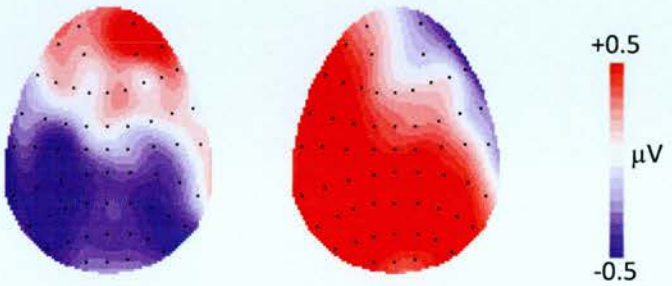

Topographic distributions for the pre- and post-segmentations.

Comparing start- and breakpoint-passive-coarse

Pre-segmentation time window (-550 to -450ms)

ANOVA Result	Interaction
[F(1, 23) = 6.61; p < 0.05]	condition*location

Post-segmentation time window (650 to 750ms)

ANOVA Result	Interaction
[F(1, 23) = 5.457; p < 0.05]	condition and hemisphere
[F(1.312, 30.170) = 4.62; p < 0.05]	condition, hemisphere and site

Topographic analysis

ANOVA Result	Interaction
Pre- vs. Post-Segmentation	
-	-
Pre-Segmentation	
[F(1, 23) = 6.21; p < 0.05]	condition*location
Post-Segmentation	
[F(1, 23) = 8.27; p < 0.01]	condition*hemisphere
[F(1.39, 30.67) = 6.39; p < 0.05]	condition*hemisphere and site

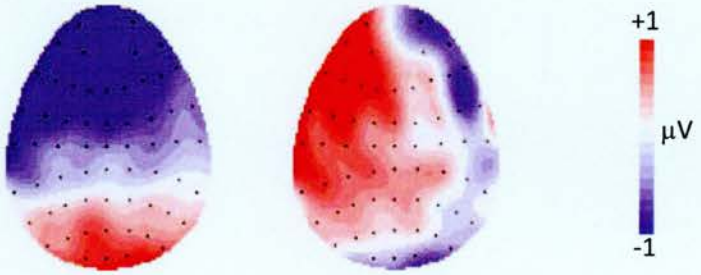

-550 to -450ms 650 to 750ms

Topographic distributions for the pre- and post-segmentations.

Comparing start- and breakpoint-passive-fine

Pre-segmentation time window (-600 to -500ms)

ANOVA Result	Interaction
[F(1, 23) = 4.73; p < 0.05]	condition

T-test pairing results

Left-Frontal Electrodes		Right-Frontal Electrodes	
F5	[t(23) = 2.76; p < 0.05]	F6	[t(23) = 2.15; p < 0.05]
F3	[t(23) = 1.97; p < 0.1 (0.06)]	F4	[t(23) = 1.75; p < 0.1 (0.093)]
F1	[t(23) = 2.05; p < 0.1 (0.052)]	F2	[t(23) = 1.98; p < 0.1 (0.06)]
Left-Parietal Electrodes		**Right-Parietal Electrodes**	
P5	[t(23) = 2.34; p < 0.05]	P6	-
P3	[t(23) = 2.07; p = 0.05]	P4	-
P1	-	P2	-

Post-segmentation time window (1300 to 1500ms)

ANOVA Result	Interaction
[F(1, 23) = 4.45; p < 0.05]	condition*hemisphere

T-test pairing results

Left-Frontal Electrodes		Right-Frontal Electrodes	
F5	[t(23) = -2; p < 0.1 (0.058)]	F6	-
F3	-	F4	-
F1	-	F2	-
Left-Parietal Electrodes		**Right-Parietal Electrodes**	
P5	[t(23) = -2.75; p < 0.05]	P6	-
P3	[t(23) = -2.44; p < 0.05]	P4	-
P1	-	P2	-

Topographic analysis

ANOVA Result	Interaction
Pre- vs. Post-Segmentation	
-	-
Pre-Segmentation	
[F(1, 23) = 5.08; p < 0.05]	condition*location
Post-Segmentation	
[F(1.87, 41.05) = 3.5; p < 0.05]	condition*hemisphere and site

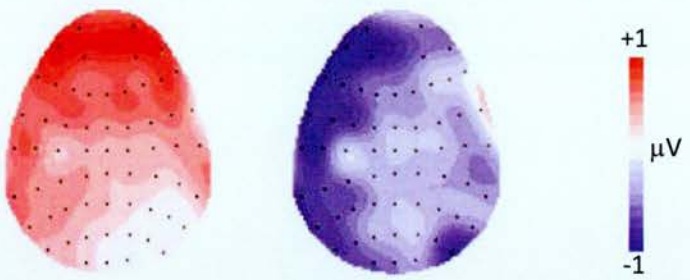

-600 to -500ms 1300 to 1500ms

Topographic distributions for the pre- and post-segmentations.

Comparing end- and breakpoint-passive-coarse

Pre-segmentation time window (-700 to -600ms)

ANOVA Result	Interaction
[F(1.76, 40.43) = 3.9; p < 0.05]	condition, location, hemisphere and site

T-test pairing results

Left-Frontal Electrodes		Right-Frontal Electrodes	
F5	-	F6	-
F3	-	F4	-
F1	-	F2	-
Left-Parietal Electrodes		**Right-Parietal Electrodes**	
P5	[t(23) = -1.84; p < 0.1 (0.079)]	P6	[t(23) = -2.12; p < 0.05]
P3	[t(23) = -1.89; p < 0.1 (0.072)]	P4	[t(23) = -2.31; p < 0.05]
P1	-	P2	[t(23) = -2.07; p = 0.05]

Post-segmentation time window (500 to 700ms)

ANOVA Result	Interaction
[F(1.53, 35.12) = 2.7; p < 0.1 (0.094)]	condition, location and site

T-test pairing results

Left-Frontal Electrodes		Right-Frontal Electrodes	
F5	-	F6	-
F3	-	F4	-
F1	-	F2	-
Left-Parietal Electrodes		**Right-Parietal Electrodes**	
P5	[t(23) = 3.62; p = 0.001]	P6	-
P3	[t(23) = 2.89; p < 0.01]	P4	-
P1	-	P2	-

Topographic analysis

ANOVA Result	**Interaction**
Pre- vs. Post-Segmentation	
-	-
Pre-Segmentation	
[F(1.71, 37.63) = 4.4; p < 0.05]	condition*location, hemisphere and site
Post-Segmentation	
-	-

-700 to -600ms 500 to 700ms

Topographic distributions for the pre- and post-segmentations.

Comparing end- and breakpoint-passive-fine

Pre-segmentation time window (-1000 to -100ms)

ANOVA Result	Interaction
[F(1, 23) = 11.87; p < 0.01]	condition and location
[F(1, 23) = 20.98; p < 0.001]	condition and hemisphere
[F(1, 23) = 11.81; p < 0.01]	condition, location and hemisphere
[F(1.27, 29.26) = 14.96; p < 0.001]	condition, hemisphere and site
[F(1.36, 31.17) = 10.23; p < 0.01]	condition, location, hemisphere and site

T-test pairing results

Left-Frontal Electrodes		Right-Frontal Electrodes	
F5	-	F6	[t(23) = 3.53; p < 0.01]
F3	-	F4	[t(23) = 3.04; p < 0.01]
F1	-	F2	[t(23) = 2.89; p < 0.01]
Left-Parietal Electrodes		**Right-Parietal Electrodes**	
P5	[t(23) = -2.97; p < 0.01]	P6	-
P3	[t(23) = -1.91; p < 0.1 (0.069)]	P4	-
P1	-	P2	-

Post-segmentation time window (100 to 500ms)

ANOVA Result	Interaction
[F(1, 23) = 5.84; p < 0.05]	condition and location
[F(1, 23) = 6.11; p < 0.05]	condition and hemisphere
[F(1, 23) = 7.43; p < 0.05]	condition, location and hemisphere
[F(1.42, 32.7) = 6.87; p < 0.01]	condition, hemisphere and site
[F(1.46, 33.51) = 6.54; p < 0.01]	condition, location, hemisphere and site

T-test pairing results

Left-Frontal Electrodes		Right-Frontal Electrodes	
F5	-	F6	-
F3	-	F4	-
F1	-	F2	-
Left-Parietal Electrodes		**Right-Parietal Electrodes**	
P5	[t(23) = 3.54; p < 0.01]	P6	[t(23) = 2.67; p < 0.05]
P3	[t(23) = 3.18; p < 0.01]	P4	[t(23) = 2.72; p < 0.05]
P1	[t(23) = 2.81; p = 0.01]	P2	[t(23) = 2.73; p < 0.05]

Topographic analysis

ANOVA Result	Interaction
Pre- vs. Post-Segmentation	
[F(1, 23) = 9.36; p < 0.01]	condition* epoch and location
[F(1, 23) = 18.76; p < 0.001]	condition* epoch and hemisphere
[F(1, 23) = 8.68; p < 0.01]	condition* epoch, location and hemisphere
[F(1.34, 29.44) = 14.75; p < 0.001]	condition* epoch, hemisphere and site
[F(1.40, 30.71) = 8.01; p < 0.01]	condition* epoch, location, hemisphere and site
Pre-Segmentation	
[F(1, 23) = 7.51; p < 0.05]	condition* location
[F(1, 23) = 12.66; p < 0.01]	condition* hemisphere
[F(1, 23) = 5.47; p < 0.05]	condition* location and hemisphere
[F(1.30, 28.60) = 8.99; p < 0.01]	condition* hemisphere and site
[F(1.42, 31.23) = 5.36; p < 0.05]	condition* location, hemisphere and site
Post-Segmentation	
[F(1, 23) = 7.59; p < 0.05]	condition* hemisphere
[F(1, 23) = 6.72; p < 0.05]	condition* location and hemisphere
[F(1.35, 29.59) = 9.42; p < 0.01]	condition* hemisphere and site
[F(1.39, 30.58) = 6.89; p < 0.05]	condition* location, hemisphere and site

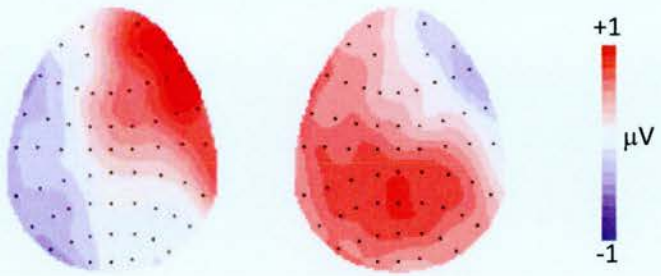

-1000 to -100ms 100 to 500ms

Topographic distributions for the pre- and post-segmentations.